INSTITUTO SUPERIOR DE ENGENHARIA DO PORTO

MESTRADO EM ENGENHARIA MECÂNICA

isep

Equipamento de ensaios a cross car beams

TIAGO DANIEL SANTOS SILVA

novembro de 2019

POLITÉCNICO
DO PORTO

INSTITUTO SUPERIOR DE ENGENHARIA DO PORTO

MESTRADO EM ENGENHARIA MECÂNICA

isep

CCB TESTER CROSS CAR BEAM TESTING EQUIPMENT PROJECT AND DEVELOPMENT

TIAGO DANIEL SANTOS SILVA

Setembro de 2019

POLITÉCNICO
DO PORTO

Instituto Superior de
Engenharia do Porto

CCB TESTER – CROSS CAR BEAM TESTING EQUIPMENT PROJECT AND DEVELOPMENT

Tiago Daniel Santos Silva

1091366

2019

School of Engineering, Polytechnic of Porto

Department of Mechanical Engineering

POLITÉCNICO
DO PORTO

POLITÉCNICO
DO PORTO

CCB TESTER – CROSS CAR BEAM TESTING EQUIPMENT

PROJECT AND DEVELOPMENT

Tiago Daniel Santos Silva

1091366

Dissertation presented to ISEP – School of Engineering to fulfil the requirements necessary to obtain a master's degree in mechanical engineering, carried out under the guidance of Mr. Fernando Ferreira.

2019

School of Engineering, Polytechnic of Porto

Department of Mechanical Engineering

POLITÉCNICO
DO PORTO

JURY

President

PhD Manuel Castro

Instituto Superior de Engenharia do Porto

Supervisor

PhD Fernando José Ferreira

Instituto Superior de Engenharia do Porto

Arguing

PhD João Ribeiro

Instituto Politécnico de Bragança

ACKNOWLEDGEMENTS

This work is the ending of the first proper project that I started in my engineering career. Since then, I've had many other challenges to surpass, most of them at EVOLEO Technologies Lda., the company which took me in as an inexperienced, college-fresh engineer and helped me evolve and become what I am today. For that I must thank my work colleagues at EVOLEO for the help and contributions for this project, especially the "batch" of 2013, you know who you are. A special thanks to Rodolfo Martins, the company's CEO, for the support and time given to me to develop my skills.

My parents, without whom I would not be here, writing these words, and walking the path that I chose and they supported.

Professor Fernando Ferreira for the wise and experienced "tips" and "out-of-the-box" ideas.

Mr. Gonçalves, from SIM-M – Sistemas Integrados em Metalo-Mecânica, Lda. For the numerous insights during the structure fabrication and assembly.

And finally, Ana, for the last push and continued support both at work and in life, and for walking the path together with me.

PALAVRAS CHAVE

Testes a produtos, Cross Car Beam, indústria automóvel, NVH, Ensaios mecânicos, NVH, Estruturas automóveis.

RESUMO

O desenvolvimento de produtos é uma parte muito importante de qualquer processo de engenharia de hoje em dia. Como tal, ferramentas para testar, avaliar e verificar o que foi desenvolvido ou construído são uma necessidade para garantir que o processo de desenvolvimento está correto e que dá resposta aos requisitos de um determinado projeto, produto ou necessidade.

Esta tese descreve o projeto e engenharia de uma ferramenta para testar, avaliar, controlar e verificar o desenvolvimento de cross car beams. Atualmente, a indústria automóvel é exigente, precisa e cara, em que um simples defeito numa estrutura mecânica pode causar uma perda monetária considerável para uma empresa, bem como, e mais importante, a possível perda de vida humana. Devido a isso, as equipas de engenharia da indústria automóvel de hoje colocam uma grande ênfase no desenvolvimento de produtos, análise e design, antes de produzir qualquer elemento estrutural, para tentar reduzir o custo após a produção e o risco de erro, criando produtos e estruturas melhores e mais económicas.

Esta ferramenta/equipamento precisa de dar resultados fidedignos da resistência mecânica a cargas estáticas e repetitivas (fadiga) assim como da capacidade de desempenho de vibração. Deve ser possível aplicar cargas de diferentes magnitudes e direções.

Este trabalho está dividido em três partes principais; uma introdução onde estão descritos os objetivos principais do equipamento assim como os seus requisitos; Desenho e desenvolvimento onde as fases de desenho e desenvolvimento são descritas, assim como as alterações, dificuldades e explicações do desenho e engenharia por detrás do equipamento e das decisões tomadas; Análise estrutural onde são mostradas algumas das partes analisadas da estrutura e equipamento. Tanto análises por elementos finitos, como analíticas/numéricas foram utilizadas neste trabalho.

KEYWORDS

Product testing, Cross car beam, automotive industry, NVH, mechanical testing, automotive structures

ABSTRACT

Product development is a critical part of today's engineering process. As such, tools to test, access and verify what has been developed or built are a necessity to ensure the development process is correct and gives answers to the requirements of a given project, product or need.

This thesis describes the design and engineering of a tool to test, access, control and verify the development of Cross Car Beams. Nowadays, automotive industry, in which the Cross Car Beam product is a part of, is a very challenging, precise and expensive industry, in which a simple defect in a mechanical structure can cause considerable monetary loss to a company as well as, and most importantly, the possible loss of human life. Given that, today's automotive industry engineering teams place a high emphasis on product development, analysis and design, before producing any structural element, to try and reduce cost after production and the risk of error, creating better and cheaper products and structures.

The tool needs to give accurate results about structural strength, vibration performance as well as fatigue resistance. All the tests needed must be able to be performed with a different variety of loads, load directions and load types.

The work is divided in three main parts; Introduction where the main objectives of the equipment as well as it's requirements are listed; Design and development where the stages of design and development are described as well as the changes, difficulties and justifications of the design and engineering underlying the equipment; Structural analysis where some of the analysis made for the structure and equipment are shown and described. Both FEM and analytical analysis were done in this work.

GLOSSARY OF TERMS

2D	Two dimensions
3D	Three dimensions
CAD	Computer aided design
CAM	Computer aided manufacturing
CCB	Cross Car Beam
DIN	Deutsches Institut für Normung
ISO	International Standards Organization
NP	Norma Portuguesa
NTM	Normal, Transverse, Moment – internal forces and moments diagrams
NVH	Noise, vibration and harshness
UPN	U shaped profile beam
HEA	H shaped profile beam
IPE	I shaped profile beam
FEA	Finite Element Analysis

FIGURE INDEX

TABLE INDEX

INDEX

INTRODUCTION

1 INTRODUCTION

In this chapter, the scope of the thesis and of the project itself are described. The client's requirements for the project and tests are also detailed.

1.1 Scope of the project

The scope of the project is to design and construct an equipment capable of testing CCBs in various ways with different loads, directions of loads and amplitudes so that designers and manufacturers of this type of structures have a way to validate their drawings and ensure internally, that the structure they offer complies with the necessary requirements.

The project was developed during work at the company EVOLEO Technologies Lda. for a client company. Due to these factors, some points of this work are confidential and there are no references to the client company.

The main objectives of this project are to design, develop and build an equipment capable of testing the client's range of CCBs. The tests must provide accurate results that can be reproduced. The system must be configurable and adaptable to new structures and tests.

1.2 Scope of the thesis

This dissertation covers only the structural and mechanical part of the project, not showing the parts of the acquisition systems, hydraulic unit and sensors, it may, however, refer to certain points to these components for information purposes only.

It should also be noted that, being an extensive work and owned by a private company, not every element of the structure will be fully detailed. Given that, some structural analysis and details were left out of this work. Still, most of the critical elements are described and the structural analyses done are also shown in this work.

Some of the solutions and explanations given might not be as academic or scientific as expected, the author of this work had to take fast and practical approaches to solve the problems presented by the requirements of the client's needs, given the economical and time restrictions that a project like this is subject to. Still, effort was put in explaining the whole process as much as feasible and in layman's terms as much as possible.

The purpose of the work is to mainly show the ideas and implementation of the project, from the concept to the actual built and working equipment.

1.3 Project requirements

The project requirements, for the structural and mechanical part, will be listed below. This list is not intended to be exhaustive and has been compiled to allow for an easy understanding of the type of tests and products that it is expected to support.

It should also be mentioned that there were two distinct phases of requirements, in a first phase the requirements of maximum dimensions, weight and tests and static loads were dealt with, and in a second phase the vibration requirements (NVH).

- Maximum dimensions of the structure:
    - It should be possible to transport the equipment in a standard marine container:
        - 2,34x2,28x5,898m max;
- Dimensions of the products to be tested (Figure 1-1):
        - 2x2x1,8m max;

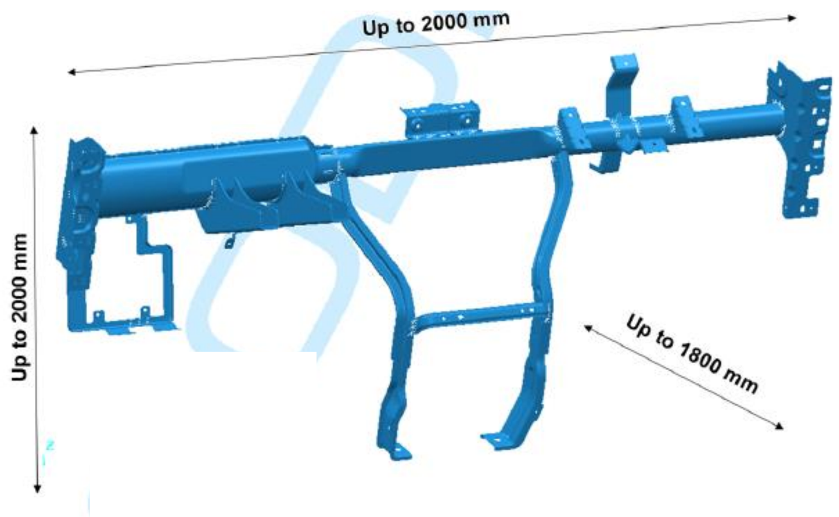

Figure 1-1 – Requirements: Maximum dimensions of the product to be tested

- Features:
    - Product fixation:
        - Flexibility to fix the product in various positions with varying attachment points (Figure 1-2);

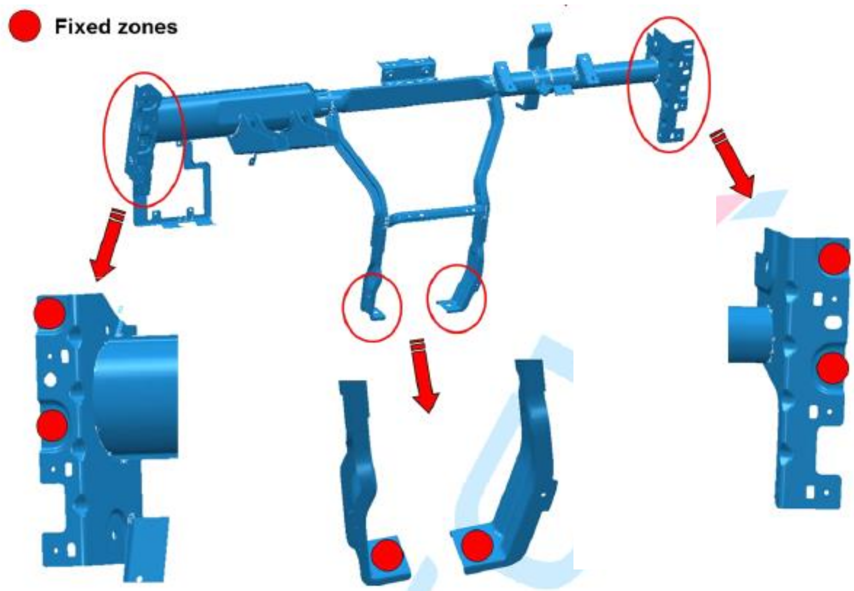

Figure 1-2 – Requirements: Fixing points of the product to be tested

- Product testing:
  - Tensile and compression tests with maximum load of 20kN and in various directions (Figure 1-3);

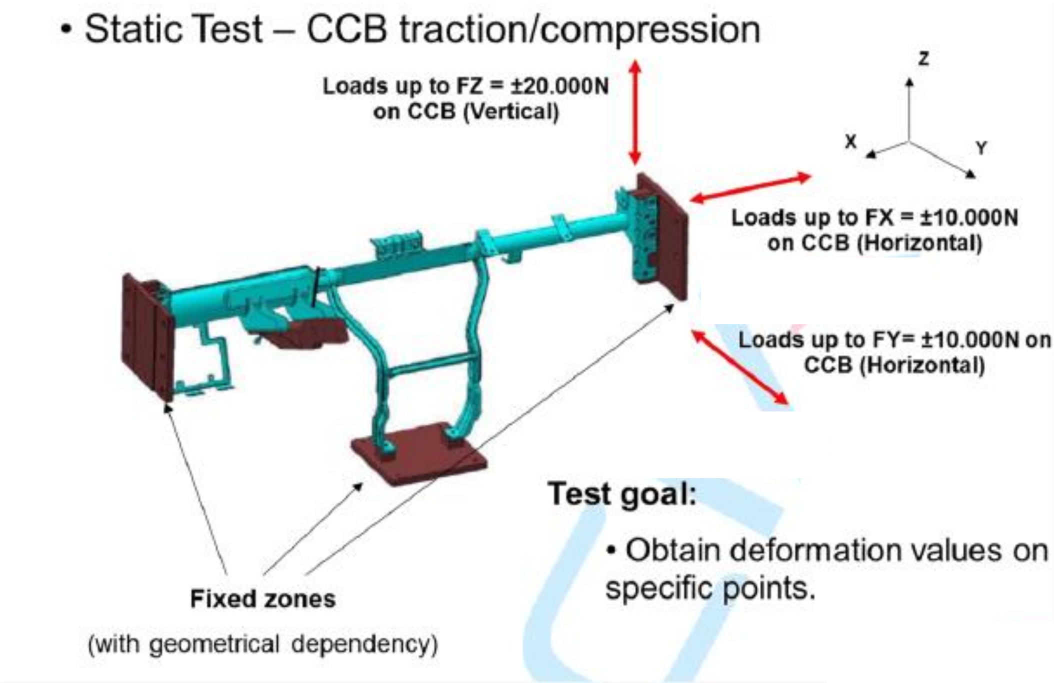

Figure 1-3 – Requirements: Traction/compression test directions and loads

  - Bending tests with a maximum load of 20kN in various directions (Figure 1-4);

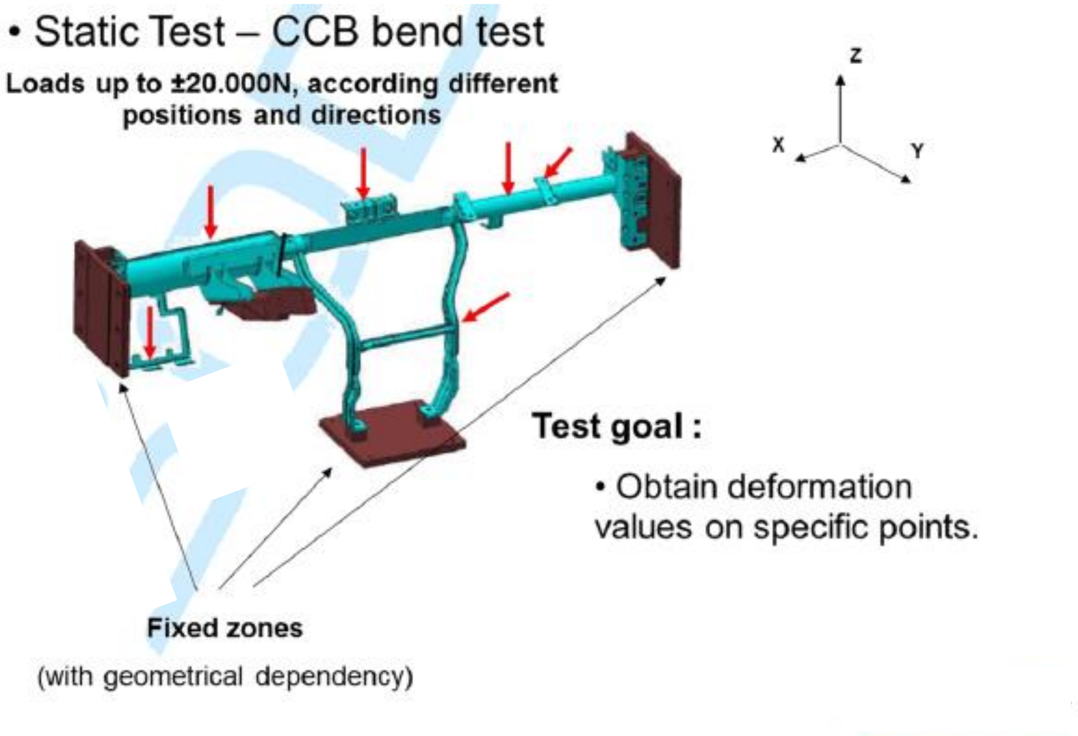

Figure 1-4 – Requirements: Bending test directions and loads

- Fatigue tests with up to 1 million cycles per actuator allowing to define load, displacement and direction.
- Measurement/Data Acquisition system
    - The equipment must have associated a system capable of measuring data from various sources simultaneously. These sources can be extensometers and accelerometers;
    - It should be possible to program the test in a "virtual" way in order to predict all possible configurations and/or steps to be performed to configure the equipment.

In a second phase, as previously mentioned, vibration requirements were added for the performance OF NVH tests. These requirements are listed below.

- Vibration Tests(NVH), (Figure 1-5)

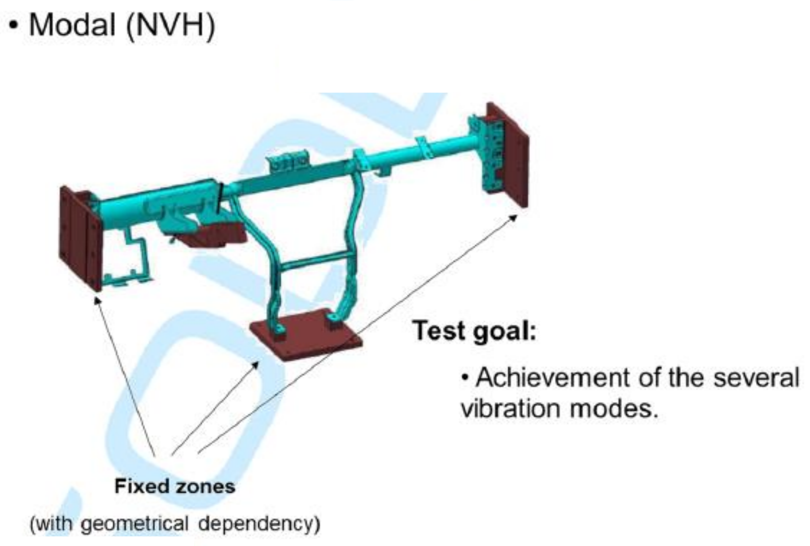

Figure 1-5 – Requirements: Vibration test (NVH)

- The NVH test brackets must have the first natural vibration mode above 400Hz

LITERATURE REVIEW

2 LITERATURE REVIEW

In this chapter, some background information that is useful to understand the current setting of CCB testing and the methods used are described.

2.1 Mechanical testing in automotive design

Mechanical testing has been very important in the automotive industry, proof of that are the ever-increasing quality levels of the vehicles we ride in today. Even at low prices, we can find cars that provide a comfortable ride vibration and acoustic -wise.

Cross Car Beams (CCB) are very common structures in today's automobile construction, Figure 2-1 shows where a CCB is mounted inside a vehicle and Figure 2-2 shows an example of a CCB with greater detail. Being a structure that generally binds the driving and directional axle of the vehicle to its user and driver, it has special requirements regarding its performance and dynamics that it passes on to the driver, than other automotive structures. It needs to withstand different loads applied by the rest of the vehicle's structure as well as to limit vibrations and noises to the inside of the vehicle as much as possible. Because of this it has quite specific and high requirements of vibration and Noise (NVH) so that the journey inside is as comfortable as possible.

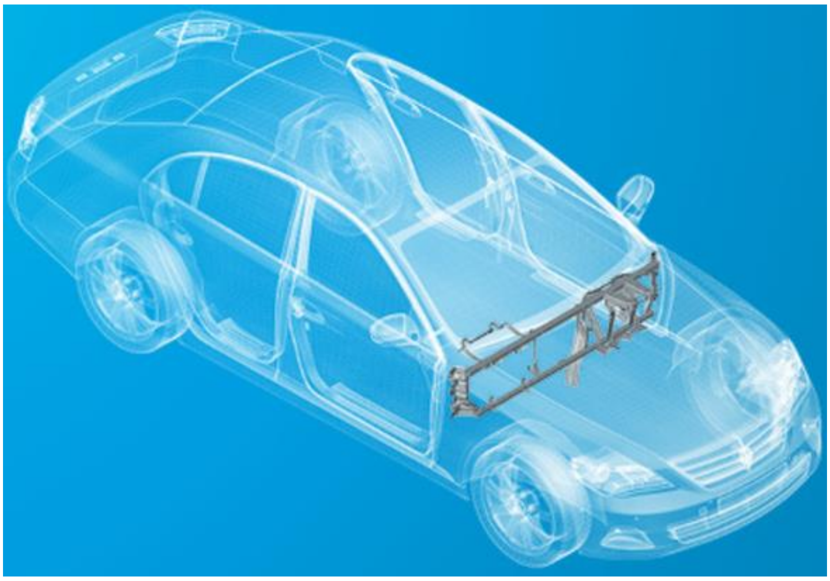

Figure 2-1 – CCB position inside car (example). Copyright Kirchhoff Automotive

Figure 2-2 – Example of a CCB. Copyright Kirchhoff Automotive

The current panorama for vehicle testing is mostly made up of large equipment, sometimes the size of whole rooms. Other are very specific for a certain part of a vehicle. Figure 2-3 shows an example of a room sized test bench for the automotive industry.

Figure 2-3 – Multi-Channel Test Bench designed for fatigue test, static strength test and module durability test, suspension module. Copyright KNR SYSTEMS INC.

The need for more economical and smaller testing equipment is what drives this work, and it is one of the main objectives.

2.2 Finite element method

This work as used, extensively, the finite element method (FEM) to design and predict the structural performance of the system due to its complexity and time it would take to describe numerically the whole system. The major advantage of computational simulations should be the significant shortening of time for testing and, inevitably, the costs reduction (Tabacu, Stefan, Ion Tabacu and Anton Hadar, 2011).

Vibration performance of the structure was also an important part of the project, as such simulations and analysis were run using modal analysis. Modal analysis is an efficient tool for describing, understanding, and modelling structural behaviour. The study of modal analysis is an excellent means of attaining a solid understanding of structural dynamics. (Brüel & Kjær, 1988)

DEVELOPMENT

3 DEVELOPMENT

On this chapter the whole design and dimensioning process of the equipment will be described, starting by the initial sketches and concepts and finishing with dimensioning of the final structure.

In this chapter, the entire design and development process is described and detailed, starting with the initial sketches, the suggestions and help of the advisor of this thesis and ending in the final design of the equipment.

3.1 Development process

The development process used follows a division of the project by different phases. In this work, the three main phases of design and engineering are presented. The pre-project, production and commissioning phases were excluded

Table 3-1 – Development process

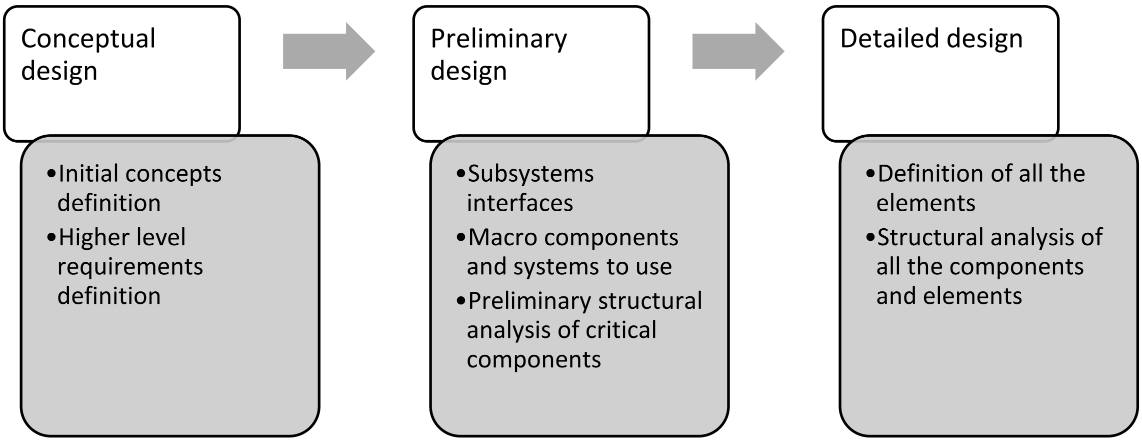

Being a prototype, there were test activities within the detailed design phase, in order to validate some points of the design and provide data to be able to advance with other parts of the project. These test activities proved to be extremely important for the final phase and response to NVH test requirements, as can be seen further ahead in this work.

3.2 Concepts and preliminary design

In this chapter are presented the initial sketches, concepts and preliminary design of the equipment, without going into much detail, because the goal is to present to the reader, in a general way, of the path and guiding lines of the project and design process of the whole developed work.

With this premise, the first sketches attempted to answer to the high-level requirements of the equipment, and those that are most important, that set this equipment apart from other mechanical testing equipment.

3.2.1 First sketch: answering the imposed flexibility

This sketch was the first attempt to meet the client's needs.

On a first approach, to try and maximize the number of directions that it would be possible to apply loads, a system of pulleys and cable was conceived. This approach allows for great flexibility because a pulley is easy to relocate in the structure and it would be possible to maintain the main actuator in one place in most cases, that would pull the cable attached to the CCB.

Based on that, two concepts were developed with a few differences on how the loads would be applied.

The first concept is based on a moving gantry and two other beams to place the pulleys at to apply the loads. Figure 3-1 and Figure 3-2 show those concepts.

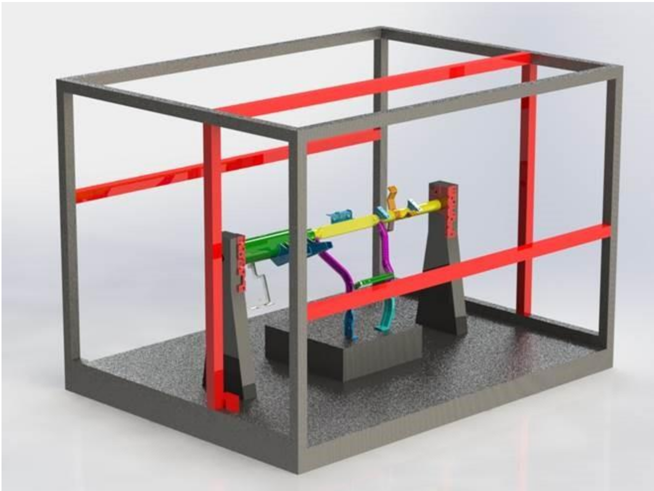

Figure 3-1 – Initial sketch 1 – Gantry and movable bars

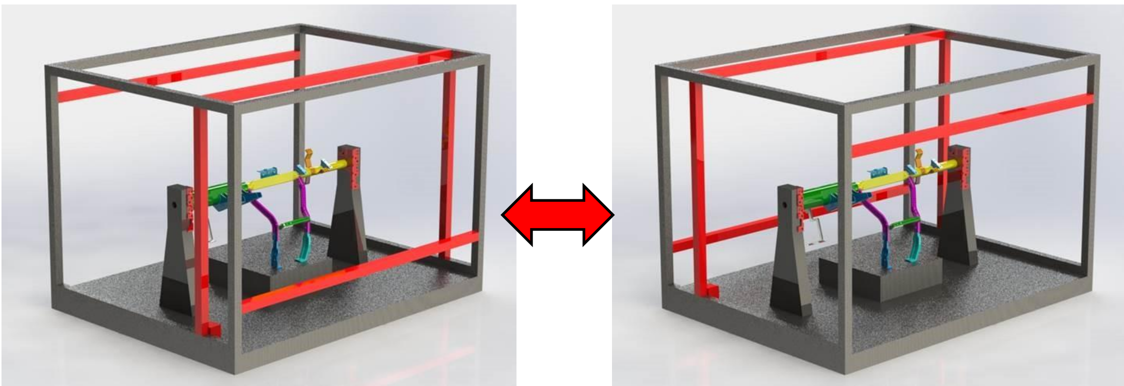

Figure 3-2 – Initial Sketch 1 – Example of possible configurations

The red elements would be movable and would allow the placing of pulleys in different positions to obtain the maximum possible load direction flexibility.

The main disadvantage of this concept is that it has many moving parts and it would be difficult to configure and setup the equipment due to the high number of parts to position.

Based on that disadvantage, the second concept was born. This concept is based around a rotating gantry around the CCB, as shown in Figure 3-3.

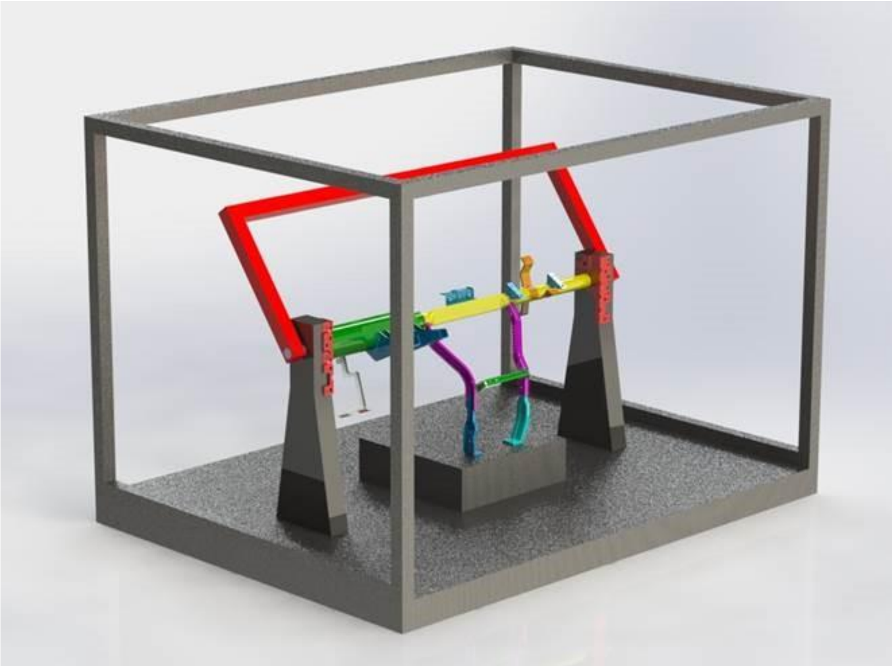

Figure 3-3 – Initial sketch 2 – Rotating gantry

This concept allows for a system with less moving parts but keep the same or similar load direction flexibility. Figure 3-4 shows two different configurations of the equipment.

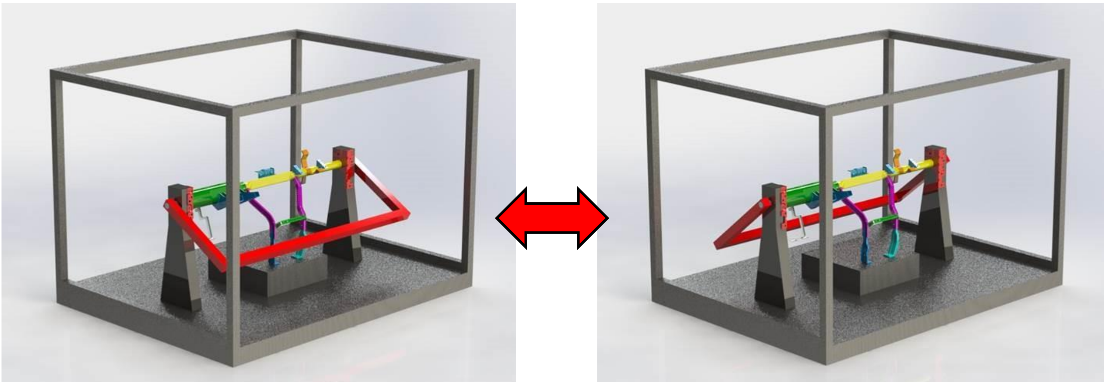

Figure 3-4 – Initial Outline 2 – Example of possible options

This version was the chosen one to take into the next development steps because from the two it is the best solution for being simpler, more economical and easier to use all the while maintaining the equipment’s flexibility and usability. At this phase, this solution still did not answer to how the product fixation would be carried out neither how the traction/compression loads along the main axis of the CCB are applied.

3.2.2 Preliminary design: getting pratical

The next sketch aimed at developing the rotating gantry chosen before, adding a few more elements to the concept and getting it closer to reality. Figure 3-5 shows an overview of the next concept.

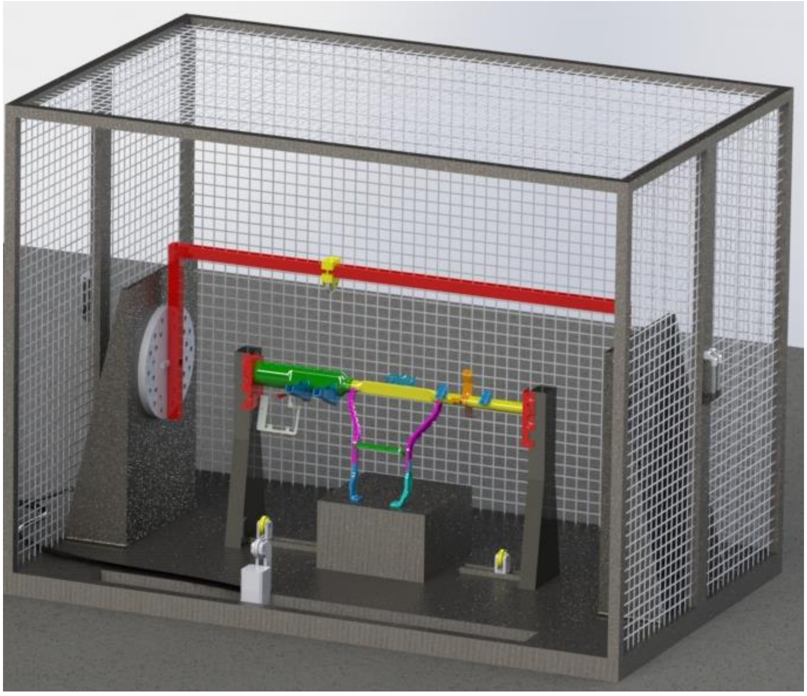

Figure 3-5 – Final sketch of conceptual design

On this new version, the rotating gantry system is made possible by using a holed plate that would fix the rotation at pre-defined angles.

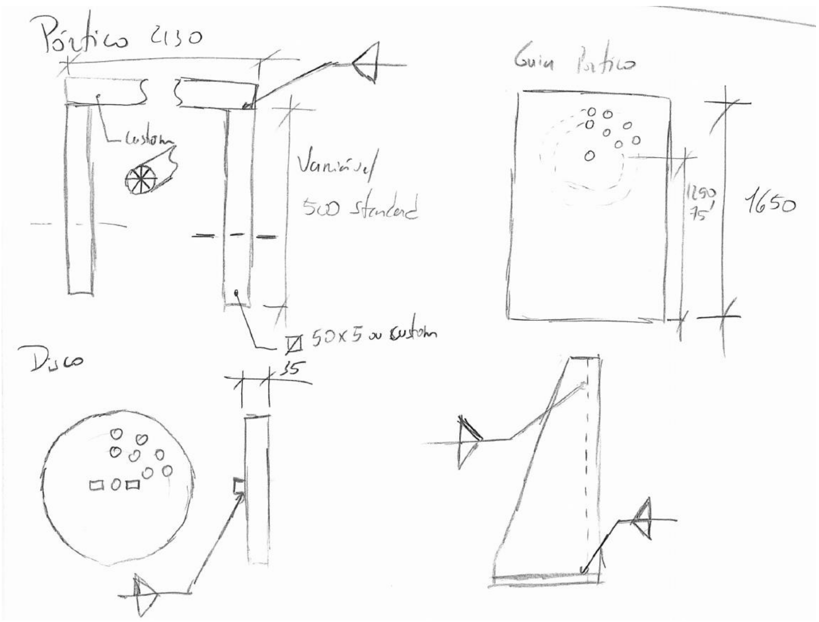

Figure 3-6 – Sketches used to idealize the concept

Pulleys at different positions were added to better represent how the testing would be carried out.

The loads would be applied using an hydraulic actuator and pulleys with cables, to pull on the structure in different directions. Figure 3-7 shows an early sketch of the proposed solution.

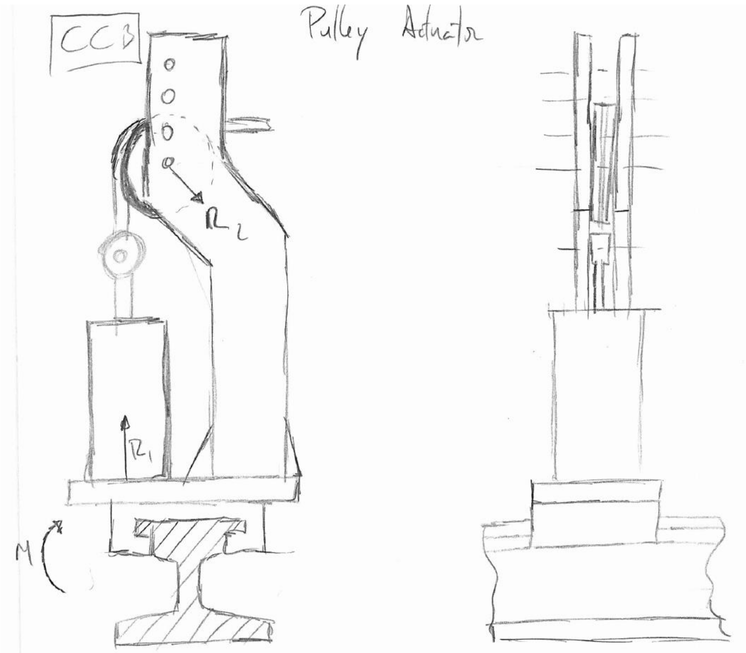

Figure 3-7 – Initial sketch of the central pulley, pulley bracket and hydraulic actuator for load application

The pulley bracket would be fixed to a linear guide, so that its position would be adjustable and thus cover the entire dimension of the CCB as shown in Figure 3-8.

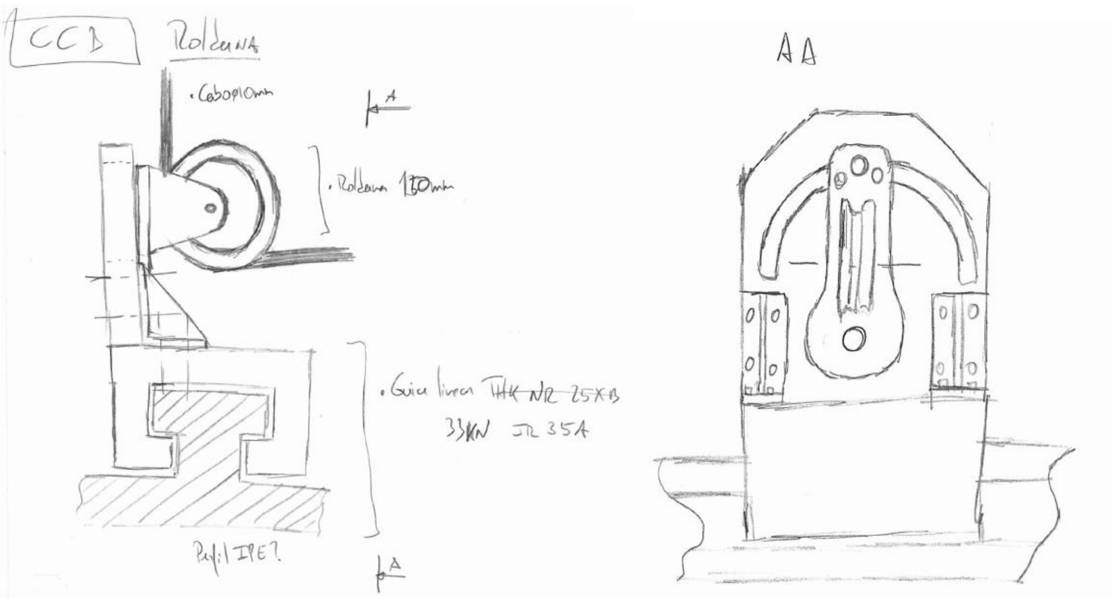

Figure 3-8 – Initial outline of the floor side pulleys

Next is the pulley that would be on the gantry, and that would give the flexibility to apply loads in different directions, by rotating around the central axis of the left sketch of Figure 3-9 and, by being fixed to the gantry, to be positioned along the trajectory of the rotating gantry, as show in Figure 3-10 (Flexible top pulley positioning). Both Figure 3-10 and Figure 3-11 also show the main components of the system, in this phase.

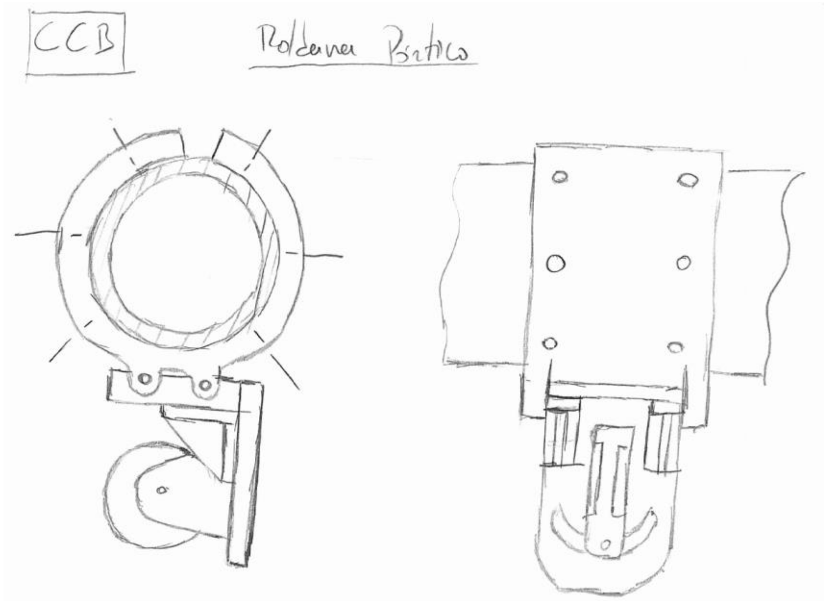

Figure 3-9 – Initial outline of the gantry pulley's support

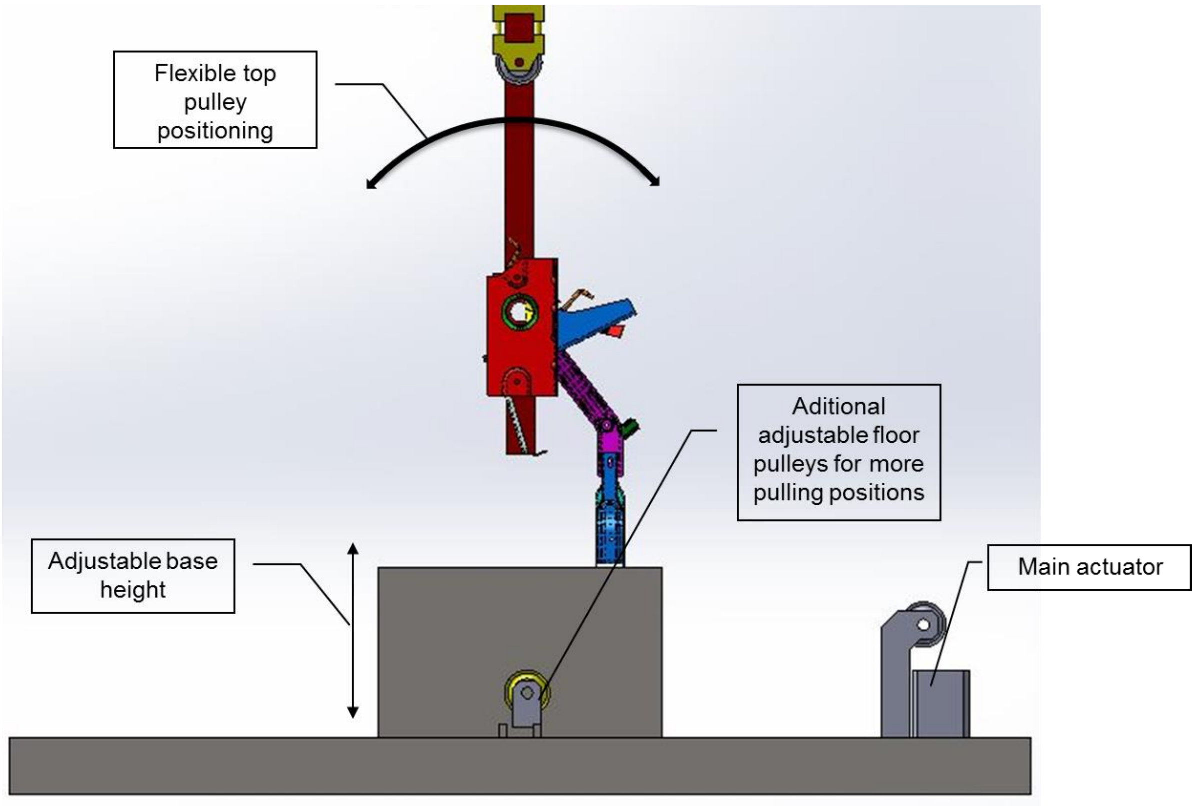

Figure 3-10 – Description of the main components of the system

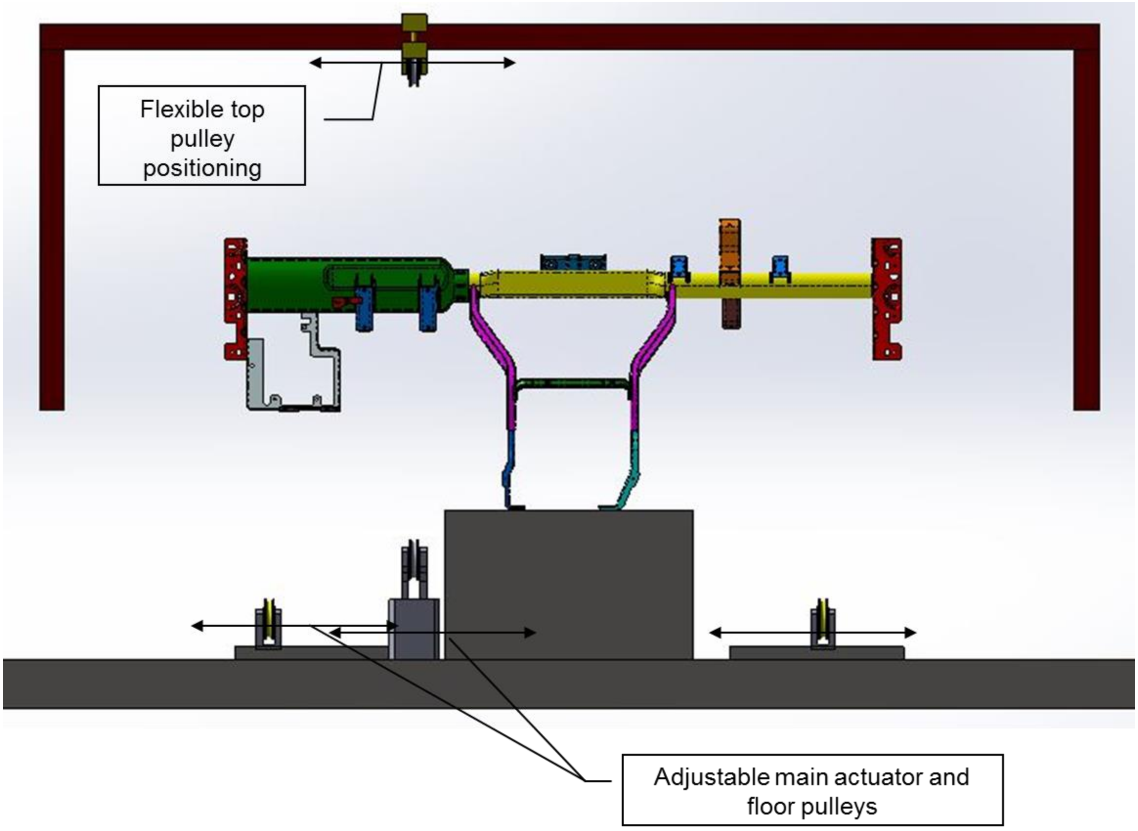

Figure 3-11 – Description of the main components of the system

The following figures show a few configurations for the equipment and the load applying through cable and pulleys would work out.

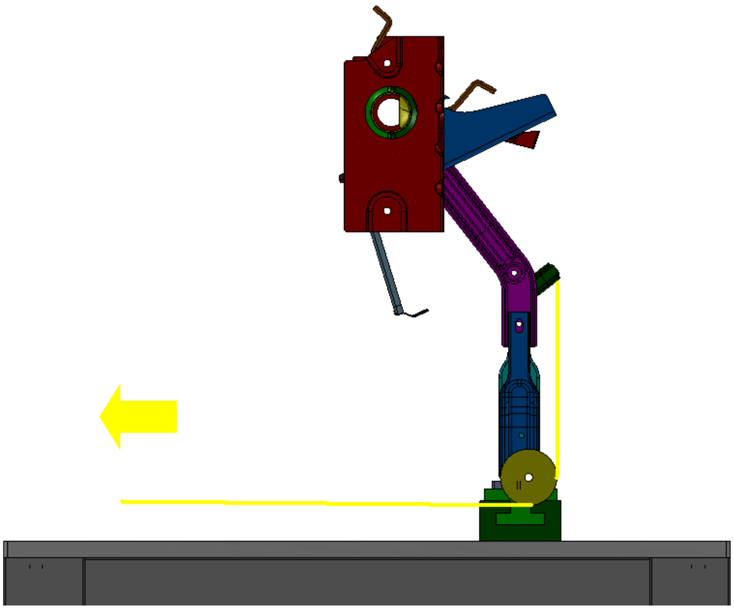

Figure 3-12 – Configurations for load application via pulley

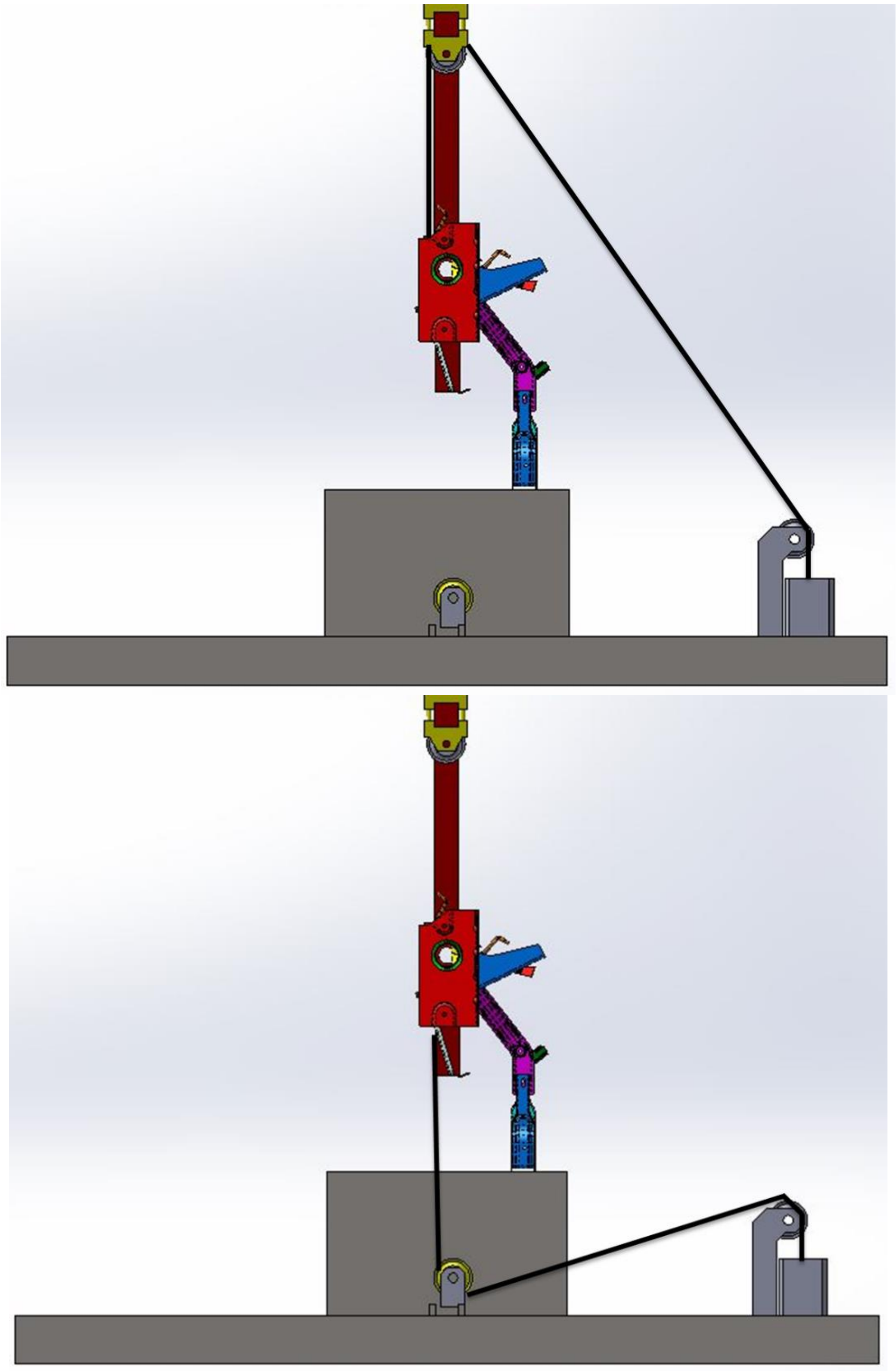

Figure 3-13 – Configurations for load application via pulley, pulling up and down on the CCB

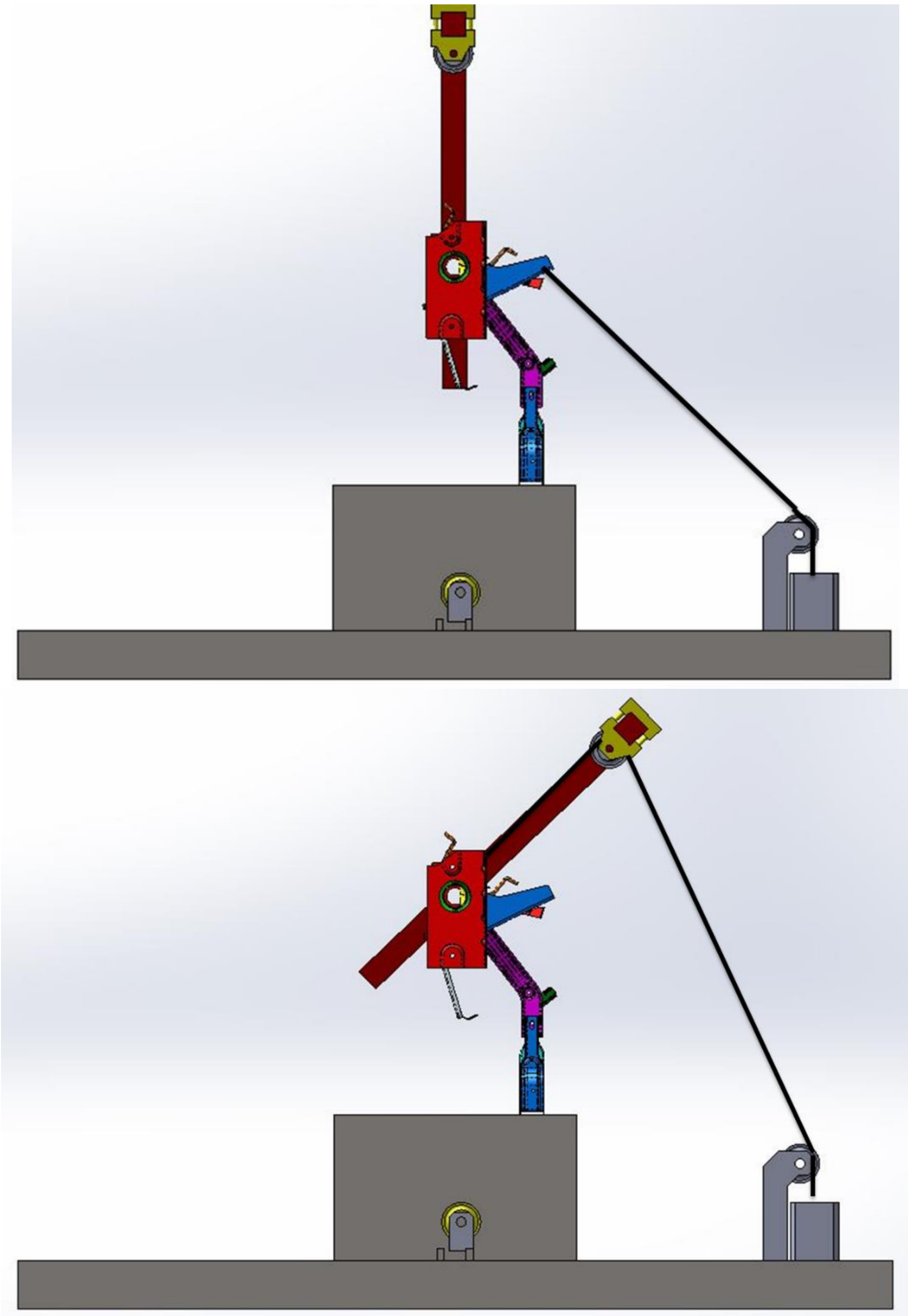

Figure 3-14 – Configurations for load application via pulley, pulling in more complex directions

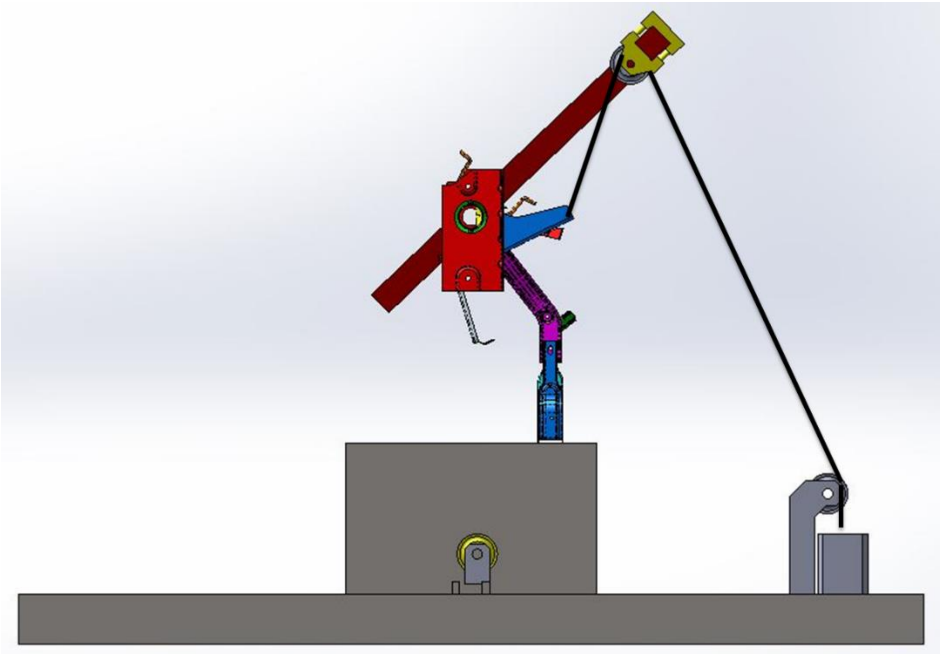

Figure 3-15 – Configurations for load application via pulley, pulling in more complex directions

After analysing this concept, it became clear that there would be a major flaw in the design. Applying loads through a cable, although possible could present a few undesired results because of the cable elasticity. This would give out wrong readings for the measurement devices and it would be very difficult to have a reliable fatigue test due, again, to the cable flexibility which would make it much harder to apply short frequency cycles.

The next concept would have to address that problem as well as get the whole idea closer to reality, starting to introduce even more standard construction and structural elements that would be able to represent the final structure.

3.2.3 Preliminary design: Closing the concept

After the first two sketches, it was time to start thinking "practical" and start developing a few ideas that would make sense in the "real world" and that would bring the concept closer to the real model.

Since the idea of using pulleys was dismissed, the new concept would make use of electric or hydraulic actuators. This final concept incorporates now many elements that were not considered on the previous sketches. Figure 3-16 shows the final version of this concept.

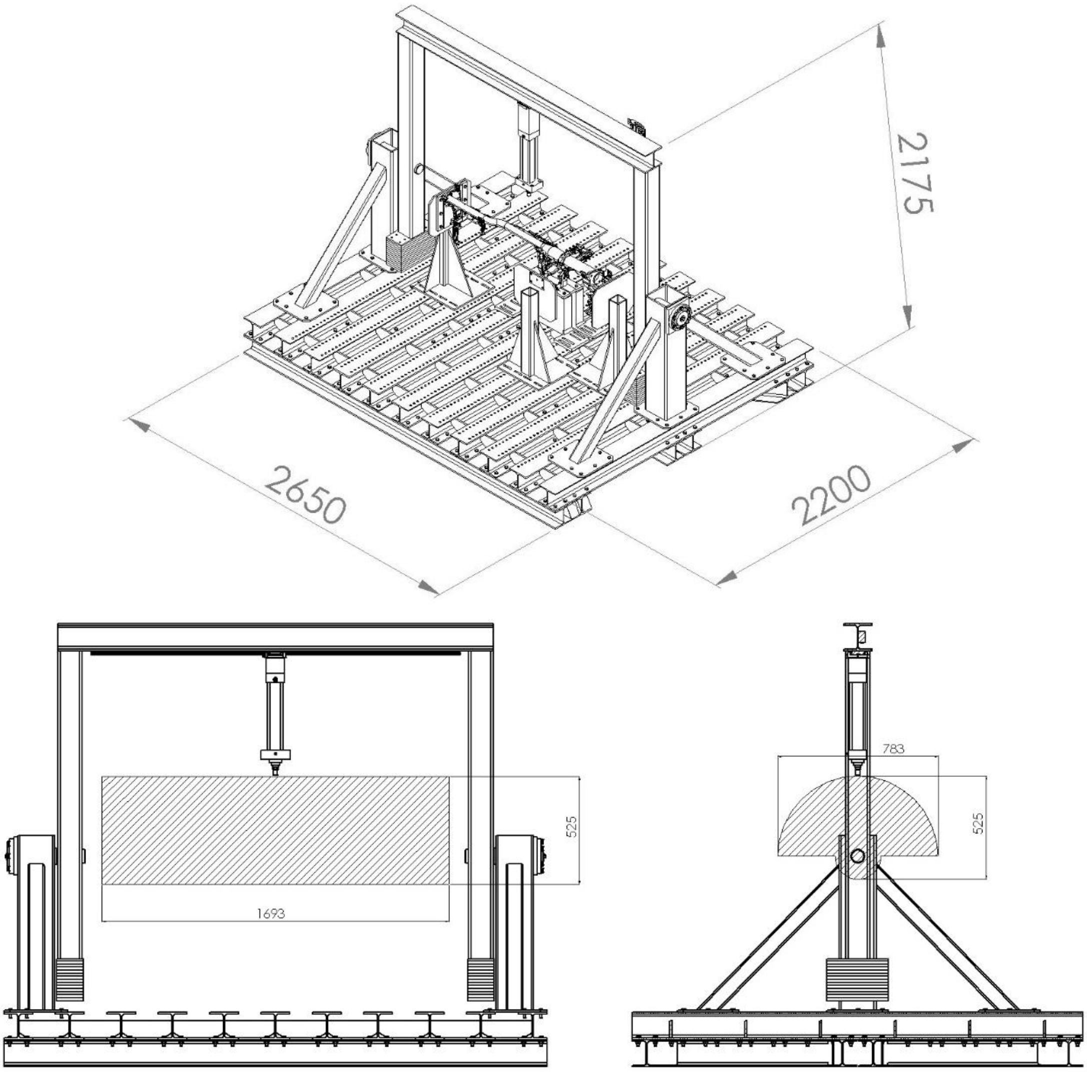

Figure 3-16 – General dimensions of the final concept of the equipment

On this final concept, there were included a few elements that would later be present on the final model and that already are able to better represent in a more realistic way, the structure.

Figure 3-17 shows the names of the main parts of the concept.

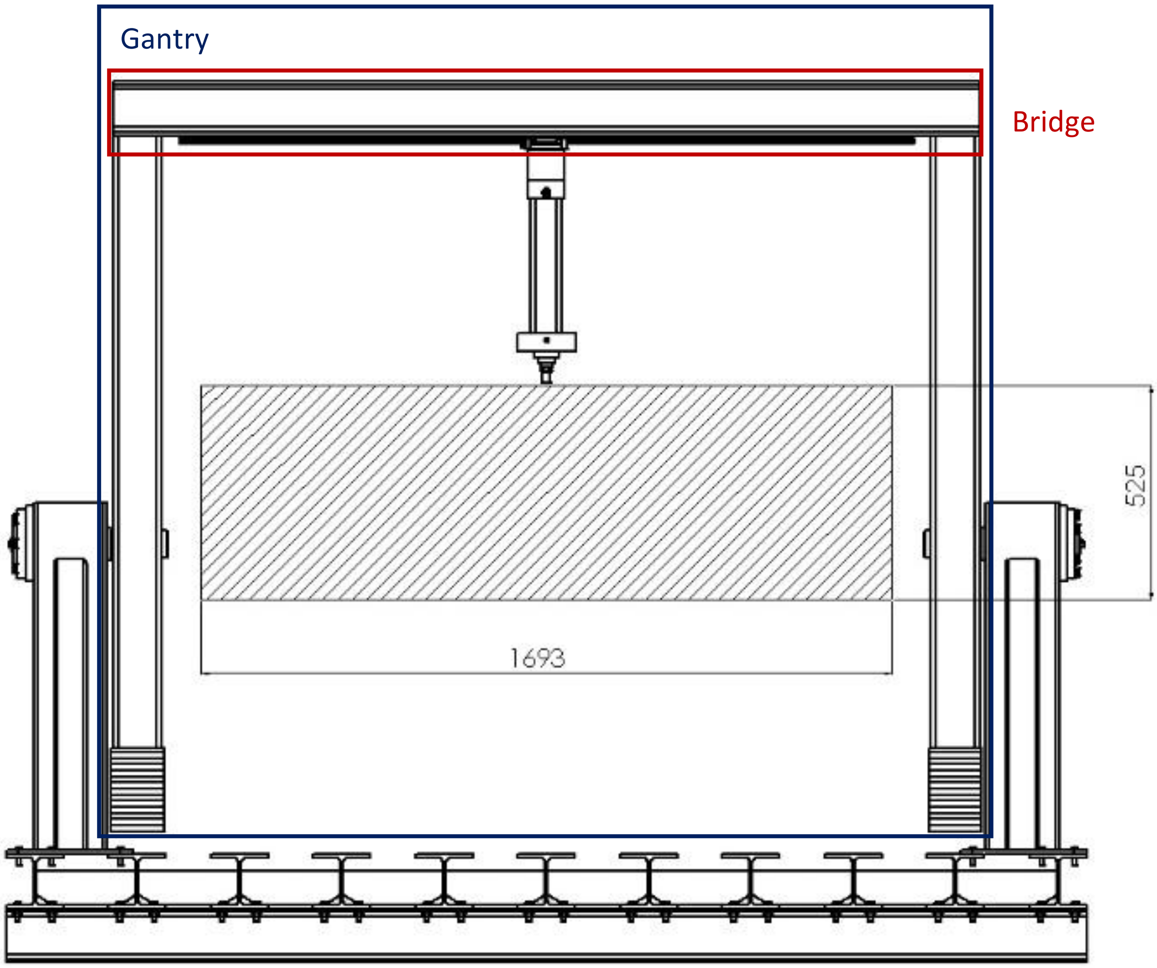

Figure 3-17 – Names of the main components

This new concept drops the idea of pulleys to apply the loads in favour of applying them directly using an hydraulic actuator. Based on the simple components from previous sketches, new and real components were used. The gantry is now made of square tubes and an IPE beam and the base is made of a matrix of HEA beams.

The hydraulic actuator can be positioned along the gantry using a rail and the gantry can rotate on a shaft placed inside the pillars, the rotation is controlled by a holed plate which gives some freedom on the selection of gantry angles. Figure 3-18 shows the system used to fix the gantry's rotation and Figure 3-19 shows the components used in greater detail.

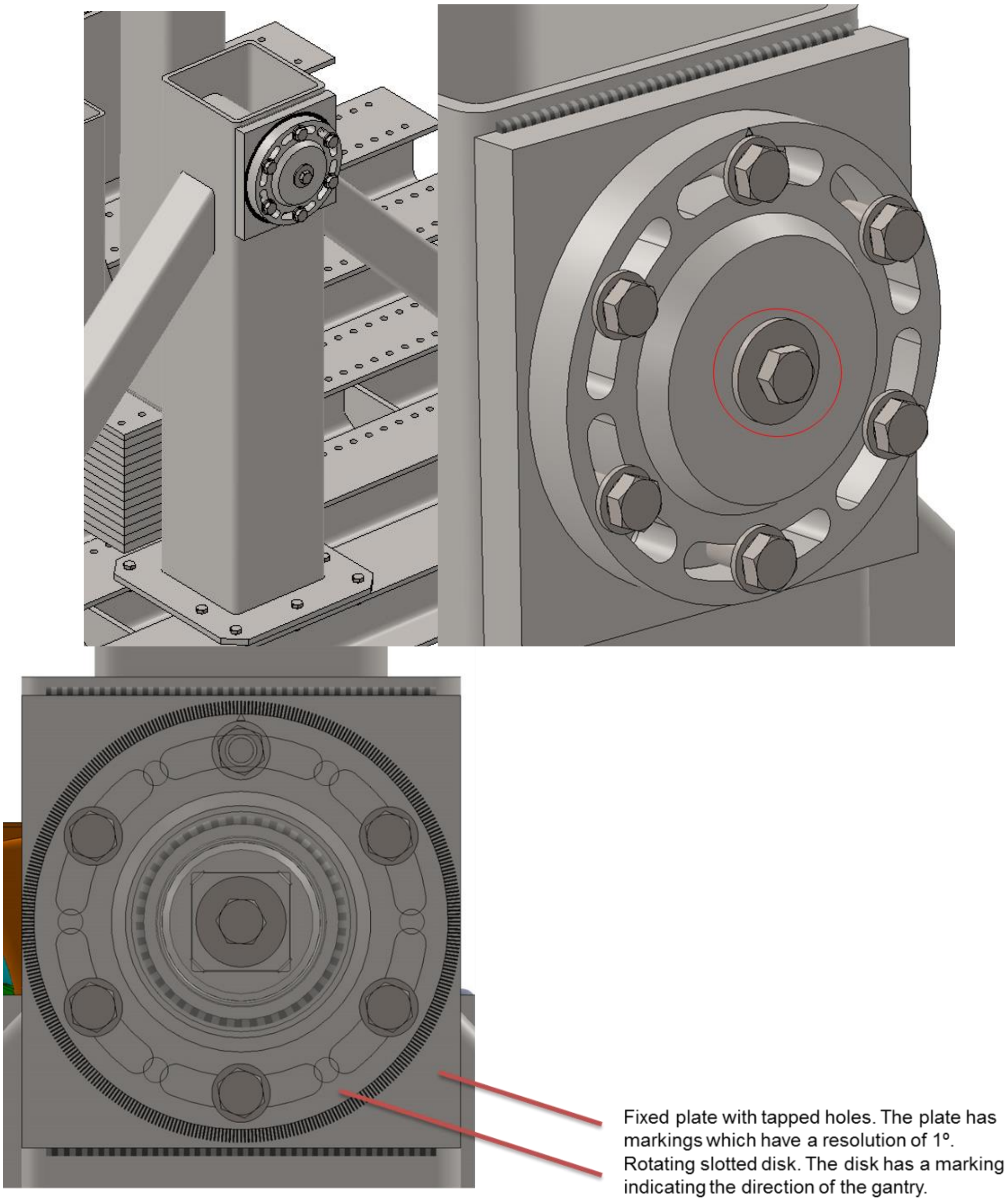

Figure 3-18 – Fixing system for the gantry's rotation

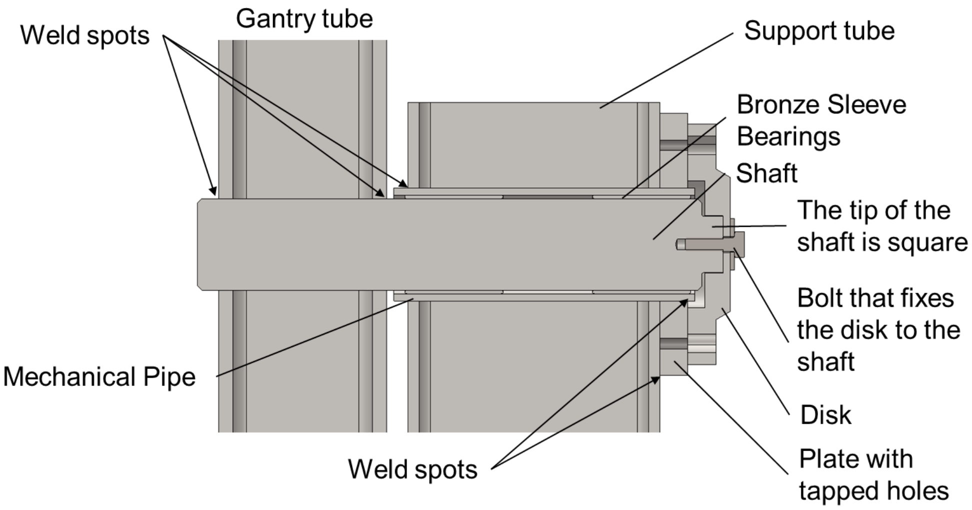

Figure 3-19 – Description of the components used in the gantry rotation system

The hydraulic actuator can be positioned anywhere along the bridge, by using a rail to mount it, as shown in Figure 3-20. To increase the flexibility in the system it would be possible to mount the actuator on a slotted plate, as shown in Figure 3-21, that would allow the actuator to rotate in a different axis.

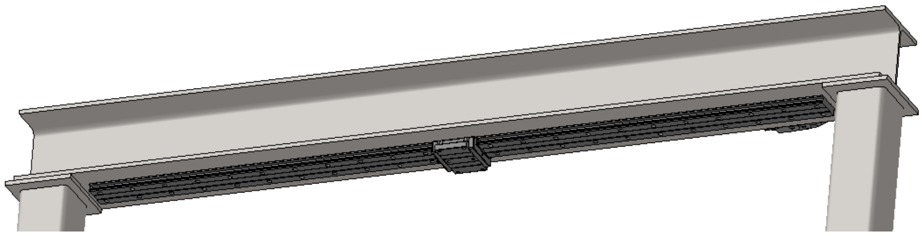

Figure 3-20 – Rail to mount the actuator on the bridge

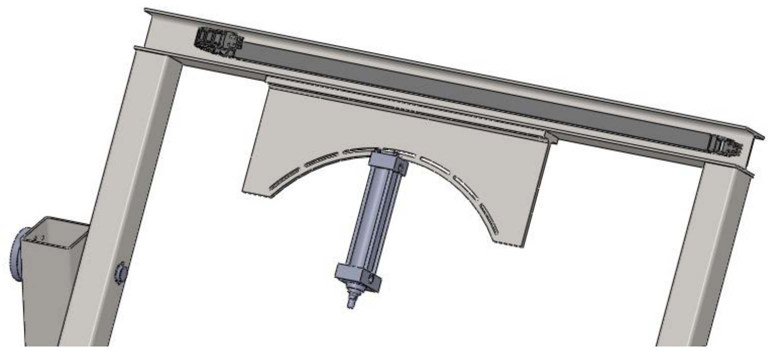

Figure 3-21 – Actuator mounted on slotted plate to increase actuator positioning flexibility

To mount the CCBs with greater flexibility the base of the equipment would have a hole matrix do accommodate the CCB’s supports in different positions and distances, as shown in Figure 3-22.

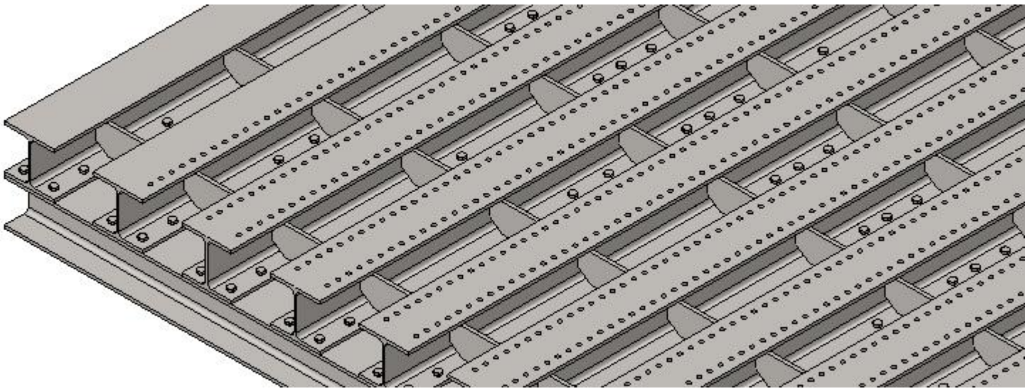

Figure 3-22 – Base's hole matrix

Still, in this design, some flaws were identified, such as the gantry rotation being somewhat limited and its fixation unreliable, the rail for the actuator would be a weak element in the assembly, which could cause failure and the gantry would still be limited due to the actuator not being able to be positioned closer to the CCB (no vertical adjustment).

After analysing these flaws, the final and design was conceived which is described in detail on the following sections.

3.3 Equipment description

In this chapter, an overview of the equipment with its specifications and dimensions.

3.3.1 Overview

Taking into account all the concepts conceived before, the Figure 3-23 shows the final representation of the equipment, and the one that was built.

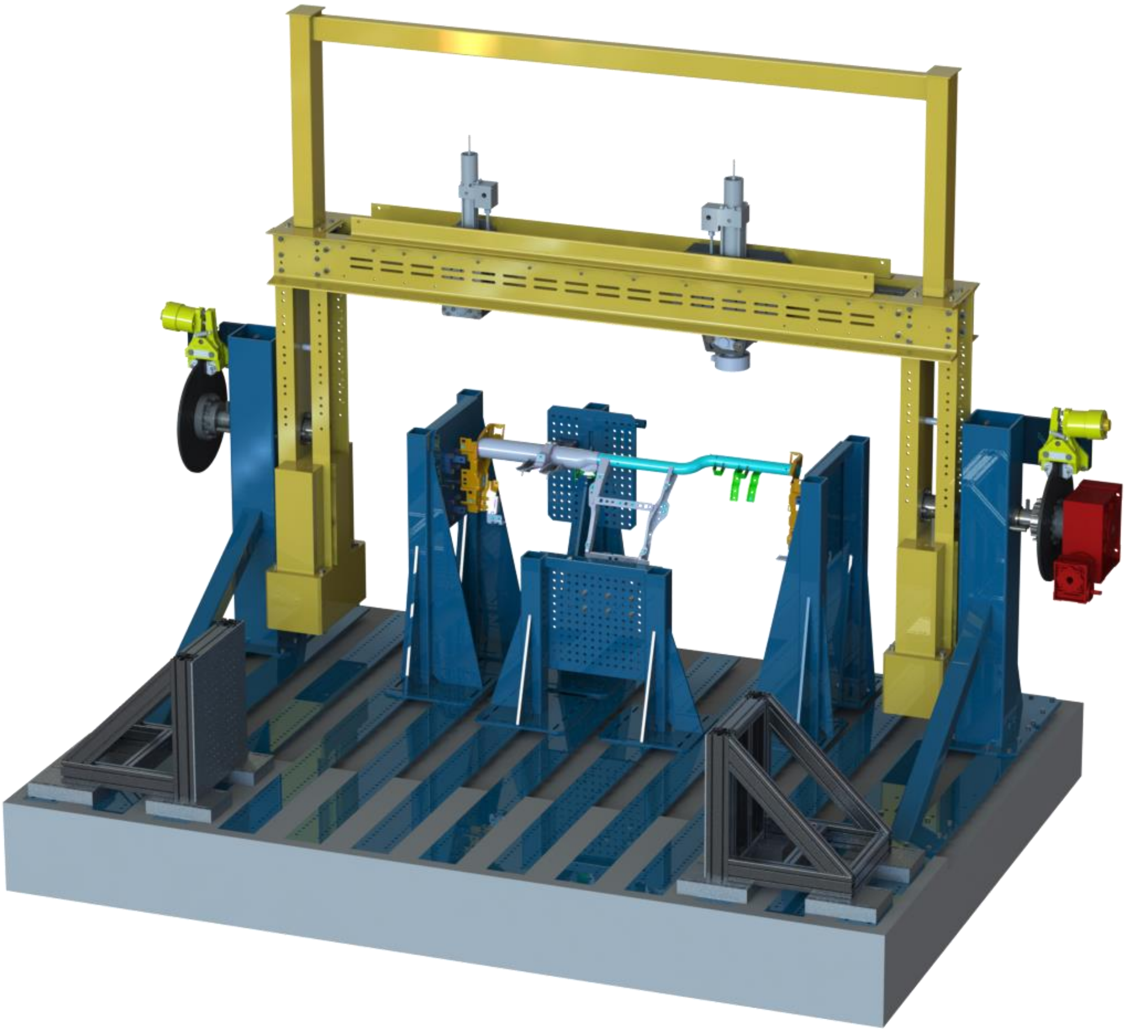

Figure 3-23 – CCBTester Overview

This design, being the final, has all the details and components needed to assemble the equipment. The following chapters describe the equipment, and its parts, in detail.

Aiming to maintain and increase the flexibility of the equipment, the major advantages of the previous concepts were kept, which allow for the multiple configurations shown in the following pictures.

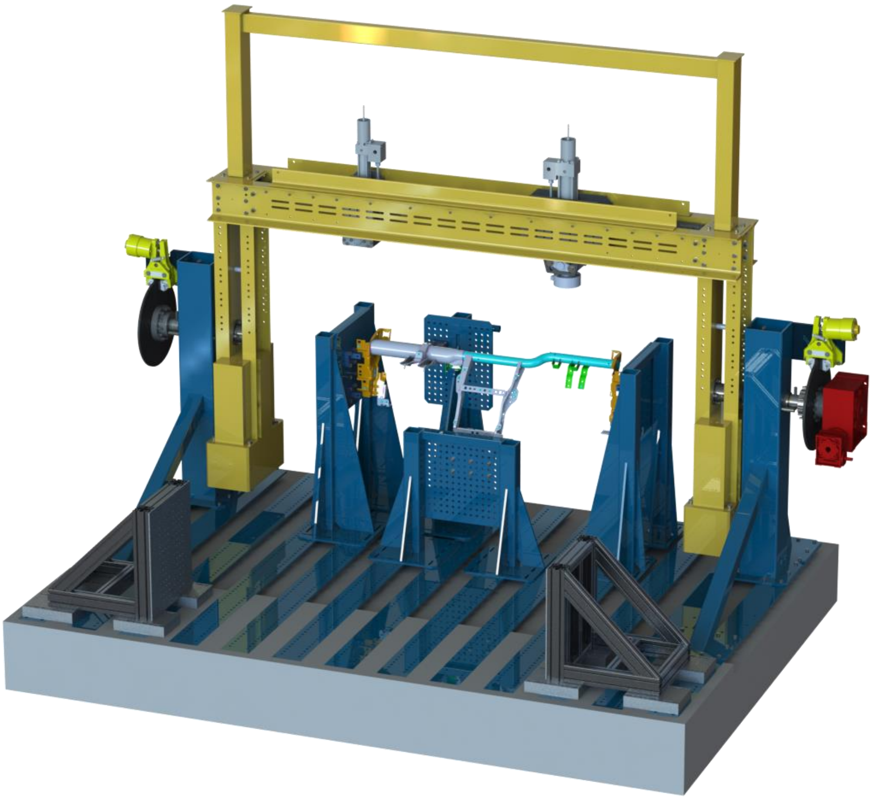

Figure 3-24 – CCBTester Overview: Bridge on top position

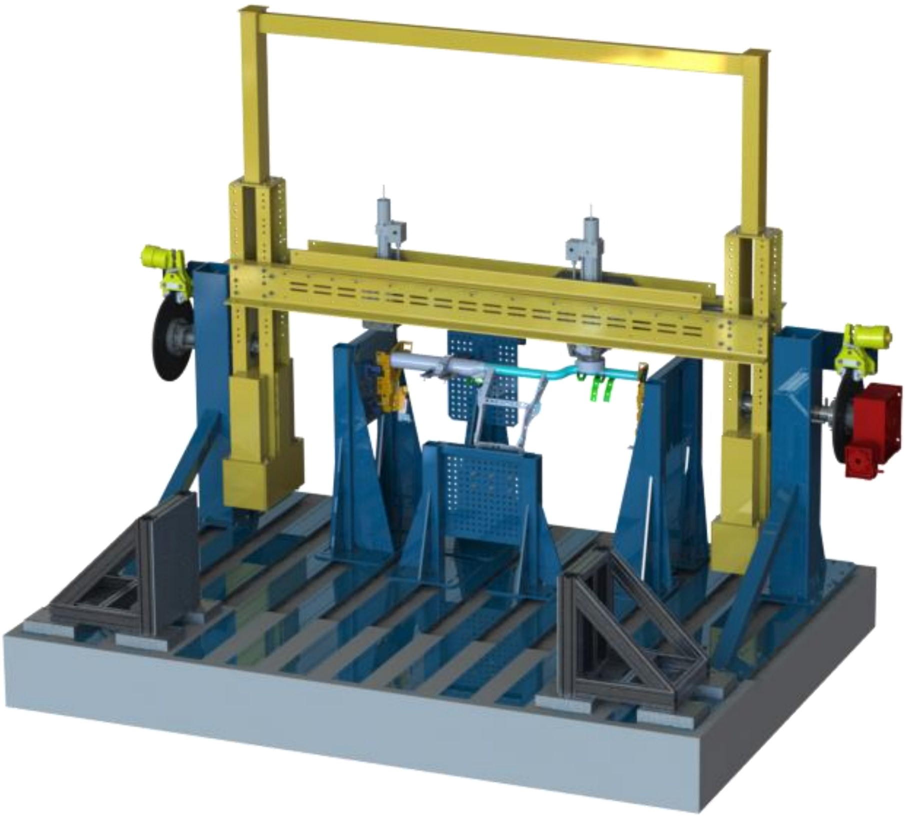

Figure 3-25 – CCBTester Overview: Lowered Bridge

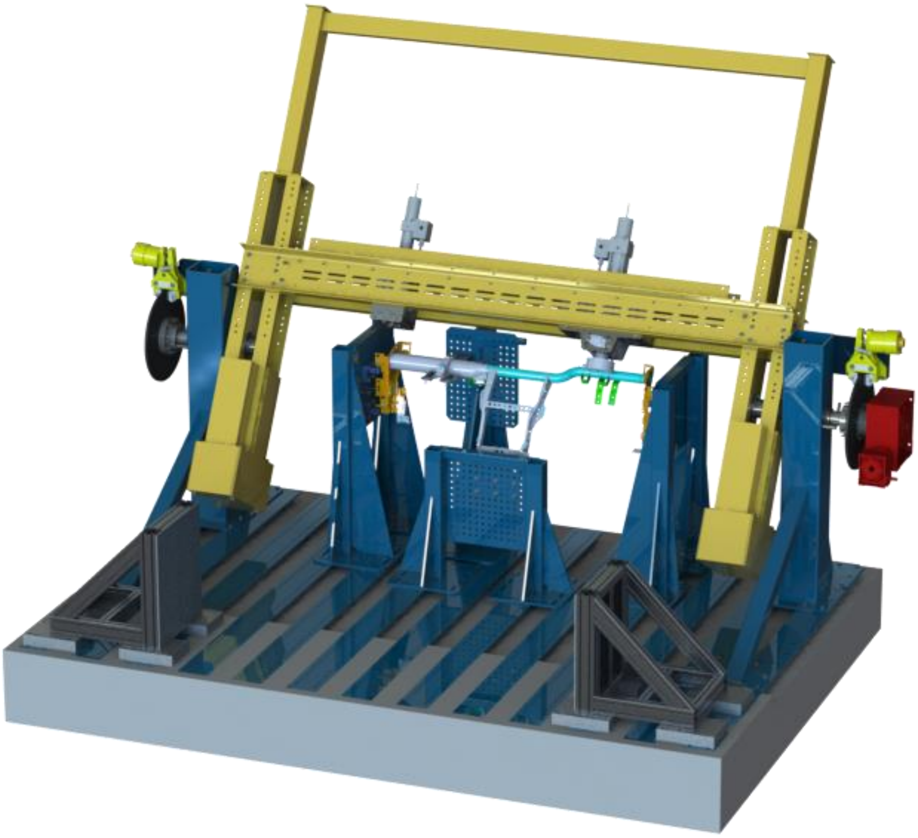

Figure 3-26 – CCBTester Overview: Rotated gantry front view

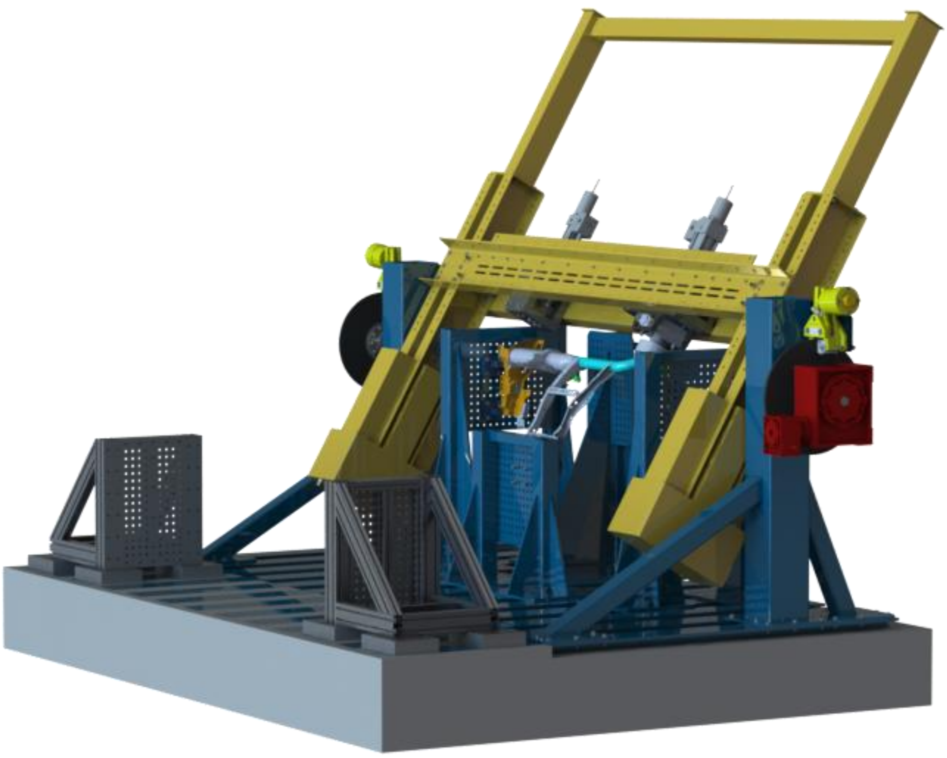

Figure 3-27 – CCBTester Overview: Rotated gantry side view

3.3.2 Main components

Figure 3-28 and Table 3-2 show the main components of the equipment as well as the names used throughout this work, for ease of understanding.

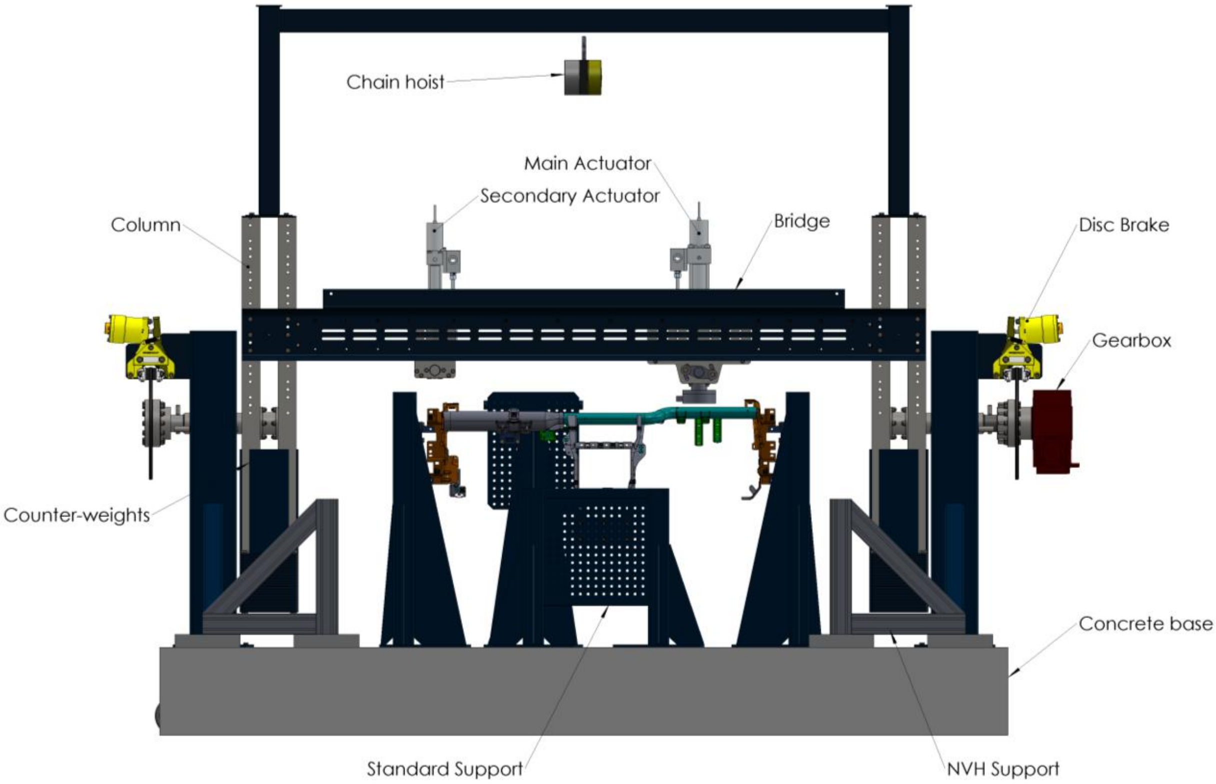

Figure 3-28 – Main components and respective names of the final equipment

Table 3-2 – Main structure groups of the equipment

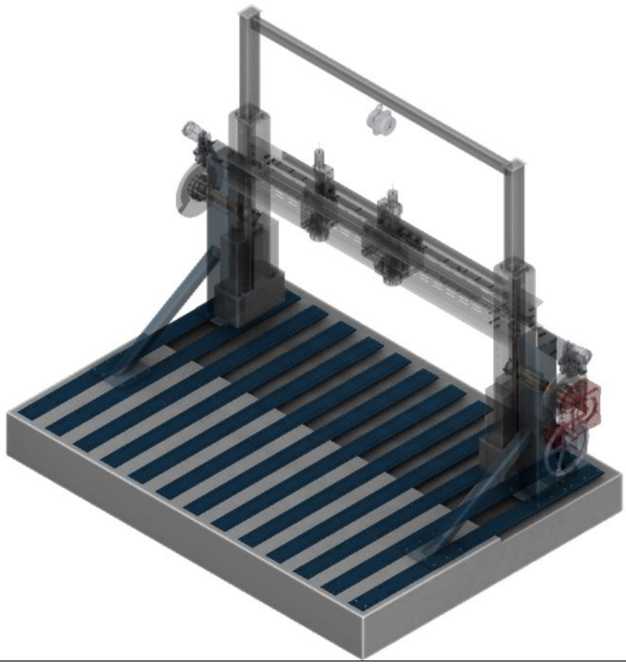

Base

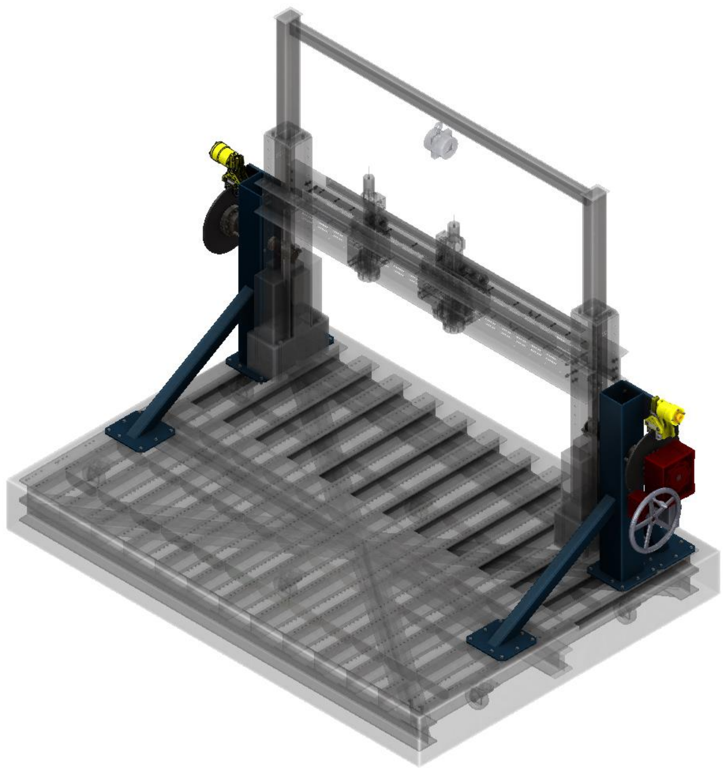

Pillars

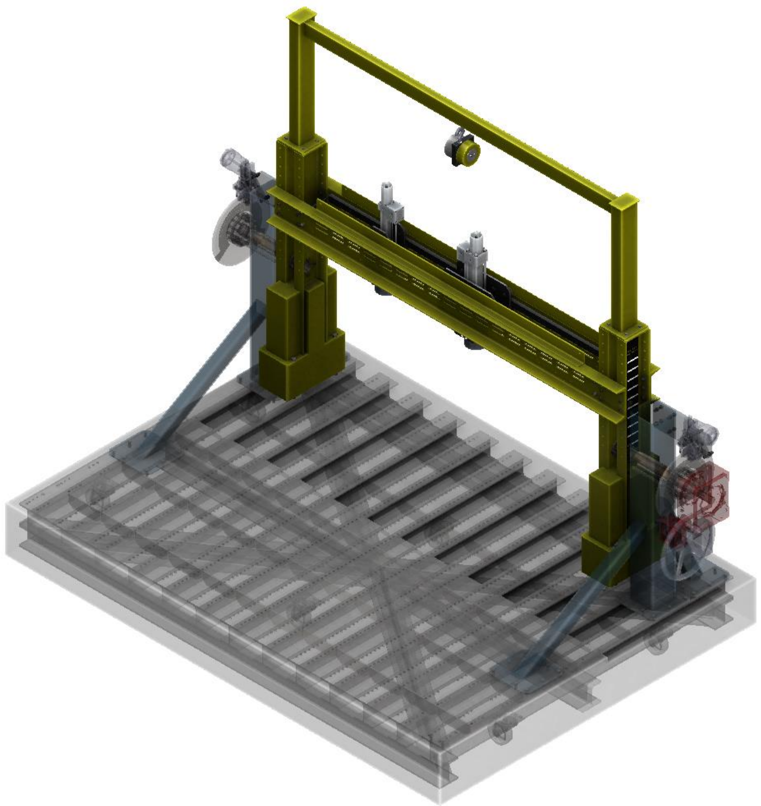

Gantry

3.3.3 Overall equipment dimensions

Below are the overall dimensions of the structure.

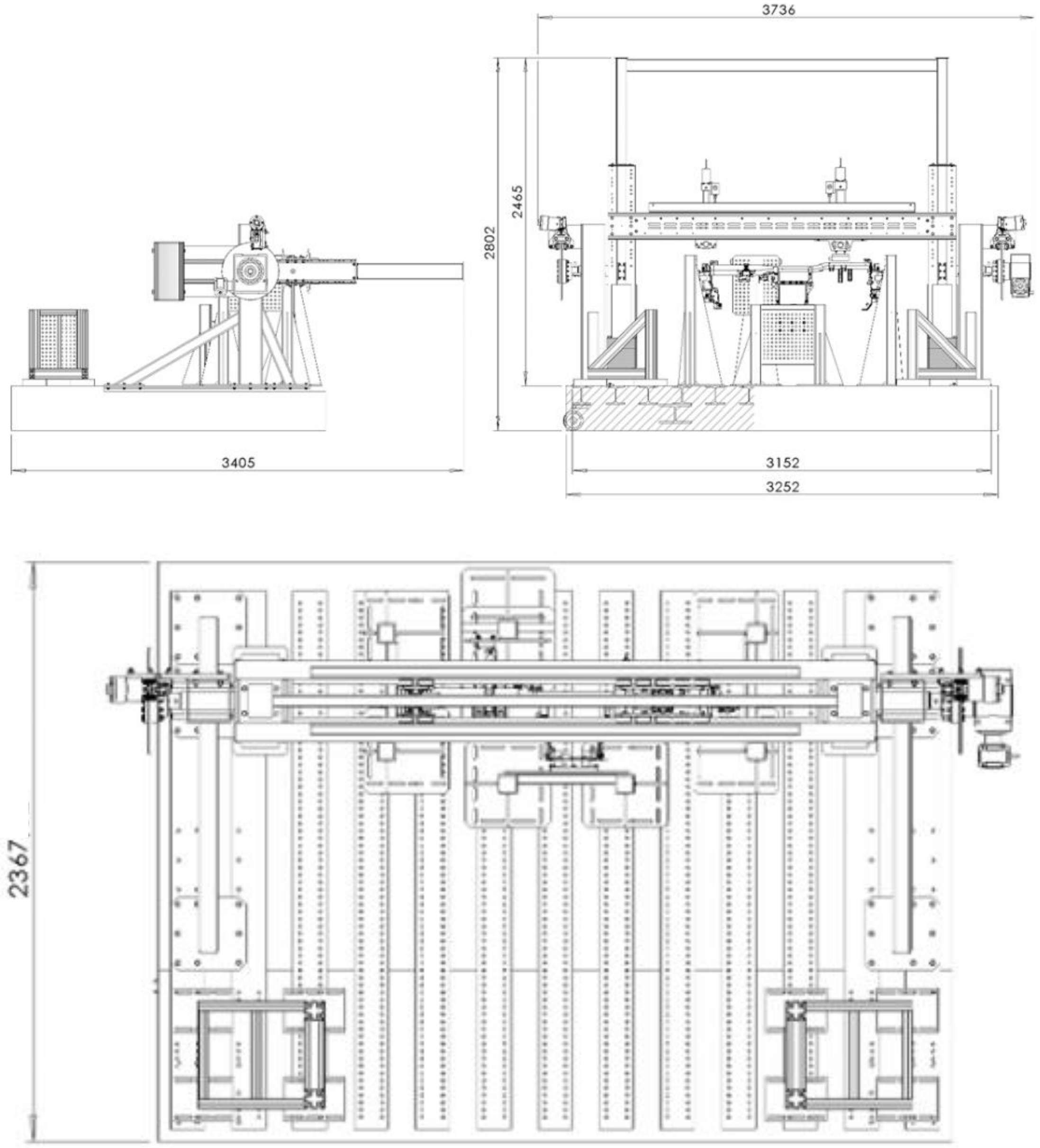

Figure 3-29 – Overall structure dimensions

3.3.4 Actuator reach

The reach of the actuators is shown below.

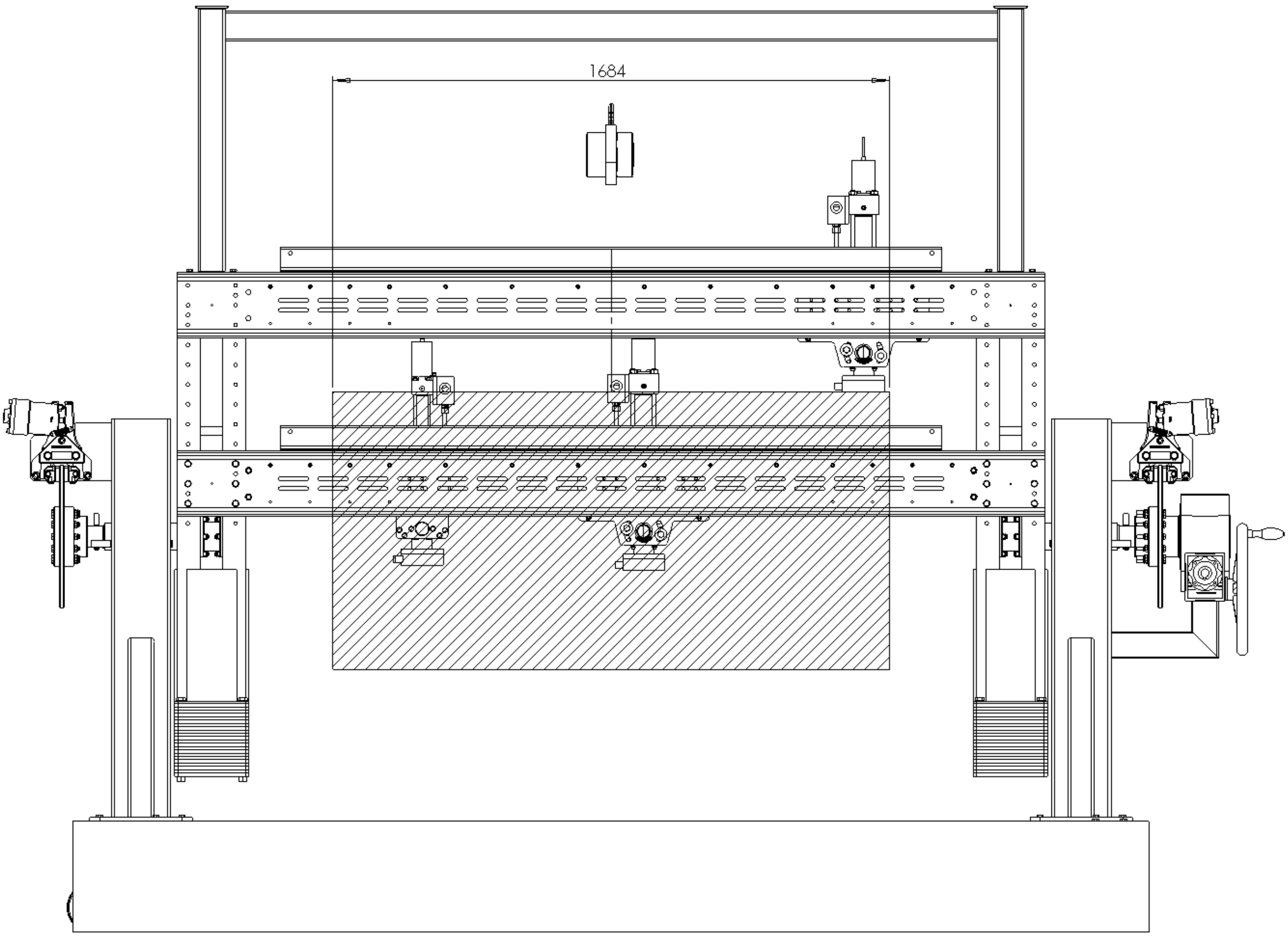

Figure 3-30 – Actuator reach

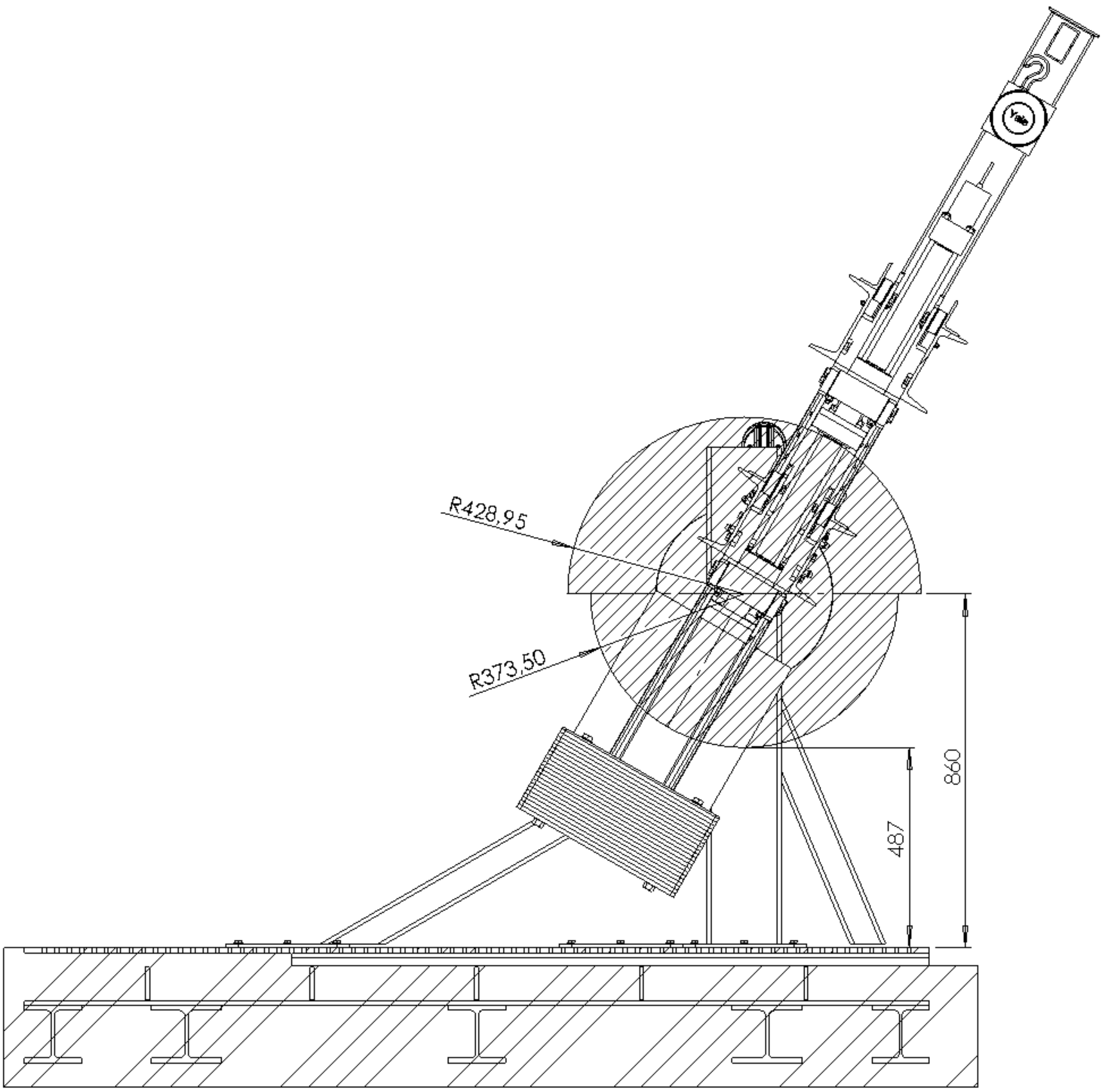

Figure 3-31 – Actuator angular reach

3.3.5 Equipment specifications

Table 3-3 – Equipment specifications

Specifications	Value
Maximum load	7,5 ~ 25 kN
Minimum load	50 ~ 500 N
Load resolution	20 ~ 50 N
Displacement resolution	0,1 mm
Load Frequency range	0 ~3 Hz
Maximum CCB Size	2x1x1 m
Maximum single loads	Two simultaneous maximum loads applied
Setup type	Manual with rotational gantry with 1° steps, planar hole matrix for the device under test positioning, height adjustable bridge in 10 positions, horizontal and angular adjustable actuators with 1 mm and 1° steps respectively
Structure Weight	~3,5 ton
Full system embedded weight	~10 ton – Embedded base to isolate the test bench from outside vibrations and loads
Dimensions	3,7x3,4x2,4 m
Data acquisition	Acquisition cabinet with capacity for 48 BNC input channels (accelerometers) and 24 ENET input channels (extensometers)
Measurement sensors	Extensometers and accelerometers
Work area	1684xø373mm

3.4 Structure description

In this chapter, all the elements of the structure are described with greater detail.

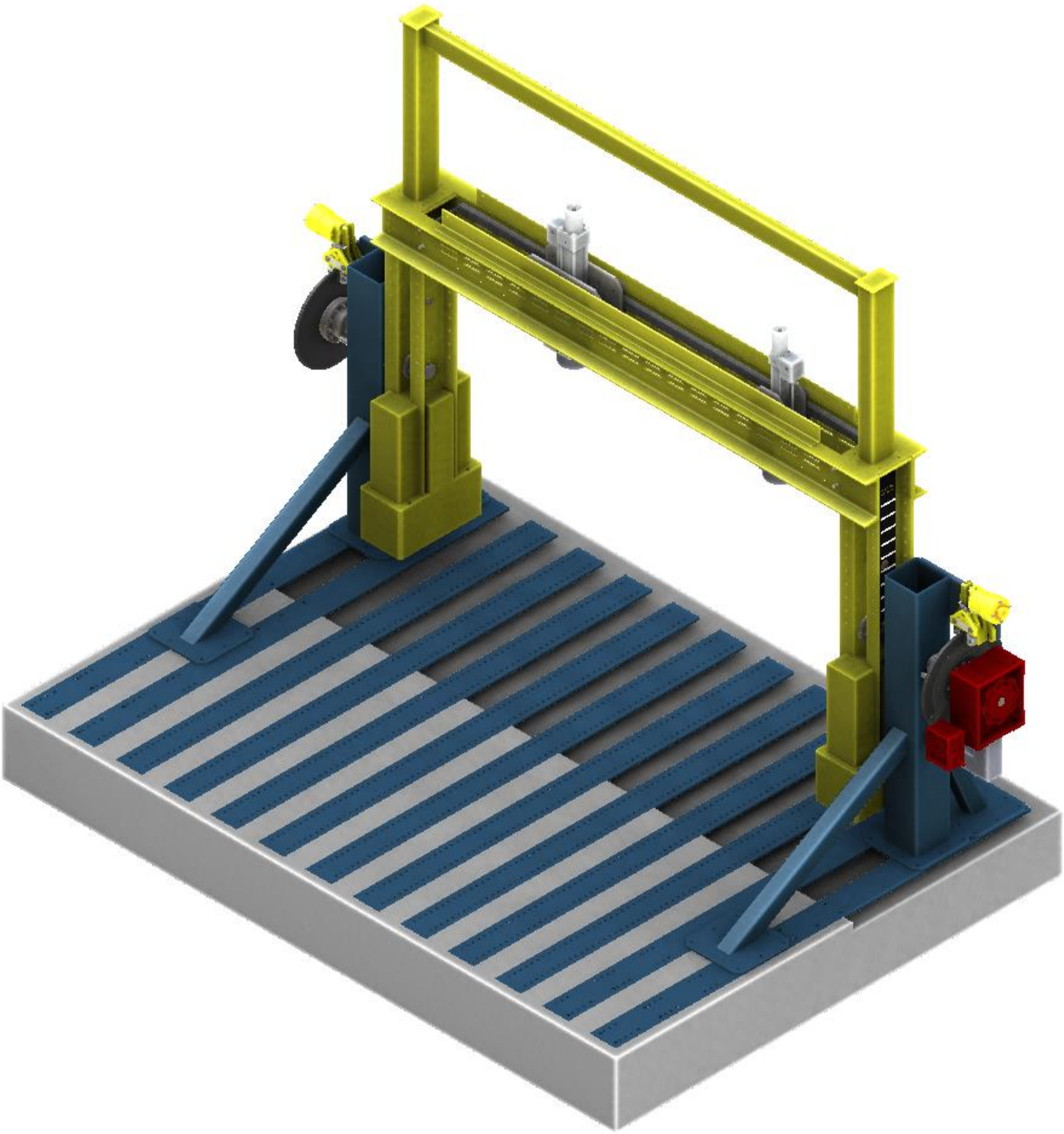

Figure 3-32 – Structure of the equipment

3.4.1 Base structure

This chapter describes the base of the equipment in detail and gives some explanations for the decisions made.

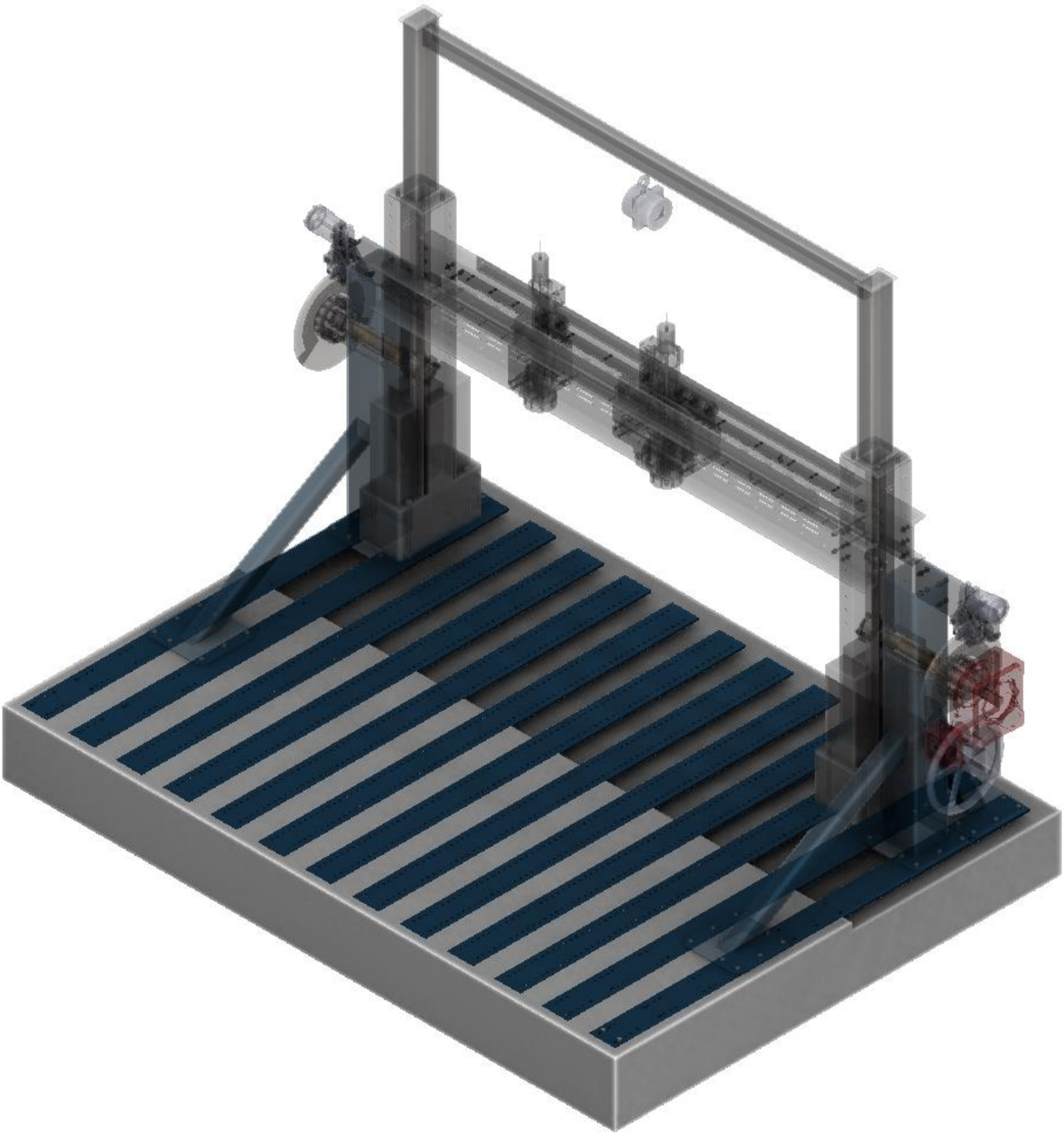

Figure 3-33 – Base of the equipment (rest of the structure in transparent)

The base of the structure is a crucial element because it serves as the main support for the whole structure and as a positioning matrix for the device to be tested. As such, special considerations had to be taken into account during its design and engineering.

The base is made up of two layers of profiles. The top layer has the function of supporting and fixing the product to test as well as gantry support while still giving flexural rigidity. The bottom has the function of increasing the stiffness of the base having some profiles arranged in specific directions to increase its resistance to torsion and bending. Figure 3-34 shows an isometric view of the base.

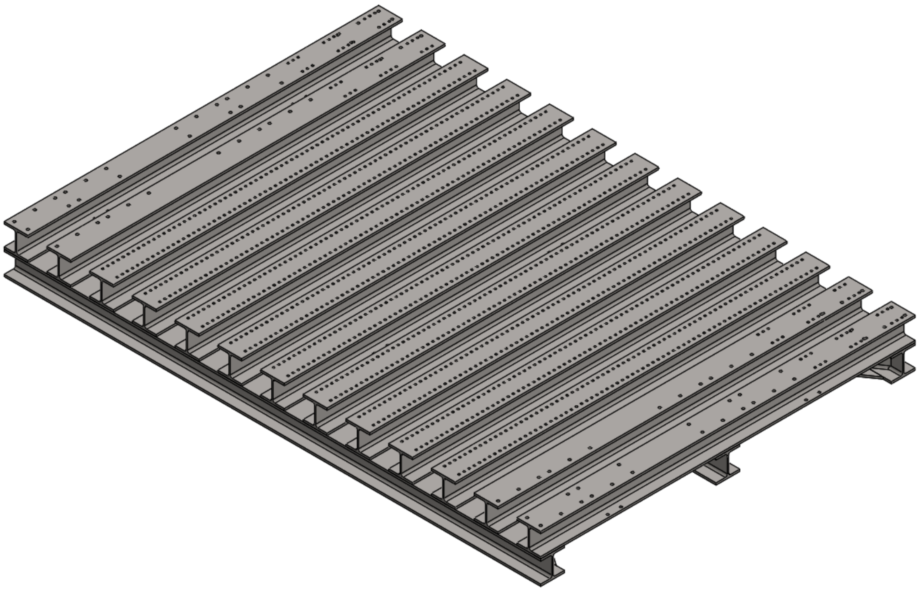

Figure 3-34 – Isometric view of the base

The flanges of the upper beams have holes for fixing the brackets of the product to test. To increase the resistance to the bending of the webs, these were welded to each other using gusset plates as shown in the figures below.

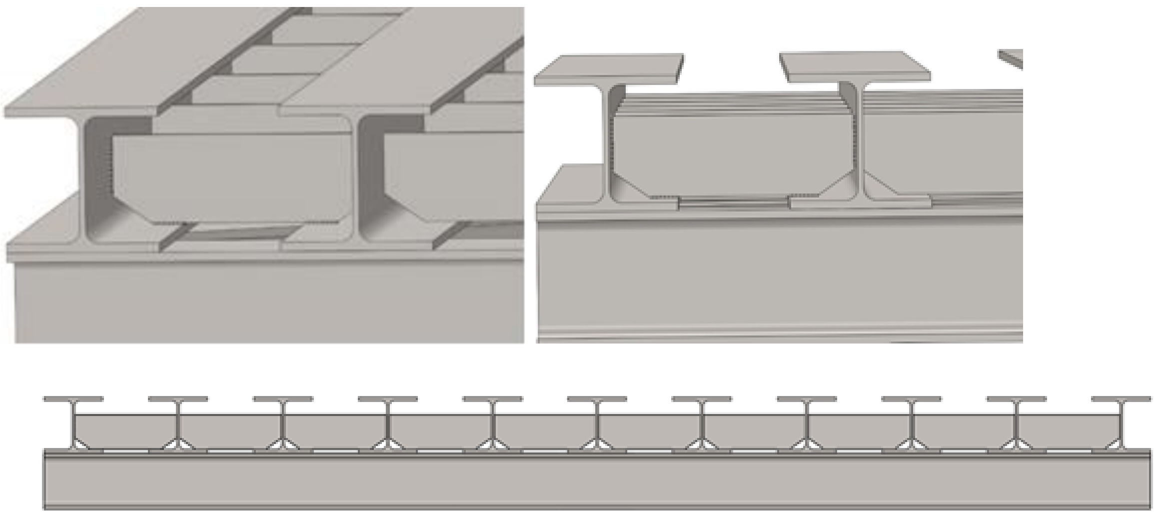

Figure 3-35 – Welded gusset plates connecting the webs

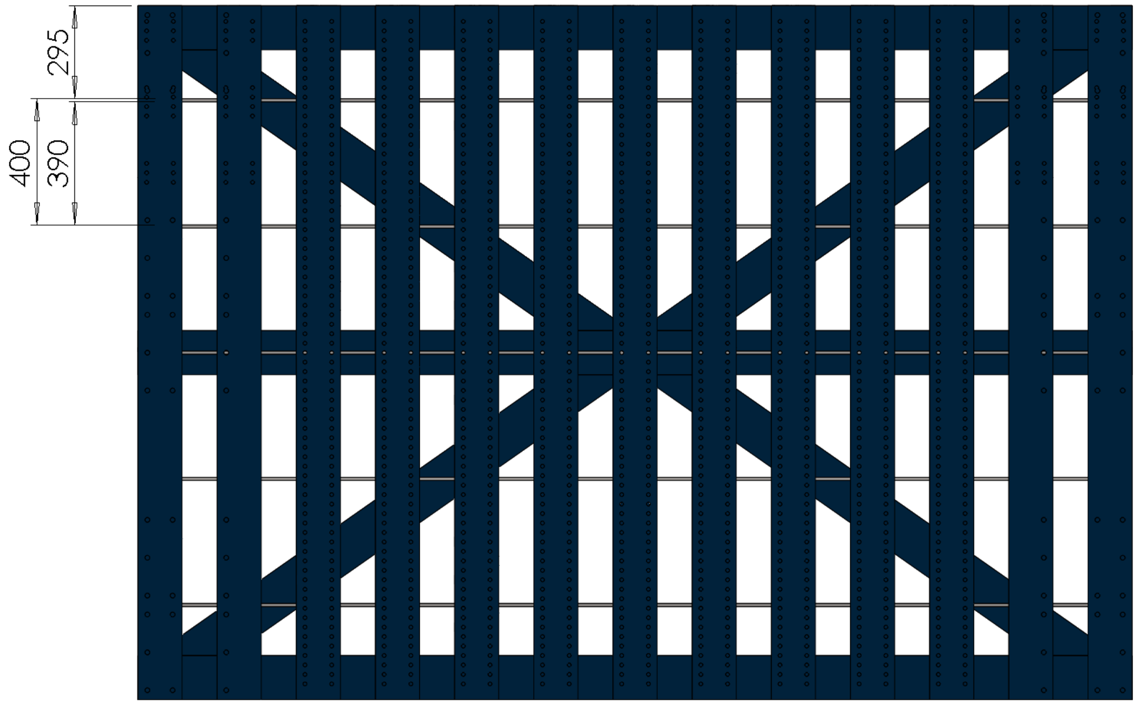

Figure 3-36 – Distance between gusset plates

The lower profiles are arranged in a cross formation to increase the torsion resistance of the set as shown in the figures below.

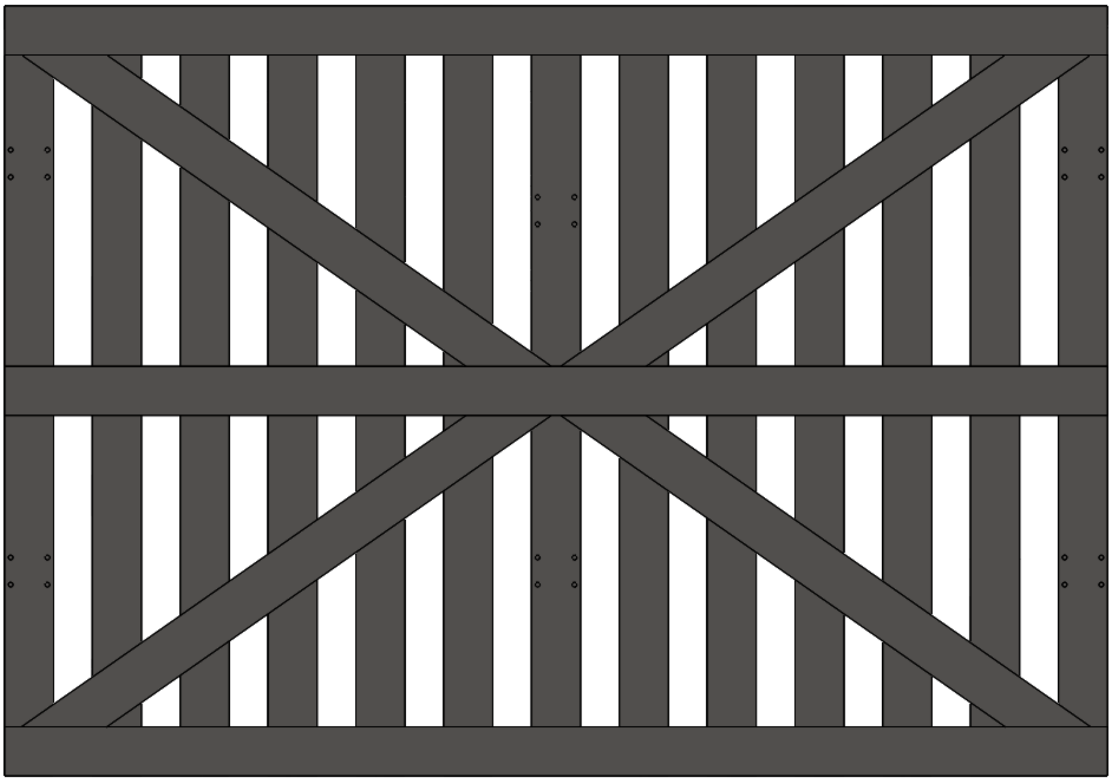

Figure 3-37 – Bottom view of the base

The two layers of profiles work in tandem to increase the rigidity of the whole system. For that they were arranged in different orientations, as mentioned before, and Table 3-4 shows the main structural function of each group.

Table 3-4 – Function of the profile groups

Beam	Main structural function
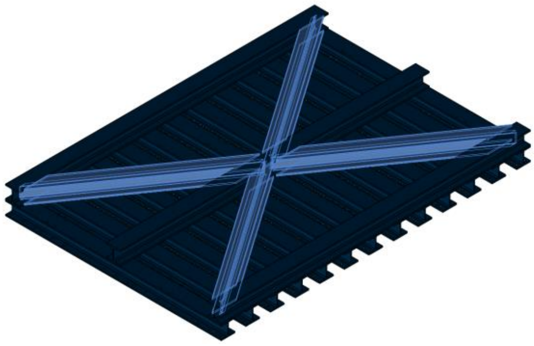	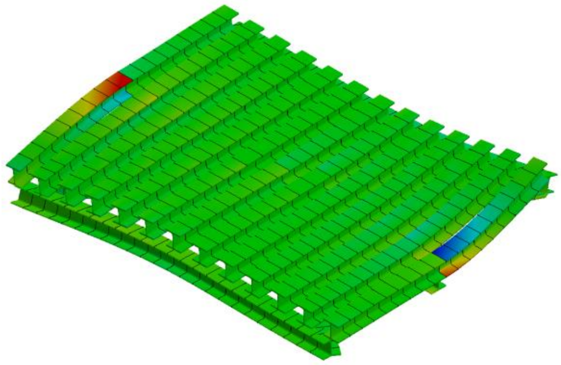
Cross beams	Torsion resistance
	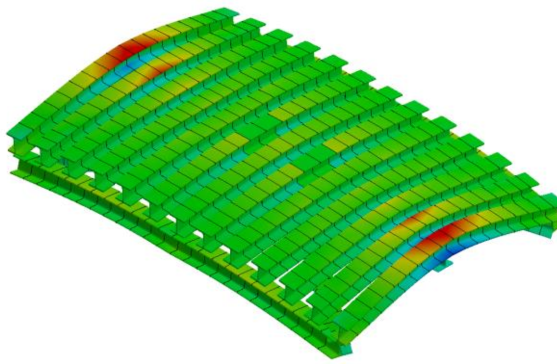
Top beams	Flexural resistance
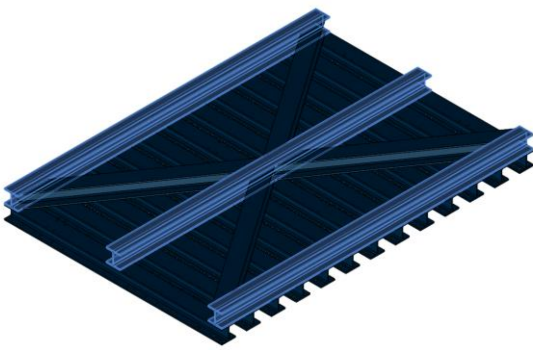	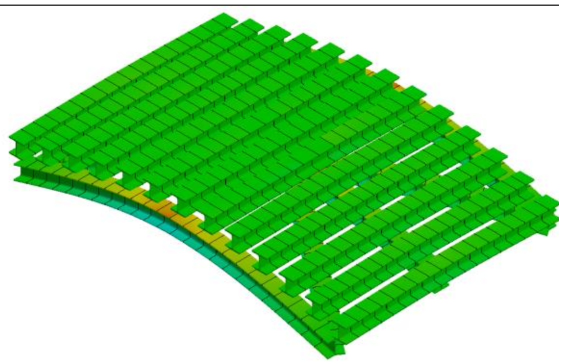
Bottom beams	Flexural resistance

Two methods of bonding of profiles were considered: with weldments or with fasteners. Using fasteners has the advantage of flexibility for assembly and disassembly, but since the need for disassembly of the base profiles does not apply, it was decided to follow with the welding process that was faster and easier to do by the supplier. However, the welding has some disadvantages such as the distortion of the metal due to the heating when welding, which is necessary to correct afterwards.

To make the structure cheaper and lightweight, HEA 140 profiles were used.

This profile was chosen because it is more compact than an IPE profile keeping the base height relatively low, but still having a good supporting area for the CCB supports fixation. The HEA profile has a larger flange which allows for a greater flexibility in the hole matrix for the fixing holes. The lower height of the web also helps increasing the first natural frequency in the Z direction, or longitudinal axis. The next table highlights the advantages of the HEA profile versus the IPE profile.

As we can see in the figure below, the profile IPE 140 has a shorter flange when compared to the HEA 140, to obtain a flange identical to the HEA 140 we would have to choose at least the IPE 270 that has a considerably greater height, which is something unwanted for equipment functionally, structurally and aesthetically. Figure 3-38 shows the dimensions of the three aforementioned profiles and Table 3-5 shows the detailed dimensions of the chosen HEA 140 profile.

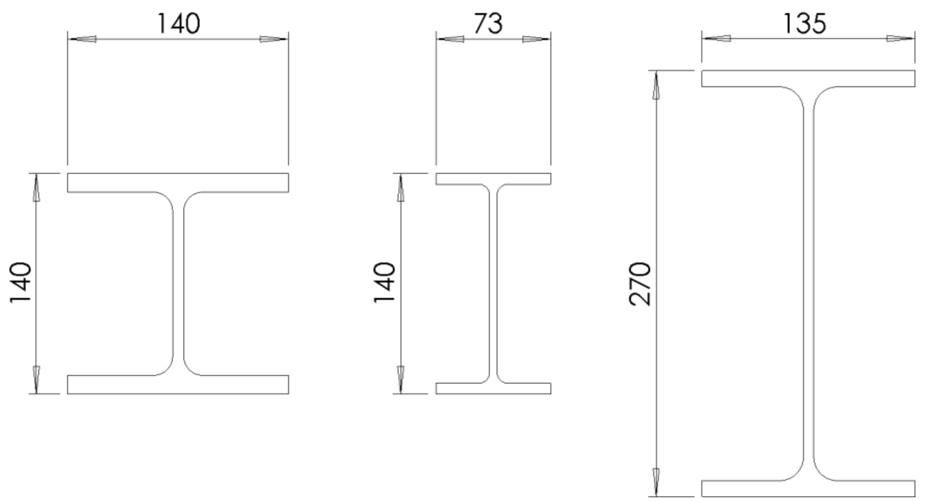

Figure 3-38 – Dimensions comparison between HEA140 and IPE140/IPE270 profiles

Table 3-5 – HEA 140 profile dimensions

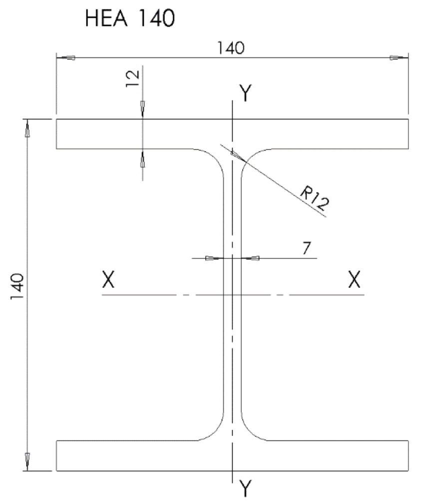	A=31,4 cm^2 P=24,7 kg/m Ix=1033 cm^4 Ix/Vx=155 cm^3 ix=5,73 cm Iy=389 cm^4 Iy/Vy=56 cm^3 iy=3,52 cm

Summing all the points mentioned before, the next table highlights the main benefits of using HEA 140 over the IPE options.

Table 3-6 – Advantages of the HEA profile versus the IPE profile

Advantages of the HEA 140 beam compared to equivalent IPE beams	
Lower base height	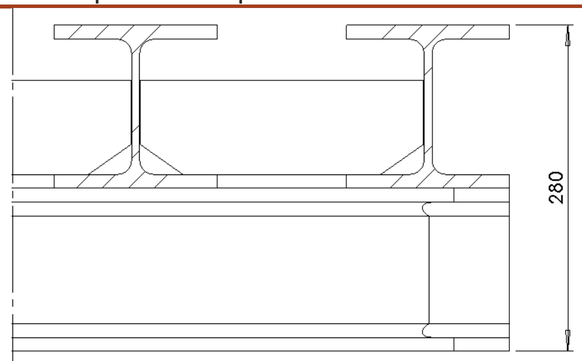
Higher support area	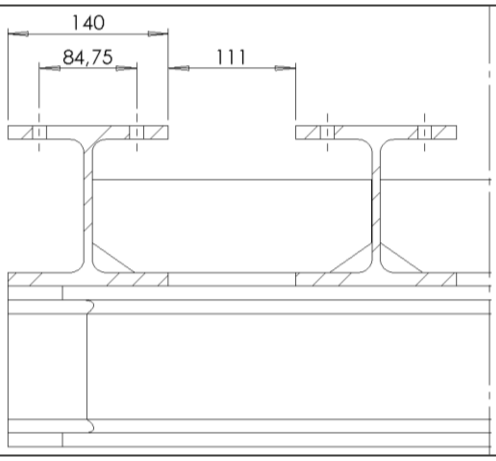
Higher natural frequency in this case (thicker web than the IPE140 and shorter web than the IPE270)	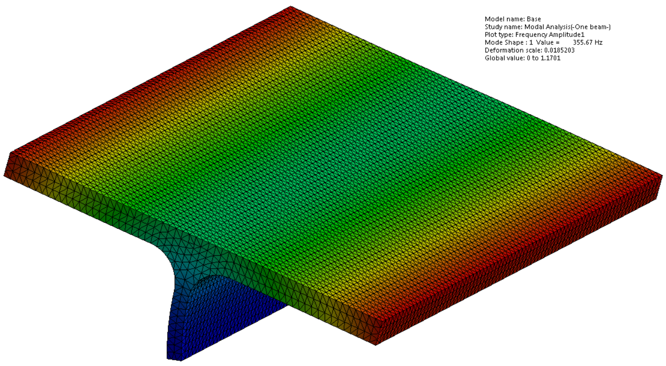

A hole matrix was added to the base to allow for flexibility to the positioning of the product to be tested in the equipment. These holes have access to both the upper and lower faces to allow the placement of nuts. Figure 3-39 shows the base hole matrix and Figure 3-40 shows the holes spacing.

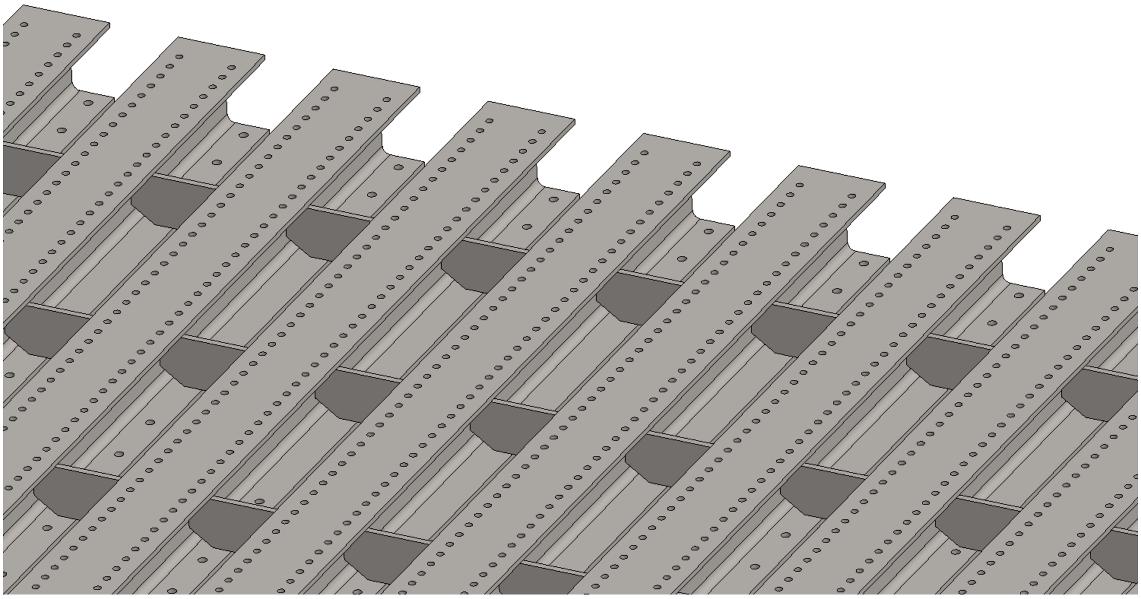

Figure 3-39 – Base hole matrix

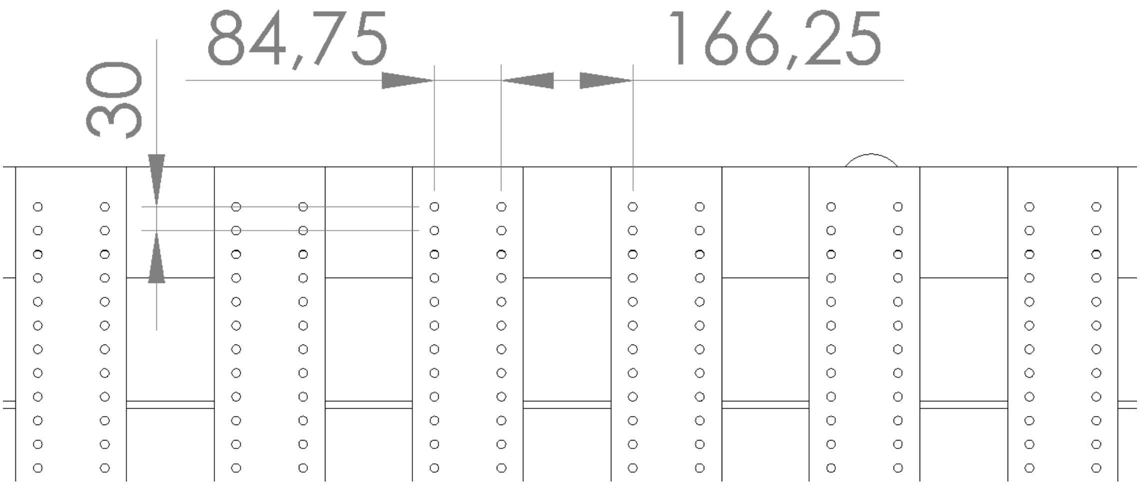

Figure 3-40 – Base hole matrix spacing

The holes have a diameter of 12mm to use M10 screws but with some clearance to increase the positioning flexibility. This matrix thus transforms the HEA profile set into a robust and flexible working base for the use of the equipment.

3.4.2 Pillars

This chapter describe the pillars in detail and gives some explanations for the decisions made.

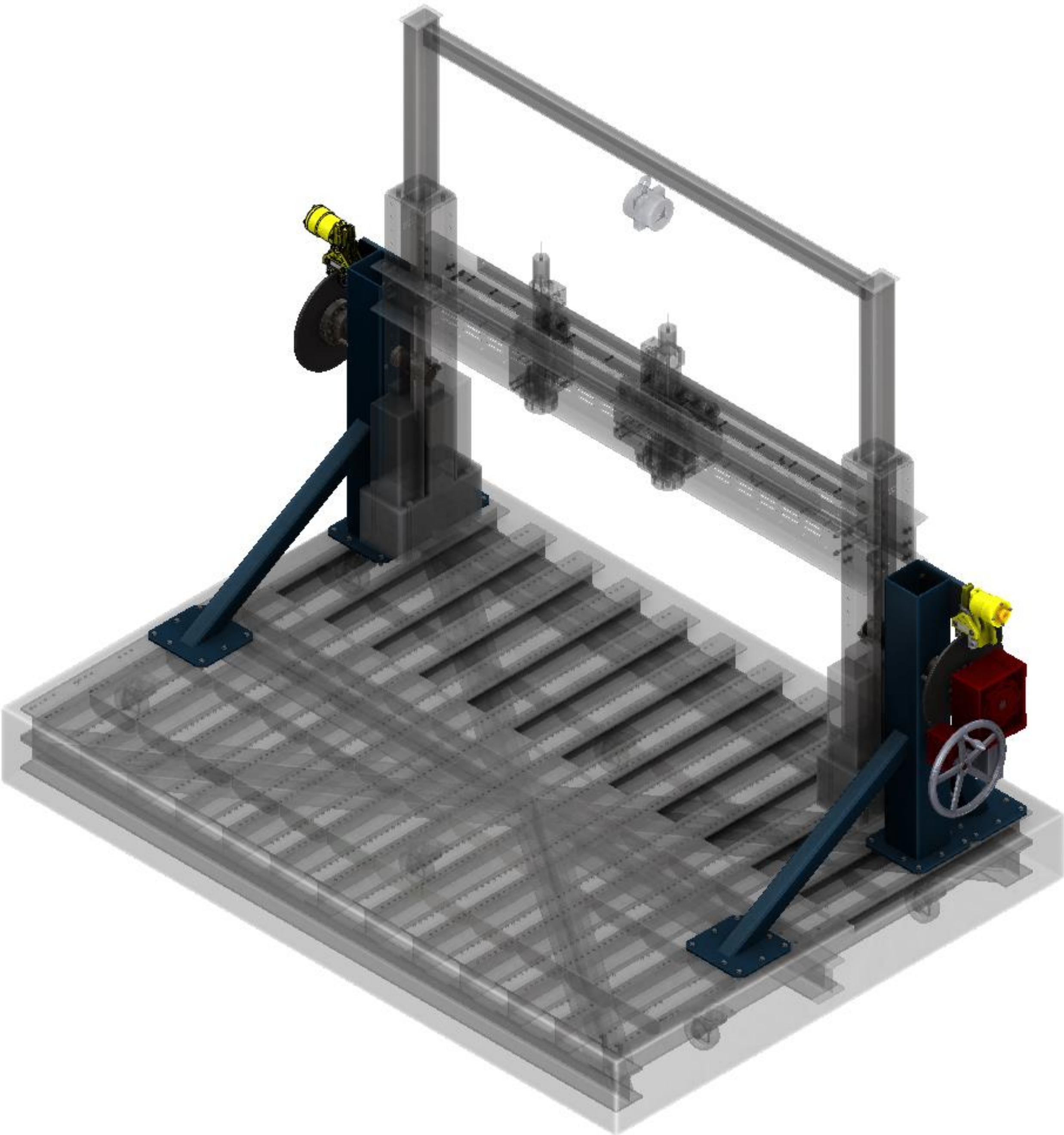

Figure 3-41 – Pillars of the equipment (rest of the structure in transparent)

The gantry, the main feature of this system, is supported by two square tube pillars which are bolted to the base structure as well as welded to two other square tubes each, to increase their flexural rigidity. Figure 3-42 shows both the left and right pillars and Figure 3-43 shows the main components of the pillars.

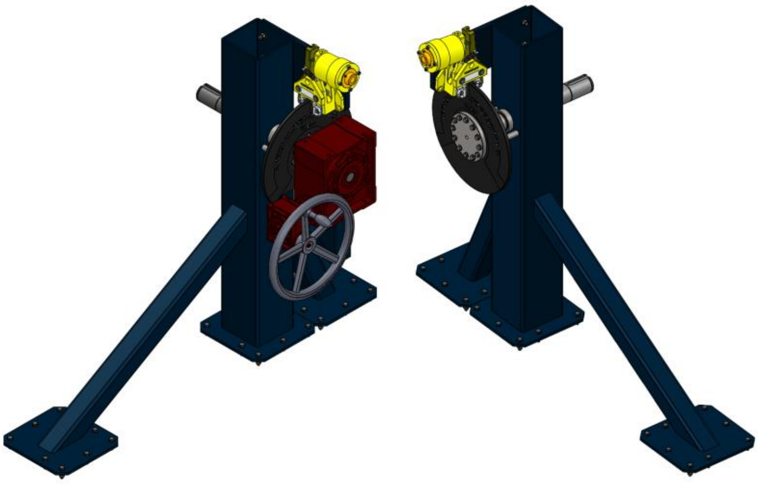

Figure 3-42 – Isometric views of the pillars

The pillars support the gantry and the rotational system along with the braking system.

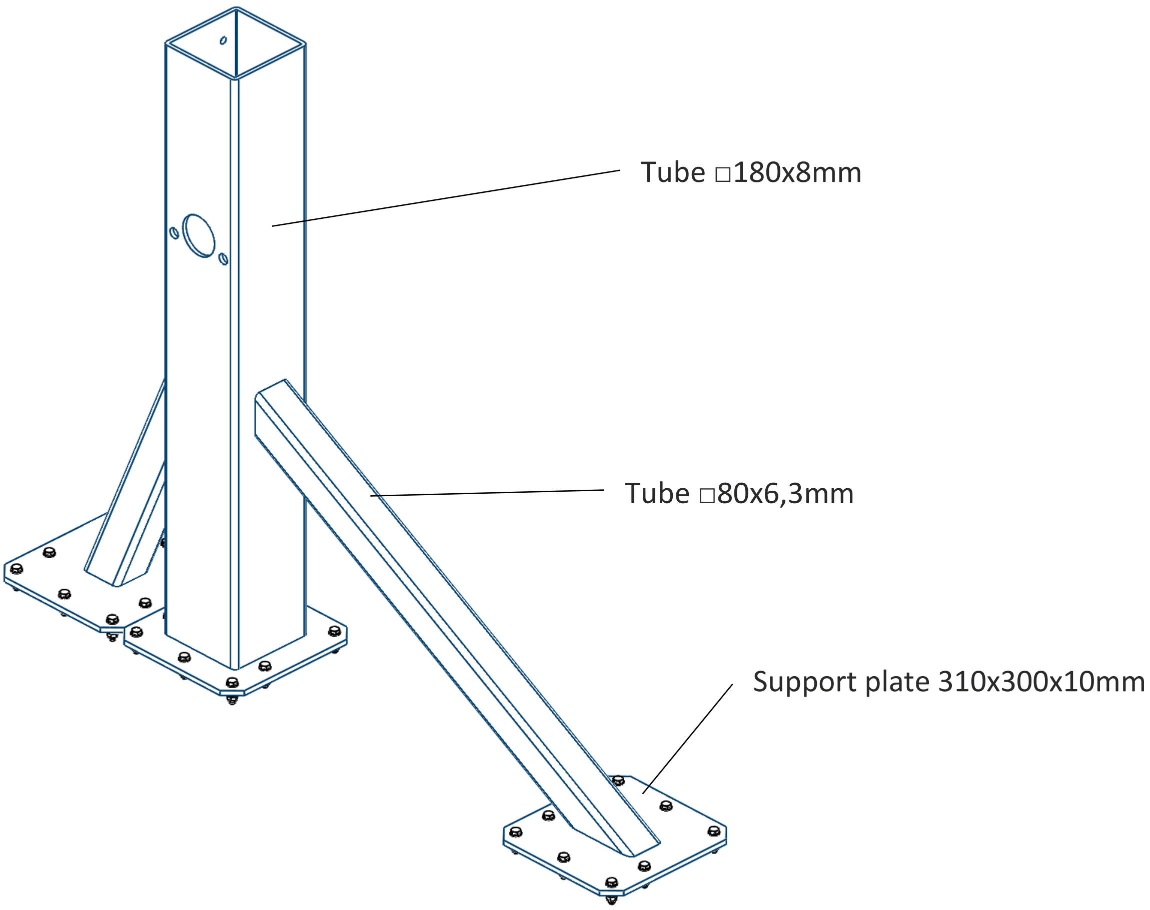

Figure 3-43 – Base structure with the pillars

There are two shafts, one in each pillar, which support the gantry and allow its rotation.

The shafts are inserted into a mechanical tube with self-lubricated bronze sleeves, which in turn is inserted into the pillars. These sleeves will allow the rotation, with minimum friction, of the shaft, while providing a long service life due to a low contact wear. The mechanical tube is welded to the pillar. Figure 3-44 and Figure 3-45 show the shaft inserted in the pillar. To the left of the pillar, in the figures, is the outer side of the equipment, where, in one side, the shaft is mounted to a gearbox, shown in Figure 3-48.

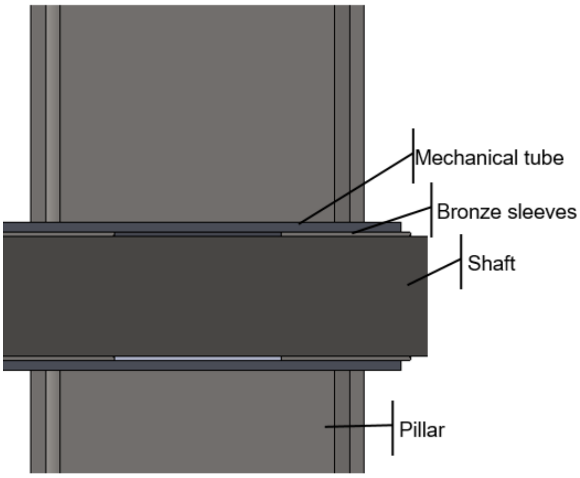

Figure 3-44 – Pillar with shaft

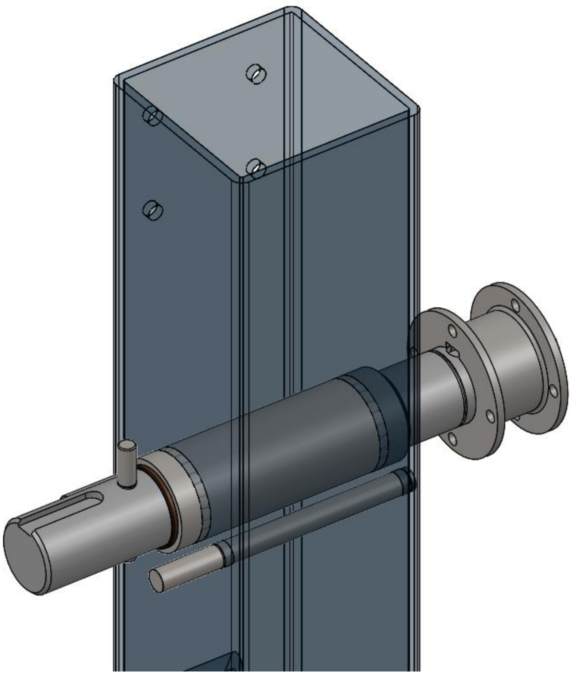

Figure 3-45 – Isometric view of the shaft inserted in the pillar

The next figure shows a cutaway of the shaft and pillar.

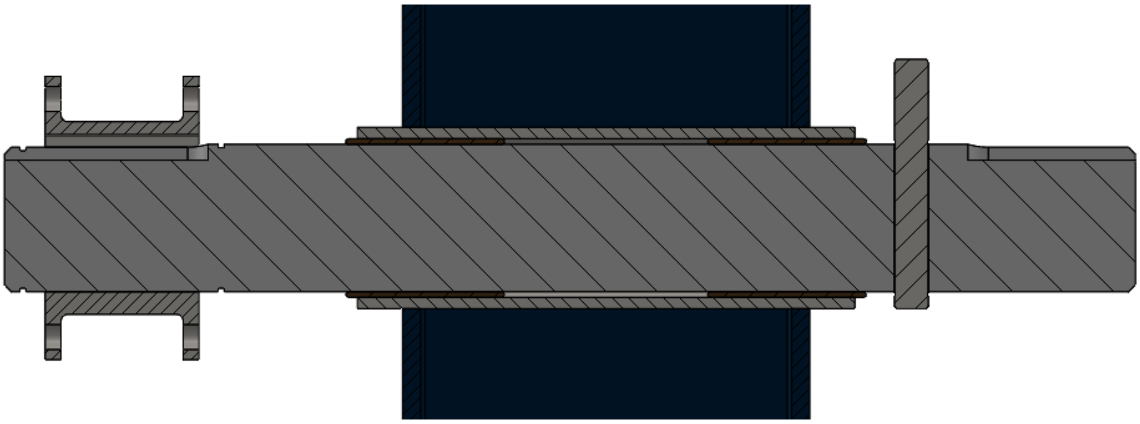

Figure 3-46 – Cutaway of the shaft and pillar

These pillars have a hole for the shaft and two stoppers each to prevent the gantry to rotate more than 90°, as shown in Figure 3-47. They have holed base plates which are bolted to the base and also support the braking system.

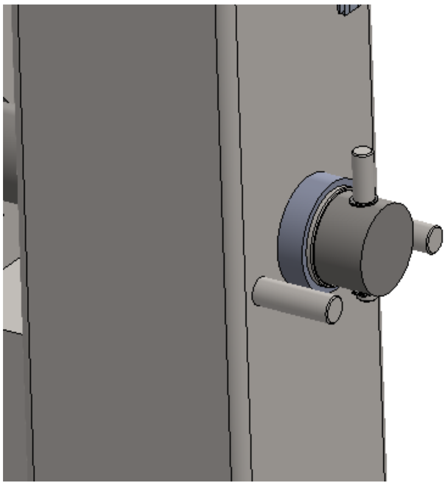

Figure 3-47 – Gantry stopping pins

One of the shafts will be mounted on a gearbox that controls the gantry's rotation as it can be seen in Figure 3-48. Rotating the gearbox wheel will rotate the gantry, to fix the gantry in its desired position, the disc brakes are used. The maximum load that needs to be applied on the hand wheel is of 3 kg, and a 90º rotation of the gantry translates into 75 rotations of the wheel.

To control the gantry angular position, disc brakes are used (Figure 3-48 and Figure 3-49). These are normally closed and to operate the gantry requires pushing a button which applies pressure on the disc calliper which releases the brake and allows the gantry to rotate. The pressure is supplied by the equipment's hydraulic unit. Two disc brakes are used, one in each side. This solution allows for the gantry to be positioned easily and with great flexibility in the angles which the gantry can be positioned.

The rotation angle of the gantry is adjusted and checked visually, by inspecting the angular scale on the disc brakes as shown in Figure 3-50.

Both the gearbox and braking system are off the shelf components.

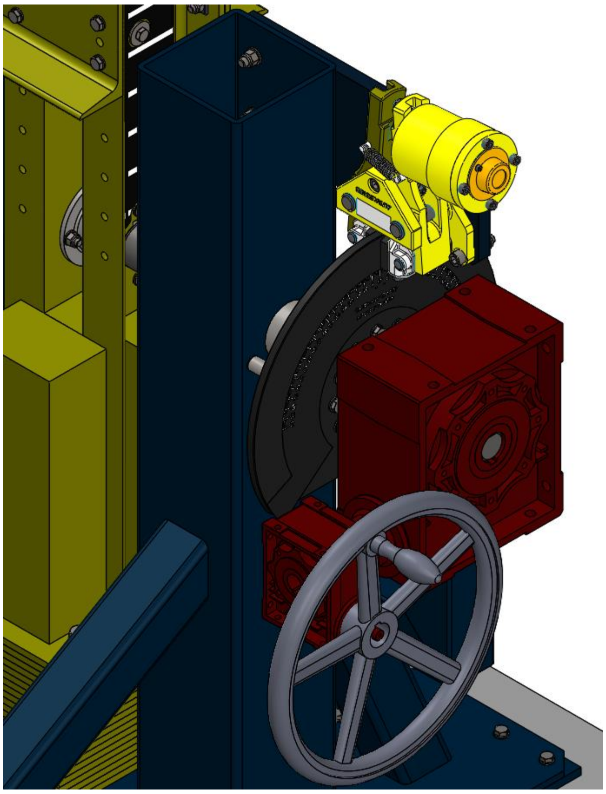

Figure 3-48 – Gantry gearbox system and disc brake

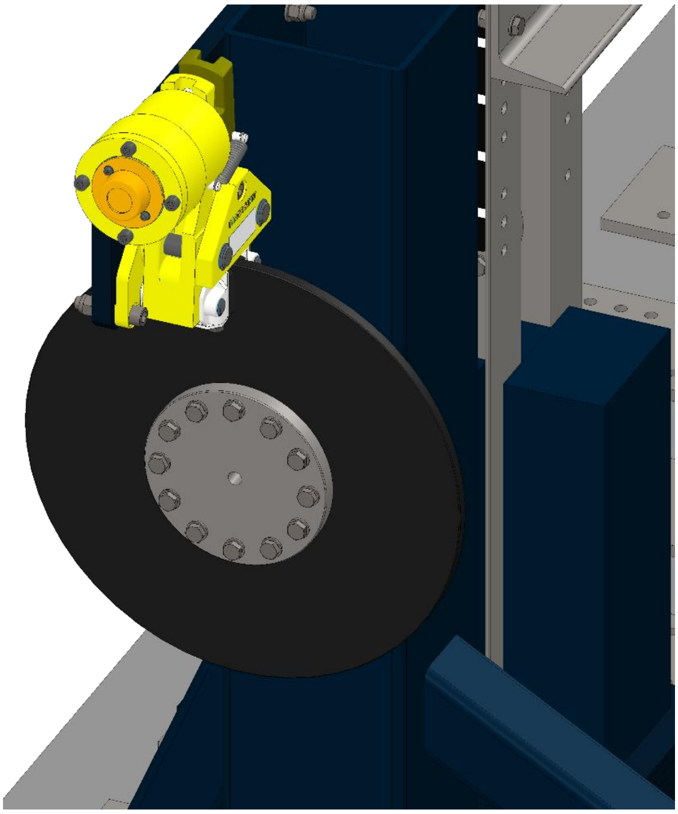

Figure 3-49 – Disc brake

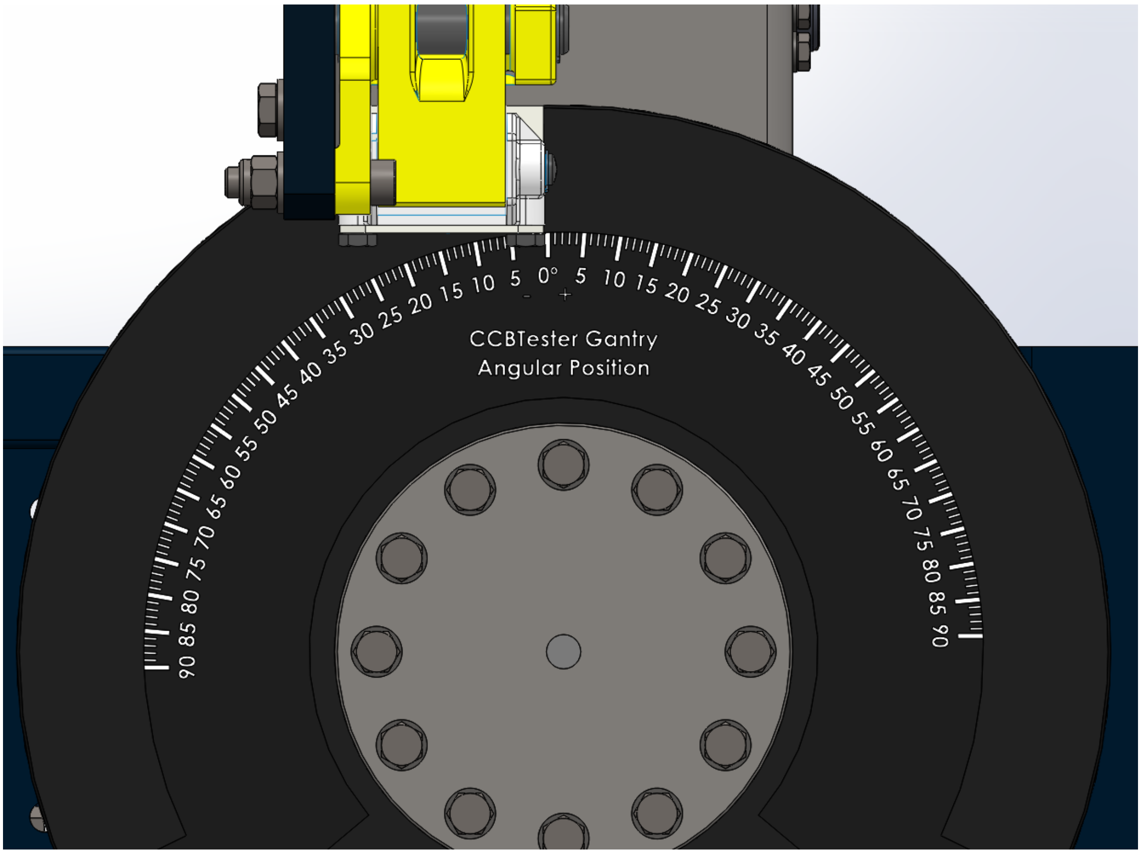

Figure 3-50 – Disc brake angular scale

3.4.3 Gantry structure

This chapter describes the gantry structure as well as all of its components.

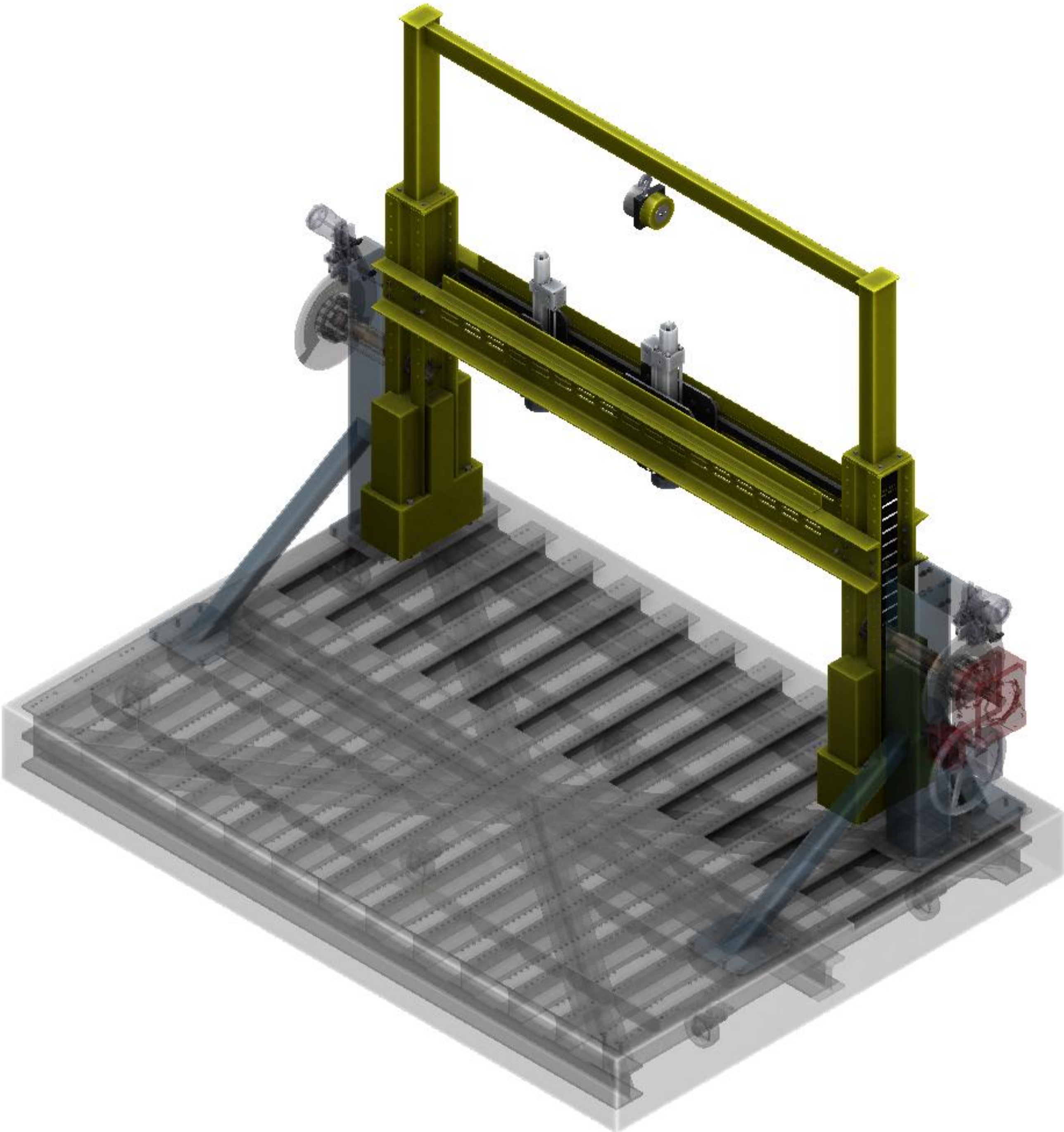

Figure 3-51 – Pillars of the equipment (rest of the structure in transparent)

The gantry is made of UPN profiles. The picture below shows the assembled gantry. The top structure is the hoist support. This part is meant to be able to be assembled and disassembled for transport. The full bridge can be seen in Figure 3-52.

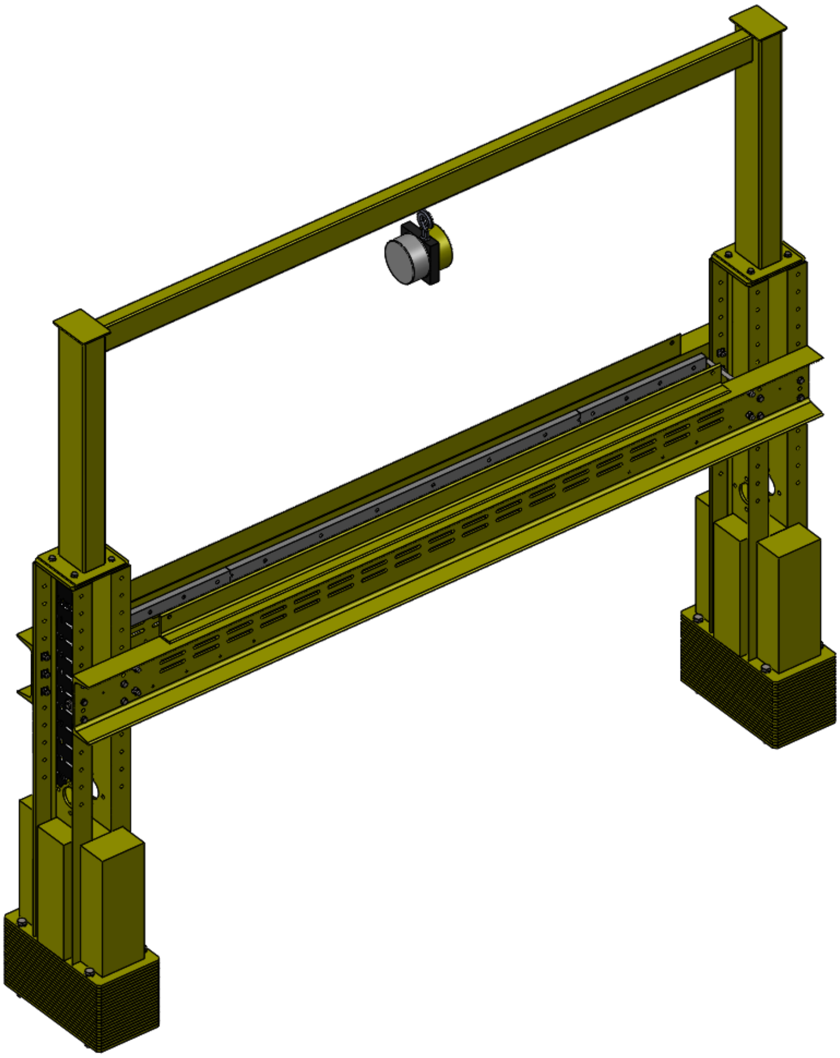

Figure 3-52 – Isometric view of the gantry

The gantry will be able to rotate along the shaft's axle, allowing a flexible positioning for the actuation system, as described in chapter 3.4.2.

The horizontal beams, called the bridge, work as a support for the actuation system. The centre of the bridge has slotted holes to position the actuator support and has holes on its extremes to fix it to the vertical beams. L angle beams are fixed to the top of the UPN profiles to increase its rigidity, lowering the total displacement when a load is applied. Figure 3-53 shows the bridge's horizontal beams.

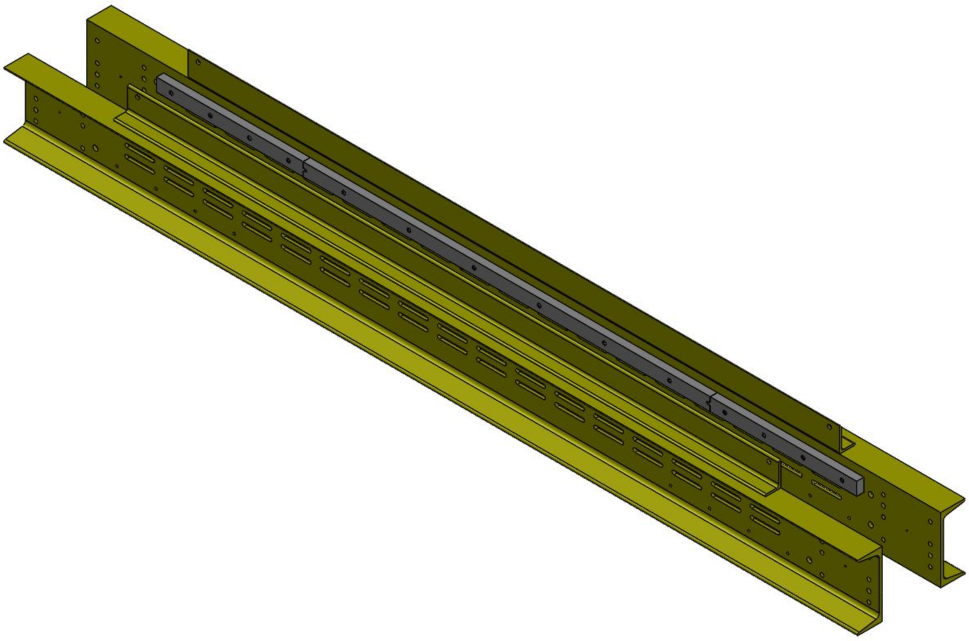

Figure 3-53 – Bridge horizontal beams

The bridge also has a rail to move the actuator along it, which also prevents the actuator from falling or dislodging itself from the bridge when not fixed (shown in brown and purple in Figure 3-54.

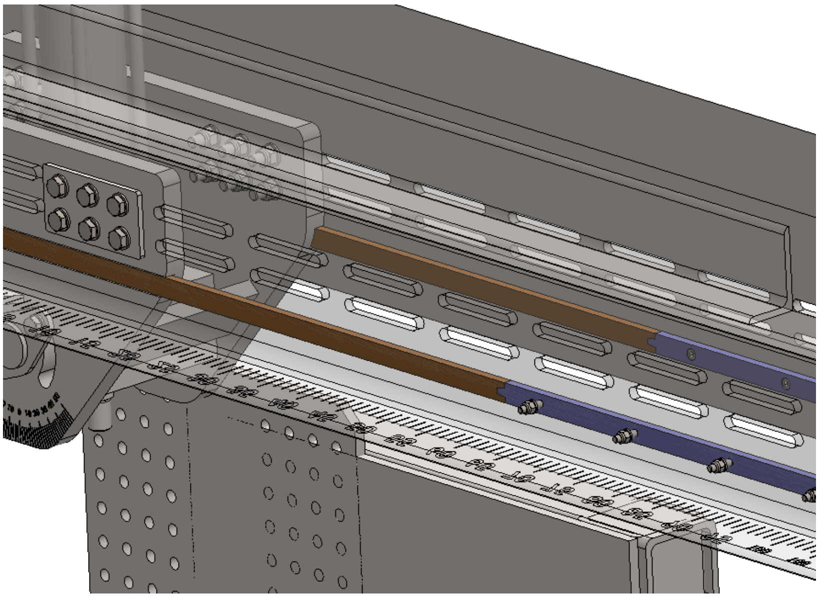

Figure 3-54 – Bridge rail to support the actuators

The bridge also has a scale with markings with a 1mm resolution ruler to position the actuator.

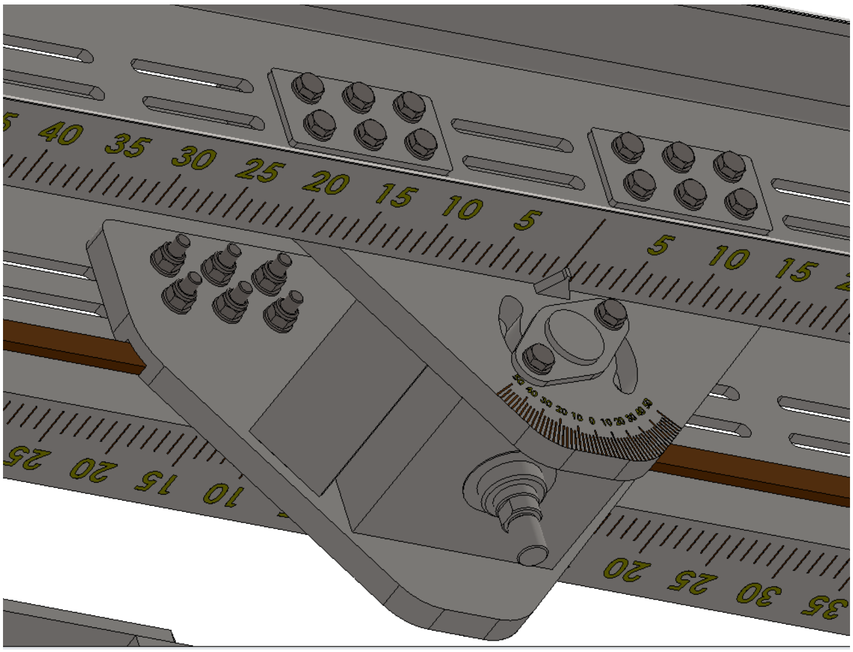

Figure 3-55 – Markings below the bridge to position the actuator

The columns are used to support the bridge. Each column is composed of two UPN180 beams, held together by small shafts (see Figure 3-58), and on the rotation axis with a shaft trough a flanged tube which helps transmit the torque from the gearbox to the gantry. They feature a hole matrix composed of bolt holes. Figure 3-56 and Figure 3-57 show details of the connection.

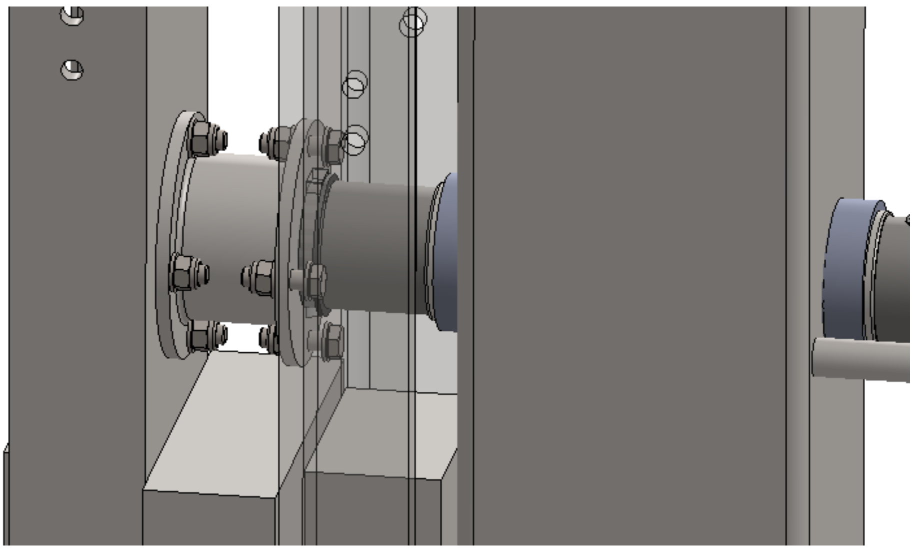

Figure 3-56 – Columns to pillars connection

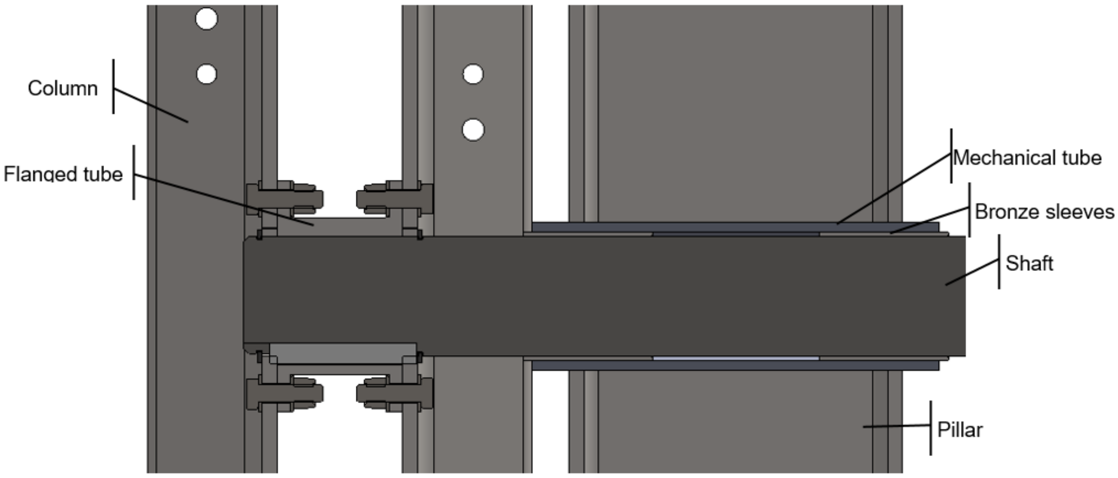

Figure 3-57 – Cutaway view of the columns-pillars connection

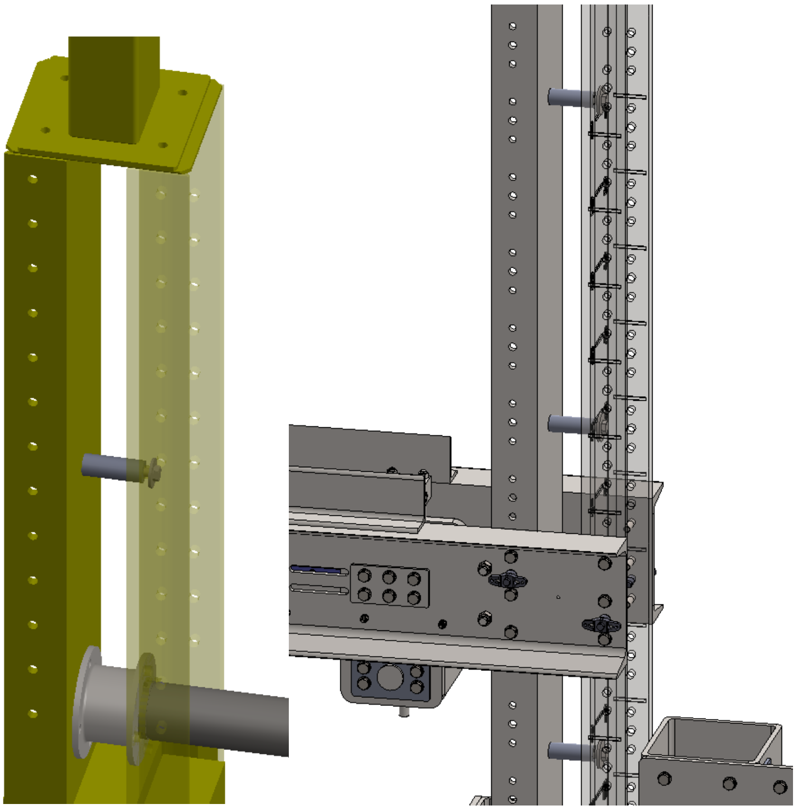

Figure 3-58 – Shafts connecting the two UPN profiles of the column

The columns have markings to indicate the possible positions of the bridge as shown in Figure 3-61. These markings allow for 11 predefined positions which have a resolution of 60mm. The columns are also holed on the flanges. These holes are used to fix the horizontal beams as shown in Figure 3-59.

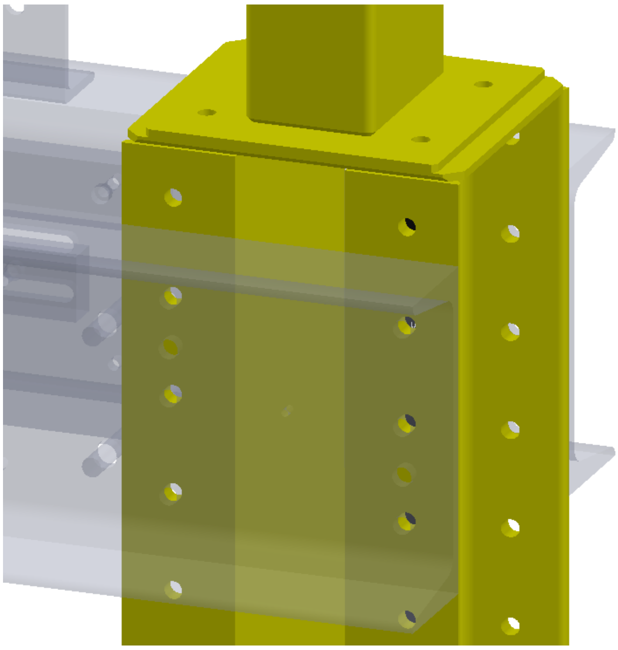

Figure 3-59 – Holes in the flanges of the columns

To fix the bridge to the columns, bolts and precision pins are used, as shown in Figure 3-60. The columns have defined positions for the bridge, due to the loads that it needs to support as shown in Figure 3-61.

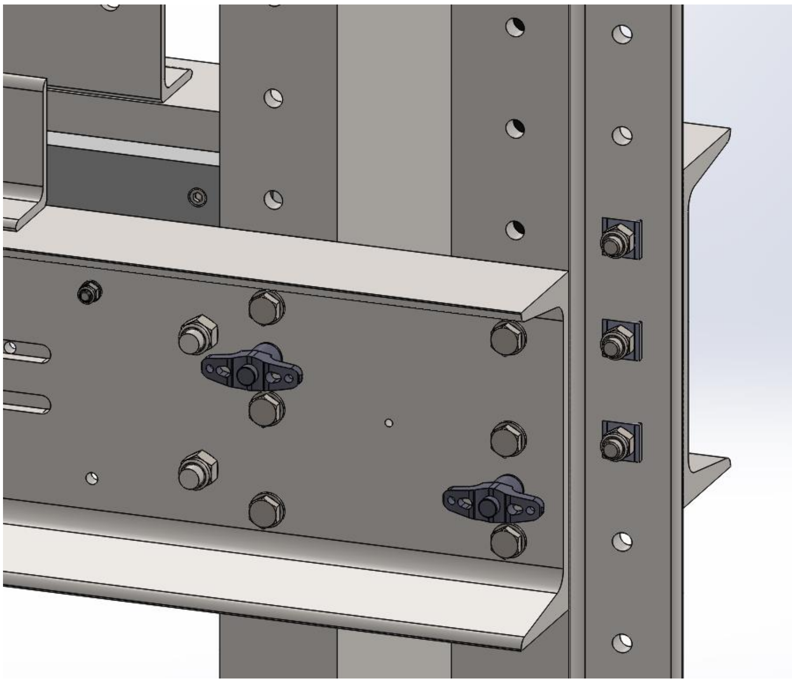

Figure 3-60 – Bridge to columns fixation with bolts and pins

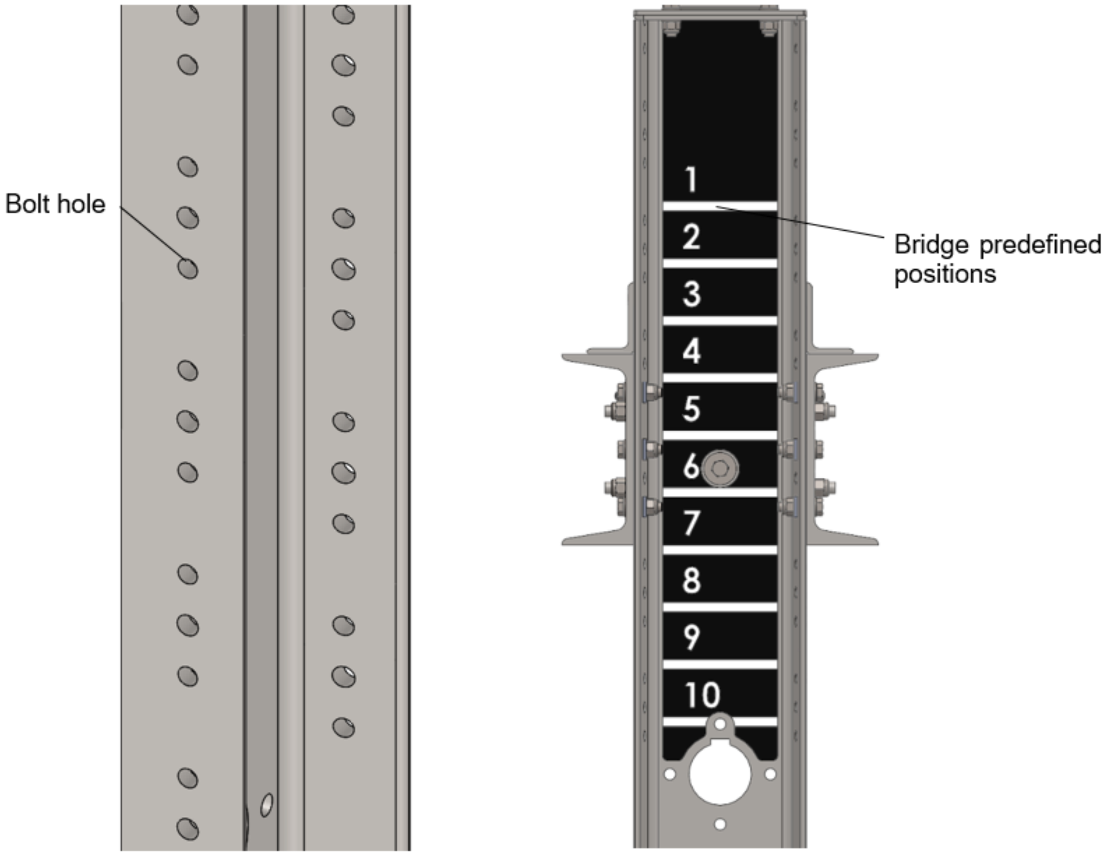

Figure 3-61 – Holes to position the bridge along the columns and markings on the columns to help position the bridge

On the lower part of each column there are a group of permanent counter-weights and removable counter-weight plates to balance the gantry as needed. Figure 3-62 shows the removable counter weight plates and Figure 3-63 shows both the permanent and removable counter weight plates.

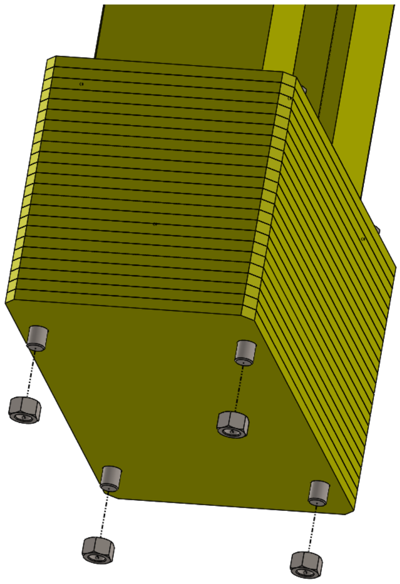

Figure 3-62 – Variable counter weight plates

The position of the bridge is the determining factor for the number of counter-weights to be used to keep the gantry as balanced as possible.

The removal of the counter-weights is done by removing the nut holding the plate in place on the bottom side of the plate group and removing the plate. The following table shows the number of plates that should be used for a given bridge position, to balance the gantry when it is rotated to the horizontal position. This was achieved by doing a simple force balance with the masses of each assembly.

Table 3-7 – Number of counter weight plates needed to balance the gantry for each bridge position

Bridge position	Number of plates
1	23
2	23
3	22
4	21
5	19
6	17
7	16
8	14
9	12
10	11

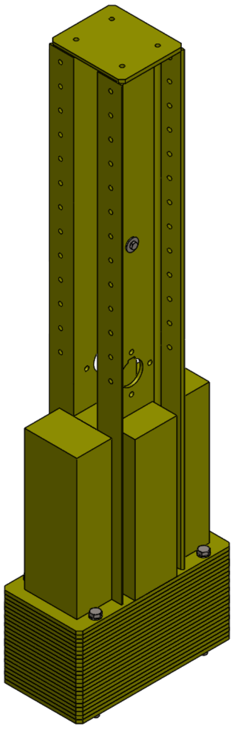

Figure 3-63 – Counter weights for the gantry

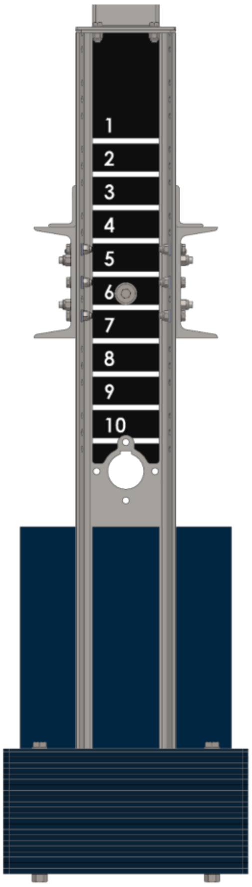

Figure 3-64 – Assembled column with counterweights

3.4.4 Vibration isolation system

To provide accurate results for the vibration tests, the whole structure must be isolated from its surroundings as well as internally between components. The reasons for this necessity are described in chapter 3.11.

To achieve that, the base must be embedded in concrete and the whole structure supported on a spring bed installed in a hole in the room where the equipment will be installed. The concrete helps isolating the vibrations of the different structure parts and components from the base, which could affect the readings and results of the CCB. Figure 3-65 shows the base embedded in concrete.

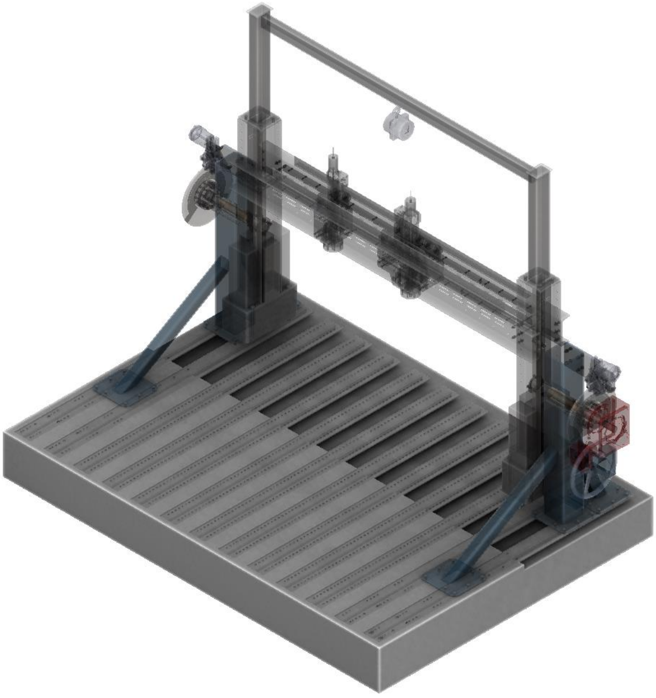

Figure 3-65 – Structure embedded in concrete

To isolate the CCB supports from the rest of the structure, the base is embedded with two height levels. The figure below shows those two levels. Figure 3-66 shows the two levels of concrete in the base.

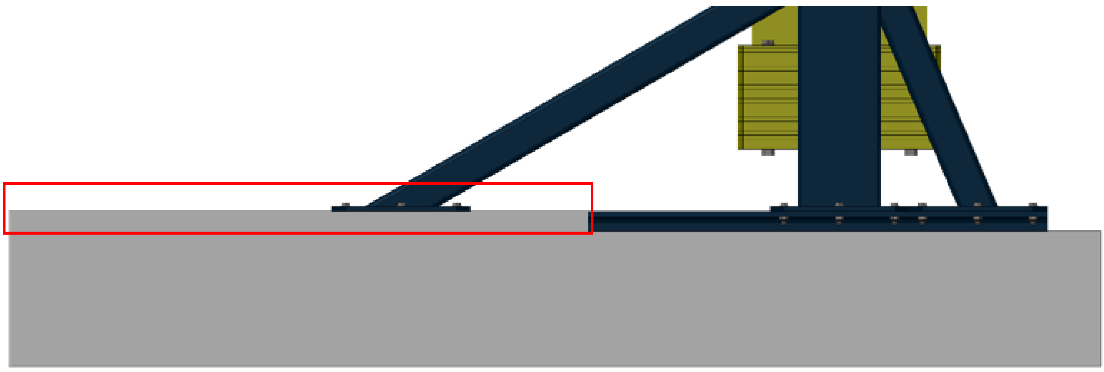

Figure 3-66 – Concrete height levels on the base

The concrete up to the base beam top level makes the whole base very stiff, which in turn isolates the CCB supports from the rest of the structure as the vibrations from the gantry and other elements are dissipated in the concrete. The rest of the base has the concrete up to a level where it is still possible to fasten the nuts to the base beams. The two levels of concrete were used to make the solution more economical, because by having the concrete up to the top of the flange of the beams, it is needed to add threaded bushings in all the holes of the base. By reducing the need by about half (about half of the base is covered up to the flange of the beams) it also reduces the amount of accessories to purchase and mount in the equipment, thus lowering the overall price of the application.

For external vibrations isolation, the whole structure needed to be “separated” from the surrounding ground. For that, a company that works in vibration isolation was contracted and they developed a solution for that, which is shown below.

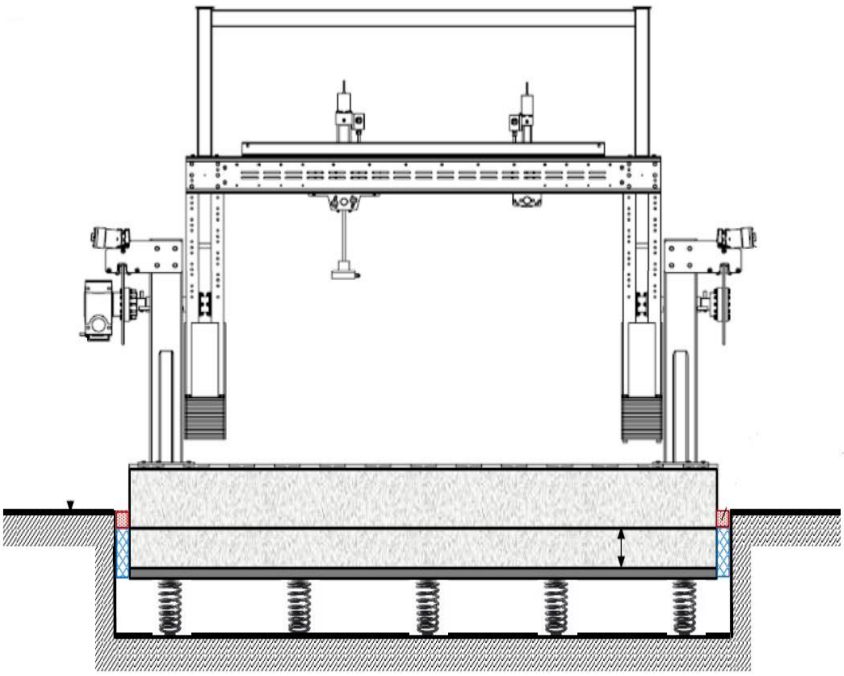

Figure 3-67 – External vibration isolation system

The system is made up of springs that support the structure, on the bottom, and flexible materials on the side walls that also, disconnect the structure from the surrounding ground.

To install the equipment properly, the installation area must be prepared. The preparation includes having a hole with the approximate dimensions shown below.

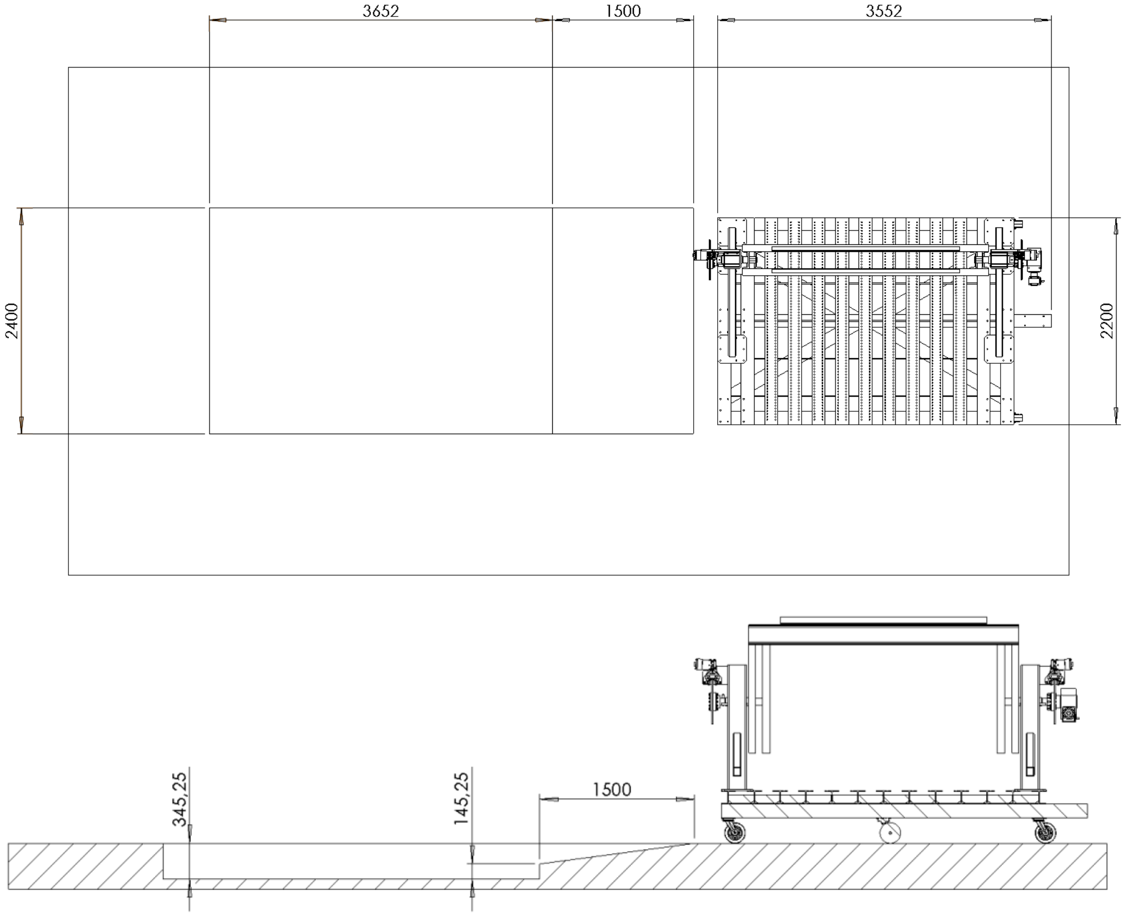

Figure 3-68 – Dimensions needed to install the equipment with the vibration isolation system

The whole solution of vibration isolation is a two-step progress and cannot be done independently. A brief description of the process is described in Table 3-8, prepared by the contracted company.

Table 3-8 – Vibration isolation system installation (Source: CDM)

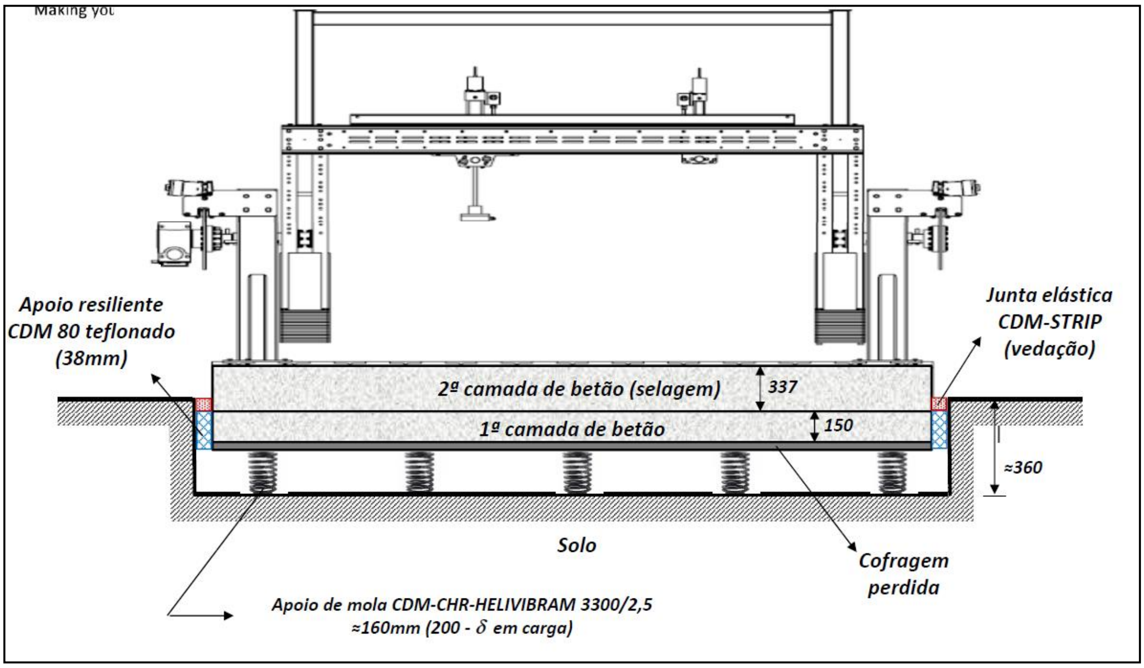

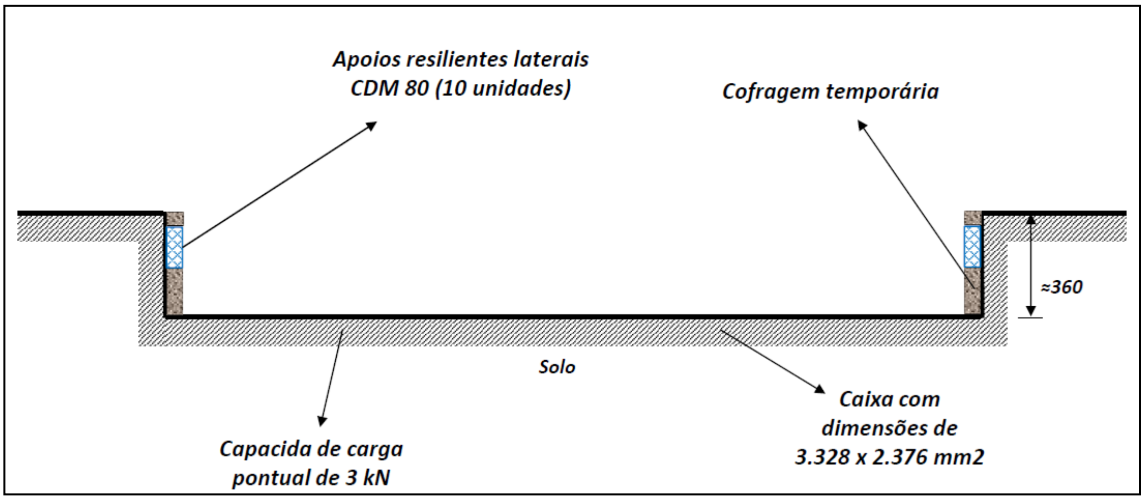

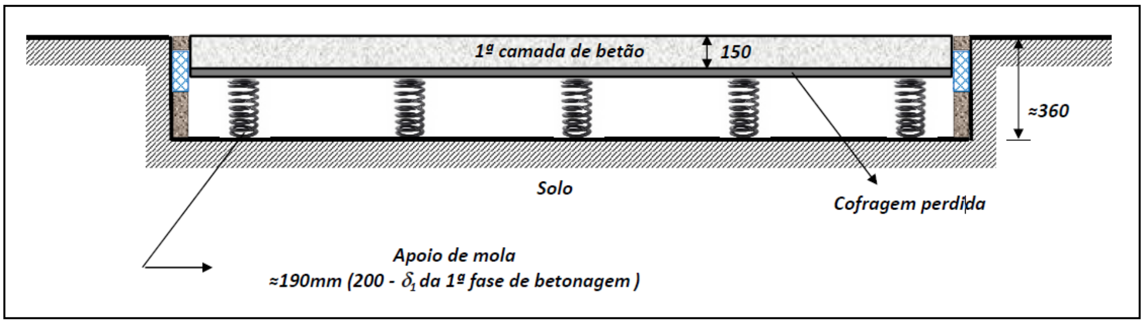

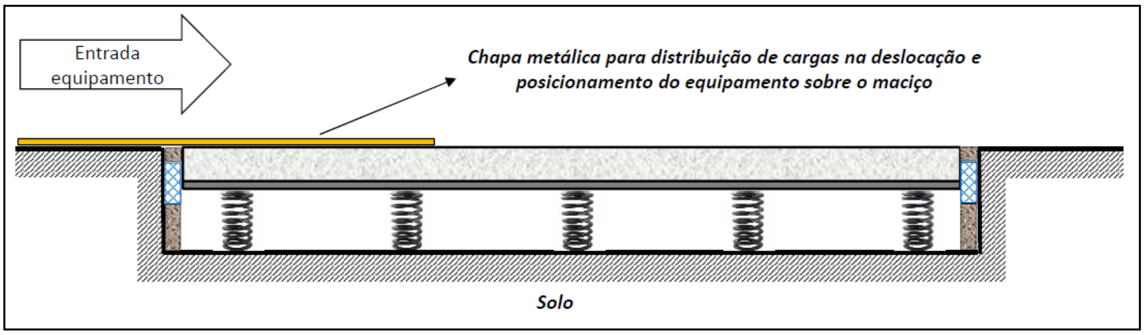
Entrada equipamento
Chapa metálica para distribuição de cargas na deslocação e posicionamento do equipamento sobre o maciço
Solo

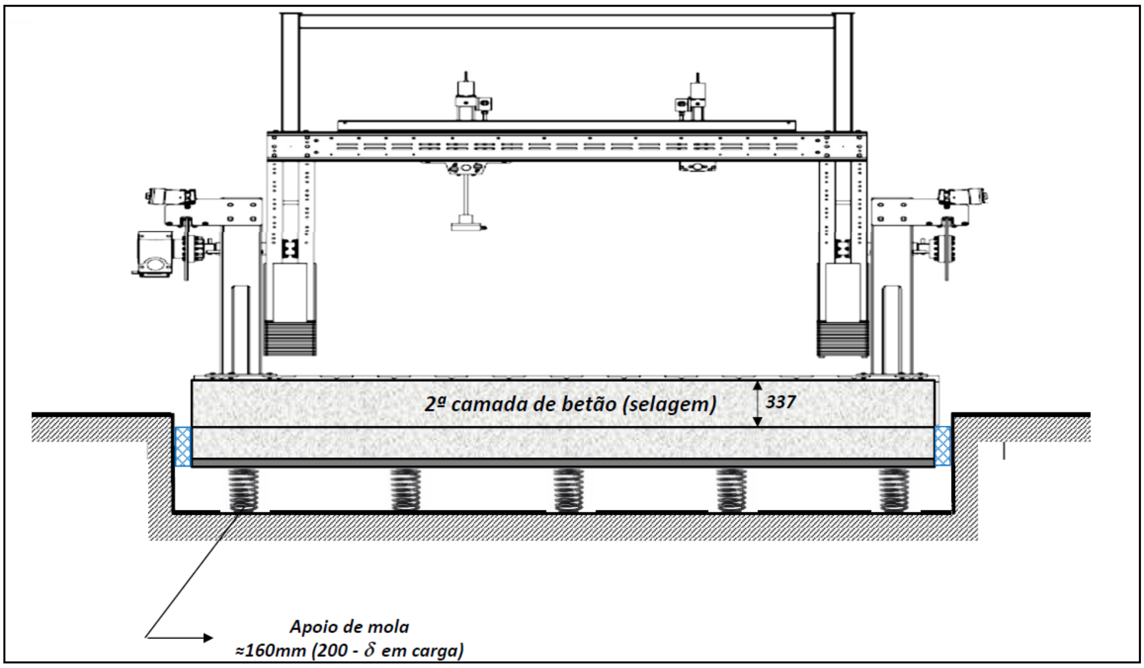
2ª camada de betão (selagem)
337
Apoio de mola
≈160mm (200 - δ em carga)

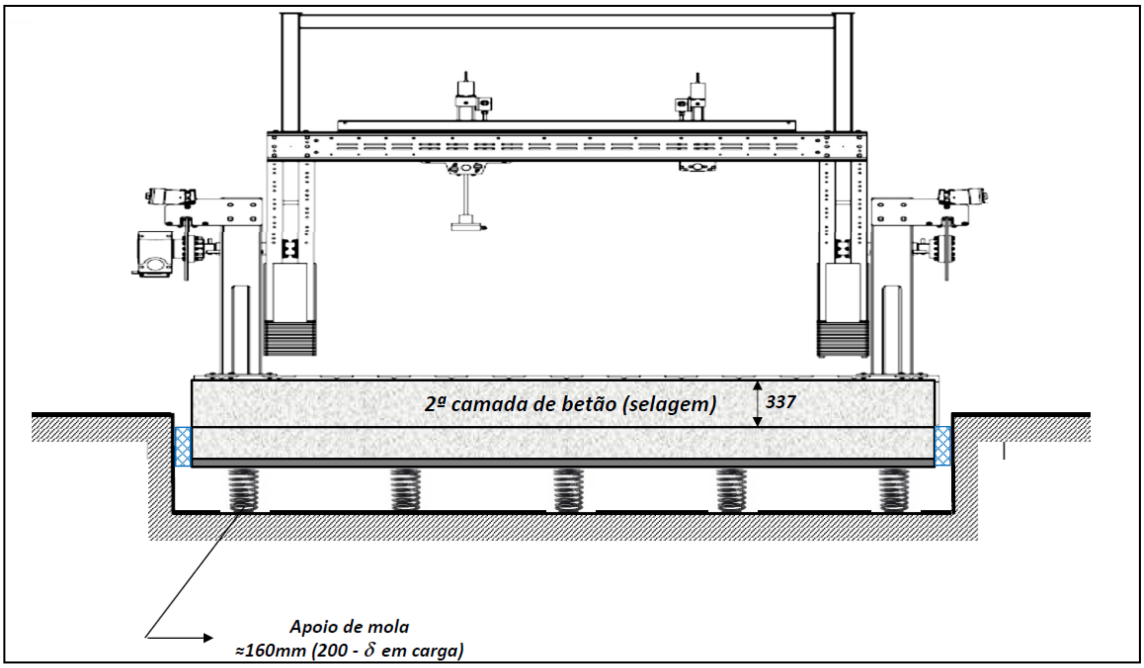
2ª camada de betão (selagem)
337
Apoio de mola
≈160mm (200 - δ em carga)

The three figures below, show a 3D representation of the main steps and the final aspect of the installation.

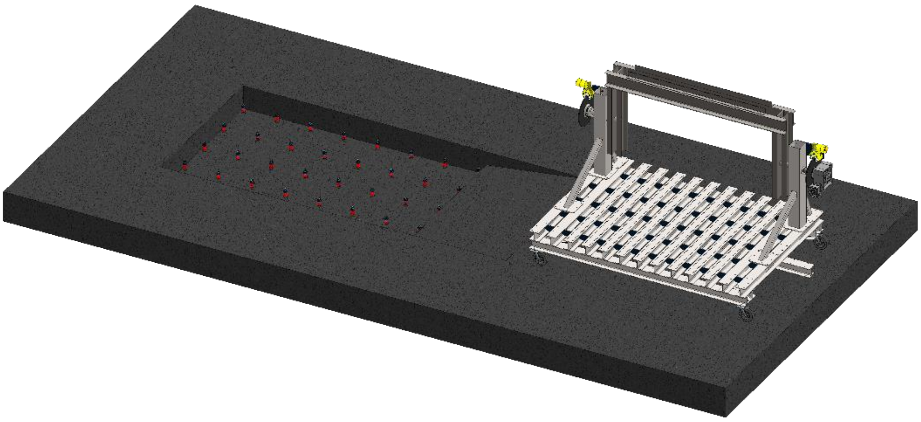

Figure 3-69 – Spring bed instalment

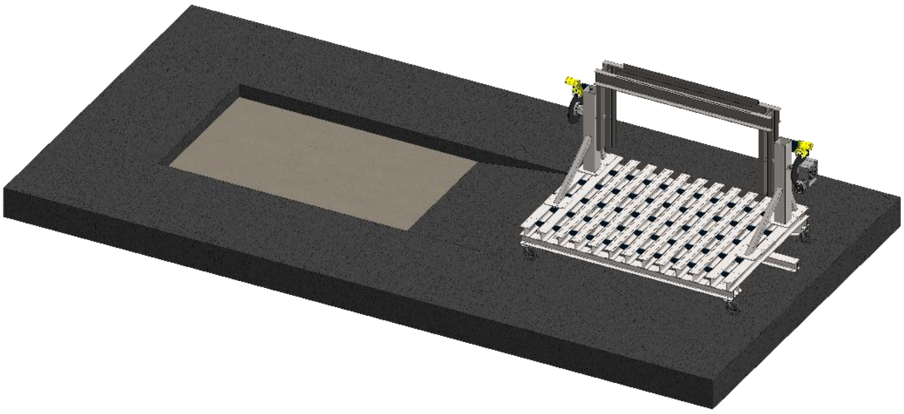

Figure 3-70 – First layer of concrete instalment

The result is shown in the next picture.

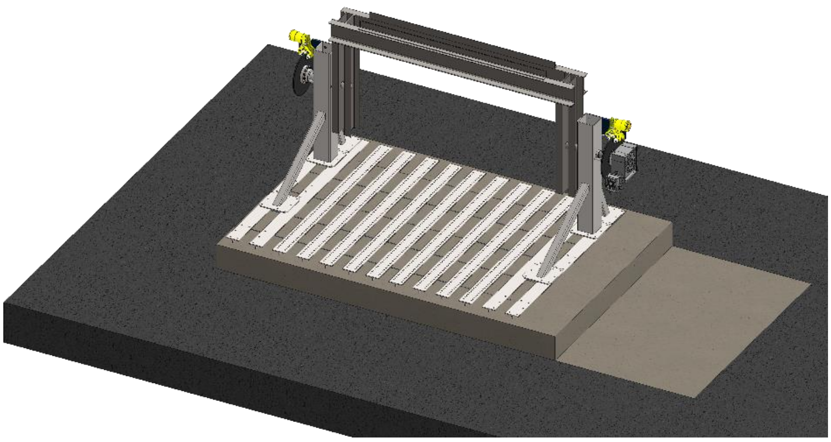

Figure 3-71 – Complete installation of the vibration isolation system (approximation)

3.5 CCB Supports

The CCB mounting is done by using custom made fixtures for each CCB model which in turn will be mounted on structures that will be bolted to the base structure. These structures can be reutilized.

3.5.1 CCB Fixation kits

Each CCB model will have its own fixation kits. These are custom made for each CCB, due to the different mounts and geometries. These are machined to the CCB specifications and are made of steel, Ck45 in this case, with black oxide coating to prevent rusting. This material was chosen because it is readily available in most suppliers, is easy to machine and is economical.

The pictures below show an example of CCB fixtures.

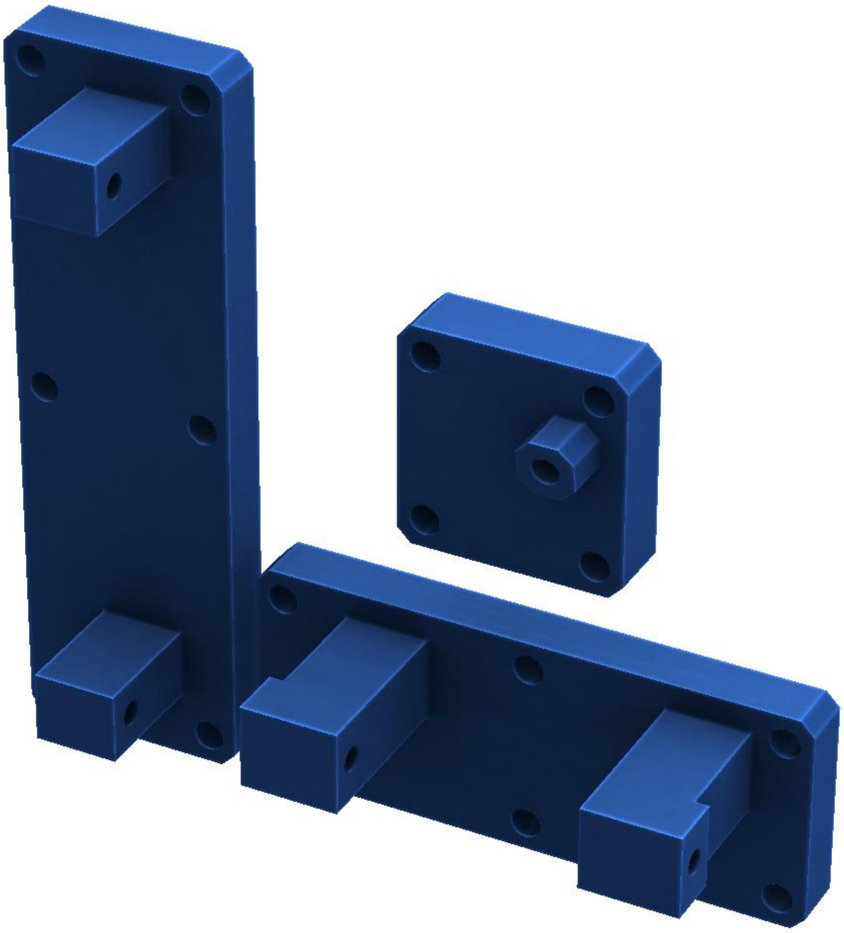

Figure 3-72 – CCB mounting fixtures

3.5.2 Static CCB Supports

To support the CCBs, four supports were designed and manufactured. These are composed of square steel tubes, welded to stiffening ribs, a holed plate to fix the CCB fixtures and base plates to fix the whole assembly to the structure base.

These have a hole matrix to fix the CCB fixtures and their fixation to the base structure is also flexible due to the use of slotted holes. Figure 3-73 shows two of the supports while Figure 3-74 an example of the fixtures fixation to the support.

Figure 3-73 – Two examples of the static test CCB supports

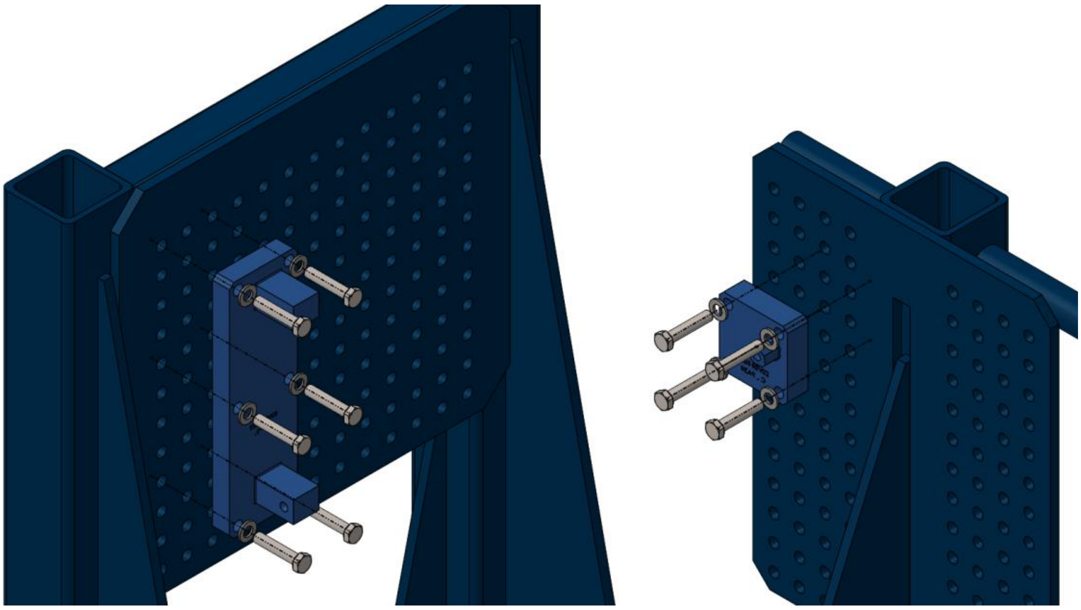

Figure 3-74 – Example of the CCB fixtures mounting on the CCB supports

The CCB is then mounted with the fixtures to the supports, as shown in Figure 3-75.

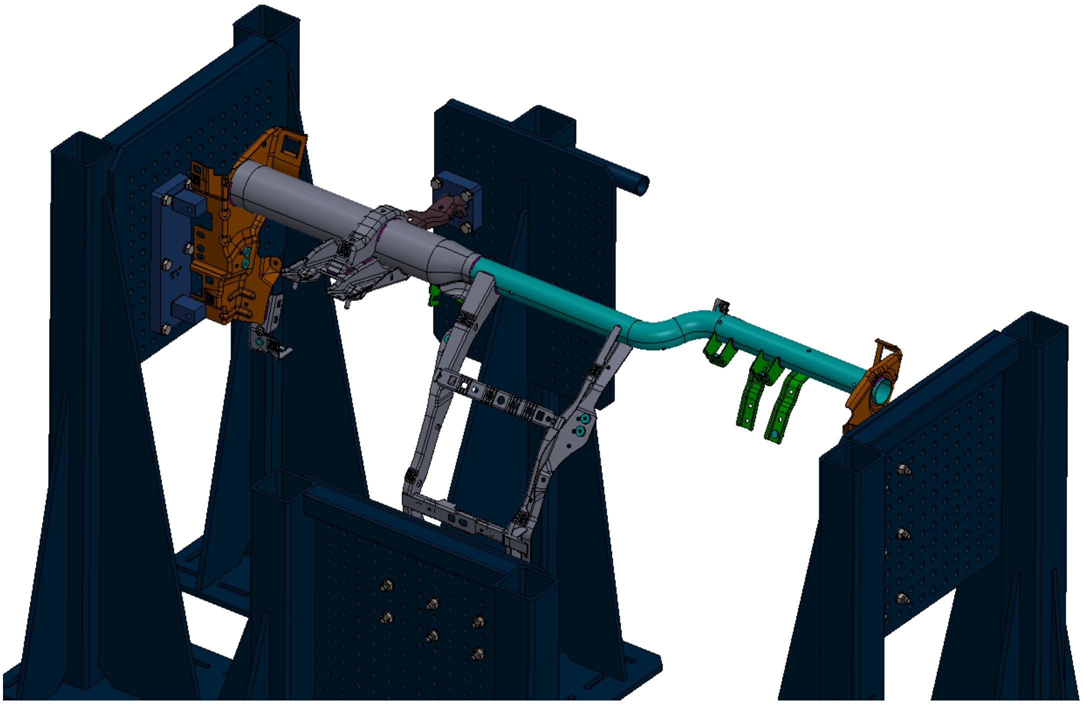

Figure 3-75 – CCB mounted to the supports

3.5.3 NVH CCB Supports

These supports are much lighter but with high stiffness to achieve the best possible results for the vibration tests.

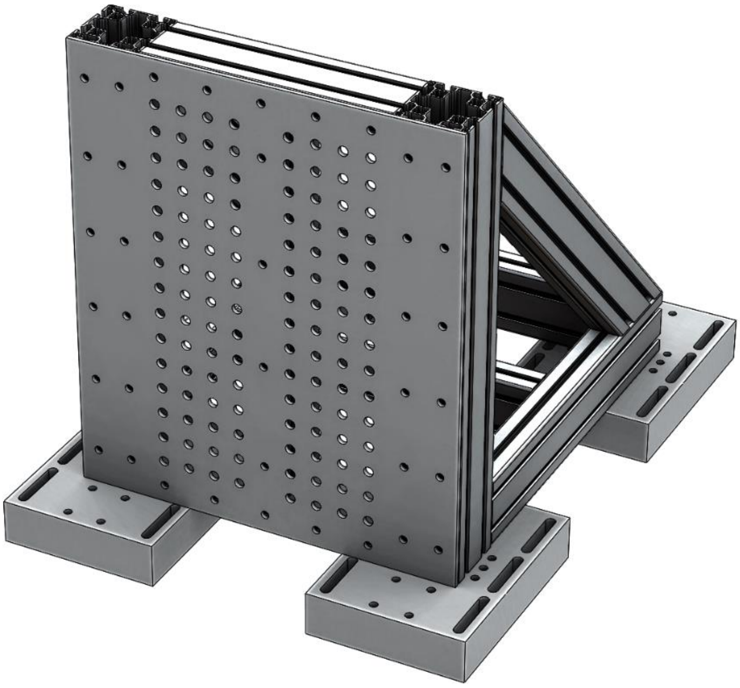

3.6 Actuation system

3.6.1 Hydraulic power station

The system has a hydraulic power station, which is a cabinet containing all the hydraulic power components such as pumps, motors and valves.

The hydraulic power station is not within the scope of this work but, for information, it was developed by an external entity based on our requirements.

This cabinet measures about 500x500x500 mm.

3.6.2 Hydraulic actuators

While the hydraulic actuators are supplied by an external supplier and as such, are not within the scope of this work, they were specified by the author to meet the client's requirements.

The actuation system features two hydraulic cylinders to apply loads on the CCBs. The main actuator is capable of higher loads, up to 25kN and the secondary actuator is used for lower loads, up to 7,5kN, with higher resolution and easier control at lower loads. The reason for having two separate actuators is, firstly to have the ability to apply a wide range of loads (from 25kN to 50N) and to be able to perform tests with two loads at the same time in the same structure, while not being an initial requirement it was requested by the client afterwards.

The main actuator is fixed to a custom support that allows the rotation of the actuator as well as horizontal positioning as the figure below shows. The secondary actuator is fixed to a similar support as the one for the main actuator but without the ability to rotate the actuator. Figure 3-76 shows both actuators.

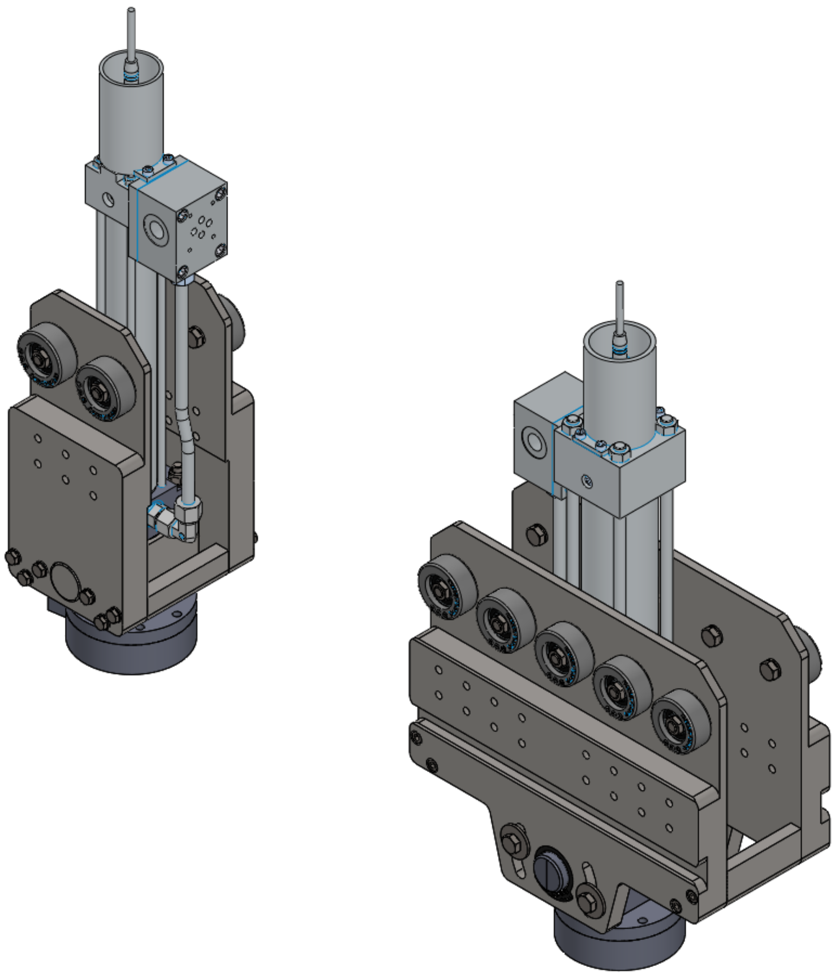

Figure 3-76 – Secondary and main actuators, left to right

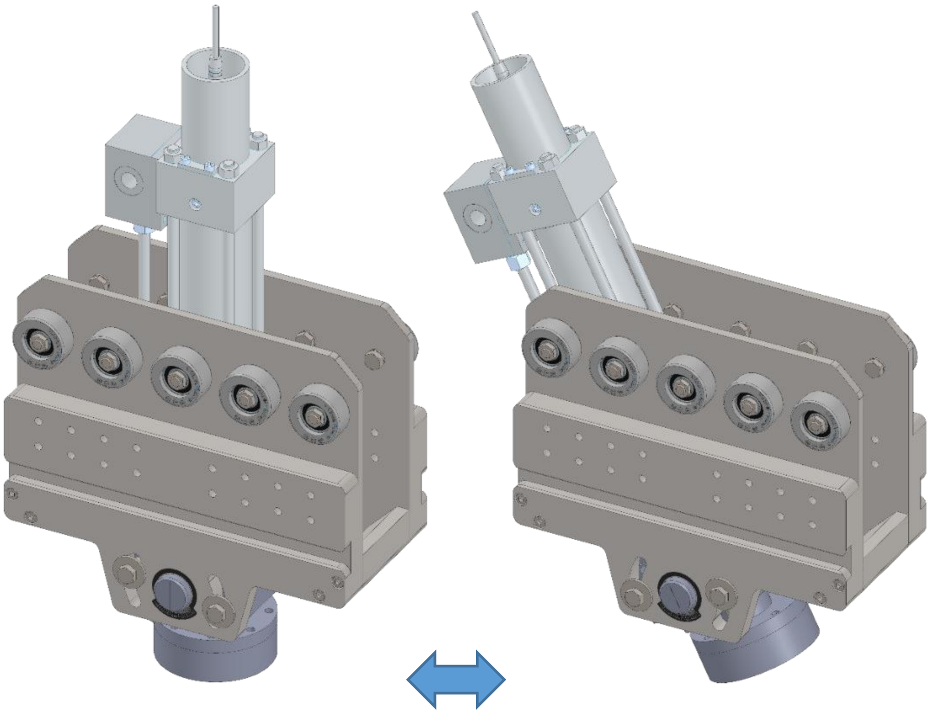

Figure 3-77 – Actuator rotation

This support will slide along on a rail that exists on the bridge. The support has markings to help setting the angular position of the actuator, these markings have a 2° resolution.

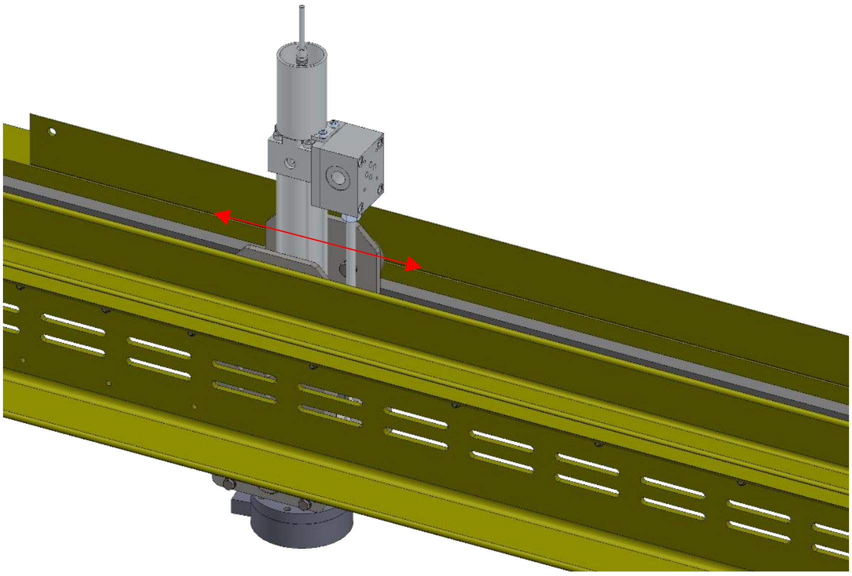

Figure 3-78 – Actuator positioning

The assembly of these actuators is done by removing a part of the rail that exists on the bridge and, with the help of the hoist, remove or place the actuators. This operation should be done while the gantry is on the vertical position. Refer to chapter 3.4.3 for more details on the bridge and gantry system.

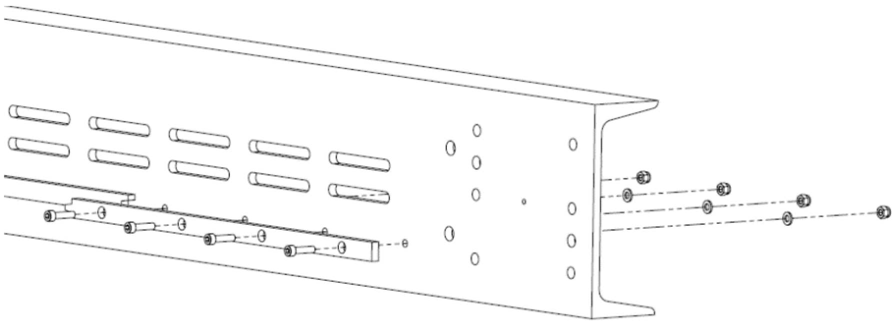

Figure 3-79 – Rail removal on the bridge to mount and dismount the actuators

Figure 3-80 and Table 3-9 show the dimensions and specifications of the main actuator and Figure 3-81 and Table 3-10 show the dimensions and specifications of the secondary actuator.

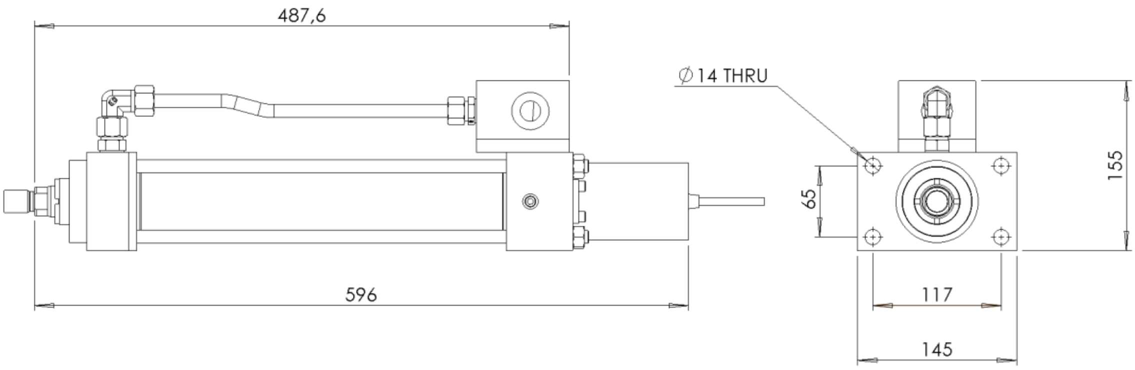

Figure 3-80 – Dimensions of the main actuator

Table 3-9 - Specifications of the main actuator

Feature	Value	Notes
Maximum load	25 kN	Static and dynamic. The software limits the maximum load at 99% for safety. Can be reconfigured.
Minimum load	500 N	Varies greatly with the actuator's speed.
Load resolution	50 N	In dynamic tests an amplitude error of 2% should be considered.
Displacement resolution	0,1 mm	In dynamic tests an amplitude error of 2% should be considered.
Stroke	300 mm	
Load cycle max. frequency	3 Hz	Low movement amplitude
Setup	Manual	Manual setup with horizontal and angular position adjustability

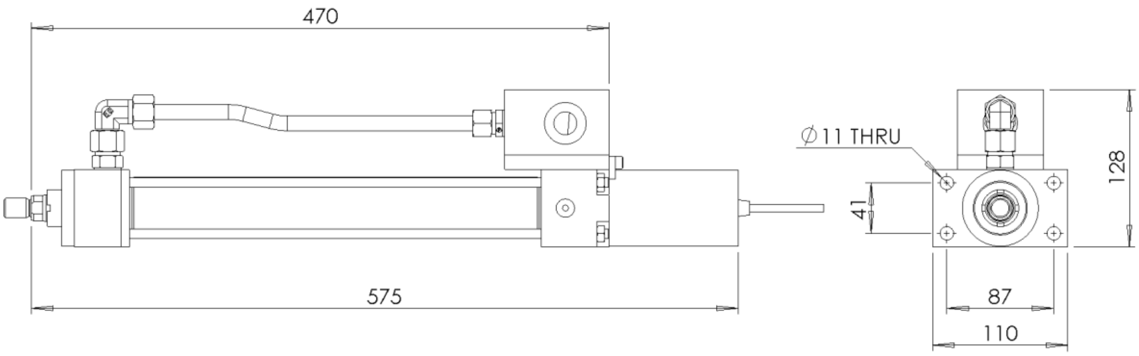

Figure 3-81 – Dimensions of the secondary actuator

Table 3-10 – Specifications of the secondary actuator

Specification	Value	Notes
Maximum load	7,5 kN	Static and dynamic. The software limits the maximum load at 99% for safety. Can be reconfigured.
Minimum load	50 N	Varies greatly with the actuator's speed.
Load resolution	20 N	In dynamic tests an amplitude error of 2% should be considered.
Displacement resolution	0,1 mm	In dynamic tests an amplitude error of 2% should be considered.
Stroke	300 mm	
Load cycle max. frequency	3 Hz	Low movement amplitude
Setup	Manual	Manual setup with horizontal position adjustability

3.7 System setup

This chapter explains the procedures necessary to setup the equipment to be used in different testing conditions.

3.7.1 Tests

The tests that we are going to show are as follows:

- Apply a load on the X axis;
- Apply a load on the Y axis;
- Apply a load on the YZ plane;
- Apply a load on the Z axis;
- NVH test.

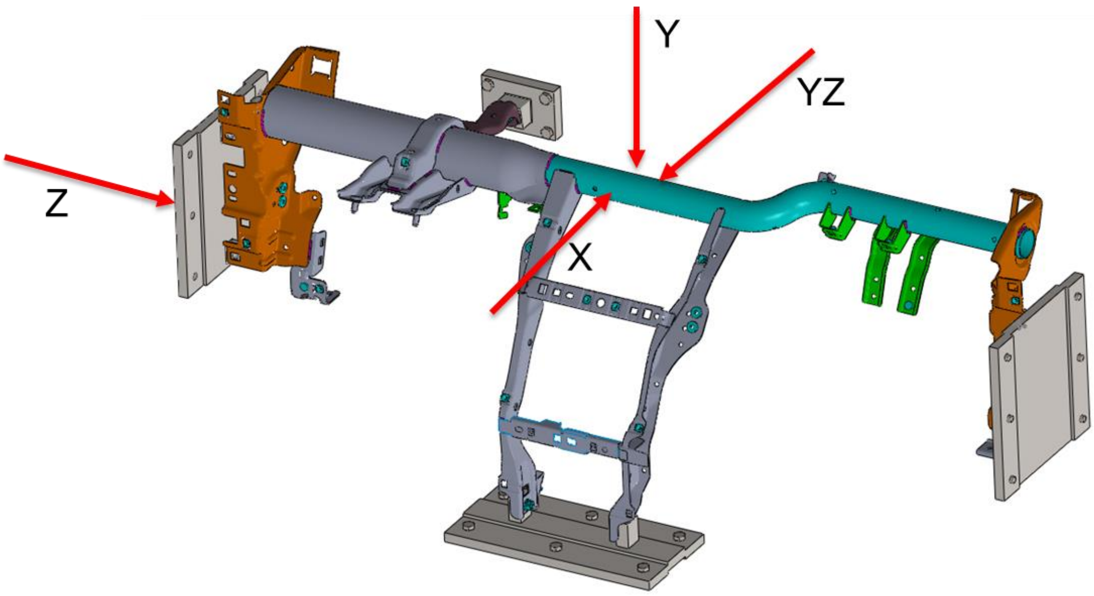

Figure 3-82 – Example CCB tests

3.7.2 CCB Mounting

The CCB models are mounted on the CCB supports, and these structures can be placed along the hole matrix that exists on the base. The custom made CCB fixtures are made according to the hole matrix on the CCB mounts.

The procedure to do so is, first, apply the custom fixtures to the CCB model to be tested, verify the tests that are going to be made and take note of the best position for the CCB to be mounted according to the CAD model, then fix the CCB to the CCB mounts according to the pre-established position.

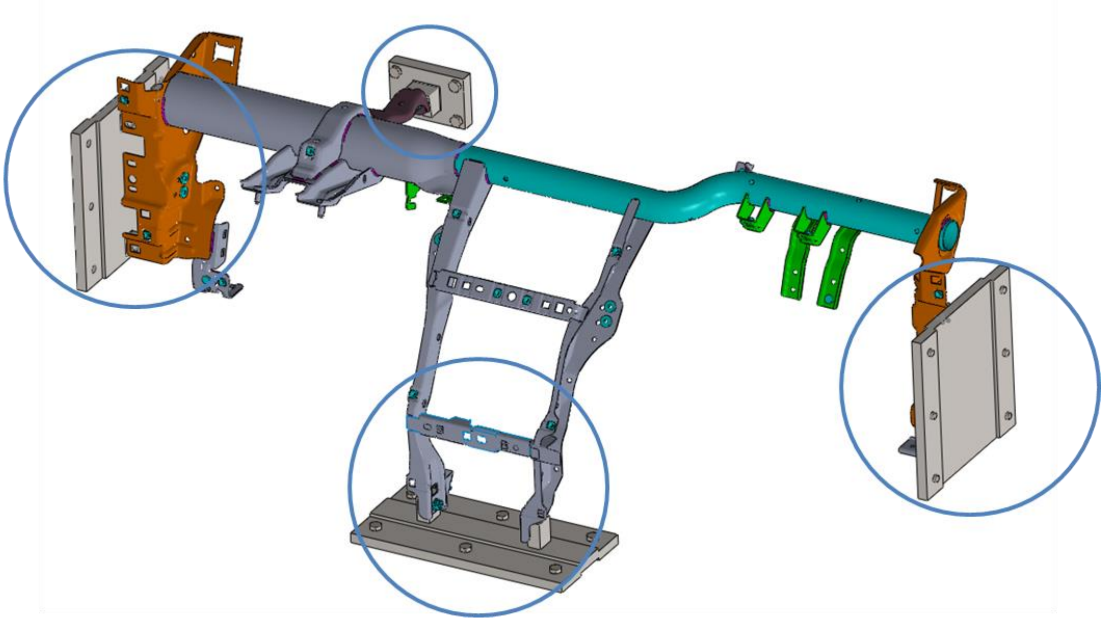

Figure 3-83 – CCB with fixtures mounted

The CCB mounts are fixed to the base using bolts and nuts.

One important rule to follow is the alignment of the CCB main axis with the axis of the CCBTester as shown in Figure 3-84:

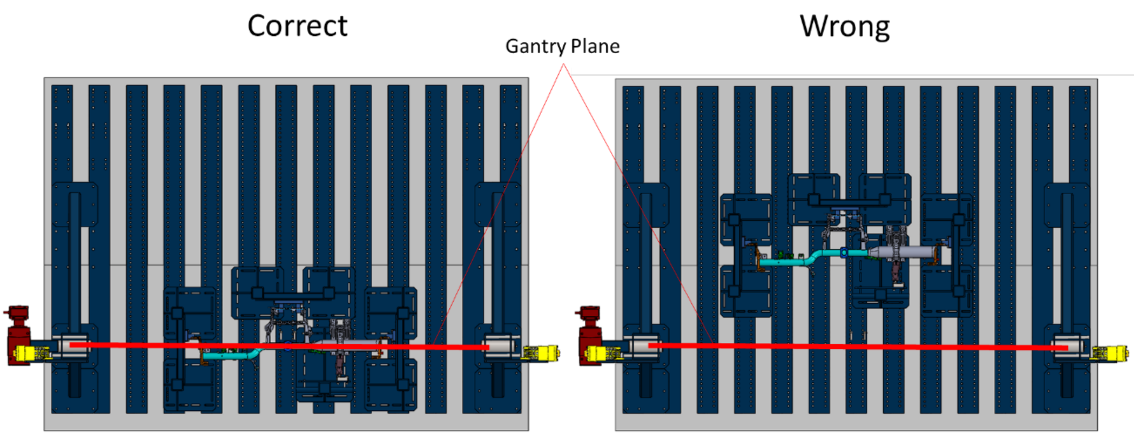

Figure 3-84 – Correct positioning of the CCB for static testing

Unless when being loaded on the X axis or the XZ plane, the CCB should always be positioned as close to the gantry plane as possible.

The CCB should then be fixed to the CCB supports. Then the whole system can be finally positioned correctly on the base and fastened using bolts and nuts.

3.7.3 Bridge Positioning

To position the bridge, a hoist is used to elevate or lower it. This procedure is done only when the gantry is on the vertical position.

To lower or elevate the bridge, remove the bolts that hold it on the columns. Using the chain hoist, lower or elevate the bridge to the desired position and insert the bolts and nuts as shown in Figure 3-85 and Figure 3-86.

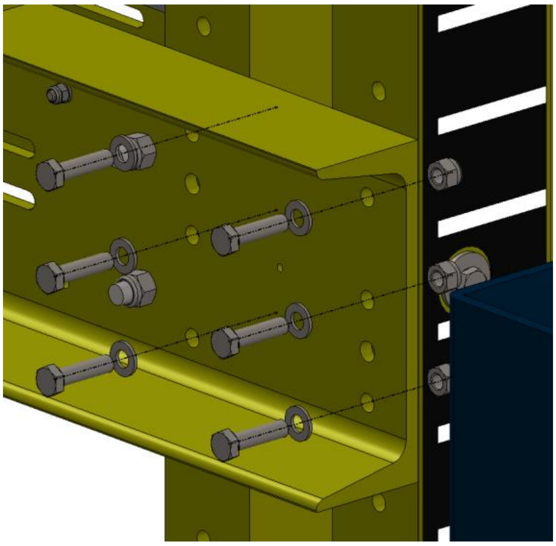

Figure 3-85 – Bridge positioning

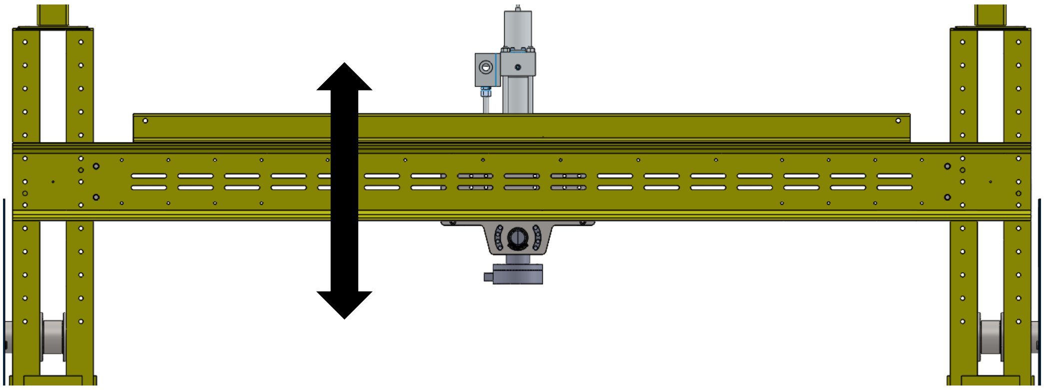

Figure 3-86 – Bridge positioning

The bridge should now be fixed and ready.

3.7.4 Gantry Rotation

The gantry rotation is controlled by a gearbox and two disc brakes.

To rotate the gantry, first release the brake, then rotate the gearbox lever until the gantry is the desired position, using the markings on the brake disc as a reference. After the gantry is on the desired position, re-apply the brakes and the procedure is terminated.

To rotate the gantry, release the disc brake and then rotate the gearbox wheel until the gantry is on the desired angular position as shown in Figure 3-87.

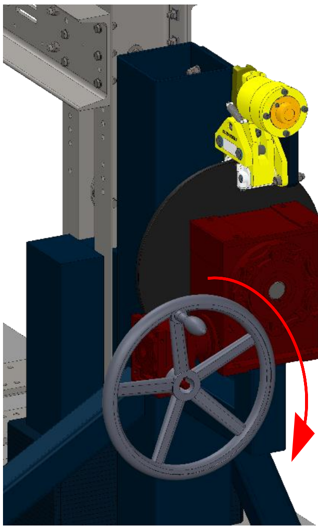

Figure 3-87 – Rotation of the gantry

After that, re-apply the brakes.

3.7.5 Actuator Positioning

The actuator has a special support that allows both the rotation of the actuator on the gantry plane as well as the linear position along the bridge. Both are secure using bolts and nuts.

To move the actuator along the bridge, first remove the bolts fixing it, then move it to the desired position using the markings on the bridge. When on the desired position, fasten the bolts to the nuts again. The actuator should now be fixed along the bridge, to fix its angular position, first remove the bolts securing it, rotate it to the desired position using the markings as a guide and then re-apply the bolts. Figure 3-88 and Figure 3-89 show this procedure.

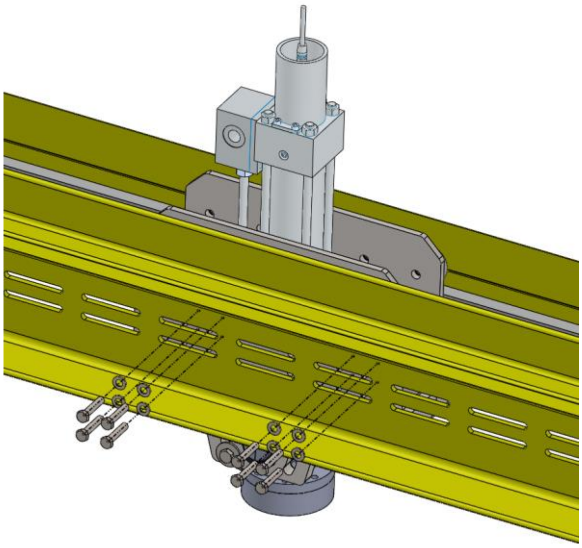

Figure 3-88 – Actuator positioning

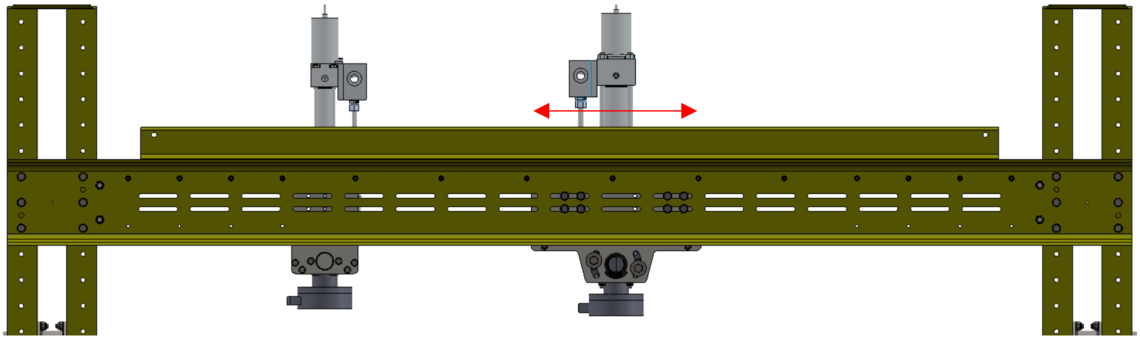

Figure 3-89 – Actuator positioning

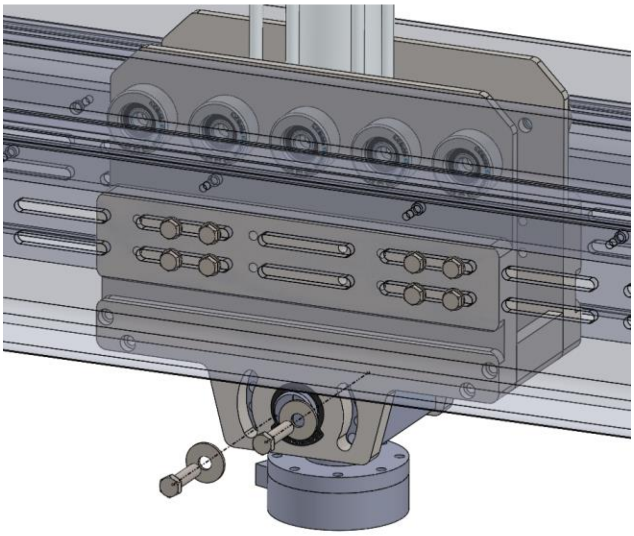

Figure 3-90 – Actuator rotation

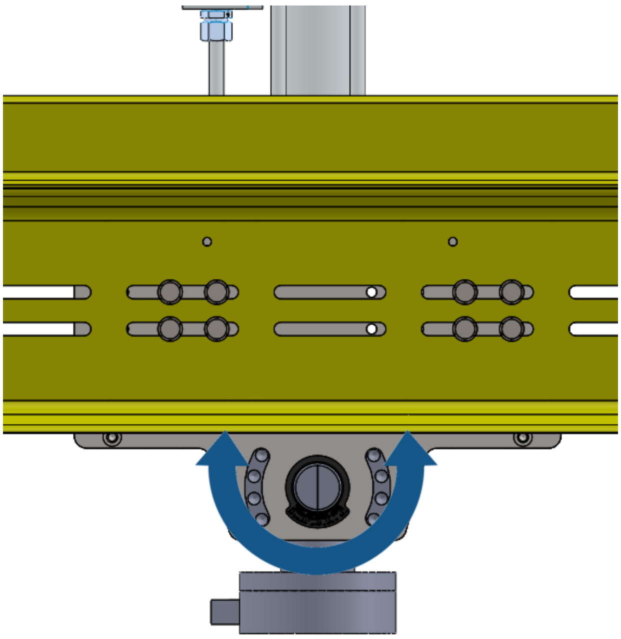

Figure 3-91 – Actuator rotation

3.7.6 Test: X axis load

For this test the first step is to correctly position the CCB model. The figures below show a possible positioning for the CCB.

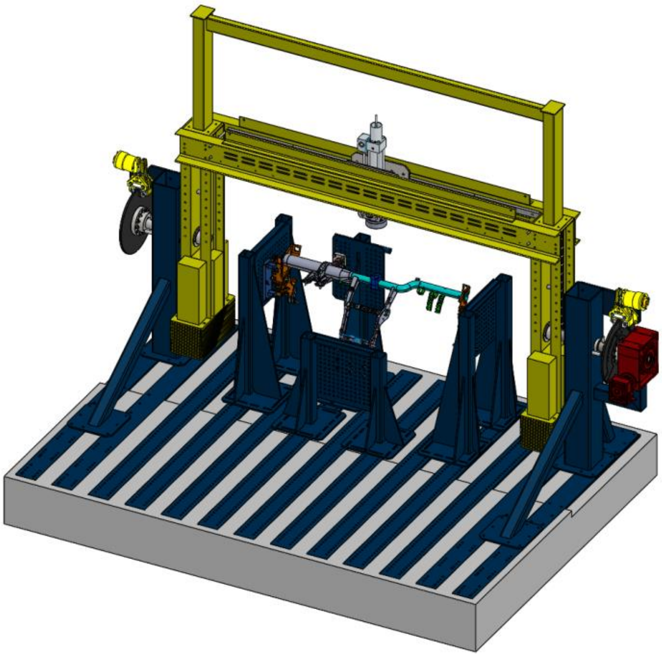

Figure 3-92 – X axis test CCB positioning

Lowering the bridge to a closer position to the CCB model, such as position number 10 is the next action.

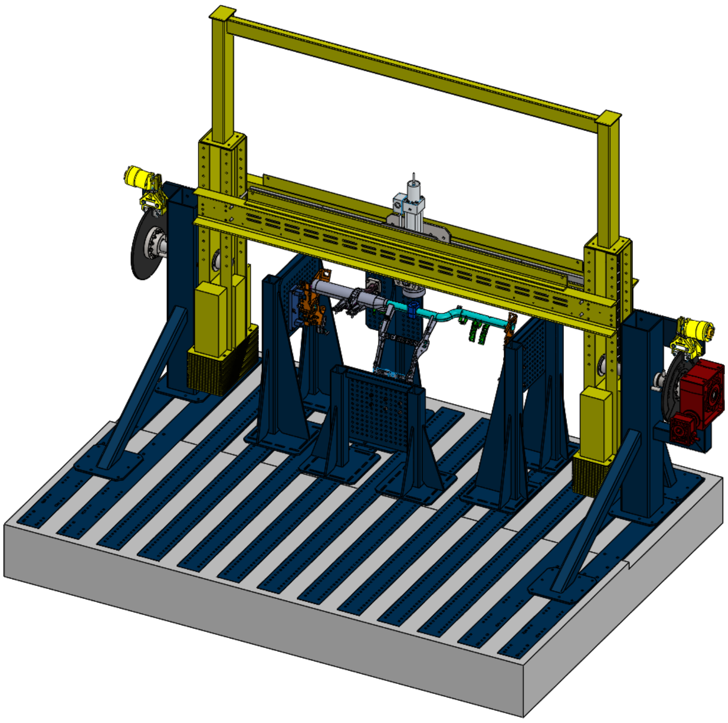

Figure 3-93 – X axis bridge positioning

Next it is needed to rotate the gantry. The gantry should be rotated to the 90º position (horizontal).

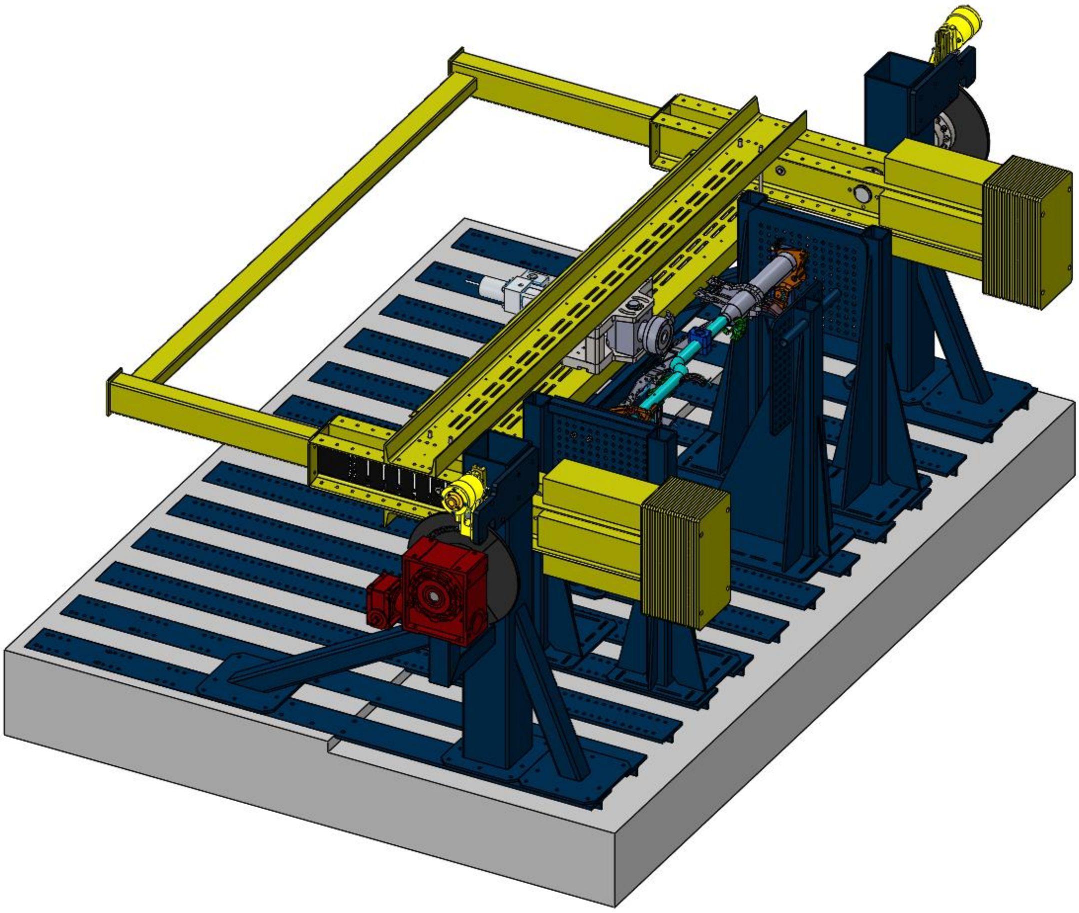

Figure 3-94 – X axis test gantry positioning

The actuator may need to the repositioned, in this case, it needs to be on the middle of the bridge It should also be perpendicular to the bridge.

After these steps, the setup should be finished and the test ready to be initiated.

3.7.7 Test: Y axis load

For this test the first step is to correctly position the CCB model. The figures below show a possible positioning for the CCB.

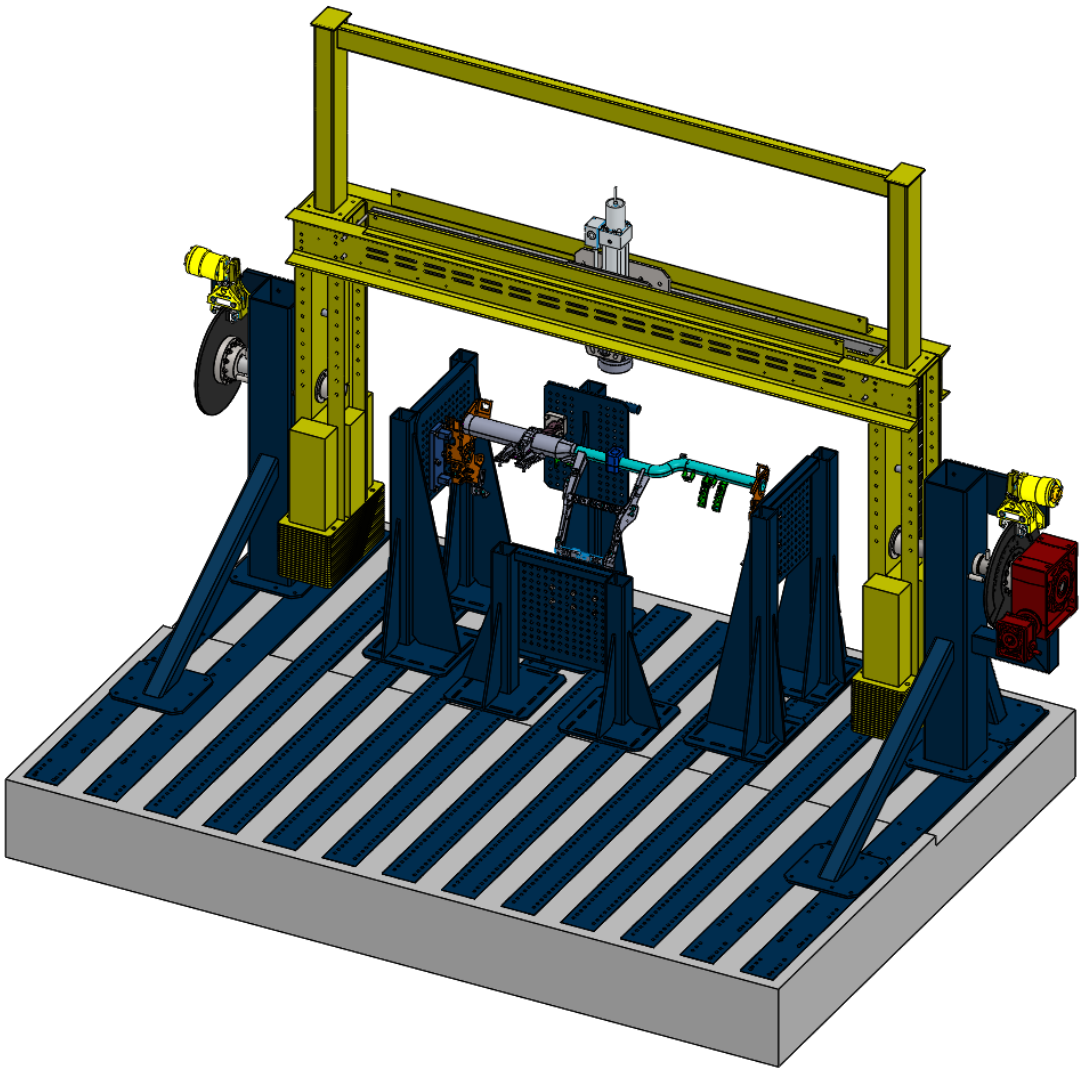

Figure 3-95 – Y axis test CCB positioning

Lowering the bridge to a closer position to the CCB model, such as position number 10 is the next action.

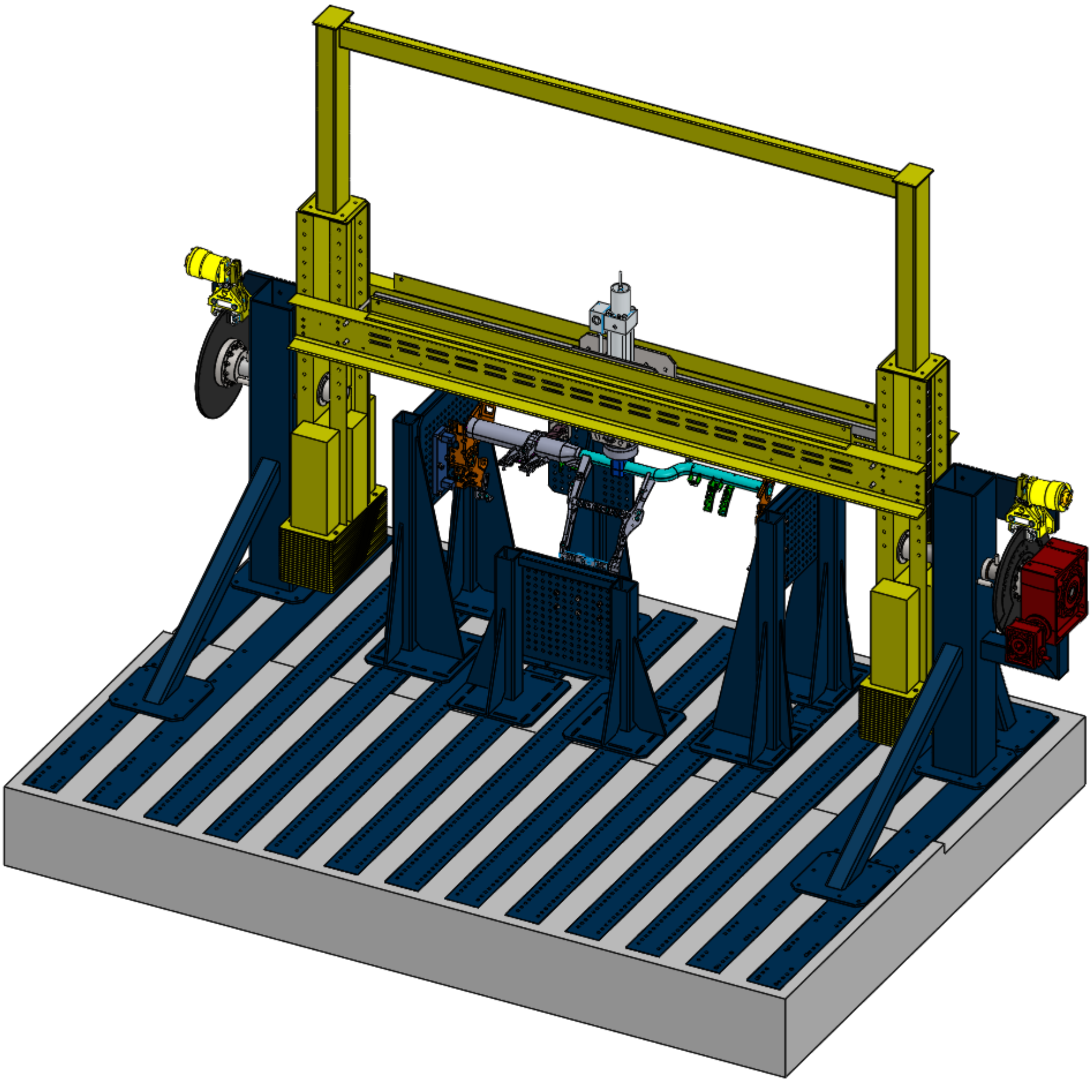

Figure 3-96 – Y axis test bridge positioning

Next it is needed to rotate the gantry. The gantry should be rotated to the 0º position (vertical).

The actuator may need to the repositioned, in this case, it needs to be on the middle of the bridge. It should also be perpendicular to the bridge.

After these steps, the setup should be finished and the test ready to be initiated.

3.7.8 Test: YZ plane load

For this test the first step is to correctly position the CCB model. The figures below show a possible positioning for the CCB.

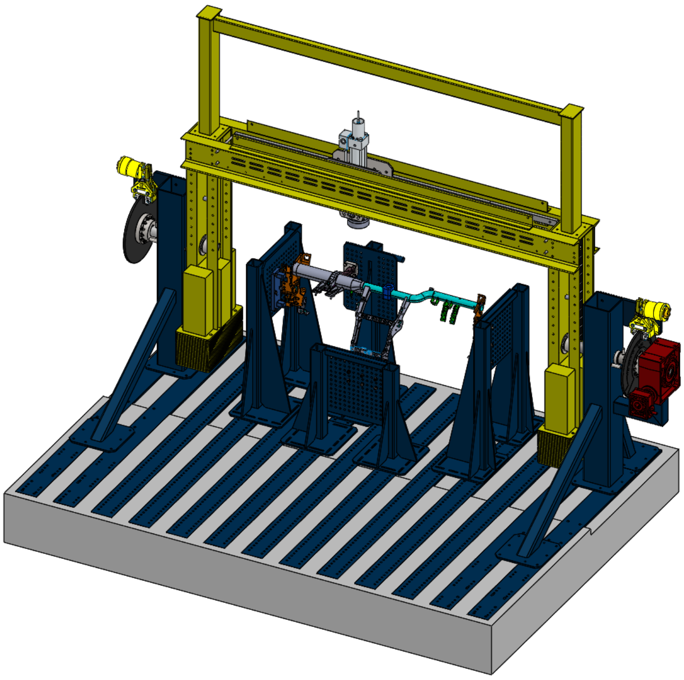

Figure 3-97 – YZ plane test CCB positioning

Lowering the bridge to a closer position to the CCB model, such as position number 10 is the next action.

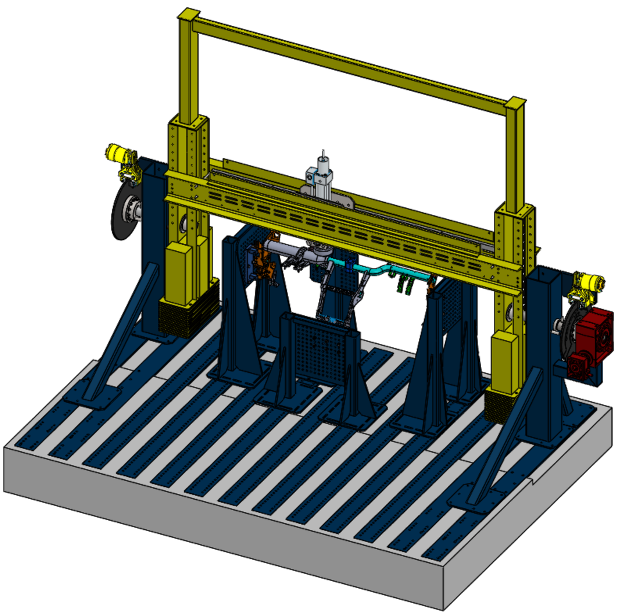

Figure 3-98 – YZ plane test bridge positioning

Next it is needed to rotate the gantry. The gantry should be rotated to the 0º position (vertical).

The actuator may need to the repositioned, in this case, it needs to be on the middle of the bridge. It should also be at about 45º to the vertical direction.

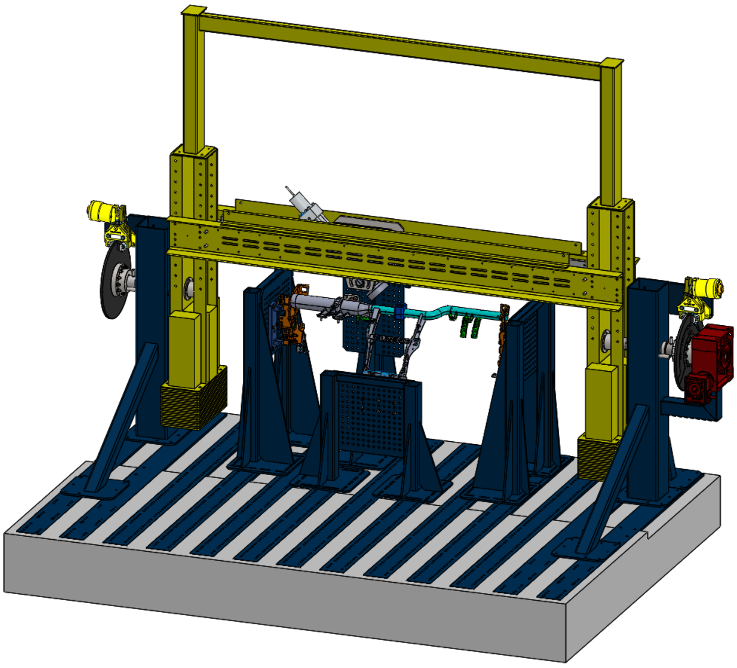

Figure 3-99 – YZ plane test actuator positioning and rotation

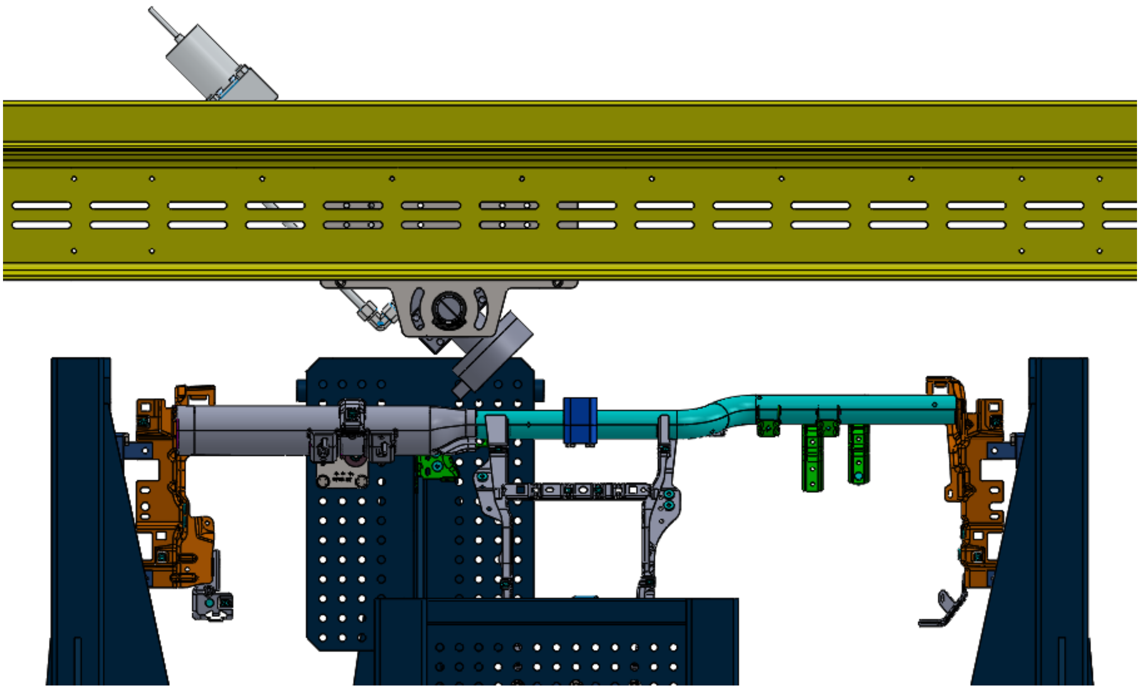

Figure 3-100 – YZ plane test actuator positioning and rotation

After these steps, the setup should be finished and the test ready to be initiated.

3.7.9 Test: Z axis

For this test the first step is to correctly position the CCB model. The figures below show a possible positioning for the CCB. On this test, the CCB must be positioned differently from the other tests, the figures below show the correct orientation.

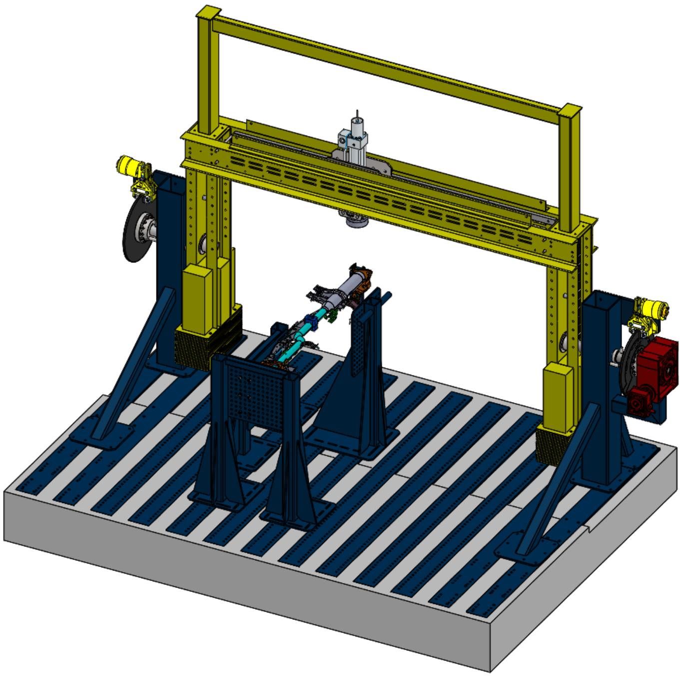

Figure 3-101 – Z axis test CCB positioning

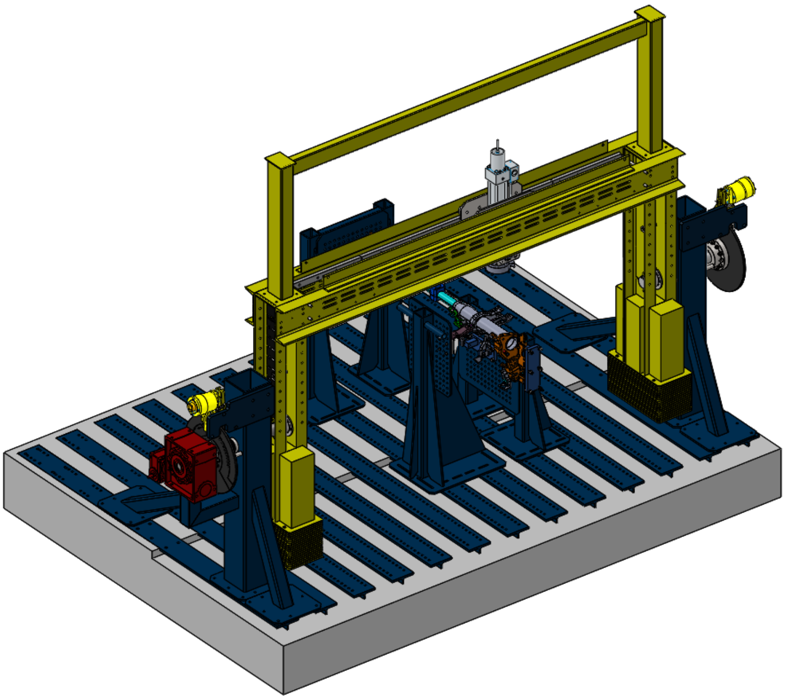

Figure 3-102 – Z axis test CCB positioning

Lowering the bridge to a closer position to the CCB model, such as position number 7 is the next action.

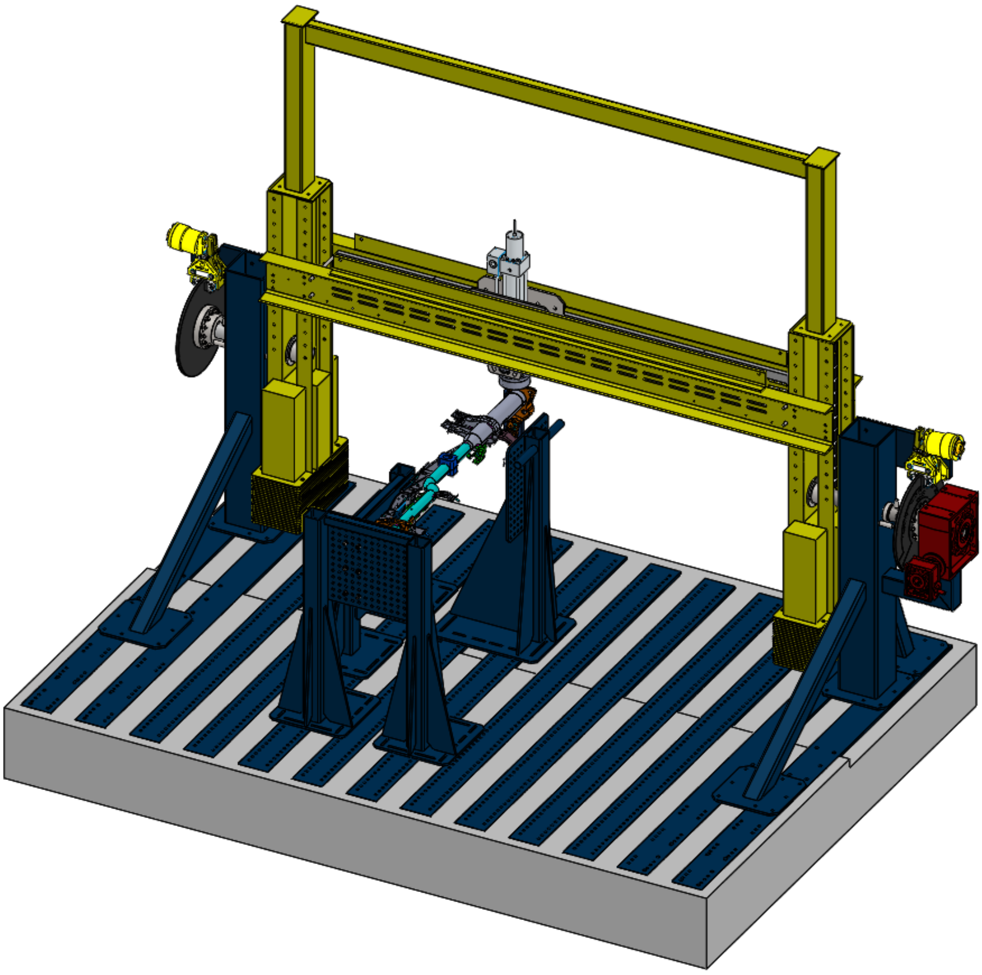

Figure 3-103 – Z axis test bridge positioning

Next it is needed to rotate the gantry. The gantry should be rotated to the 90º position (horizontal).

The actuator may need to the repositioned, in this case, it needs to be on the middle of the bridge. It should also be at perpendicular to the bridge.

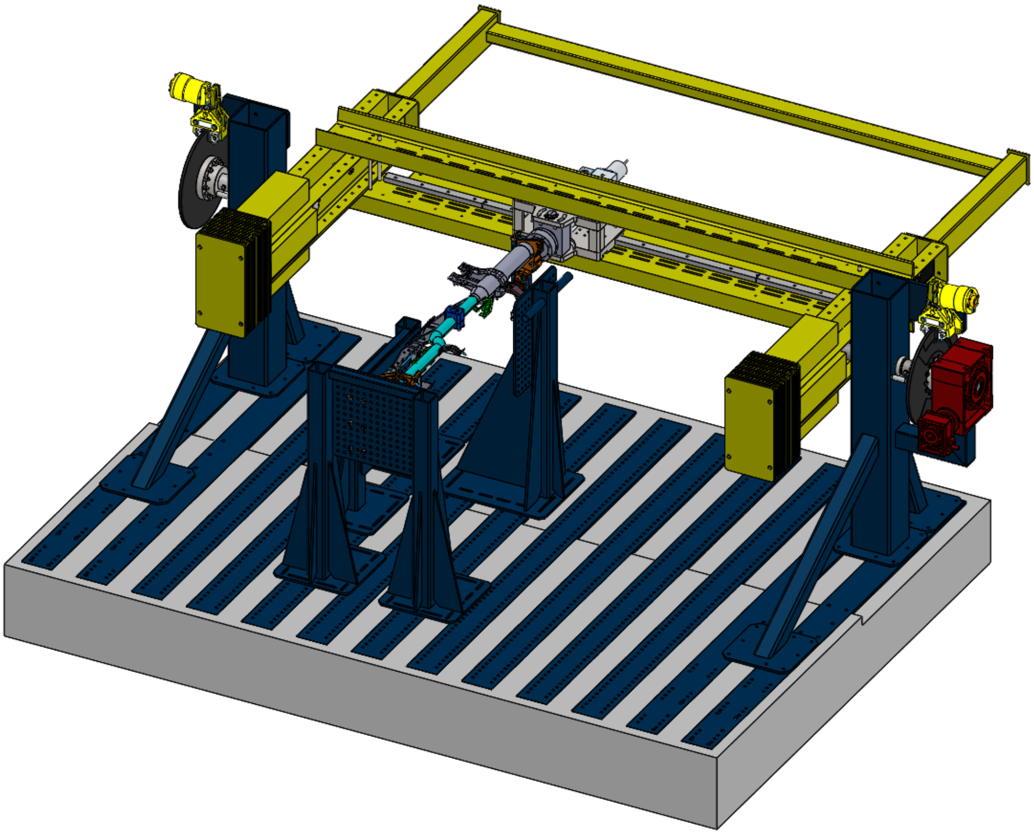

Figure 3-104 – Z axis test gantry rotation

After these steps, the setup should be finished and the test ready to be initiated.

3.7.10 NVH test

NVH testing is done on a special zone of the equipment, specifically designed to meet the vibration analysis. The base on the NVH zone is fully embedded in concrete to better isolate all the components from the rest of the structure.

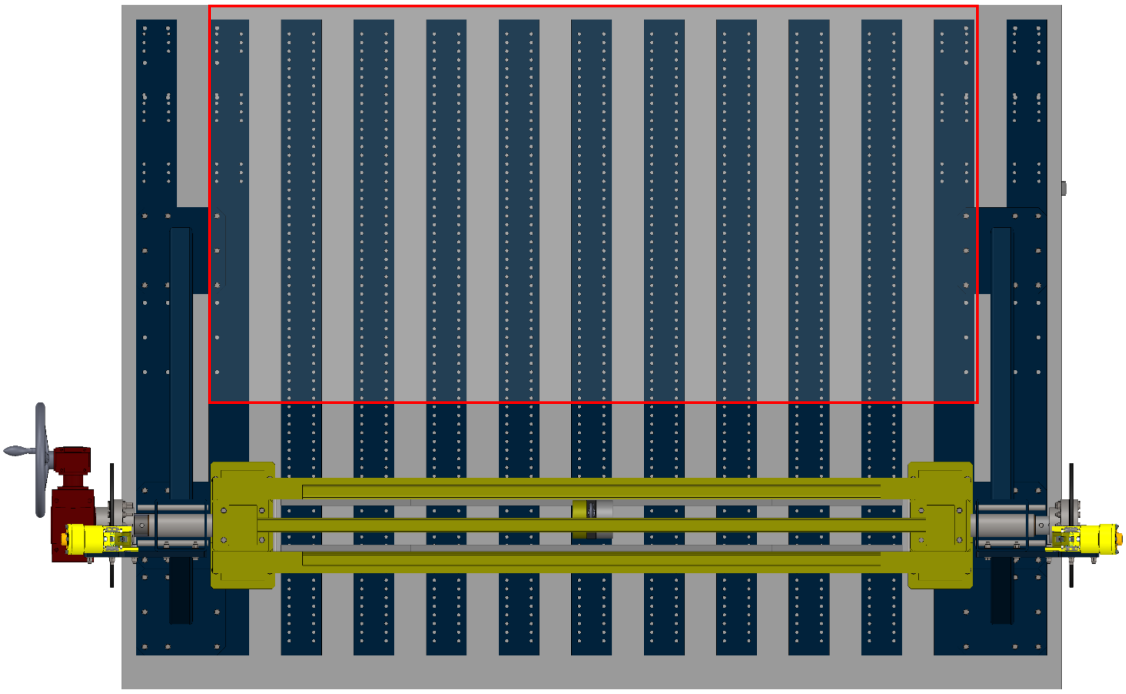

Figure 3-105 – NVH test zone

The supports for the NVH test are different from the standard supports. The fixation of these is identical to the standard, using bolts and nuts. The CCB fixtures are also compatible with the hole matrix on the front plate of the NVH supports.

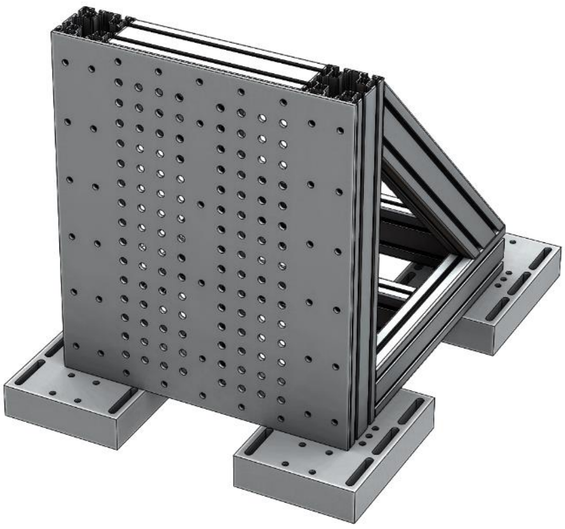

Figure 3-106 – NVH test CCB support

During the vibration testing, the rest of the equipment such as CCB supports should be removed from the base and the gantry should be resting with the brakes applied at the maximum rotation.

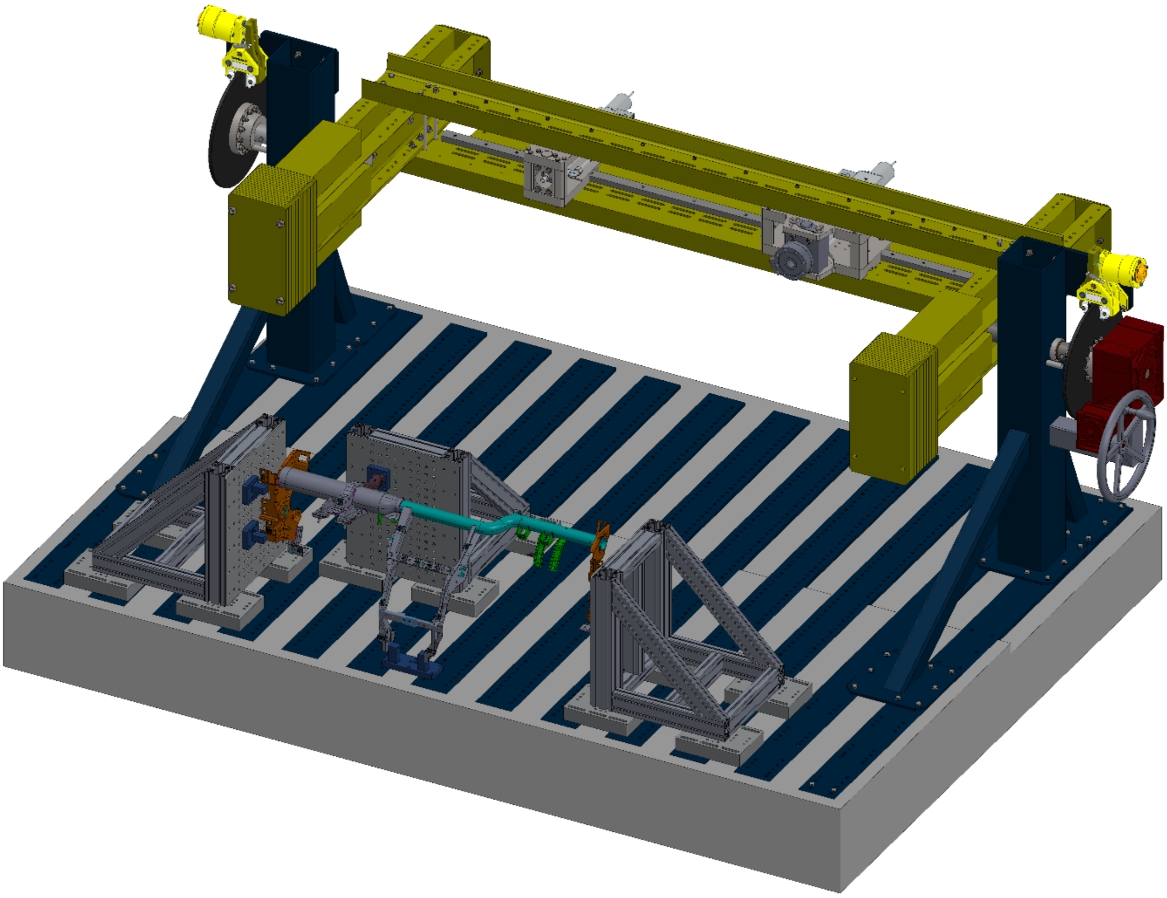

Figure 3-107 – NVH testing configuration

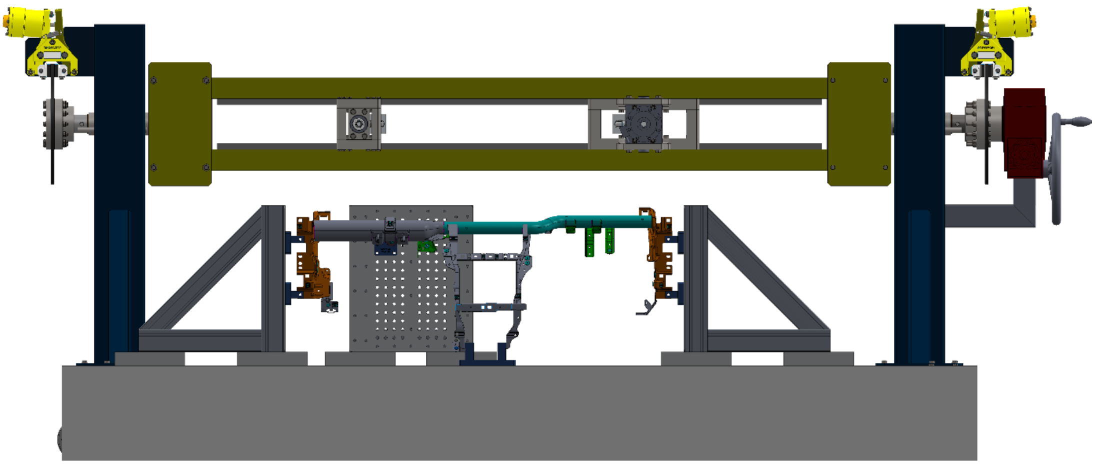

Figure 3-108 – NVH testing configuration

3.8 Structure dimensioning description

In this chapter the structural analysis is described in detail. This analysis considered the various conditions, tests, loads and types of failure that the equipment can suffer. Also, given that this equipment was developed to a privately-owned company, some parts of the dimensioning and features are not disclosed.

3.8.1 Method

This analysis was done in two ways. First an analytical model was created considering the loads and conditions of the equipment. Then a Finite Element Analysis was done considering all the different load cases.

The critical elements and zones were calculated using proper material mechanics and machine elements equations and models, using the results from the analytical model.

The software used for FEA was Solidworks Simulation.

3.8.2 Assumptions

Neither the FEA nor the analytical analysis can cover the whole spectrum of loads and dimensioning calculations, so the analysis is two-fold, the study will be divided into the general displacements and stresses for the FEA analysis and local stresses and calculations for the analytical analysis. This is due to the fact that FEA analysis not being ideal for local stresses such as bolt connections and such, and due to the fact that analytical analysis for the whole load cases is too time consuming, and this is where the FEA analysis is best, analysing the general structure.

The analytical results also serve as proof that the FEA analysis is correct and that it can be used in more complex configurations, by comparing the results in a simpler configuration.

3.8.3 Materials

For the main parts of the structure the material considered was the S275 structural steel, although the structure will be built in S355 material, which being a higher strength material, increases the factor of safety. The choice for this material is based on the commercial availability of it.

The shaft, which is one of the critical elements uses the alloy steel number 1.6582, 34CrNiMo6 material which is a high strength material commonly used in applications that require resistance to very high loads. Several other materials were considered for this element and are later mentioned in the document.

The bolts are of stainless steel grade A2-70. The ball lock pins also use high strength stainless steel, material number 1.4542, AISI 630.

3.8.4 Load cases

Different load cases were considered to better represent the real conditions when the equipment is working.

These include mostly the worst-case scenarios for the loads that the equipment was designed to support.

For all this load cases, it was applied a higher load of 50 kN (FOS of 2).

The rest of the page has been left intentionally blank

3.8.5 Analytical approach

The analytical approach was done following a frame structure analysis.

With the results, local stresses on connections and critical elements was done.

These include:

Bolt connections	Bolt shear resistance is calculated, although the expected working conditions consider friction contact, due to the pre-load applied to the bolts, this is to guarantee a worst scenario condition
Pin connections	Pins are dimensioned to support the whole load applied to the beams, this way if a bolt pre-load fails, the pin will still maintain the structure
Shaft analysis	Analysis of the shaft stress for maximum loads and for fatigue

3.8.6 Finite Element Analysis approach

On the FEA approach, the model was simplified to be able to be meshed and simulated. These simplifications have little impact on the results that are expected from this kind of analysis, because the local stresses, strains, and other local calculations are done analytically. The main output from this analysis is the general displacements, stresses and forces present on the different components.

Due to privacy restrictions of the client and employer, most FEA results were not disclosed.

The modal analyses of some elements were included and can be seen in chapter 3.11.

3.9 Analytical results

On this chapter are the results of the analytical analysis results.

3.9.1 Structure Model

The figure below shows the theoretical model of the structure. All the joints between beams are rigid. The software used to model the structure and obtain the values shown was FTOOL.

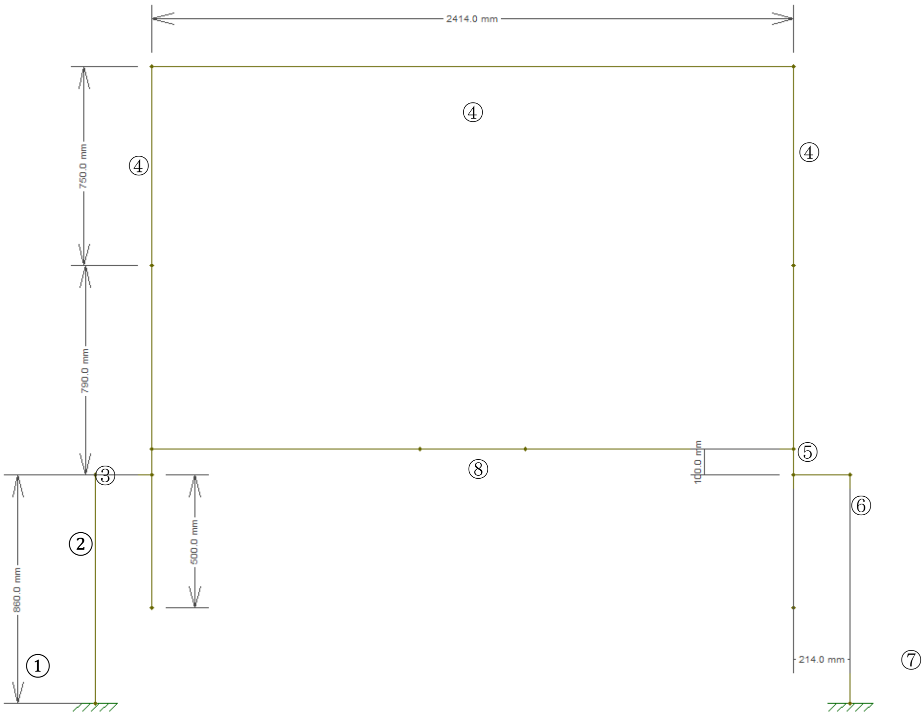

①		Square pipe 180x6,3 mm
②		Machined Shaft Ø65 mm
③		2x UPN 180 spaced by 68 mm
④		Rectangular Tube 120x80x8 mm
⑤		2x UPN 180 spaced by 68 mm
⑥		Machined Shaft Ø65 mm
⑦		Square pipe 180x6,3 mm
⑧		2x UPN 200 spaced by 180 mm

3.9.2 NTM diagrams (internal forces and moments)

3.9.2.1 Bridge mid-span load

The next figures show the axial, shear, moment and displacement diagrams.

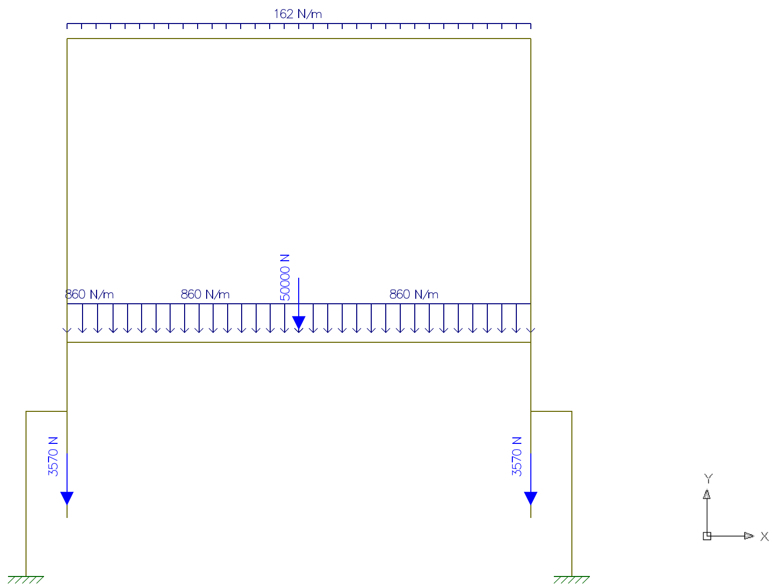

Figure 3-109 – Analytical model, bridge mid-span loads

The previous picture shows the loads applied to the structure. The distributed loads represent the self-weight and accessories, while the node loads represent the main load (50 kN) and the counter-weights (3570 N each).

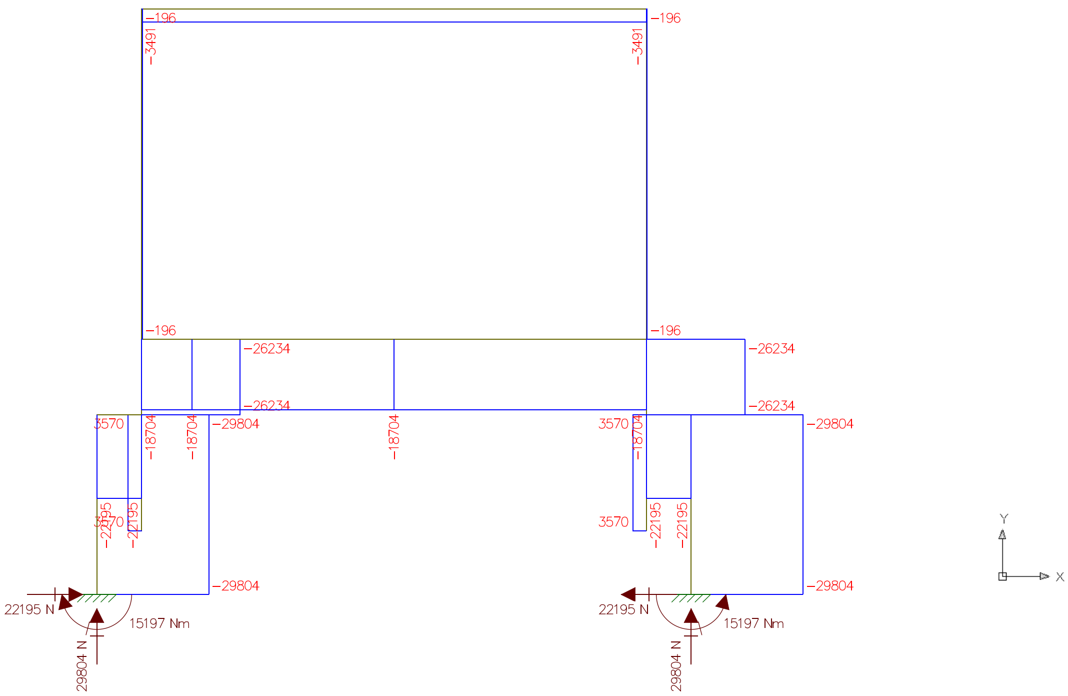

Figure 3-110 – Analytical model, bridge mid-span axial force

The maximum axial force on the bridge is of 18704 N, and on the shaft of 22195 N. The pillar has an axial load of 29804 N.

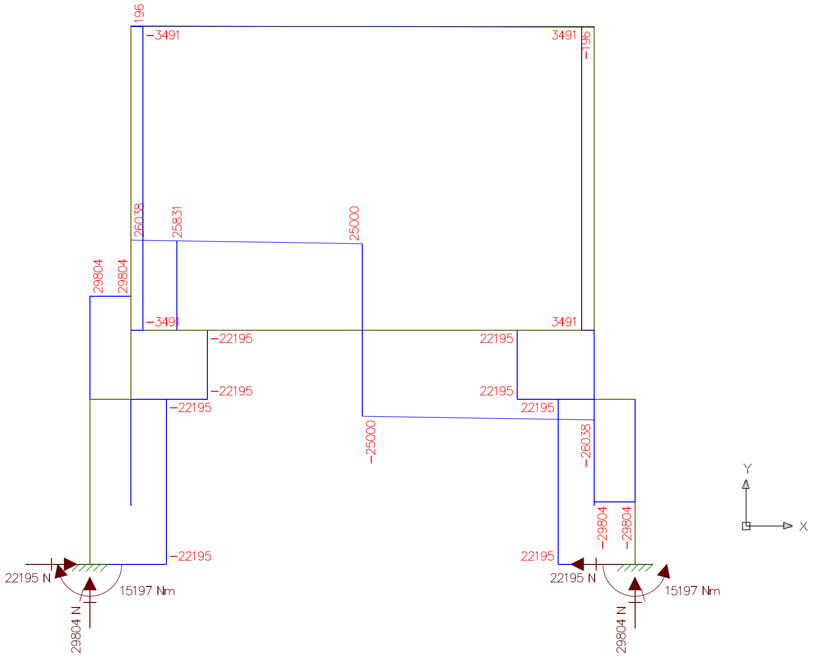

Figure 3-111 – Analytical model, bridge mid-span shear force

The maximum shear force on the bridge is on the end with the value of 26038 N. On the shaft the maximum shear force is of 29804 N.

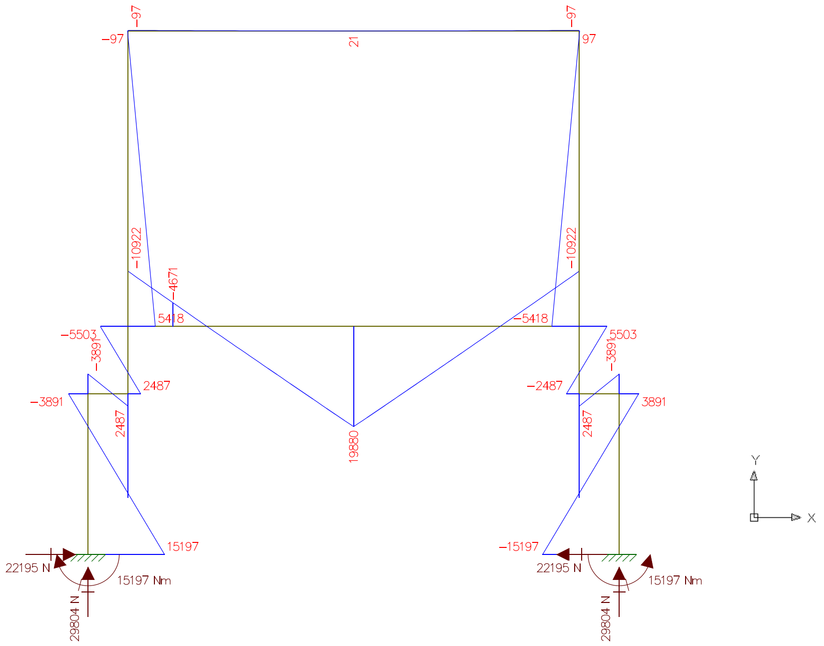

Figure 3-112 – Analytical model, bridge mid-span moment

The maximum moment is on the middle of the bridge with the value of 19880 Nm. The maximum moment on the shaft is on pillar/shaft connection with the value of 3891 Nm. The bottom of the pillar also as a considerable moment of 15197 Nm.

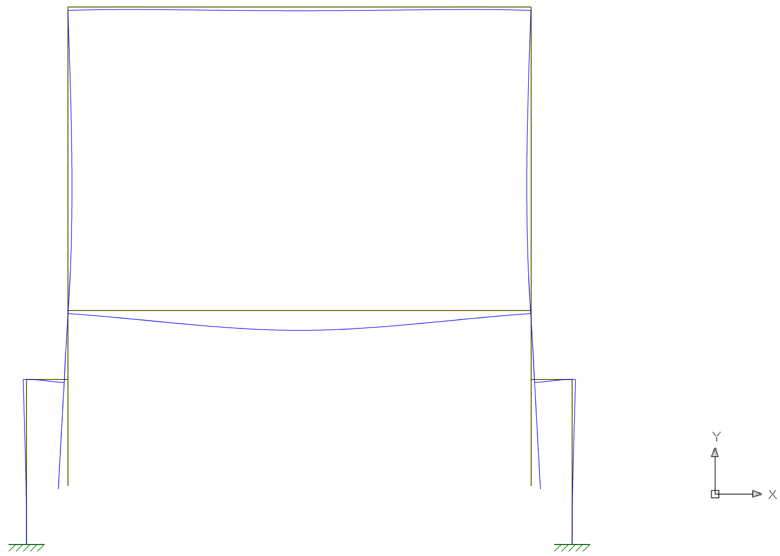

Figure 3-113 – Analytical model, bridge mid-span displacements

The maximum displacement on the middle of the bridge is of 1,049 mm on the Y direction. The displacement shown on the figure has a scale factor of 100.

3.9.2.2 Bridge end load

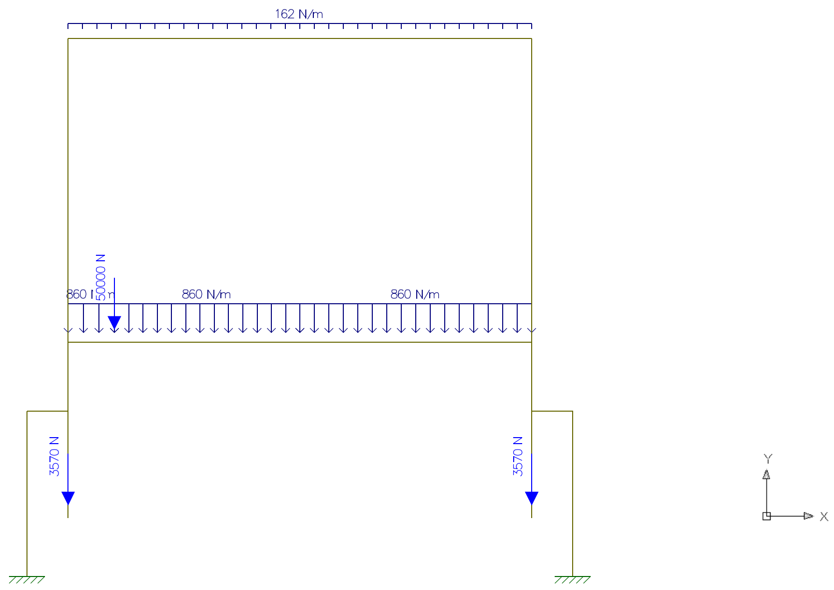

Figure 3-114 – Analytical model, bridge end loads

On this case, the load is applied on the end of the beam (as far as the actuator can reach). This loading causes different, more extreme forces on some of the elements due to the load distribution being different.

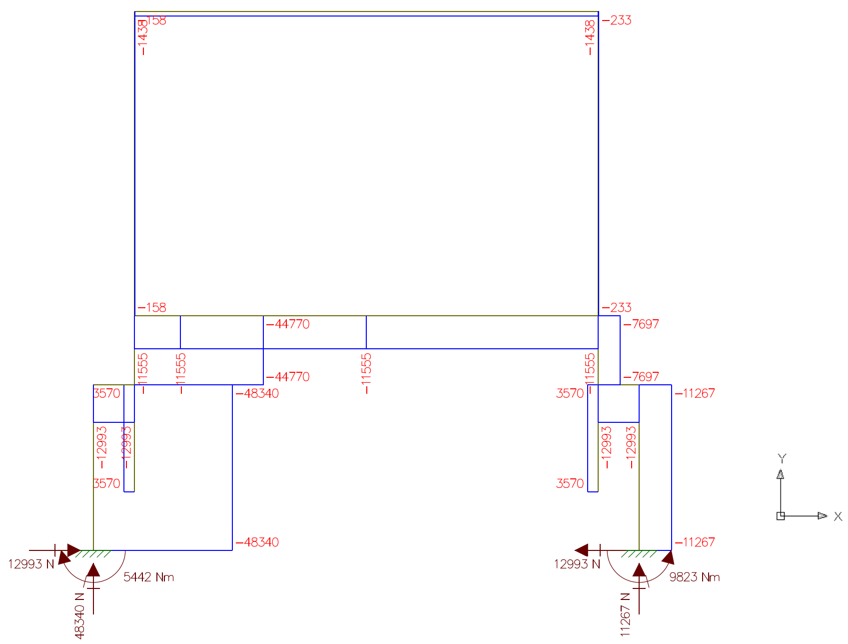

Figure 3-115 – Analytical model, bridge end axial force

The axial force is greater on the left pillar, with a value of 48340 N. The shaft supports an axial load of 12993 N. The left column has an axial load of 44770 N.

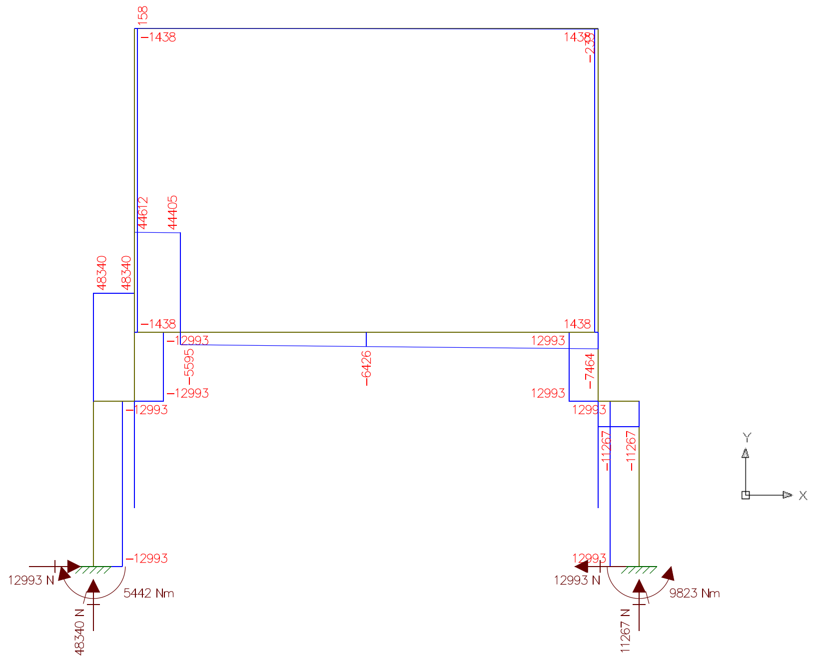

Figure 3-116 – Analytical model, bridge end shear force

The shear force is greater on the left shaft with a value of 48340 N. The bridge supports a shear force of 44612 N on the bridge/column connection. The pillar has a maximum shear force of 12993 N.

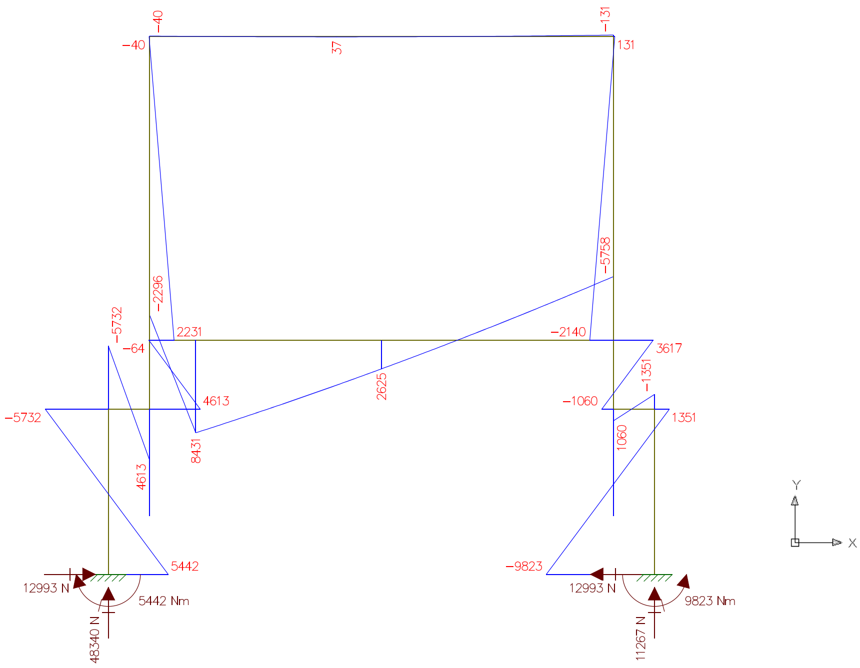

Figure 3-117 – Analytical model, bridge end moments

The maximum moment load on the bridge is where the load is applied with a value of 8431 Nm. The shaft as a maximum moment load of 5732 Nm while the pillar has a maximum moment load of 9823 Nm.

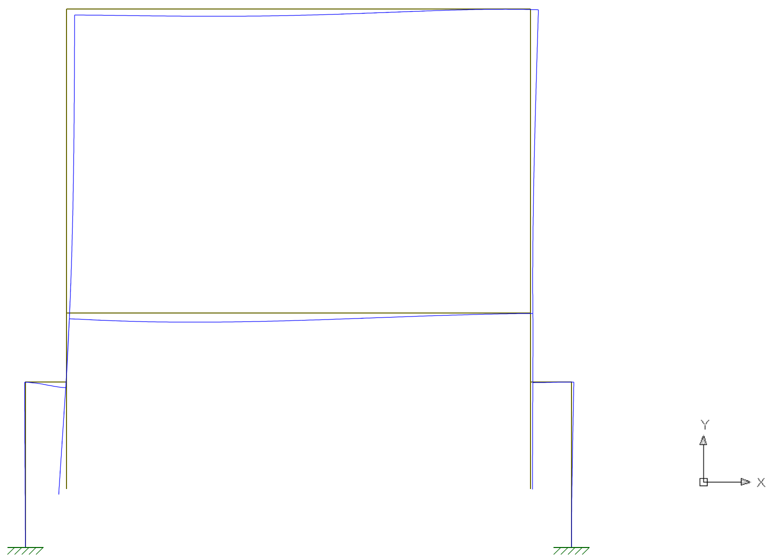

Figure 3-118 – Analytical model, bridge end displacements

The maximum displacement of 0,48mm is on the bridge on the local X=660 mm (starting from the joint of the bridge/column connection). The displacement has a scale factor of 100.

3.9.2.3 Bridge mid-span 45º load

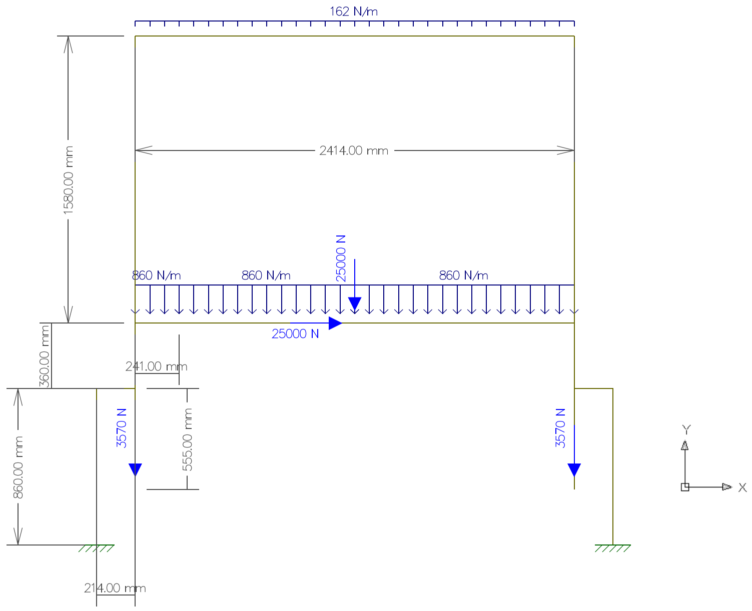

Figure 3-119 – Analytical model, bridge mid-span 45º loads

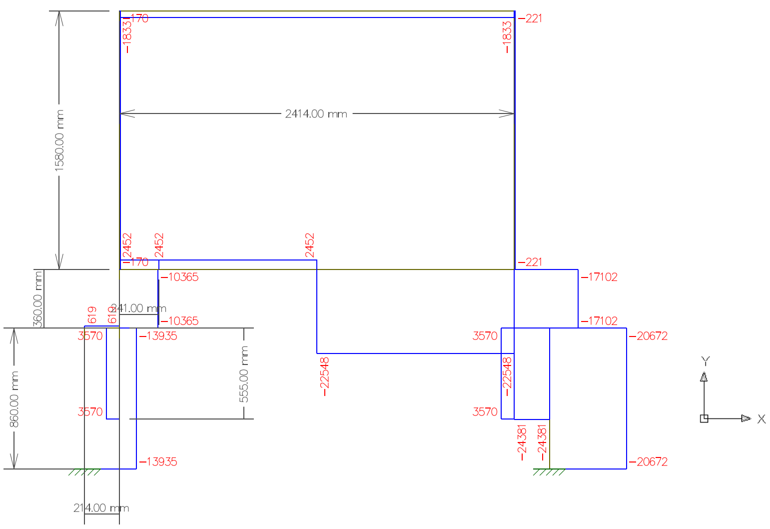

Figure 3-120 – Analytical model, bridge mid-span 45º axial force

On this case, the bridge has a maximum axial load of 23548 N, the shaft of 24381 N and the pillar of 20672 N.

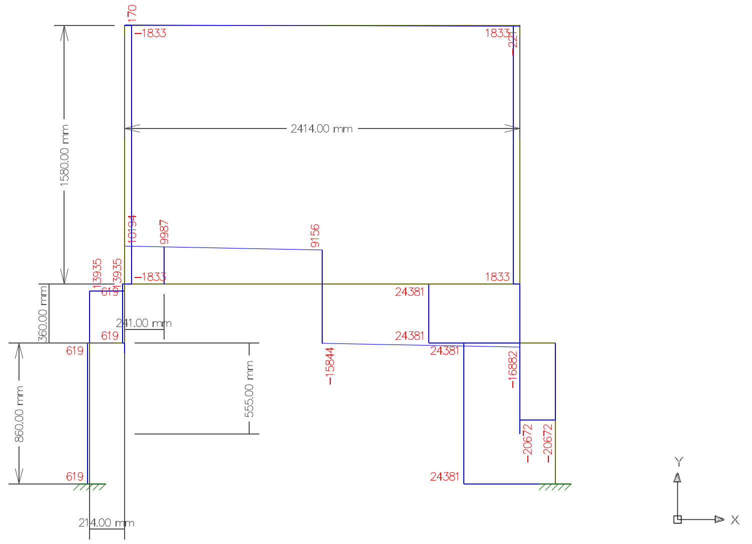

Figure 3-121 – Analytical model, bridge mid-span 45º shear force

For the shear force, it has a maximum value of 16882 N for the bridge, 20672 N for the shaft and 24381 N for the pillar.

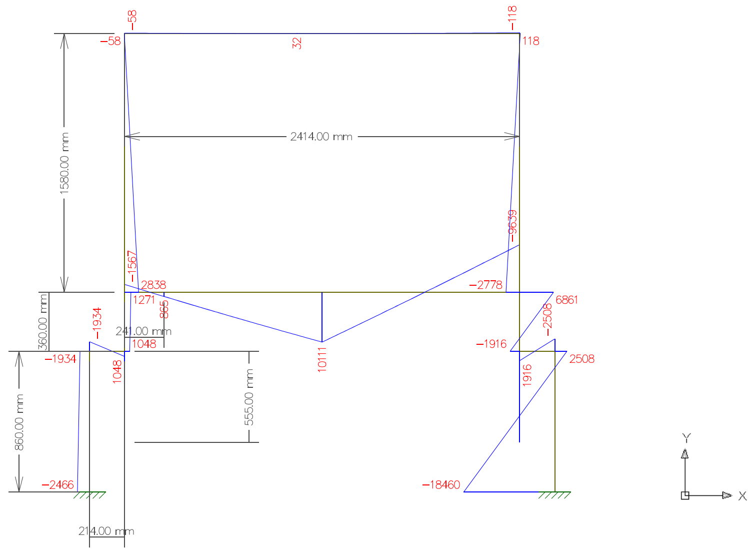

Figure 3-122 – Analytical model, bridge mid-span 45º momens

For the moment diagram, the bridge has a maximum value of 10111 Nm, the shaft of 2506 Nm and the pillar of 18460 Nm.

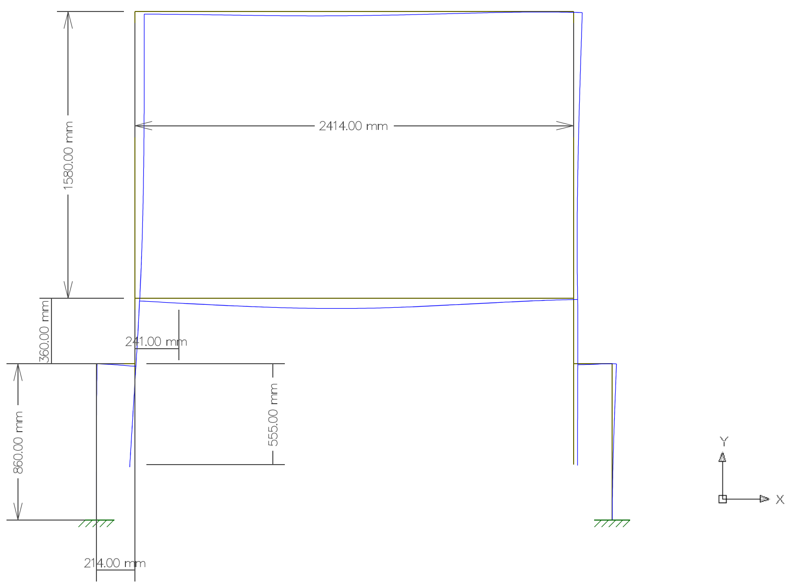

Figure 3-123 – Analytical model, bridge mid-span 45º displacements

For the displacements, the maximum displacement for the mid-point of the bridge, where the actuator is, it has a value of 0,25 mm in the X direction and of 0,54 mm in the Y direction.

3.9.3 Shaft analysis

3.9.3.1 Material selection

The shaft is a critical element on the structure. By the NTM diagrams we can see that it supports high loads, as well as being the main and only connection of the gantry to the base structure. So, it must be dimensioned in detail.

The shaft has a diameter of 65 mm and is made of a high strength material, the alloy steel number 1.6582, 34CrNiMo6.

The material selection was based on cost, availability, strength and environmental resistance.

This material 1.6582 is readily available commercially, not too expensive and has good strength and environmental resistance values.

Material properties:

Table 3-11 – Shaft material property list

Nominal Diameter (mm):	To 16	16 - 40	40 - 100	100 - 160	160 - 250
Rm - Tensile Strength (MPa) (+QT)	1200-1400	1100-1300	1000-1200	900-1100	800-950
Re - Upper yield strength or Rp0.2 - 0.2% proof strength (MPa) (+QT)	1000	900	800	700	600

For a diameter of 65 mm the tensile strength is of 1000 MPa and the upper yield strength is of 800 MPa.

- **Modulus of elasticity [MPa]:** 210
- **Density [g/cm^3]:** 7.84
- **Environmental resistance**
    - Flammability: very good
    - Fresh water: good
    - Organic solvent: very good
    - Oxidation at 500 ºC: good
    - Sea water: average
    - Strong acid: poor
    - Strong alkalis: poor
    - Wear: very good
    - Weak acid: average
    - Weak alkalis: good
    - Minimum service temperature: -73.2 to -42.2 ºC
    - Maximum service temperature: 613-653 ºC

3.9.3.2 Choosing the critical load case

On this load case, analysing the NTM diagrams, the critical section for the shaft is at the pillar connection.

The forces on that section are:

Table 3-12 – Shaft loads for each load case

Type of force	Mid-span	Beam end	Mid-span 45º
N [N]	22195	12993	24381
V [N]	29804	48340	20672
M [Nm]	3891	5732	2506

With the values from the different load cases, we can see that the worst case is when the actuator is at the beam end. We can assume this because on this kind of loadings, the shear and moment forces are always the most critical factor when determining the shaft resistance.

3.9.3.3 Shaft static resistance

$$N = 12993\ N$$

$$V = 48340\ N$$

$$M = 5732\ Nm$$

To check for the resistance of the shaft, first the stresses need to be calculated.

The section properties for the shaft are as follows:

- Section modulus: $W = 26961{,}25\ mm^3$
- Polar moment of inertia: $J = 1752500\ mm^4$
- Section area: $A = 3318{,}31\ mm^2$
- Normal stress: $\sigma_N = \frac{N}{A} = \frac{12993}{3318{,}31} = 3{,}92\ MPa$
- Shear stress: $\tau_V = \frac{V}{A} = \frac{48340}{3318{,}31} = 14{,}57\ MPa$
- Flexural stress: $\sigma_M = \frac{M}{W} = \frac{5732000}{26961{,}25} = 212{,}60\ MPa$
- Torsional Stress: $\tau_{Mt} = \frac{M_t \times r}{J} = \frac{620000 \times 65/2}{1752500} = 11{,}50\ MPa$

With the 3 stresses, we can now calculate the equivalent stress (Von Mises):

$$\sigma_{eq}^{VM} = \sqrt{\frac{(\sigma_{11} - \sigma_{22})^2 + (\sigma_{22} - \sigma_{33})^2 + (\sigma_{11} - \sigma_{33})^2 + 6({\sigma_{12}}^2 + {\sigma_{23}}^2 + {\sigma_{31}}^2)}{2}}$$

Solving the equivalent stress equation yields an installed stress of $218{,}89\ MPa$.

This value has a factor of safety of 3,65, for a load of 50 kN.

$$\sigma_{inst} = \frac{\sigma_{yield}}{n} \Leftrightarrow 218{,}89 = \frac{800}{n} \Leftrightarrow n = 3{,}65$$

3.9.3.4 Shaft fatigue analysis

The fatigue analysis takes various factors into account.

The maximum fatigue allowable stress is:

$$\sigma_f = k_a k_b k_c k_d k_e k_f \sigma_{f0}$$ – [Eq. 6 (Domingues, 2003)]

Where k_n are factors that will change the maximum fatigue stress:

k_a – surface finish

k_b – sizer

k_c – reliability

k_d – temperature

k_e – stress concentrations

k_f – other effects

σ_{f0} – fatigue strength

For steels, the fatigue strength is given as:

$$\begin{cases} \sigma_{f0} = 0{,}5 \times \sigma_r \leftarrow \sigma_r \leq 1400\ MPa \\ \sigma_{f0} = 700\ MPa \leftarrow \sigma_r > 1400\ MPa \end{cases}$$ [Eq. 6-8 (Budynas & Nisbett, 2011)]

On this case, the fatigue strength for this material is of $0{,}5 \times \sigma_r = 500\ MPa$, and the k_n factors are:

$k_a = 0{,}7$ – Machined – [Fig. 5 (Domingues, 2003)]

$k_b = 0.87$ - $8\ mm \leq D \leq 250\ mm \rightarrow 1{,}189 \times d^{-0{,}097}$ $d = 0{,}37 \times D$ – [Eq. 7, 8, 9 and 10 (Domingues, 2003)]

$k_c = 0.87 - \mathrm{R} = 0{,}95 \wedge \mathrm{S} = 8\%$ – [Eq. 14 and 15 and tables 1 and 2 (Domingues, 2003)]

$k_d = k_e = k_f = 1$ - $T \leq 350°\mathrm{C} \wedge$ No other effects – [Eq. 16, 17, 18, 19 and 20 (Domingues, 2003)]

Getting all the factors, taking into account the loads that the shaft will support, the maximum fatigue strength is of $265{,}34\ MPa$.

Both the stress values for the static load and fatigue load are below the limits and are done for twice the load expected.

With this analysis we can conclude that the chosen shaft diameter and material are appropriate.

► The higher values for factor of safety and resistance are to increase the rigidity of the system, decreasing the maximum deflections, which would interfere with the results given by the equipment.

3.9.4 Bolt connection analysis

Although the bolted connections are designed to support the loads through friction and not shear, the bolts are dimensioned to support the loads even if the axial pre-load is not enough.

3.9.4.1 Choosing the critical load

On this case, it is the bridge loading that is taken into account.

Table 3-13 – Pin loads for each load case

Type of force	Mid-span	Beam end, left node	Beam end, right node
V [N]	26038	44612	7464
M [Nm]	10922	2296	5758

On this case, due to the combination of the shear and moment forces, the critical load case is not clear, because both the mid-span loads and the beam end, left node loads are high. To solve that, the force of the most loaded bolt is calculated taking into account both the shear and moment force.

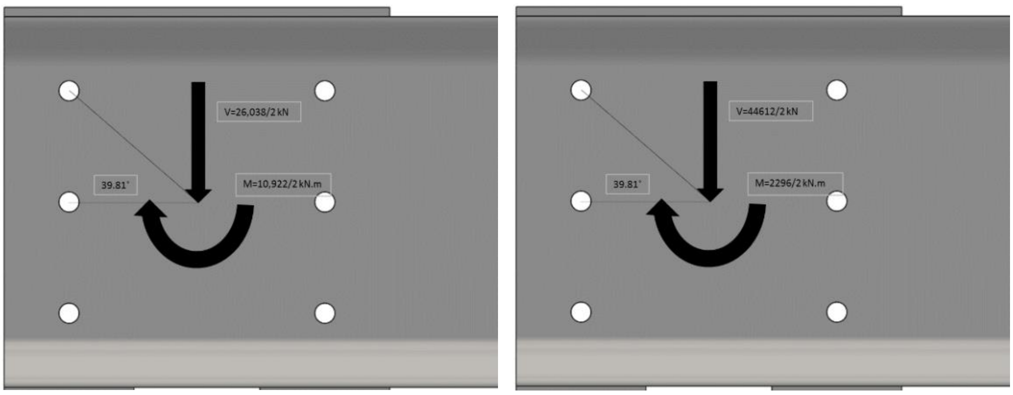

Figure 3-124 – Bolt loads, left: Mid-span, right: Beam end, left node

For the shear force of the mid-span case, the load on each bolt is:

$$F_v = \frac{V/2}{n} = \frac{26038/2}{6} = 2170\ N$$

For the moment force the distances to the centre point of the connection must be calculated and are as follows:

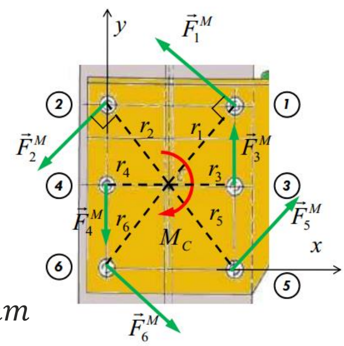

$$r_1 = r_2 = r_5 = r_6 = 93{,}72\ mm$$

$$r_3 = r_4 = 72\ mm$$

And:

$$K = \frac{M}{\sum_{i=1}^{n} r_i^2} = \frac{\frac{10922}{2}}{r_1^2 + r_2^2 + r_3^2 + r_4^2 + r_5^2 + r_6^2} = 0{,}12\ kN/mm$$

$$F_i^M = K \times r_i$$

$$F_1^M = F_2^M = F_5^M = F_6^M = 11248\ N$$

$$F_3^M = F_4^M = 8641\ N$$

The two bolts that are more loaded are the number 2, 4 and 6.

Using trigonometric relations we can obtain the total acting forces on those bolts:

$$F_2^T = F_6^T = 2170 + 11248 \times \cos 39{,}81 = 10810\ N \wedge F_4^T = 2170 + 8641 = 10811\ N$$

For the beam end, left node:

$$F_v = \frac{V/2}{n} = \frac{44612/2}{6} = 3718\ N$$

$$K = \frac{M}{\sum_{i=1}^{n} {r_i}^2} = \frac{\frac{2296}{2}}{{r_1}^2 + {r_2}^2 + {r_3}^2 + {r_4}^2 + {r_5}^2 + {r_6}^2} = 0{,}03\ kN/mm$$

$$F_i^M = K \times r_i$$

$$F_1^M = F_2^M = F_5^M = F_6^M = 2365\ N$$

$$F_3^M = F_4^M = 1817\ N$$

$$F_2^T = F_6^T = 3718 + 2365 \times \cos 39{,}81 = 5535\ N \wedge F_4^T = 3718 + 1817 = 5535\ N$$

We can conclude that the mid-span case is the worst.

3.9.4.2 Bolt resistance check

For this case:

$$F_{Max}^{Bolt} = 10811\ N$$

And the maximum allowable shear force for and M10 A2-70 stainless steel bolt:

$$F_{v,Rd} = \frac{\alpha_v \times f_{ub} \times A_s}{\gamma_{M2}}$$ – (Cl. 3.6.1 - EN 1993-1-8)

Where:

$\alpha_v = 0{,}5 -$ Shear on the threaded part – (Cl. 3.6.1 - EN 1993-1-8)

$f_{ub} = 700\ MPa -$ For an A2 – 70 Stainless steel bolt

$A_s = 58\ mm^2 -$ Shear area for an M10 bolt

$\gamma_{M2} = 1{,}25$ – (EN 1993-1-1)

$F_{v,Rd} = 16240\ N > 10811\ N$

3.9.5 Pin connection analysis

The precision pins are used to help position the bridge but also to support the loads in case the bolts fail.
M12 pins are used, and the shear force that they support:

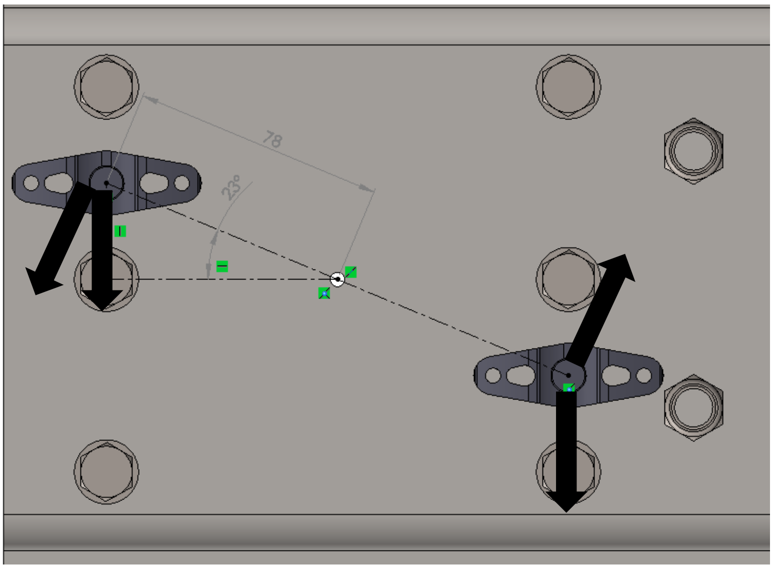

Figure 3-125 – Pin loads

$$F_v = \frac{V/2}{n} = \frac{26038/2}{2} = 6510\ N$$

$$F_M = \frac{10922/2}{0{,}078 \times 2} = 35006\ N$$

$$F_T = 6510 + 35006 \times \cos 23 = 38733\ N$$

These pins are rated at a maximum shear load of 144 kN, so we can conclude that they will support this load.

$$144\ kN > 38{,}7\ kN$$

3.10 FEA

The model used in the FE analysis was simplified. These simplifications do not change significantly the real results to be expected from the structure. The figure below shows the FEA model.

It must be taken into account that local stresses, such as the maximum values on certain connections that we can get from this FEA analysis, are not relevant to this method. The local stresses calculations were done on the analytical approach. As such, the results this analysis focus on are the displacements for the bridge.

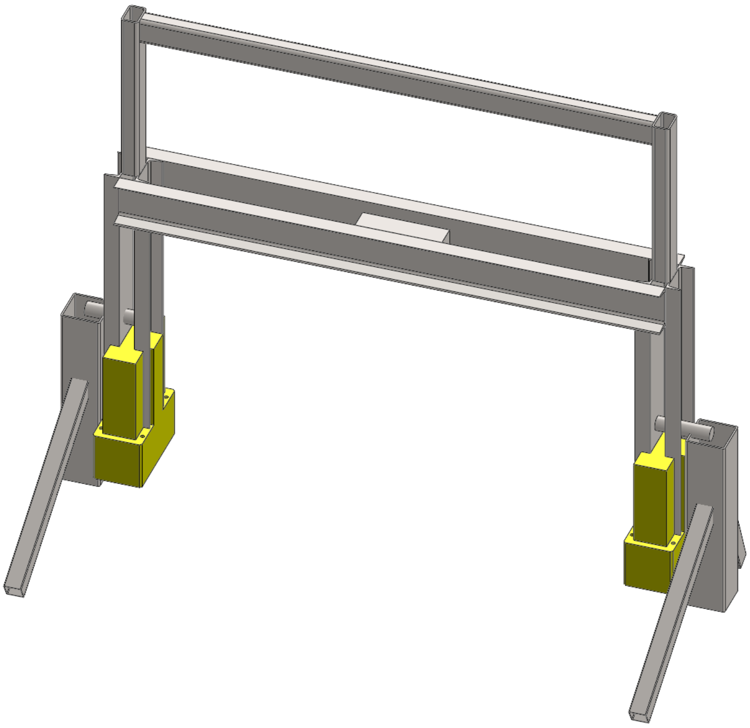

Figure 3-126 – Simplified FEA model

The rest of the page has been left intentionally blank

3.10.1 Gantry and pillars finite element model

The model for this analysis is made of mostly beam elements except for the counter weights and the actuator block which are solids but their elasticity is not considered to the analysis, only their weight and geometry for simplification and to reduce the simulation time, while still being a good enough approximation.

The type of finite elements used was quadratic tetrahedral (TET10, 10 nodes) for the solid elements and beam elements (2 nodes).

The FEA results for this part were not disclosed.

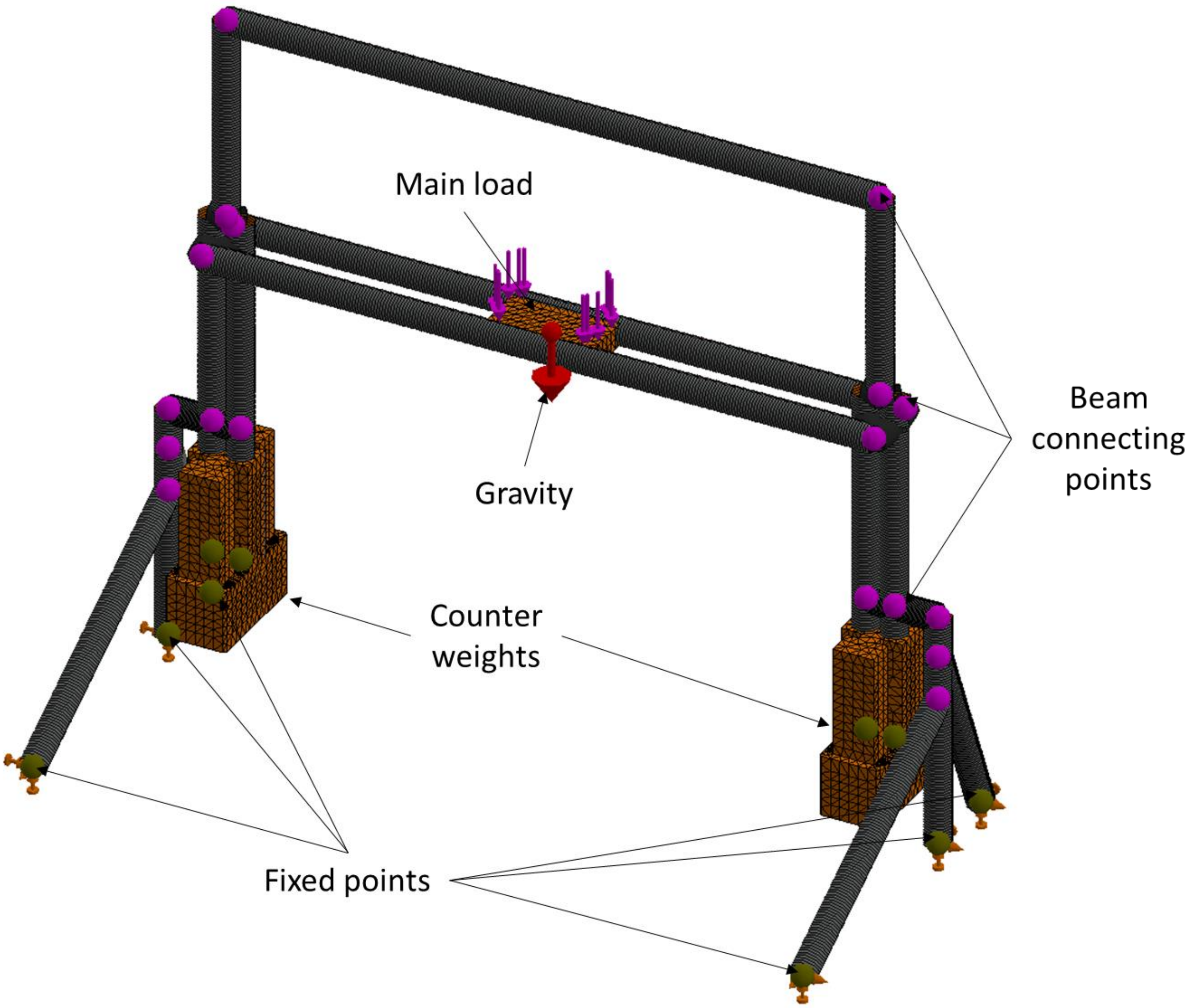

Figure 3-127 – Gantry and pillars mesh model

3.10.2 Actuator Supports analysis

FEA was also conducted for the actuator supports. In this case, contact was simulated between the hydraulic cylinder trunnion and the supporting plate. Figure 3-128 and Figure 3-129 show the meshed model of the assembly.

The complete analysis and results are not present in this work, due to privacy requirements from the employer.

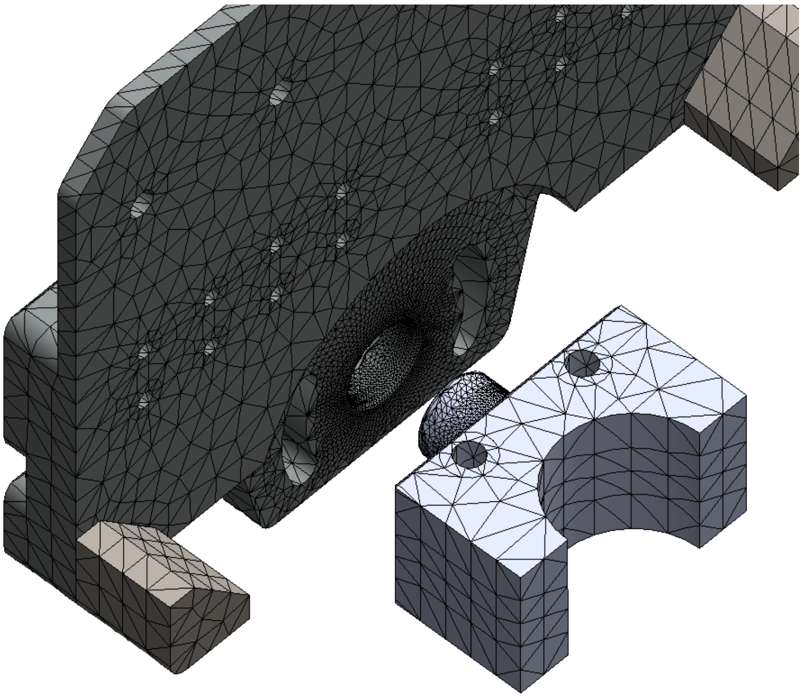

Figure 3-128 – Meshed model of the main actuator support

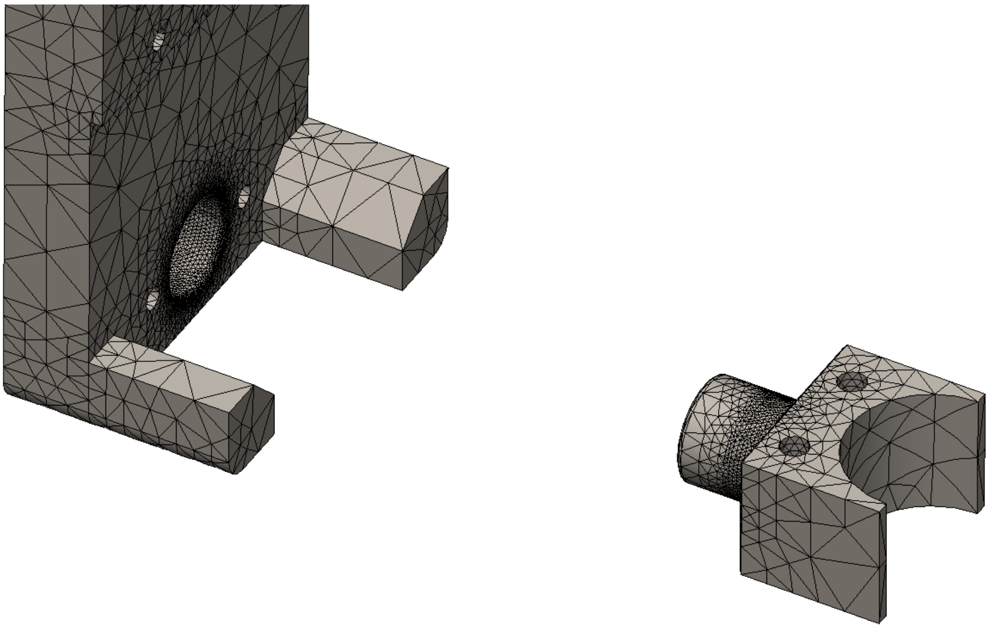

Figure 3-129 – Secondary actuator meshed model

3.11 Frequency analysis

For the frequency analysis, the goals are to isolate the equipment under test from vibrations of the structure and from the outside. The value to achieve is a minimum frequency of at least 400Hz for any part of the structure that is directly connected to the CCB.

The models shown below are slightly different from the final model, but this analysis was done in that phase of the project, so it makes sense to use them and since the last version has increased stiffness, this scenario is worse than the final one. Regardless of that, by experience, it can be assumed that the structure will have low frequency modes, and that with so many elements it would be very difficult to pinpoint the ones causing significant disturbance in the CCB readings. So, with that conclusion, the results below are just a very simplified approach to just have a general idea of the structure performance. It was assumed from the start of the resolution of the vibration performance that we would need to dampen the structure. To solve that it was specified to embed the base in concrete and save time and resources trying to optimize a structure which is not at all appropriate for vibration testing.

3.11.1 Structure

The image below shows a previous state of the structure, and its fixations/supports:

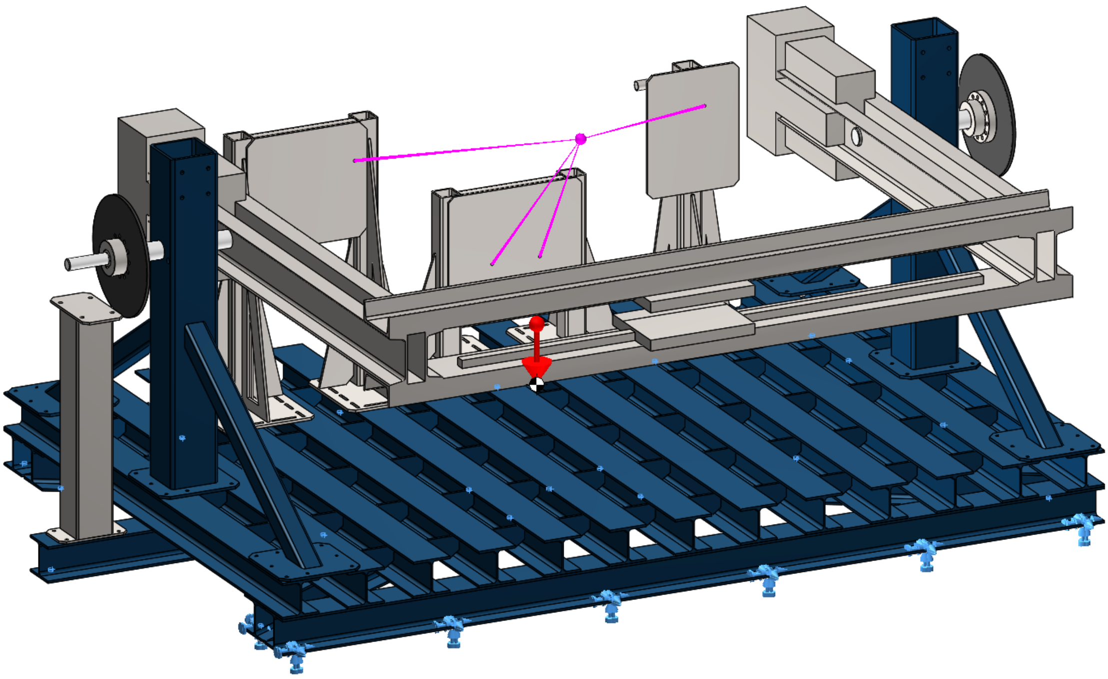

Figure 3-130 – Structure fixed to the ground

The pink lines and dot represent the CCB and its center of mass (remote mass with the correct mass and moments of inertia used, to simplify the model). The blue arrows represent the fixation of the structure to the ground.

The table below shows the first 30 modes.

Table 3-14 - Structure fixed to the ground modes of vibration

Mode No.	Frequency(Hertz)	Mode No.	Frequency(Hertz)
1	16,47	16	109,92
2	20,47	17	113,61
3	20,89	18	145,89
4	25,13	19	150,70
5	29,02	20	154,46
6	37,87	21	162,62
7	46,64	22	166,98
8	49,12	23	177,35
9	53,30	24	179,71
10	62,89	25	197,88
11	77,92	26	202,87
12	84,72	27	209,55
13	92,76	28	221,11
14	96,66	29	224,09
15	97,77	30	228,69

Below are some of the modes.

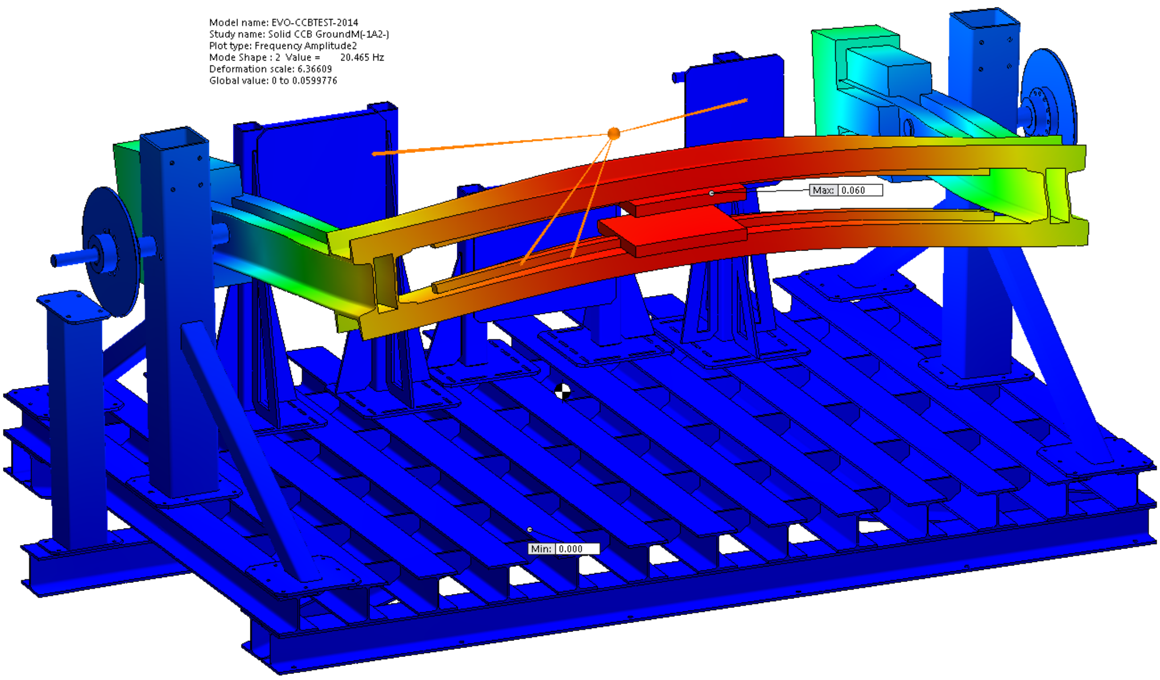

Figure 3-131 – Structure frequency analysis: 2nd mode

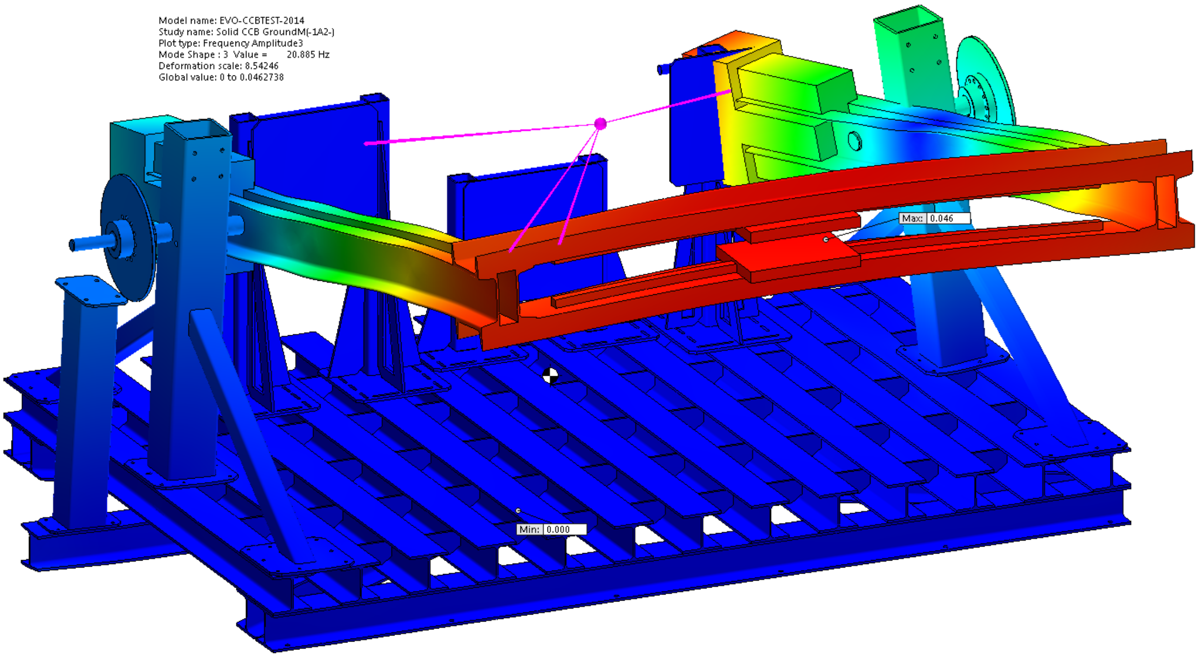

Figure 3-132 – Structure frequency analysis: 3rd mode

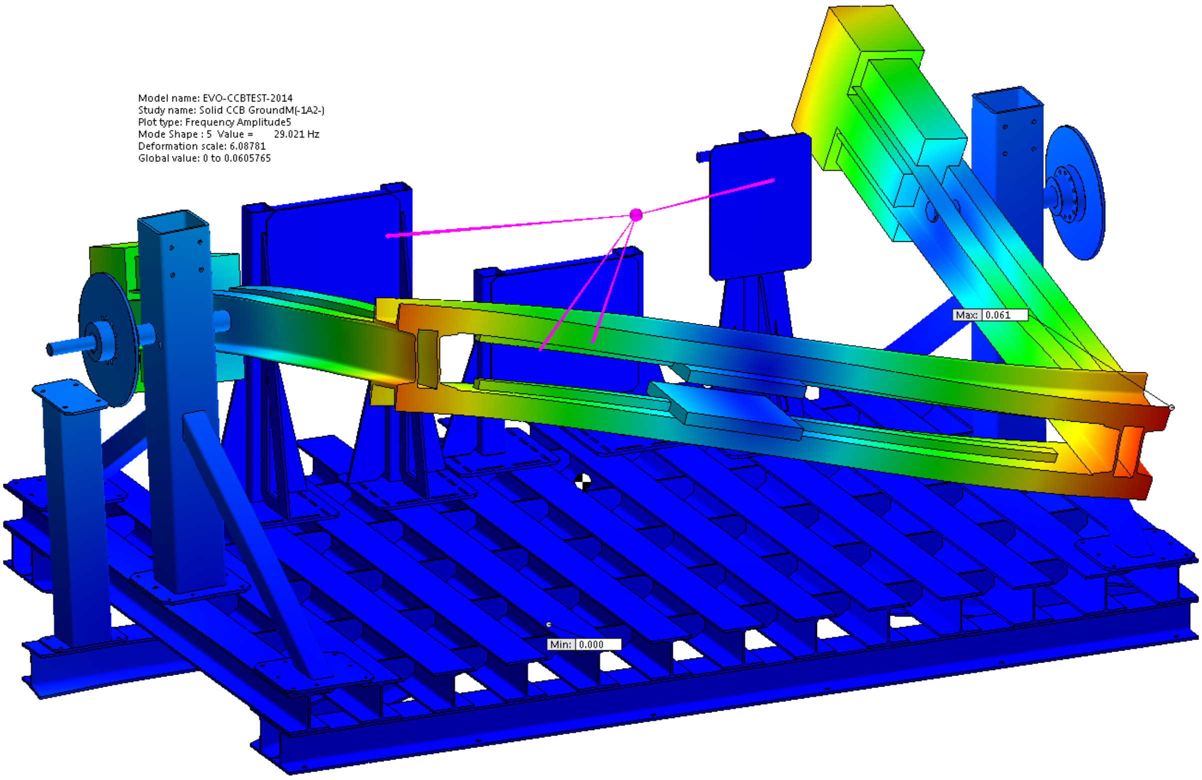

Figure 3-133 – Structure frequency analysis: 5th mode

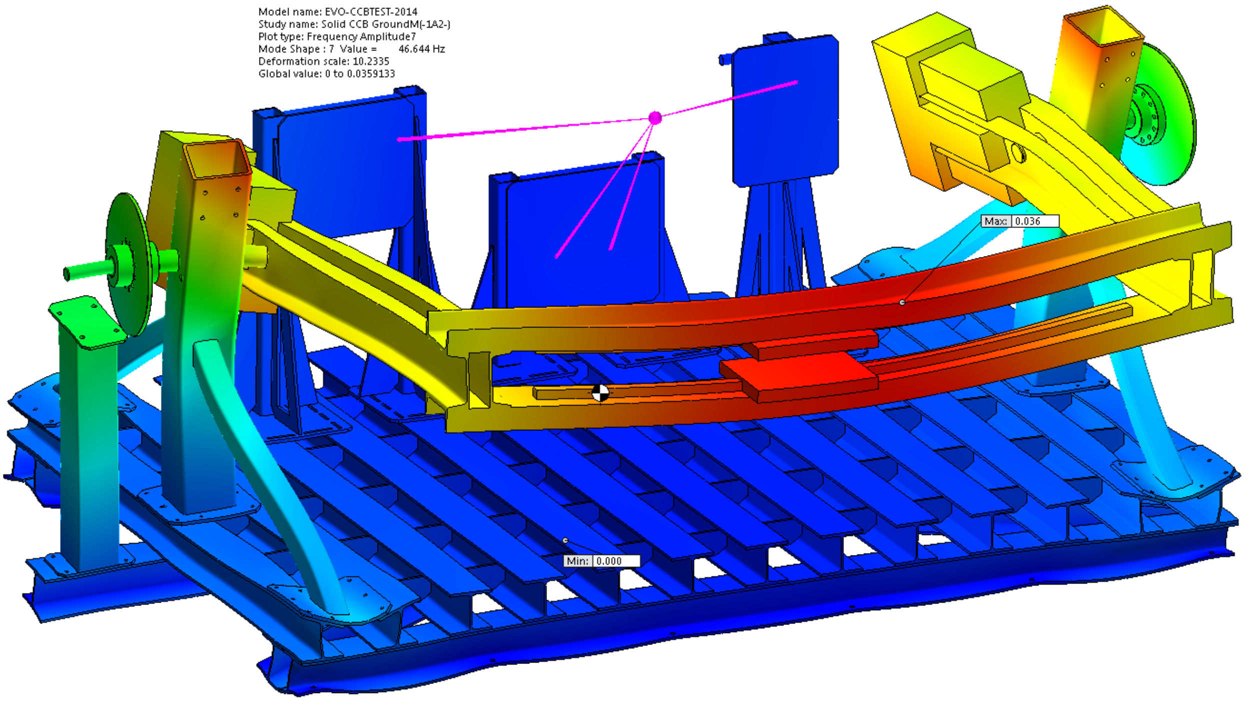

Figure 3-134 – Structure frequency analysis: 7th mode

The rest of the page has been left intentionally blank

Having so many components, it would be too time consuming to find what local modes could affect the CCB supports, if excited.

Experimental tests were conducted on the structure with accelerometers that showed that the CCB supports and the CCB itself is affected by the structure local modes.

Accelerometers were mounted on multiple parts of the structure as well as the CCB itself. Below are some pictures of the tests. The tests concluded that there are far too many residual vibrations that can affect the readings during testing.

Figure 3-135 – Experimental testing of the structure

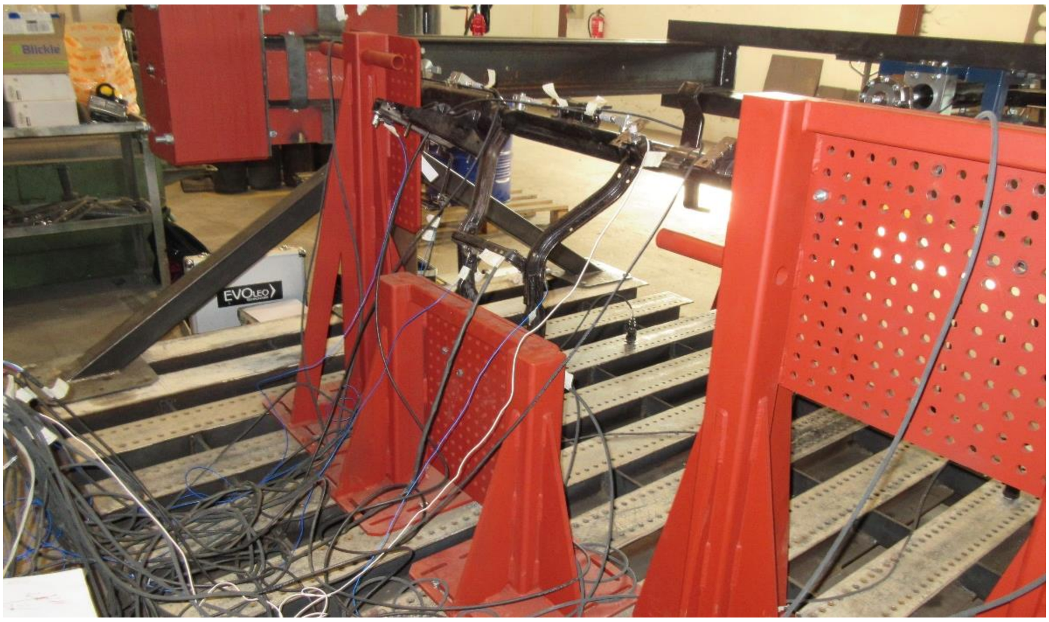

Figure 3-136 – Experimental testing of the structure

Figure 3-137 – Experimental testing of the structure

To try and isolate the CCB supports from the rest of the structure, a new solution was conceived, which is simply merging part of the base structure in solid concrete. This, in theory should dissipate any vibrations caused by the gantry system before those vibrations get to the supports. The image below shows how it would look after the base structure is concreted.

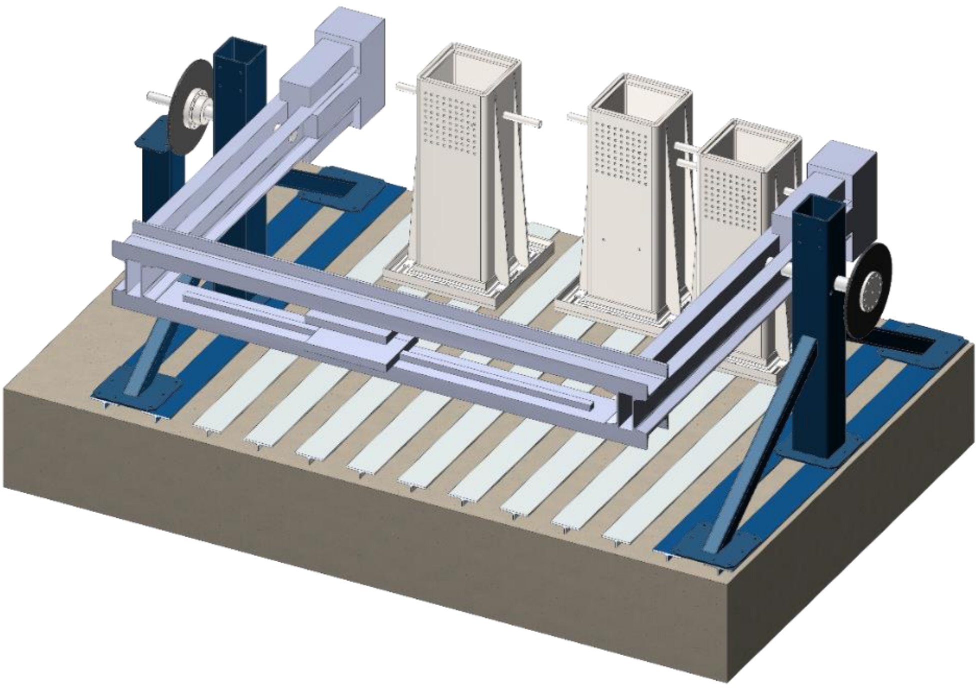

Figure 3-138 – Embedded structure

Next are the results of the simulation with the concrete base which are very similar to the previous results. The reason for this is that the first modes are all of the surrounding structure, and not of the base itself.

The structure is embedded in the concrete and the concrete base is fixed on its lower face.

Table 3-15 – Embedded structure modes of vibration

Mode No.	Frequency(Hertz)	Mode No.	Frequency(Hertz)
1	16.76	16	157.23
2	21.14	17	158.14
3	21.58	18	163.79
4	26.43	19	174.06
5	29.81	20	175.05
6	38.73	21	178.31
7	48.31	22	181.93
8	49.49	23	187.82
9	54.92	24	194.08
10	62.46	25	222.15
11	81.24	26	224.35
12	86.03	27	228.35
13	98.77	28	229.67
14	101.08	29	237.51
15	112.67	30	240.74

The images below show some of the modes.

The study shows that the concrete base does indeed dissipate the vibrations of the gantry system, this way the CCB Supports are not affected by the rest of the structure.

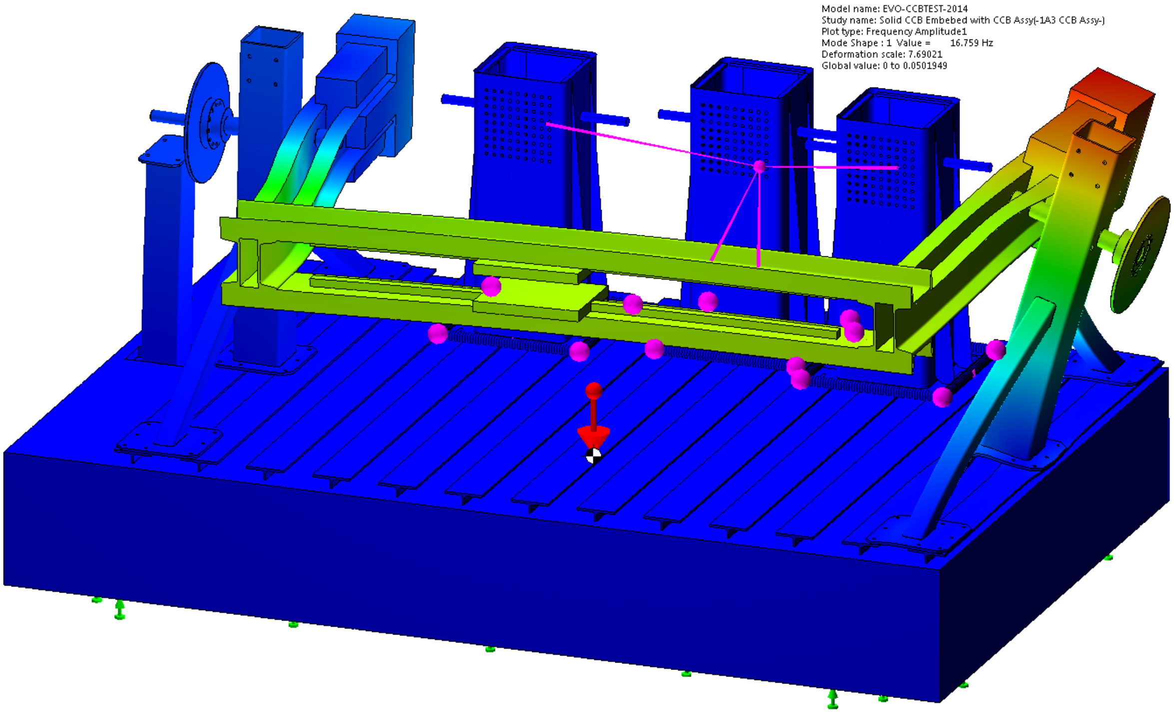

Figure 3-139 – Embedded structure frequency analysis 1st mode

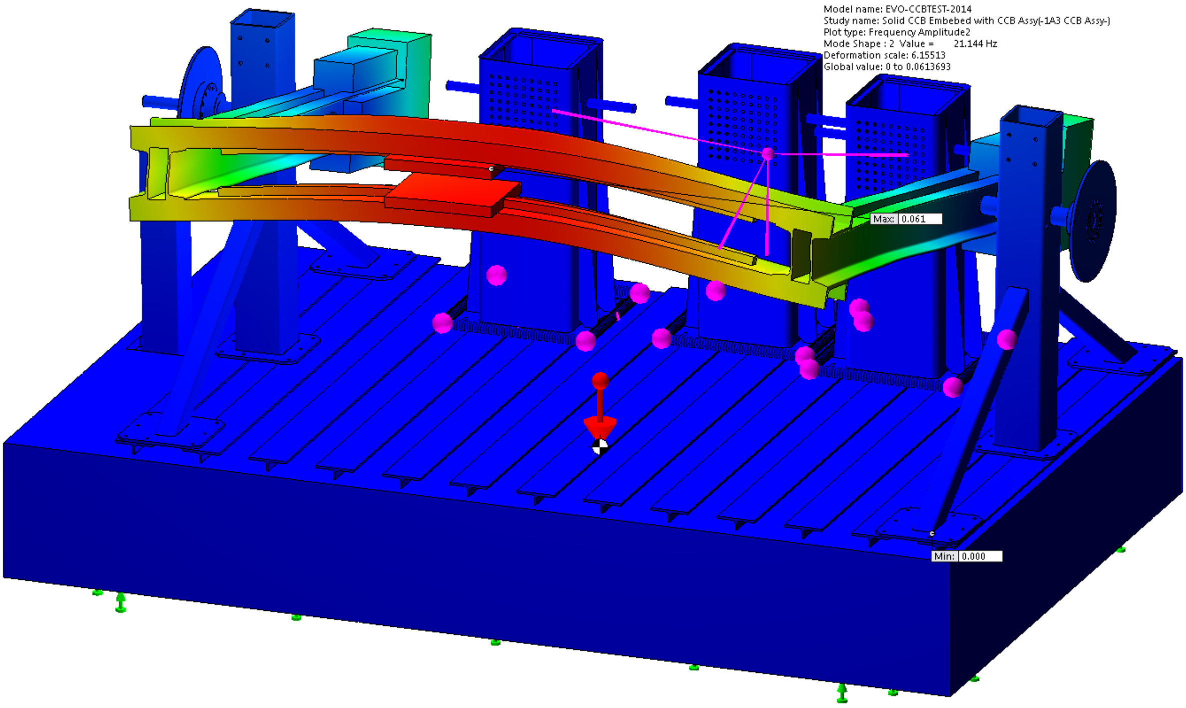

Figure 3-140 – Embedded structure frequency analysis 2nd mode

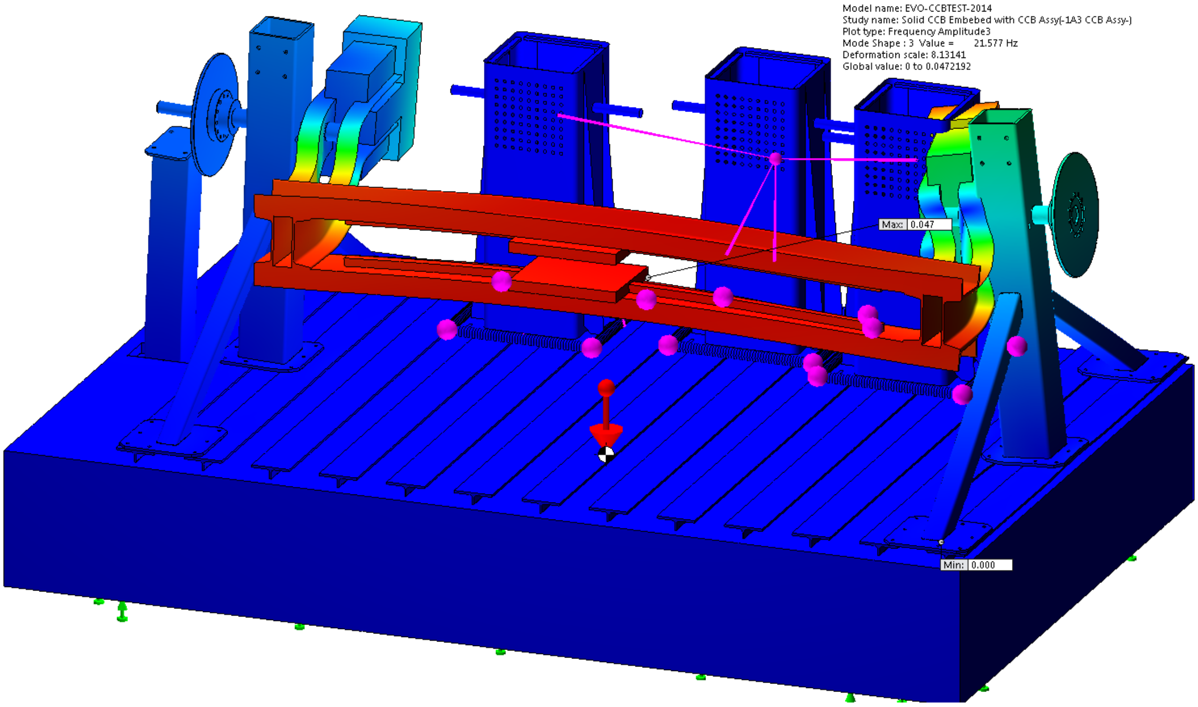

Figure 3-141 – Embedded structure frequency analysis 3rd mode

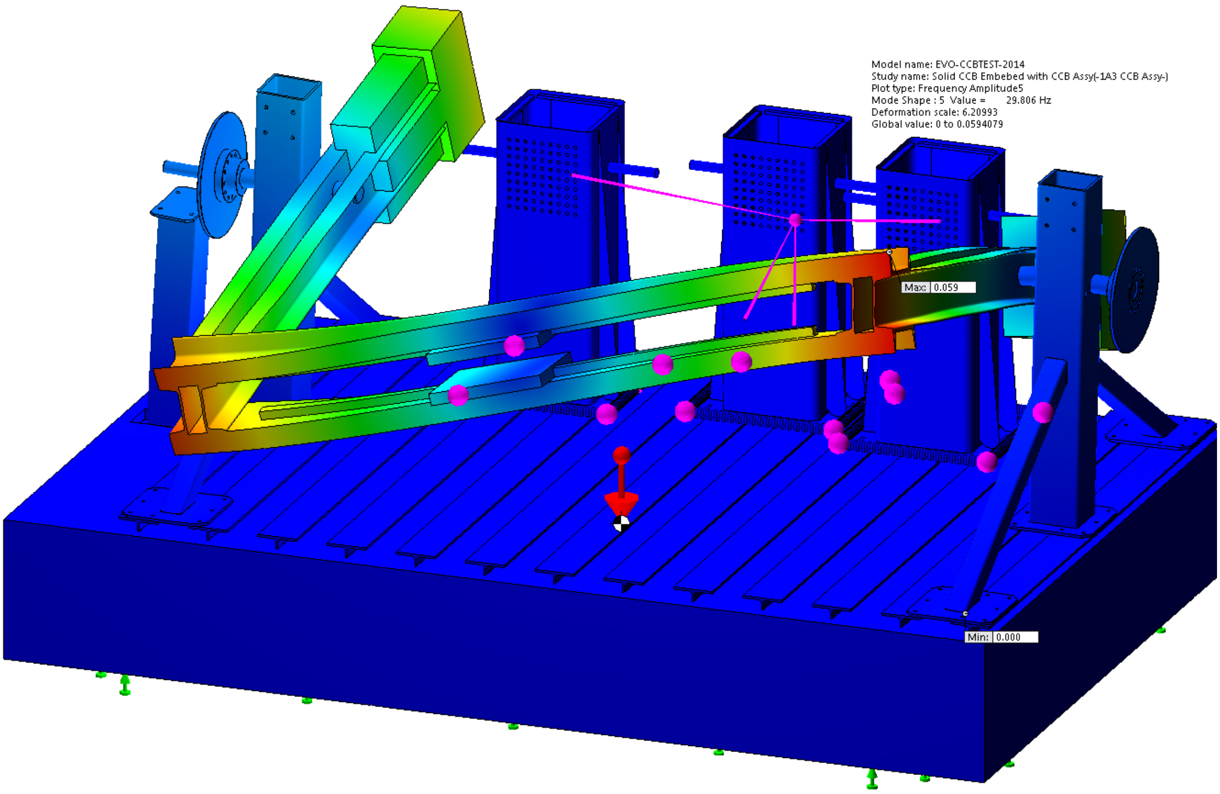

Figure 3-142 – Embedded structure frequency analysis 5th mode

We can conclude that the concrete base does work as expected, to eliminate the transfer of vibrations from the gantry to the base beams even if the gantry and other components vibrated at low frequencies, that effect does not affect the testing zone (base beams) due to the damping effect of the concrete embedding the beams.

3.11.2 Base embedded beam local analysis

With the steel base embedded in the concrete, there might be some unwanted vibrations of the portion that is free.

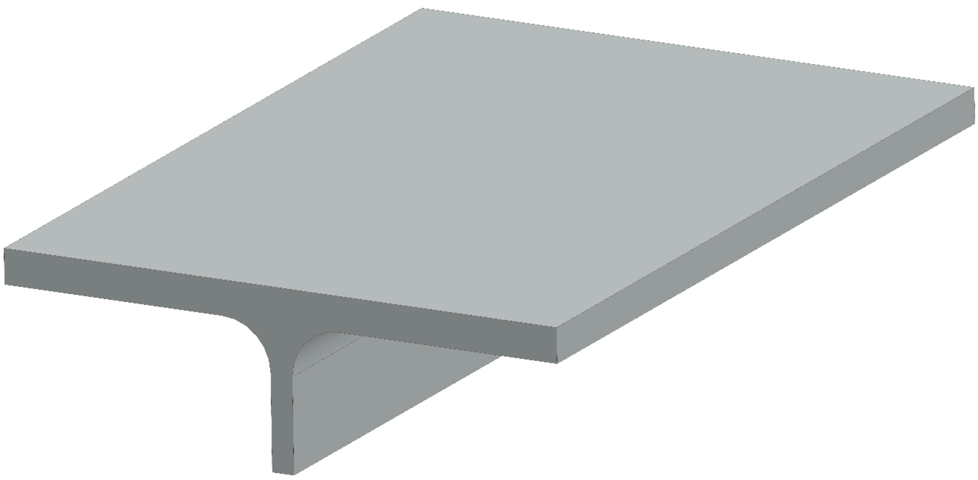

Figure 3-143 – Portion of the beam free off the concrete

The portion of the beam was fixed on its lower face and a gravity load was applied.

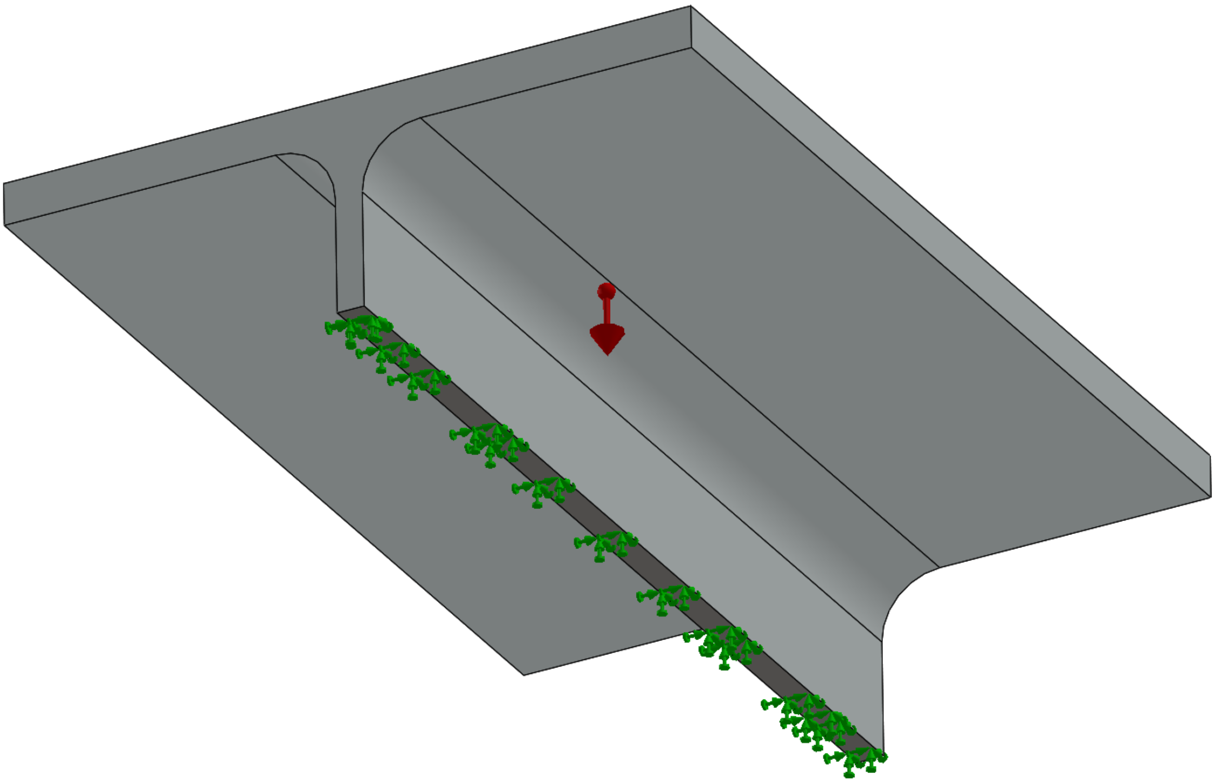

Figure 3-144 – FEA boundaries

The next figure shows the mesh utilized.

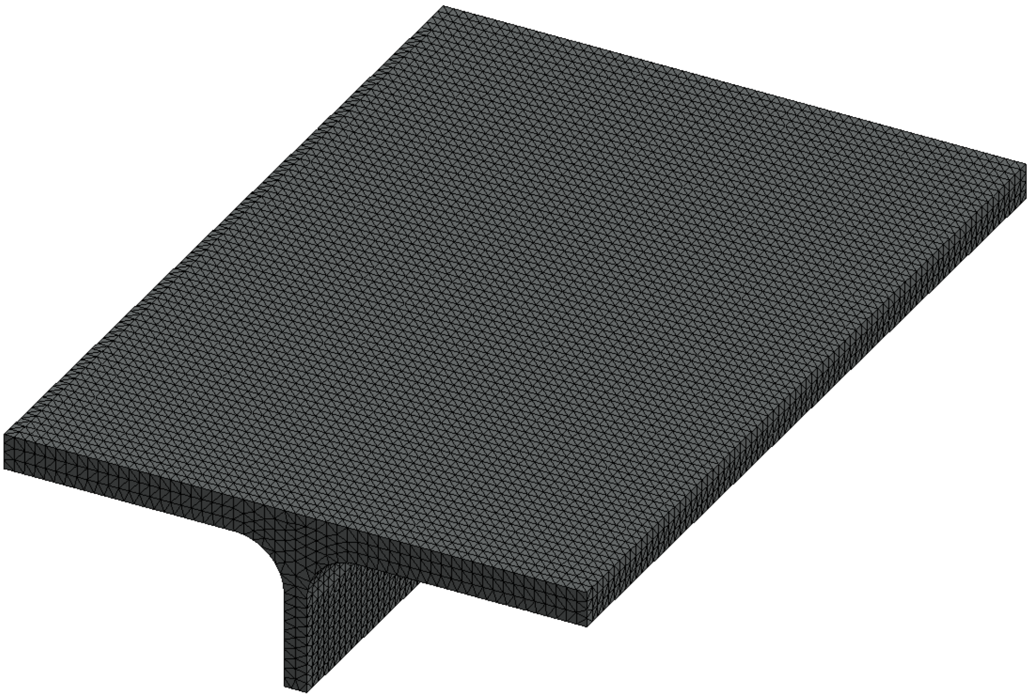

Figure 3-145 – Meshed model of the flange of the beam

As it can be seen, the mesh is very refined, providing good results. The next figure shows the first mode of vibration.

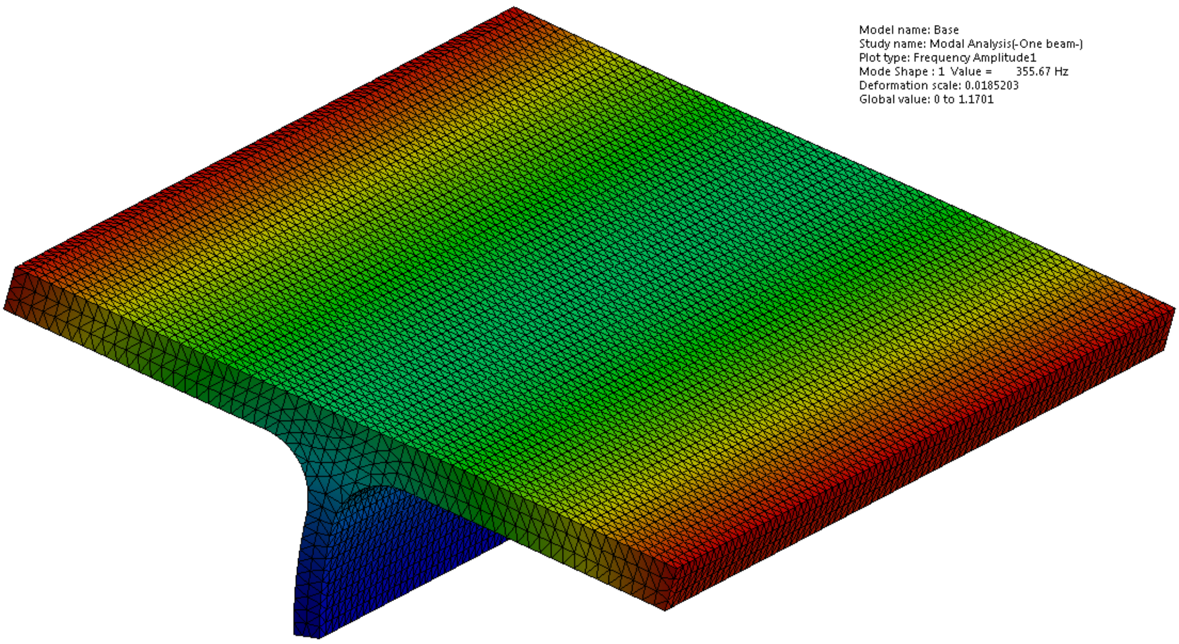

Figure 3-146 – First mode of vibration of the flange of the beam

The portion of the beam free of the concrete still shows some unwanted vibrations at 355Hz, to fix that problem, a new area for the NVH testing was developed where the concrete fully embeds the beams, this way the beam is completely fixed, providing the best fixation scenario for the CCB supports.

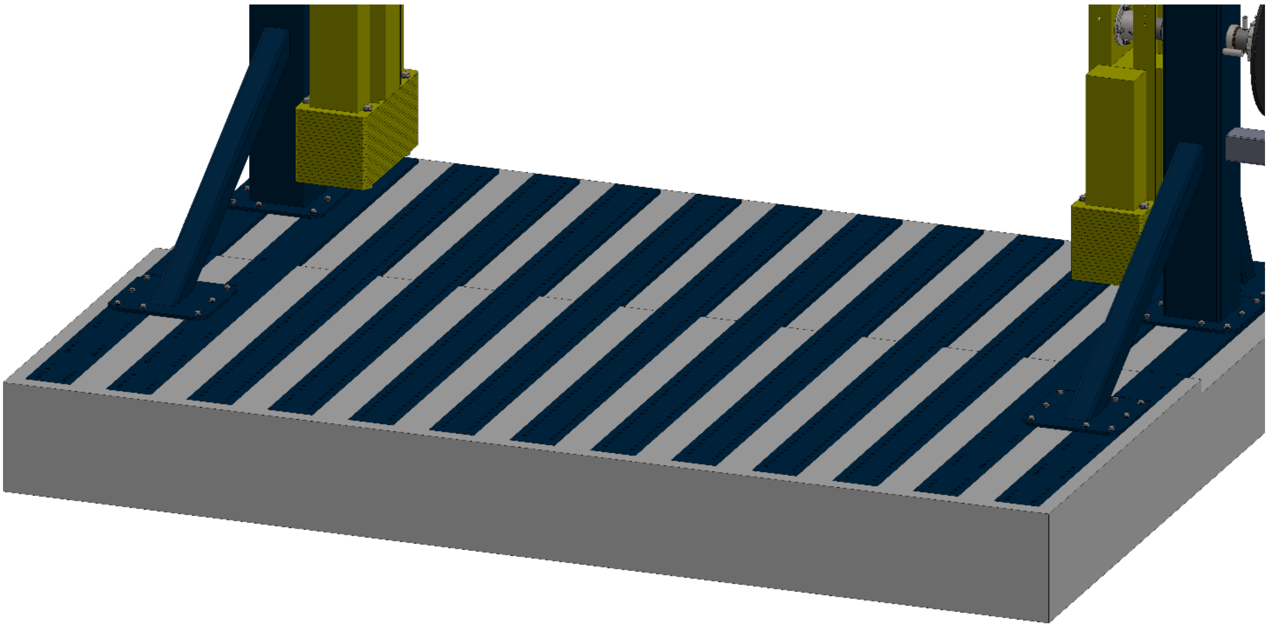

Figure 3-147 – Full concrete embedment of a part of the base

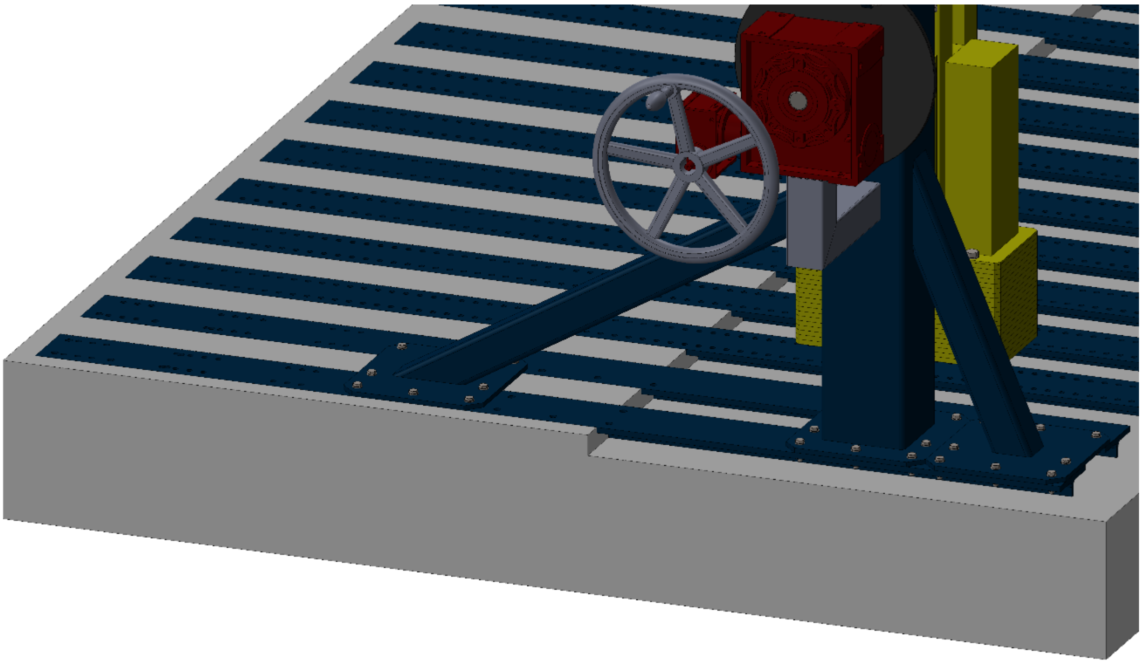

Figure 3-148 – Full concrete embedment of a part of the base

The area shown on the picture below represents the reserved area for NVH testing.

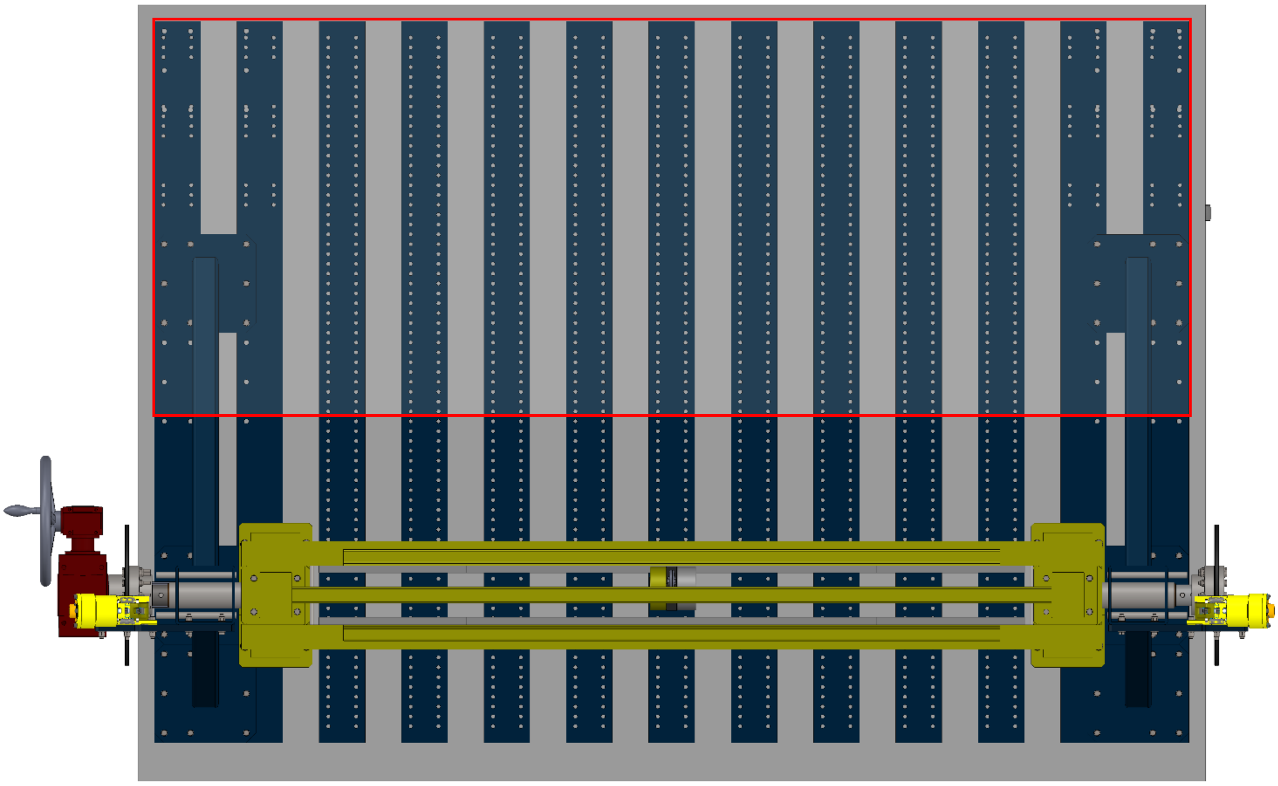

Figure 3-149 – NVH testing area

This solution completely isolates the CCB from the vibration effects of other components, creating an appropriate zone for NVH testing within the equipment.

3.11.3 CCB Supports

The first CCB supports design were engineered for high strength, in which the weight was not the main concern, as such they were made of steel sheets welded to square tubes. This kind of construction makes them very strong and capable of sustaining the loads of the static tests, but being considerably heavy, their dynamic and vibration performance was not the best, so new CCB supports were needed. Their frequency analysis is shown below.

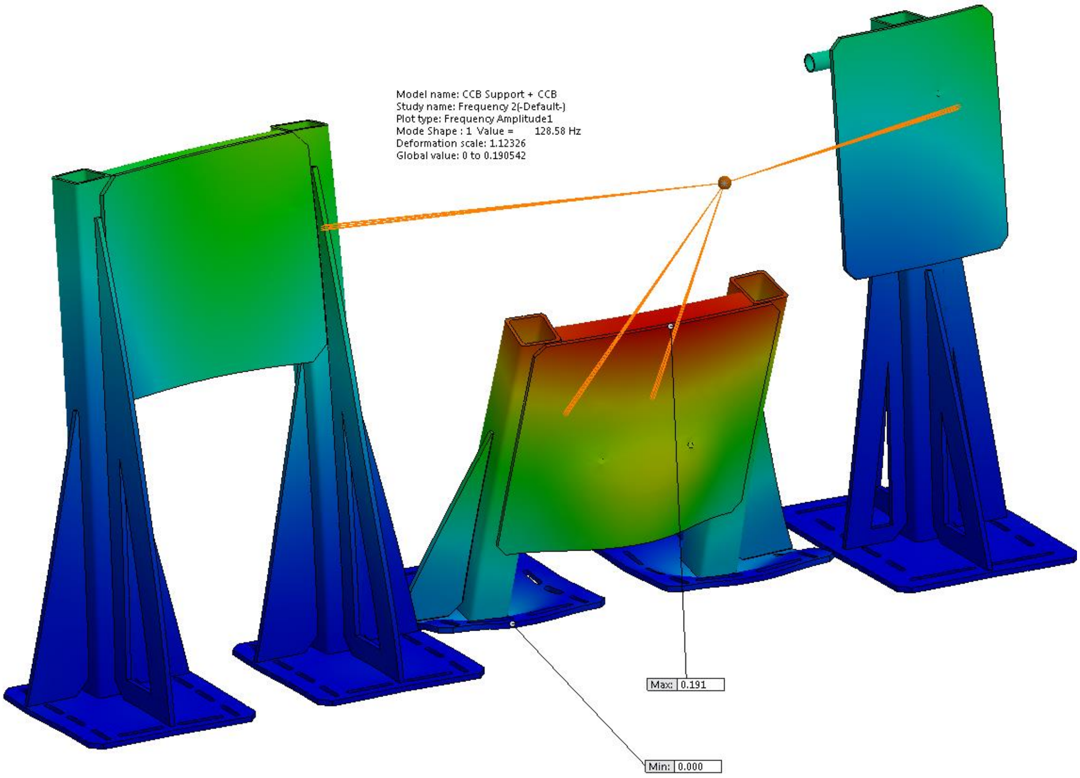

Figure 3-150 – Static test CCB supports

Due to that, a new type of support is needed. For that, we needed a lighter support, but with high rigidity, the mechanical strength of the support is not as important, so that's the attribute that will be lowered to achieve higher rigidity and lower weight values.

To make the support lighter, but with high rigidity we considered using aluminium for the material with commercial aluminium profiles. Every frame as stiffened by adding a plate to join the aluminium profiles. To fix the support to the structures base, special feet were designed, from cut L beam profiles, and with strengthening ribs welded, that allow for flexible positioning, these feet can be positioned anywhere along the aluminium profiles. To hold the CCB fixtures, two plates were added to the front of the support, these plates can be positioned anywhere along the aluminium profiles. The result was a structure like the one shown below. The goal to achieve is 400Hz.

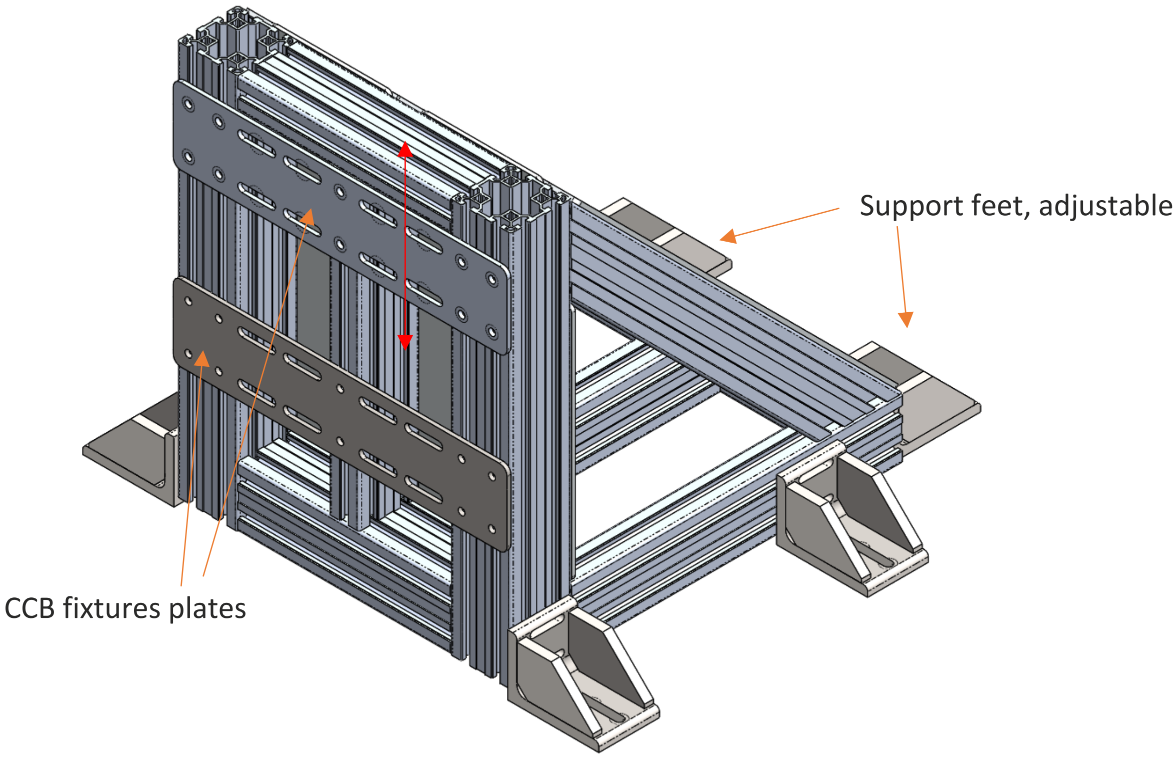

Figure 3-151 – New NVH testing CCB support

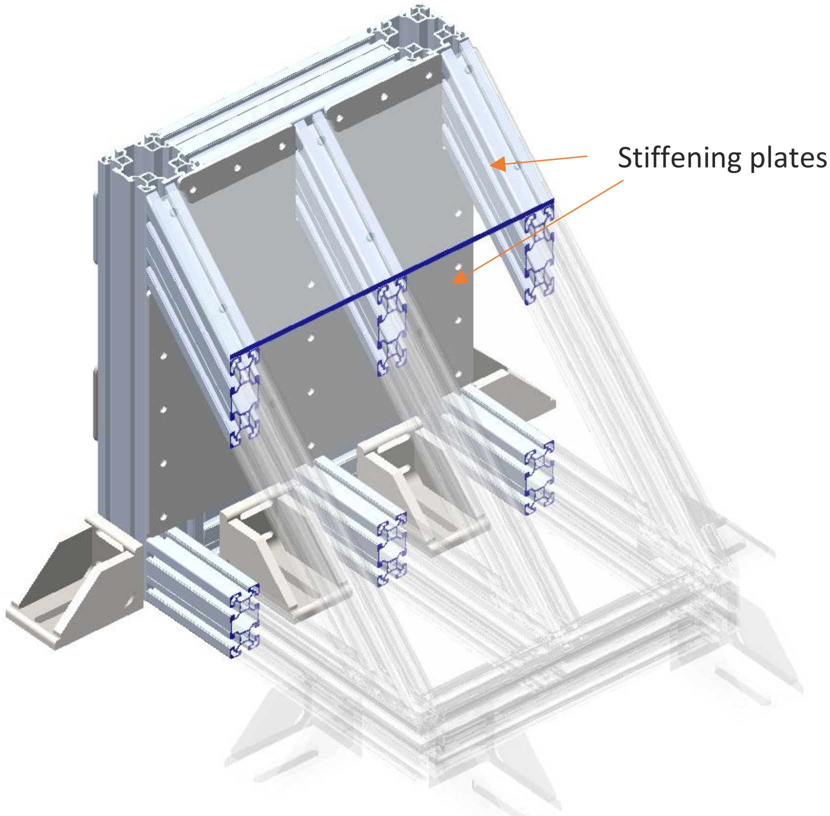

Figure 3-152 – New NVH testing CCB support

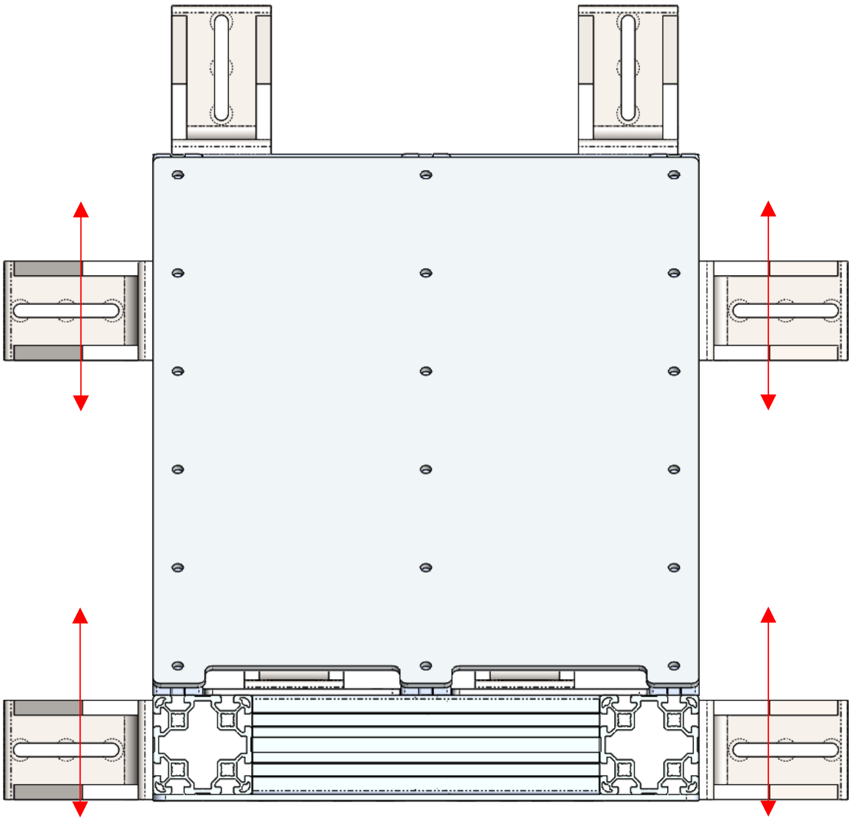

Figure 3-153 – Top view of the CCB NVH support

Different types of meshes were used in the simulation of this support. For the aluminium profiles, beam mesh was used, for the stiffening plates shell mesh and for the feet solid mesh. All the elements were considered bonded

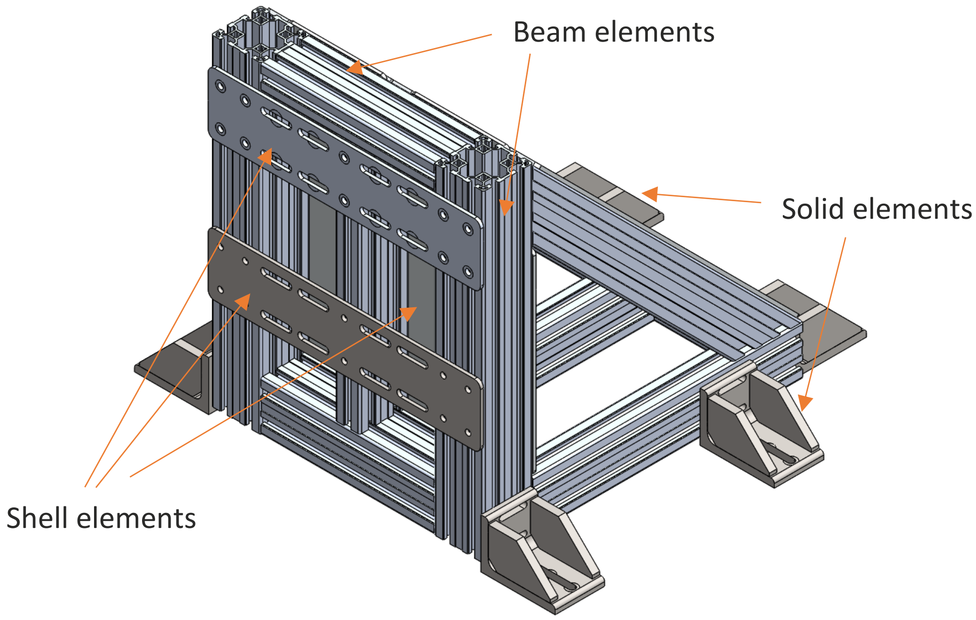

Figure 3-154 – NVH CCB support types of meshing elements

The final mesh is shown below in Figure 3-155. Shells and beams rendered in 3D.

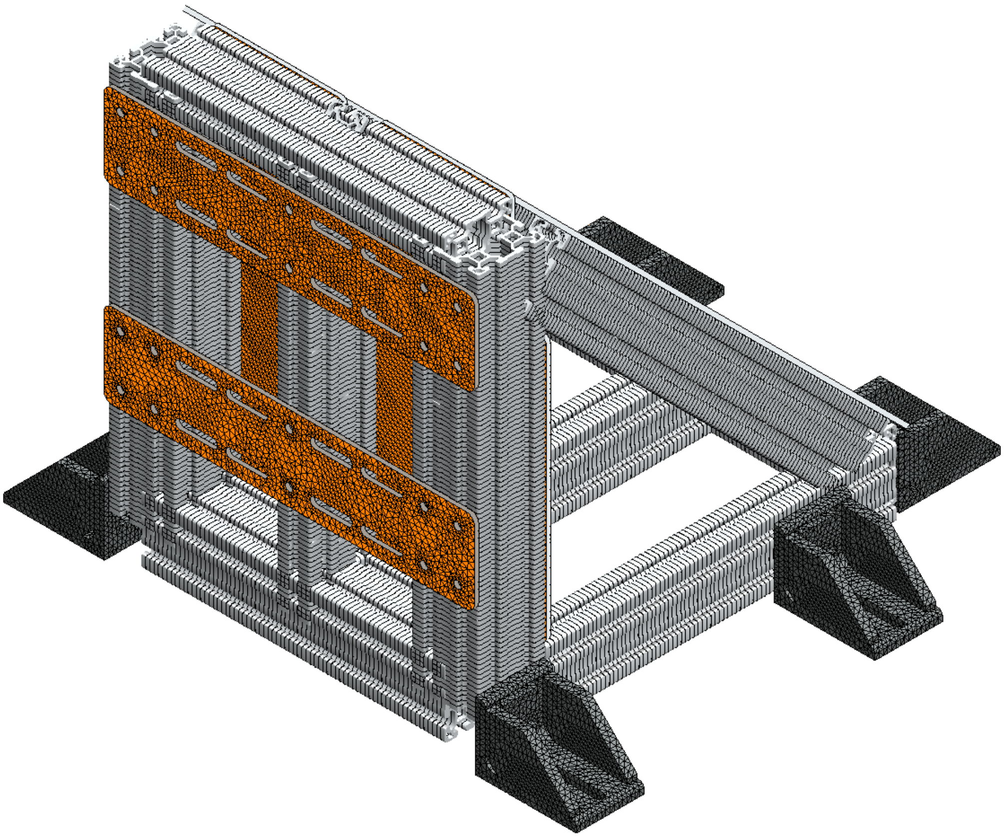

Figure 3-155 – NVH CCB support mesh

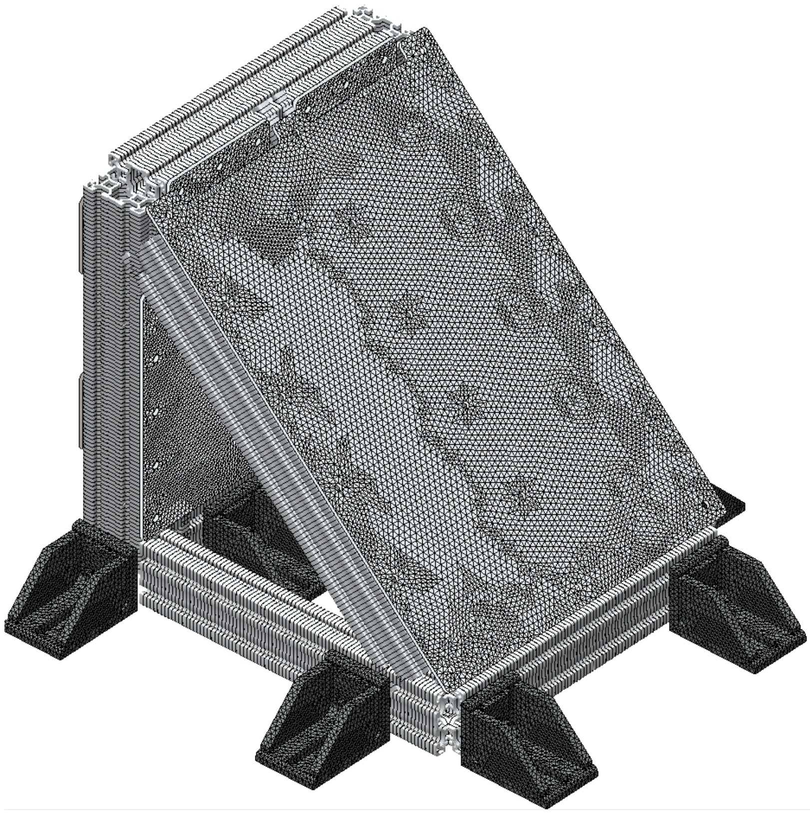

Figure 3-156 – NVH CCB support meshed model

The fixations of the support were considered taking into consideration the structure base hole pattern and the worst-case scenario. Multiple configurations were tested, and two are presented in this work, which could be considered worst-case. Nevertheless, the design allows for a very large number of configurations and predicting them all would be impossible.
The first feet configuration is shown in Figure 3-157.

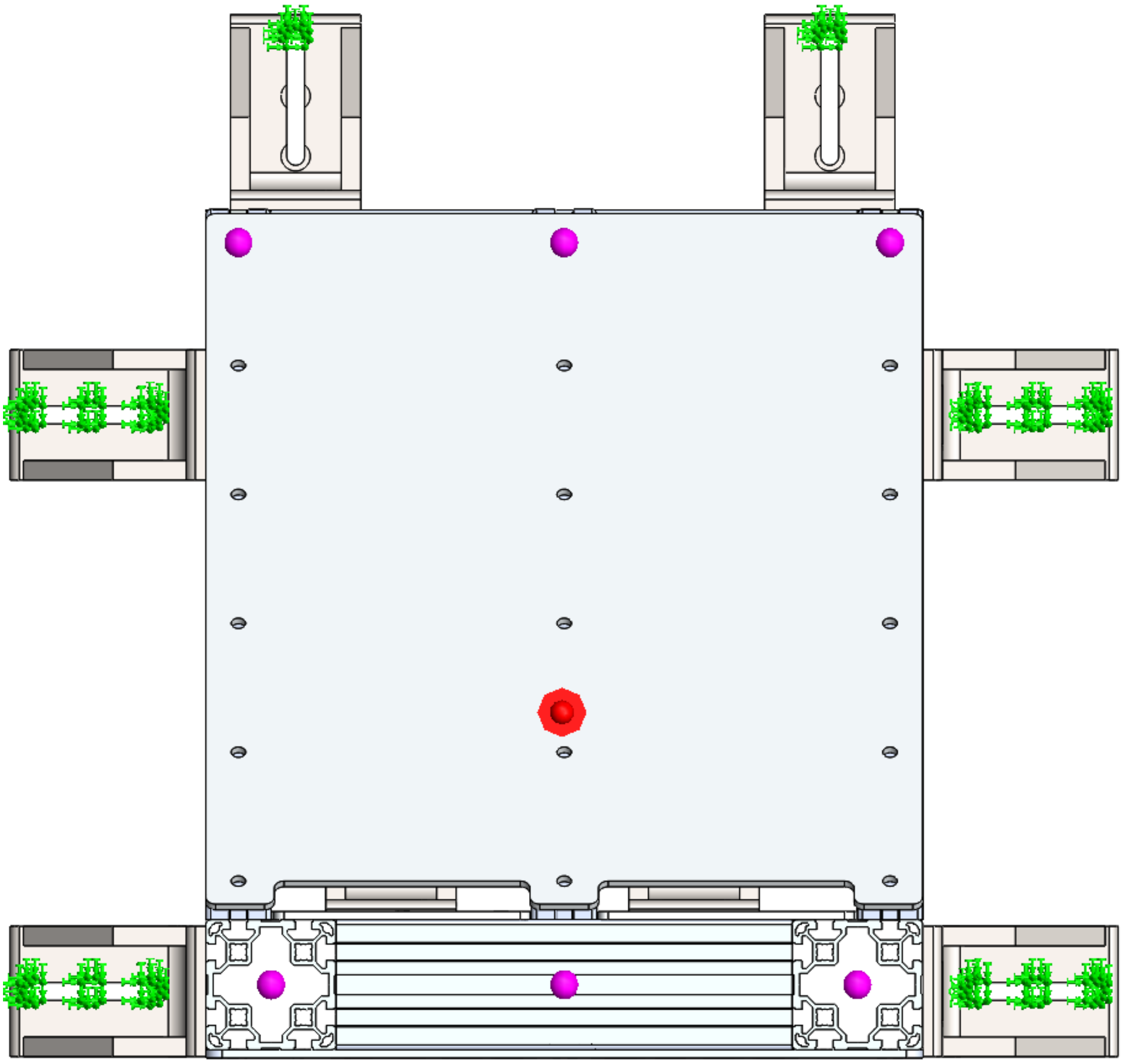

Figure 3-157 – NVH CCB support config. A simulation fixation points

To more accurately define the fixations, an area around the slots with dimensions of the screw was added and the fixation is done on that area (completely fixed).

In this case, we're only looking for the first mode of vibration, so that is the only value analysed and the focus was to find feet configurations that could not achieve the goal.

Table 3-16 –NVH CCB support config. A first mode of vibration

Mode No.	Frequency (Hz)
1	477,35

The next pages show the first mode of vibration.

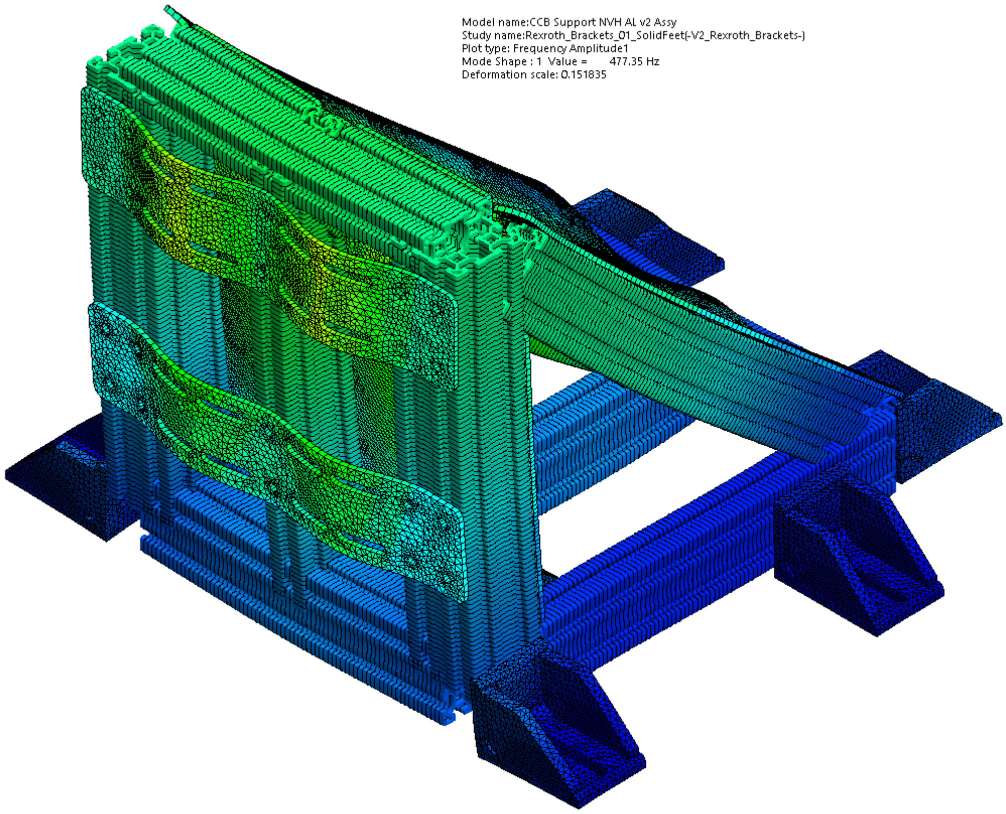

Figure 3-158 – NVH CCB support config. A 1st mode of vibration

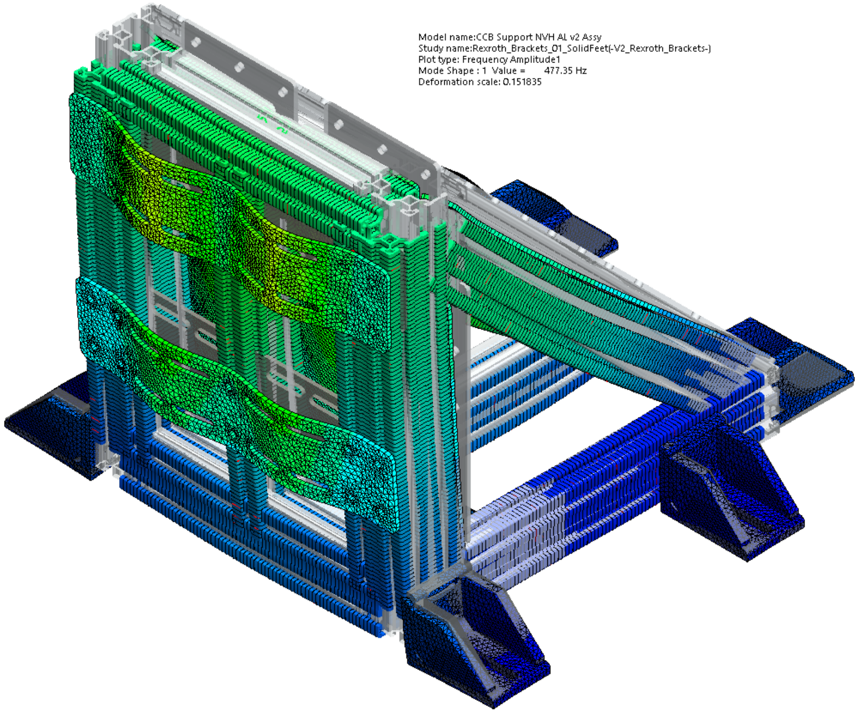

Figure 3-159 – NVH CCB support config. A 1st mode of vibration (original model superimposed)

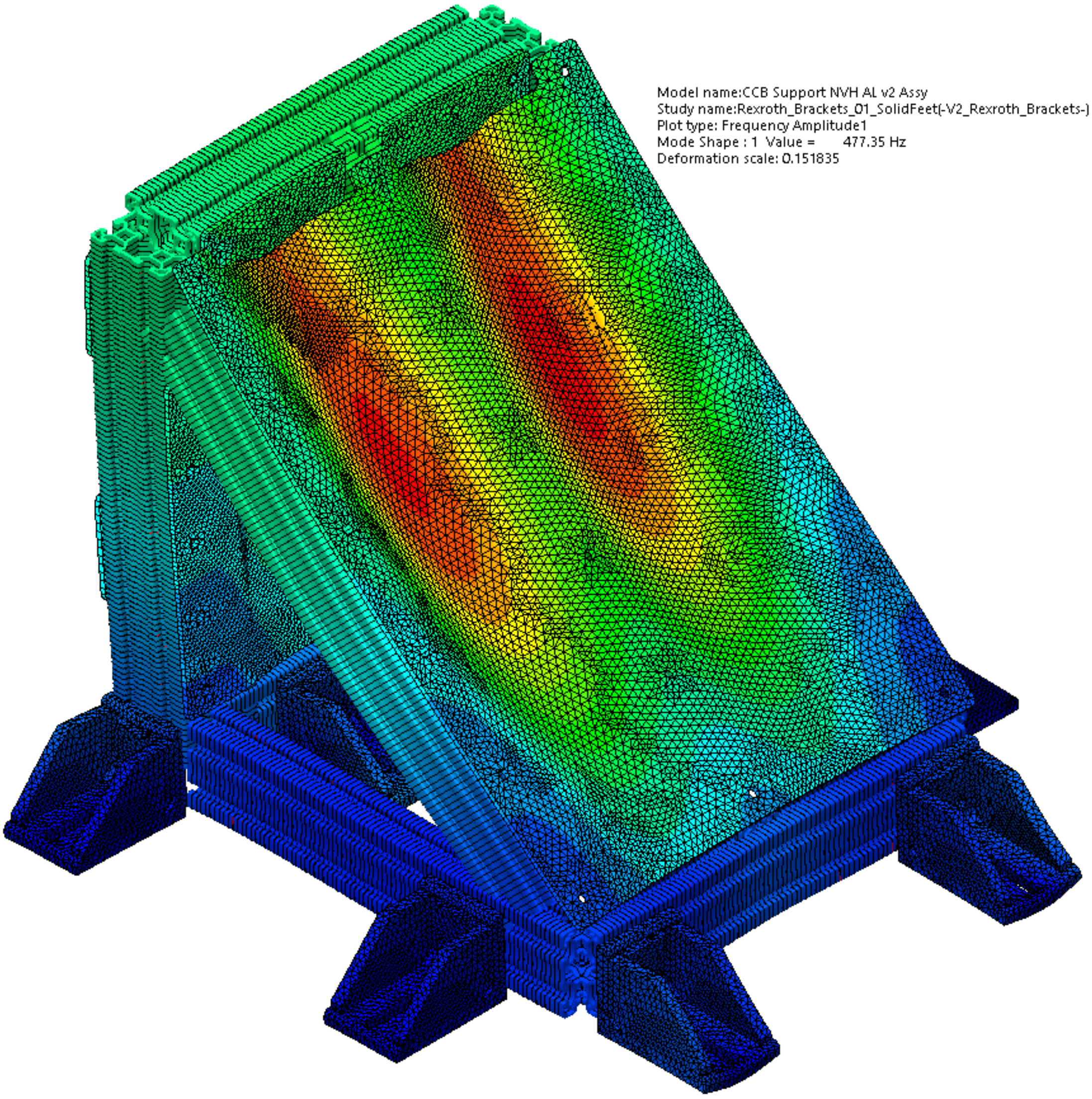

Figure 3-160 – NVH CCB config. A 1st mode of vibration (rear view)

Next is the second configuration considered.

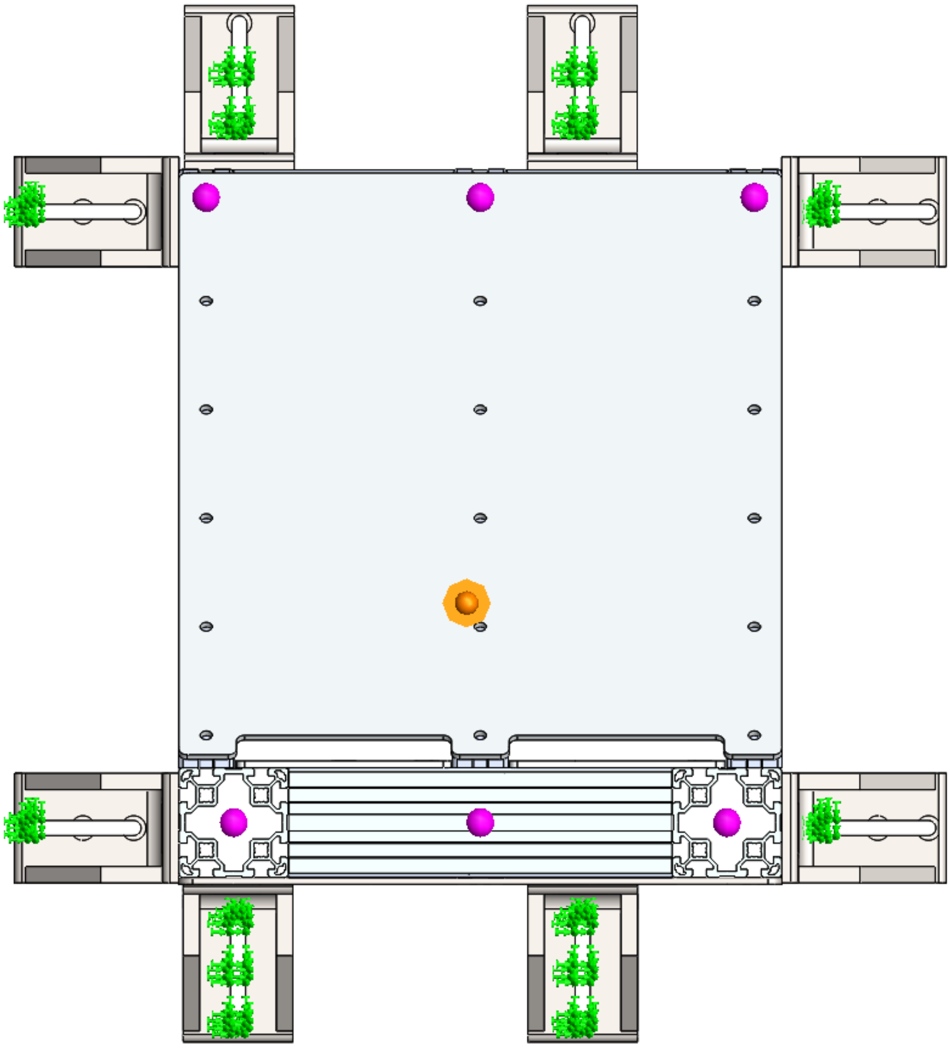

Figure 3-161 – NVH CCB support config. B simulation fixation points

As before, we're only looking at the first mode of vibration, which is shown below.

Table 3-17 – NVH CCB support config. B first mode of vibration

Mode No.	Frequency (Hz)
1	484,86

The next pages show the first mode of vibration for the config. B.

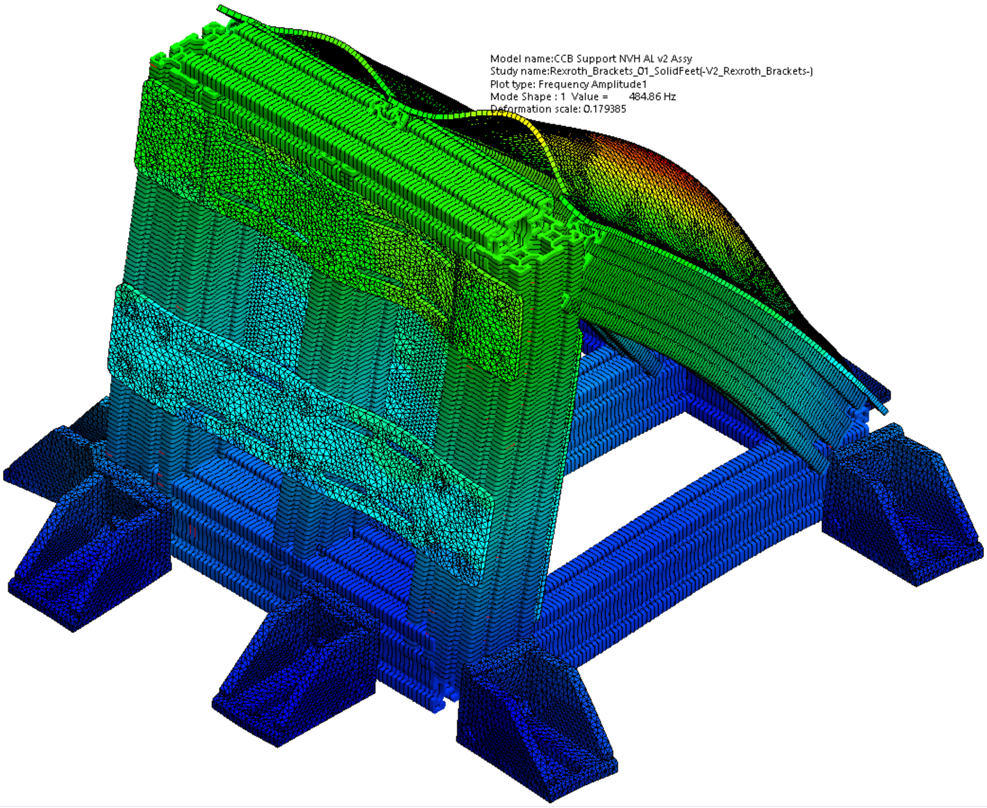

Figure 3-162 – NVH CCB support config. B 1st mode of vibration

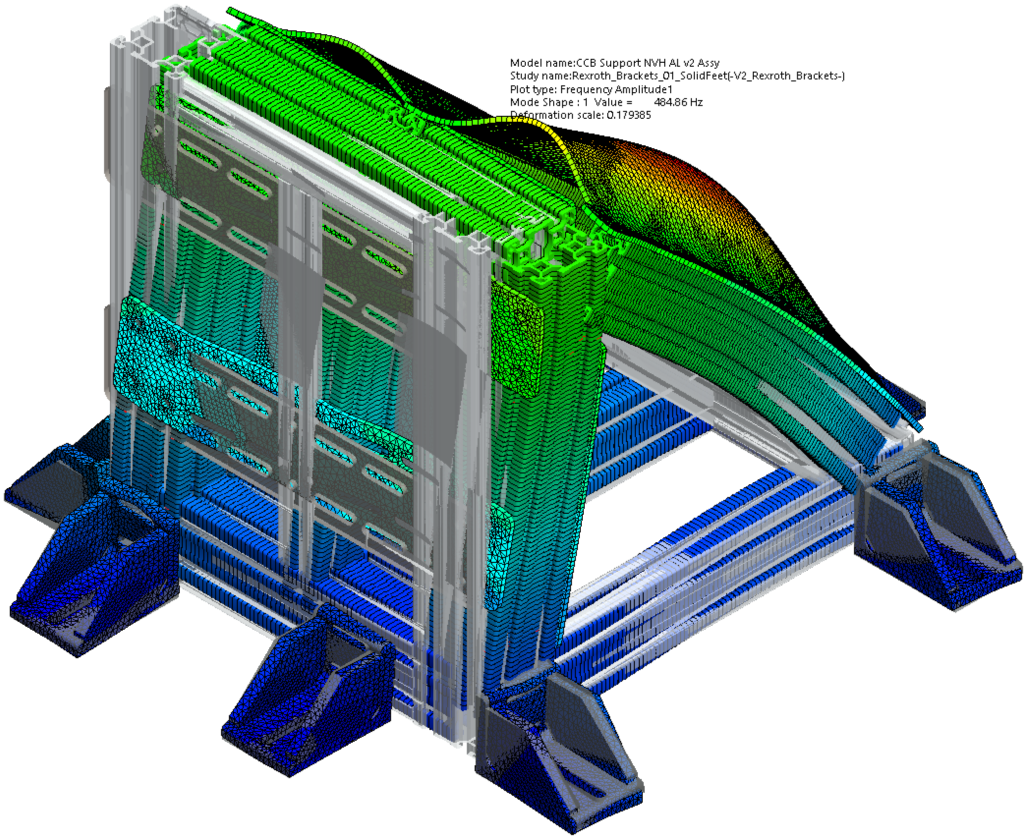

Figure 3-163 – NVH CCB support config. B 1st mode of vibration (original model superimposed)

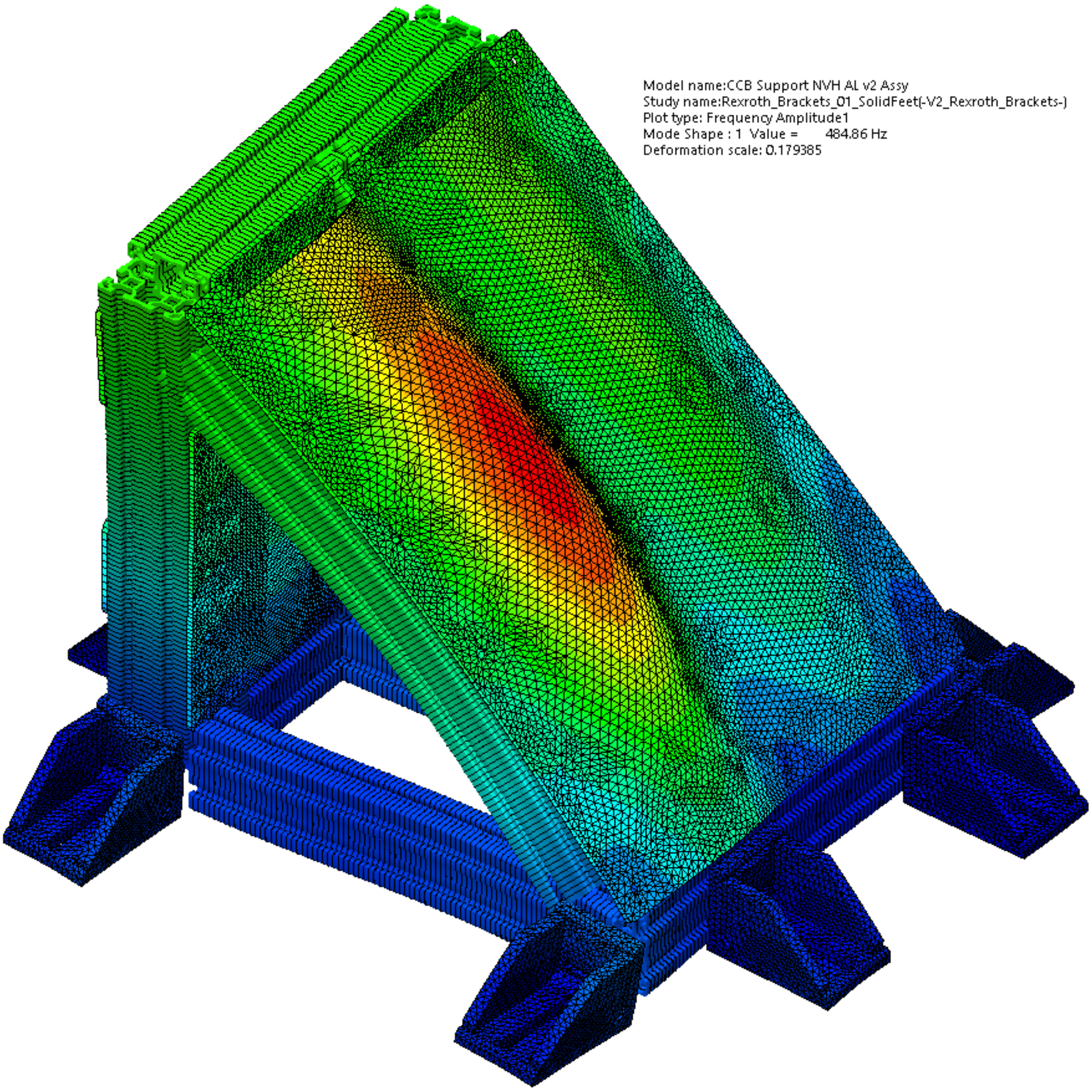

Figure 3-164 – NVH CCB config. B 1st mode of vibration (rear view)

From the studies, it can be concluded that the supports are appropriate for the NVH testing. Other configurations could give higher first modes.

The lowest result, in config. A is of 477Hz which complies with the requirement of the client of a first mode of vibration above 400Hz.

Since the aluminium profiles have a few details along the shape of the profile and the previous study considered the profile a beam, a profile with 600mm was studied to check its local modes and natural frequencies of the walls and fins of the profile.

To decrease the simulation time, some assumptions were taken into account such as, using symmetry planes to decrease the number of elements and maintain accurate results. This symmetry planes divide the profile in 8 equal parts.

The meshing was refined to get at least two elements per thin wall. Solid elements were used.

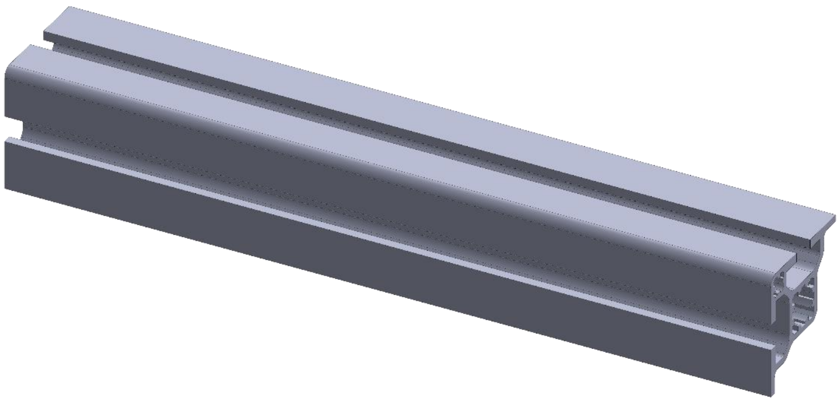

Figure 3-165 – Section of an 80x80 aluminium profile used in the NVH supports

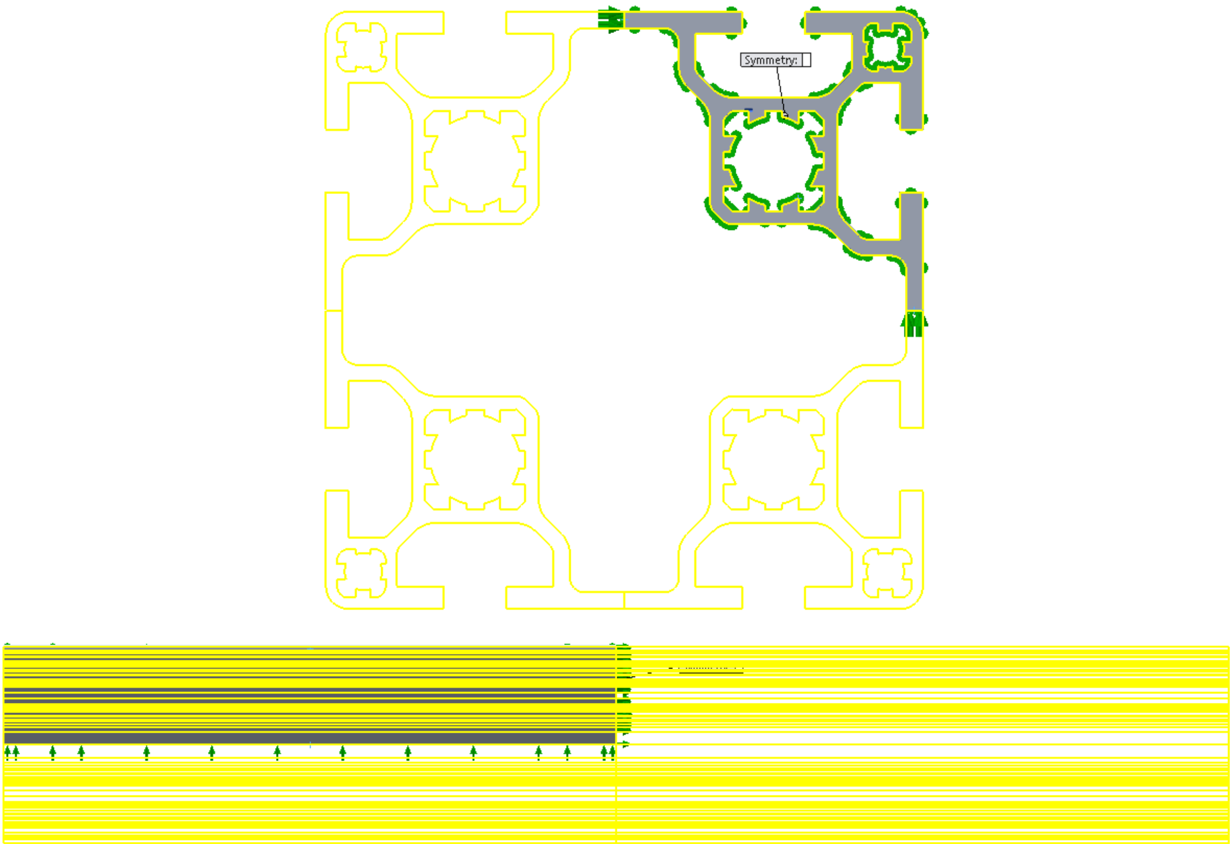

Figure 3-166 – Symmetry planes applied to the 80x80 profile

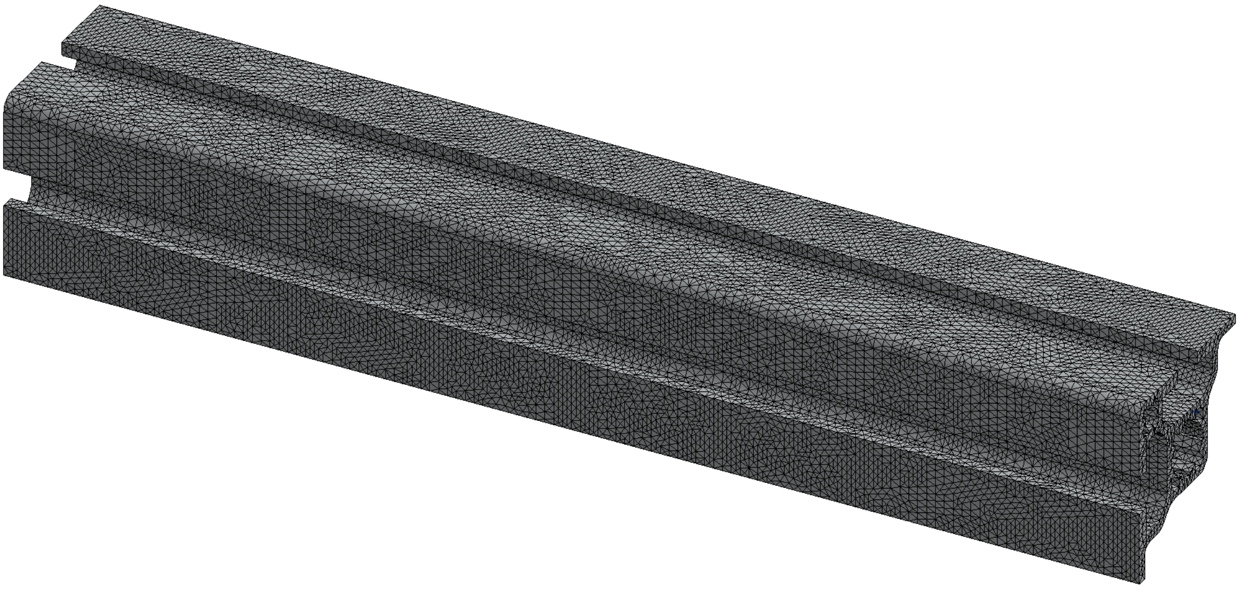

Figure 3-167 – Mesh of the 80x80 aluminium profile solid model

Table 3-18 – 80x80 aluminium profile 1st mode of vibration

Mode No.	Frequency (Hertz)
1	640,8

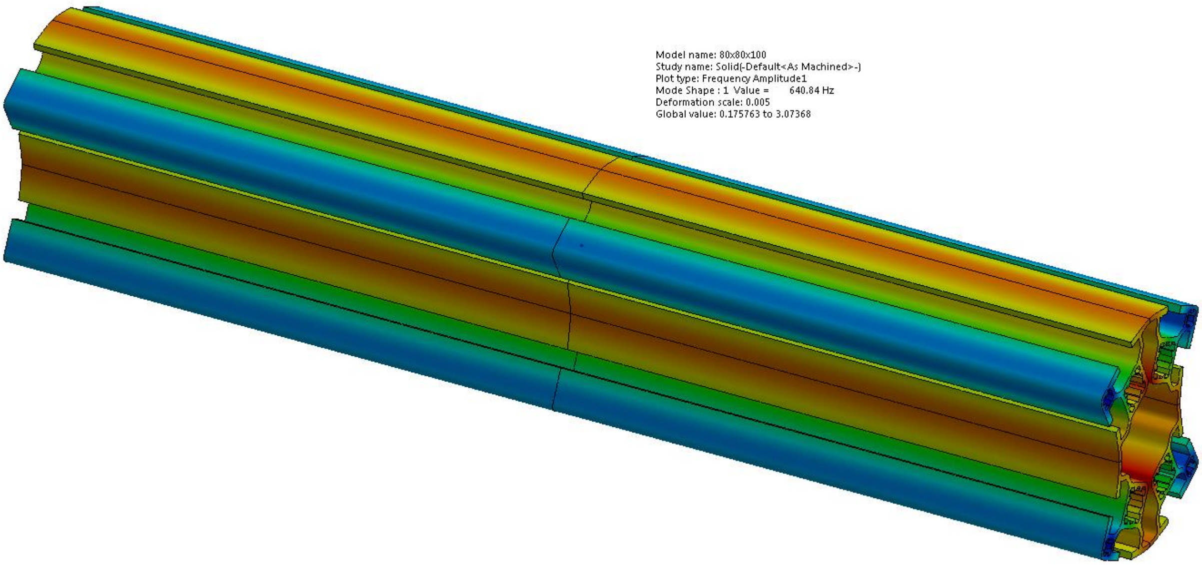

Next is the other type of aluminium profile present in the structure. The assumptions and procedure is the same as on the other profile.

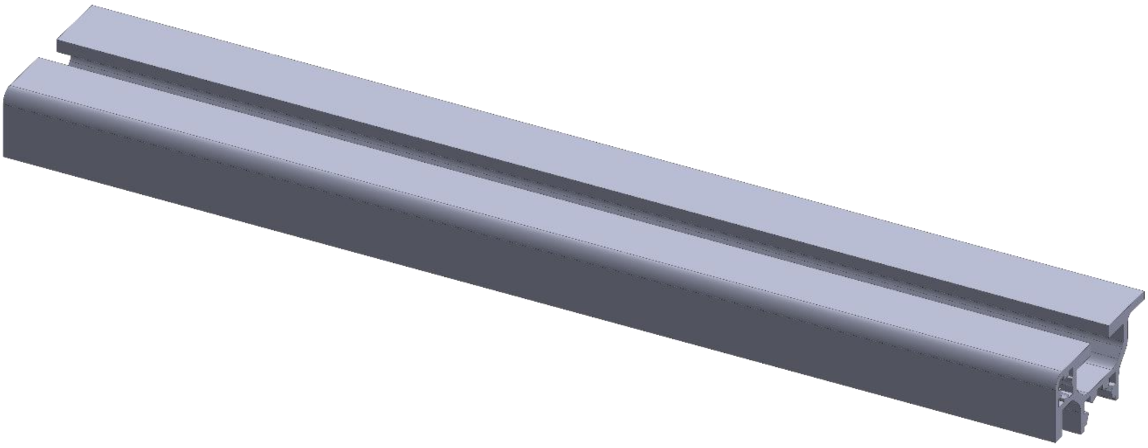

Figure 3-168 – Section of an 80x40 aluminium profile used in the NVH supports

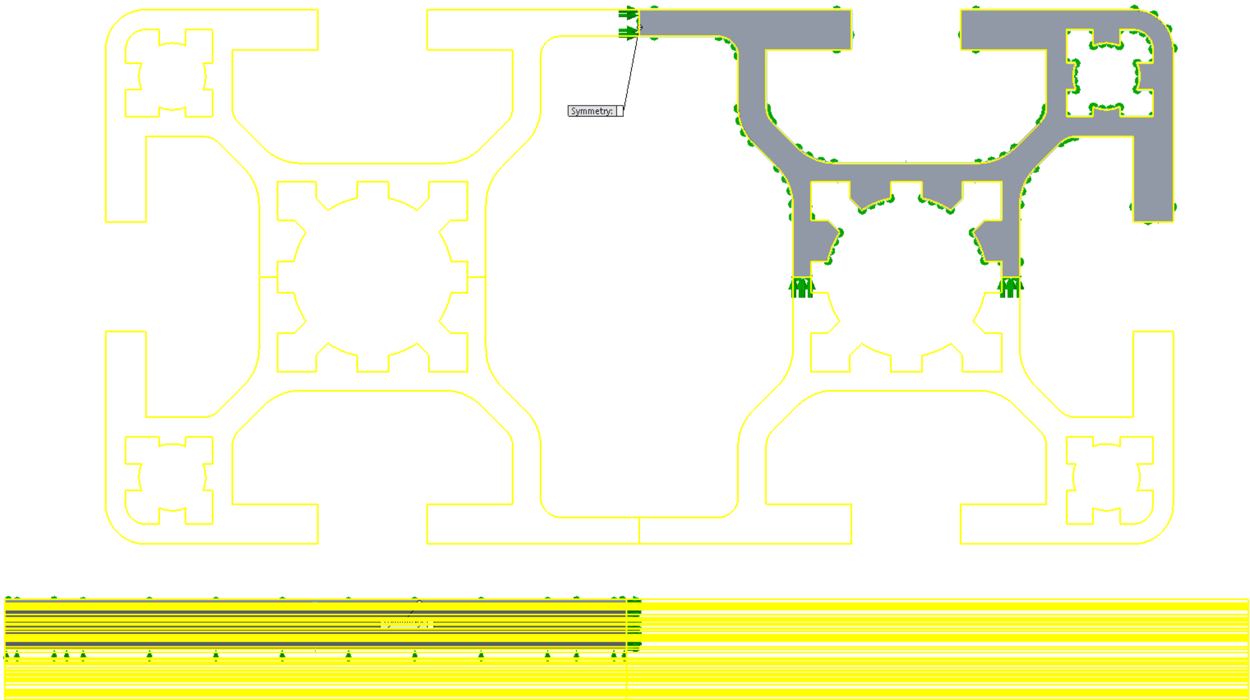

Figure 3-169 – Symmetry planes applied to the 80x40 profile

Figure 3-170 – Mesh of the 80x40 aluminium profile solid model

Table 3-19 – – 80x40 aluminium profile 1st mode of vibration

Mode No.	Frequency (Hertz)
1	1721,3

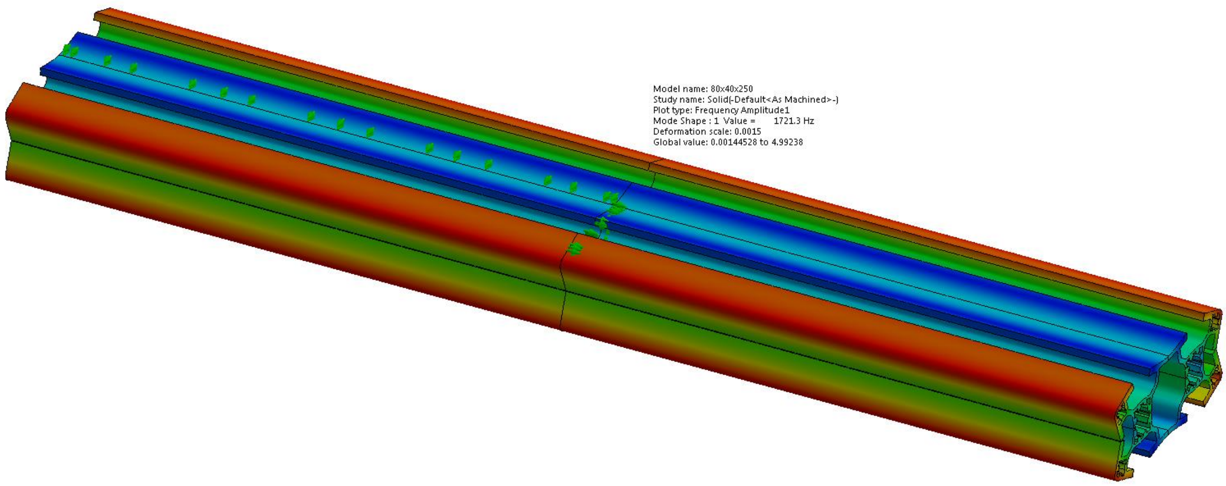

Given the results, we can conclude that, internally, there should be no issues with unwanted vibrations coming from any part of the aluminium profiles.

4 CONCLUSIONS

In this work, an equipment was designed and developed for a project of EVOLEO Technologies following the requirements of the company's client.

The initial requirements of the client were achieved, the developed and built equipment is capable of testing CCBs in static tests, fatigue tests and NVH tests. This equipment is capable of testing CCBs up to [dimensions] with the ability to apply up to two loads simultaneously with either up to 7,5kN or 25kN with a stroke of 300mm depending on the chosen actuators.

The equipment was designed to be operated by one person, not having any need for other external tools to move or operate any of the components and configure the equipment. To operate the heaviest component, the bridge, a hoist was added that helps the operator move the bridge to the desired position.

The way this equipment is designed, allows for multiple configurations, allowing the operator to apply loads in multiple directions. The adjusting components such as the bridge, gantry and the base, allow the testing of any of the client's proposed CCB models.

The whole system was designed to have its base and other parts in welded construction using structural profiles of the types IPE and HEA.

It was not part of this work to develop any control or automation system to control the hydraulic actuators.

The equipment's structure was checked for resistance and rigidity, and all the installed stresses are below the fatigue limits being that the highest deflection, under load, is on the bridge by about 1mm.

Modal analysis were also run to the system's gantry and pillars, which returned frequencies of about 5Hz, which as the base was embedded in concrete, does not affect the readings and measurements of the CCBs.

To comply with the client's requirements for the NVH tests, specific CCB supports were designed which have their first mode of vibration above the 400Hz. The whole structure is also projected to be isolated from external vibrations, by using a solution developed by a contracted company.

Below are some pictures of the equipment, after assembly.

Figure 4-1 – CCBTester after assembly

Figure 4-2 – CCBTester after assembly

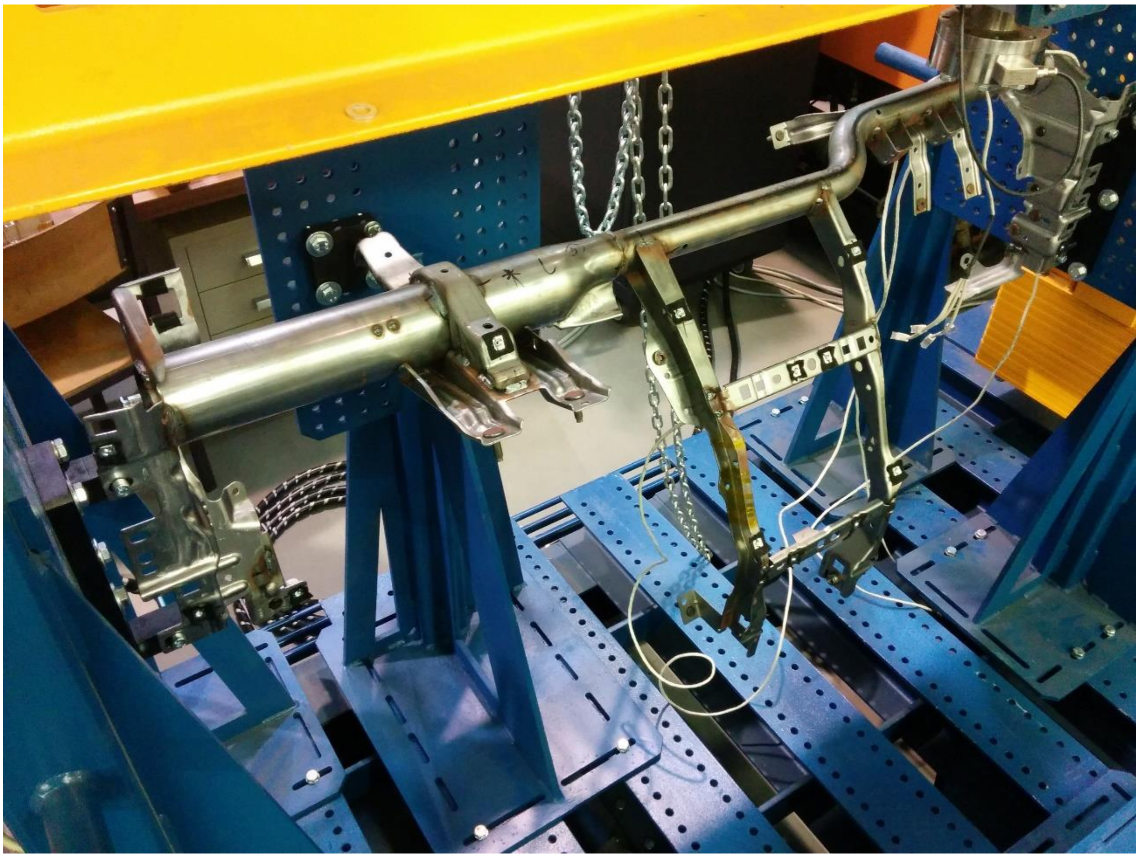

Figure 4-3 – CCBTester with CCB mounted

5 FUTURE WORK

Developing automation and control modules to program fatigue tests.

The equipment has been tested and operated, but still without the concrete base. For that, it needs to be transported to the client's laboratory after their approval. At the date of this work, the client had not yet requested that. Has such it is needed to devise a plan and workflow to install the equipment in the client's premises.

The author believes that this type of testing equipment for CCBs will start to have relevance in the future and will become ever more advanced and sophisticated and would benefit from a base manufactured using foundry processes. This type of manufacturing process allows for better vibration performance, as usually seen in older lathes and milling machines.

During this project, there were multiple budget restrictions, both for material and time. This creates the need for a practical and faster approach, one that is not an ally of scientific or academic work. Future works could include the further analysis and improvement of the current design to better know it's dynamic properties and increasing the equipment's automation level so that the setup and configuration times by the operator are diminished.

BIBLIOGRAPHY AND REFERENCES

6 BIBLIOGRAPHY AND REFERENCES

Ashby, M. F. (2010). *Materials Selection in Mechanical Design.* Butterworth-Heinemann.

Atkins, T., & Escudier, M. (2013). *A Dictionary of Mechanical Engineering (Oxford Quick Reference).* Oxford University Press.

Automotive Benchmarking. (2015, July 23). Retrieved from A2mac1: http://www.a2mac1.net

Brown, H. T. (2010). *507 Mechanical Movements: Mechanisms and Devices.* Watchmaker Publishing.

Brüel & Kjær. (1988). *Structural Testing.* Nærum.

Budynas, R. G., & Nisbett, J. K. (2011). *Shigley's Mechanical Engineering Design.*

Domingues, J. S. (2003). *Apontamentos de orgãos de máquinas.* ISEP.

Duncan, A. E. (1996). *Understanding NVH basics: Proceedings of the International Body Engineering Conference.* IBEC.

Eurocode 3 - Design of steel structrures Part 1-8: Design of joints. (2010).

Eurocode 3: Design of steel structures Part 1-1: General rules and rules for buildings. (2009).

Gentle, R., Edwards, P., & Bolton, W. (2001). *Mechanical Engineering Systems.* Elsevier.

Morais, S. (2006). *Desenho técnico básico 3.* Porto Editora.

Multi-axes test bench. (2014, July 10). Retrieved from KNR Test Systems: http://www.knrsys.com/ko/portfolio/component-testing-package-2/

Sclater, N. (2011). *Mechanisms and Mechanical Devices Sourcebook.* McGraw-Hill Education.

Tabacu, Stefan, Ion Tabacu and Anton Hadar. (2011). Computational modelling of vehicle interior components for impact applications: Thickness analysis. *International Journal of Crashworthiness*.

DRAWINGS AND APPENDICES

7 DRAWINGS

Attached are a small collection of technical drawings of some of the critical parts of the equipment.

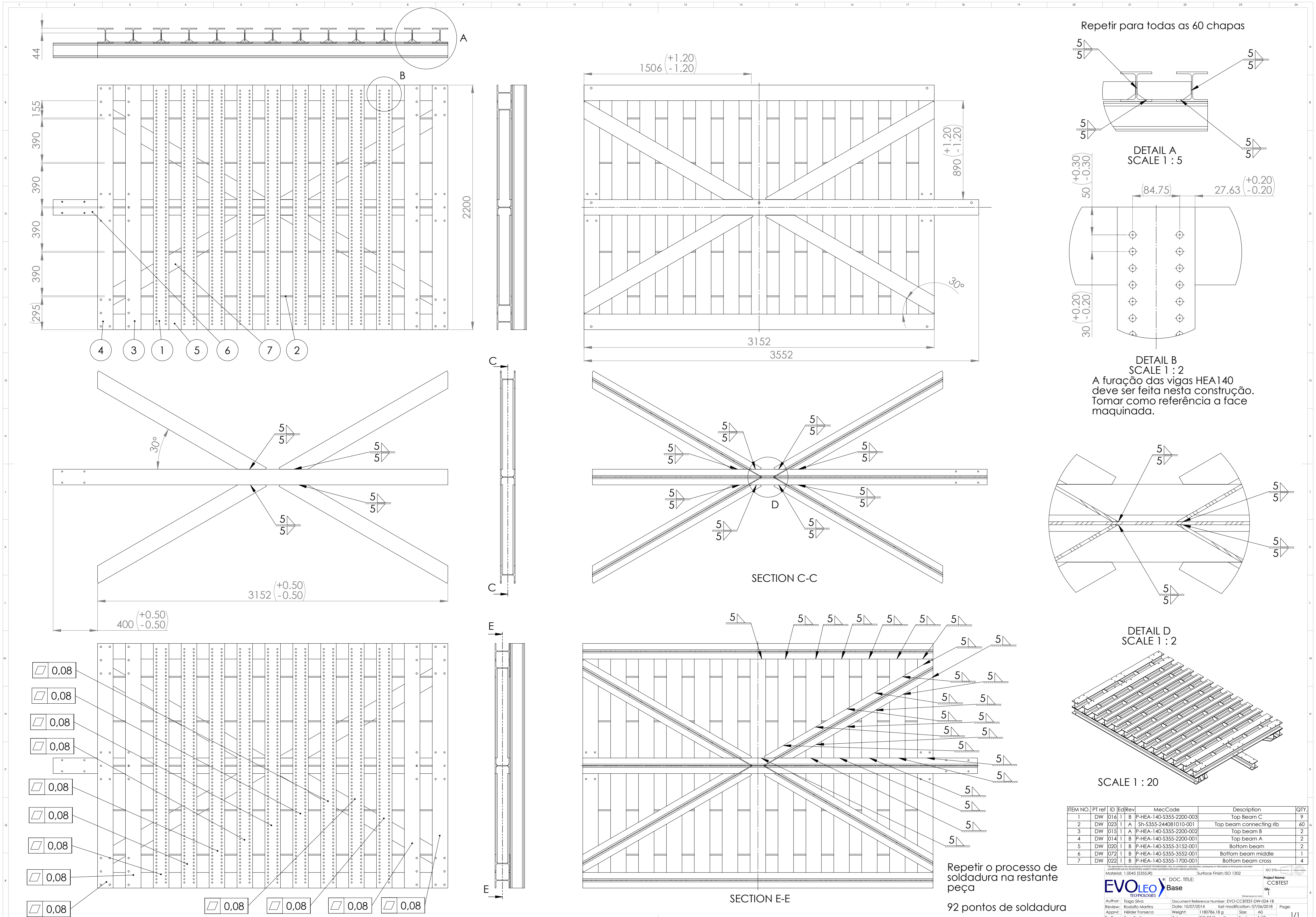

ITEM NO.	PT ref	ID	Ed	Rev	MecCode	Description	QTY.
1	DW	016	1	B	P-HEA-140-S355-2200-003	Top Beam C	9
2	DW	023	1	A	Sh-S355-244081010-001	Top beam connecting rib	60
3	DW	015	1	A	P-HEA-140-S355-2200-002	Top beam B	2
4	DW	014	1	B	P-HEA-140-S355-2200-001	Top beam A	2
5	DW	020	1	B	P-HEA-140-S355-3152-001	Bottom beam	2
6	DW	072	1	B	P-HEA-140-S355-3552-001	Bottom beam middle	1
7	DW	022	1	B	P-HEA-140-S355-1700-001	Bottom beam cross	4

Material: 1.0045 (S355JR) | Surface Finish: ISO 1302 | ISO SYS

EVOLEO TECHNOLOGIES

DOC. TITLE: **Base**

Dimensions in mm

Project Name: CCBTEST

Qty. 1

Author:	Tiago Silva	Document Reference Number: EVO-CCBTEST-DW-024-1B			
Review:	Rodolfo Martins	Date: 10/07/2014	last modification: 07/06/2018		Page:
Apprvl:	Hélder Fonseca	Weight:	1180786.18 g	Size: A0	
Pa Rev.:	Sara Freitas	Tolerance:	ISO 2768 - m K	Scale: 1:10	1/1

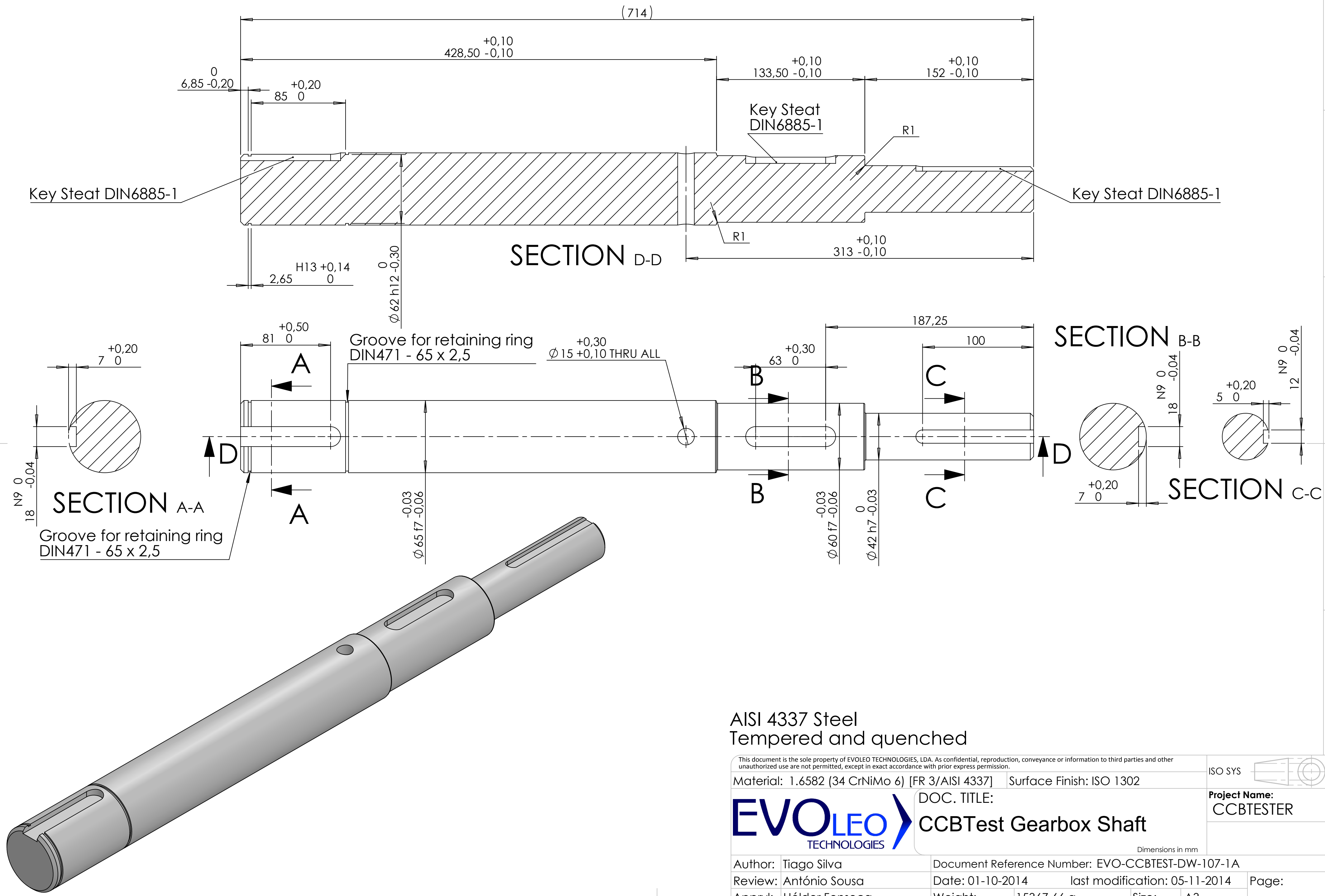

AISI 4337 Steel
Tempered and quenched

Material: 1.6582 (34 CrNiMo 6) [FR 3/AISI 4337] | Surface Finish: ISO 1302 | ISO SYS

EVOLEO TECHNOLOGIES

DOC. TITLE: CCBTest Gearbox Shaft

Project Name: CCBTESTER

Dimensions in mm

Author:	Tiago Silva	Document Reference Number: EVO-CCBTEST-DW-107-1A					
Review:	António Sousa	Date: 01-10-2014	last modification: 05-11-2014				Page:
Apprvl:	Hélder Fonseca	Weight:	15367.66 g	Size:	A3		1/1
Pa Rev.:	Sara Freitas	Tolerance:	ISO 2768 m K	Scale:	1:3		

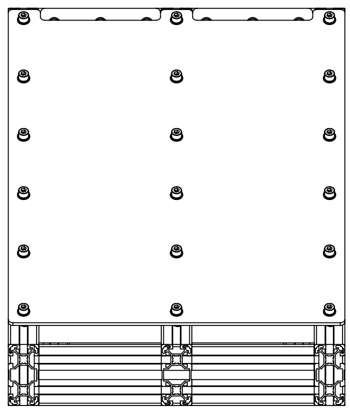

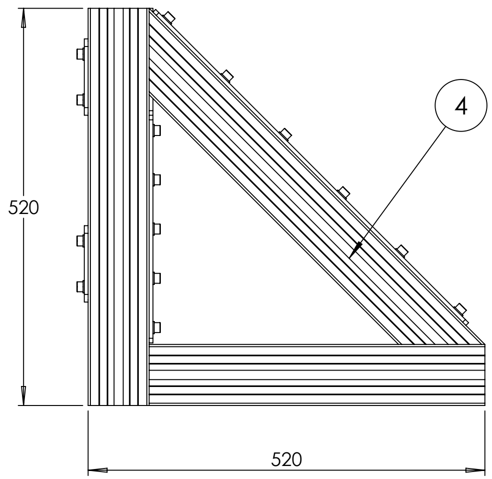

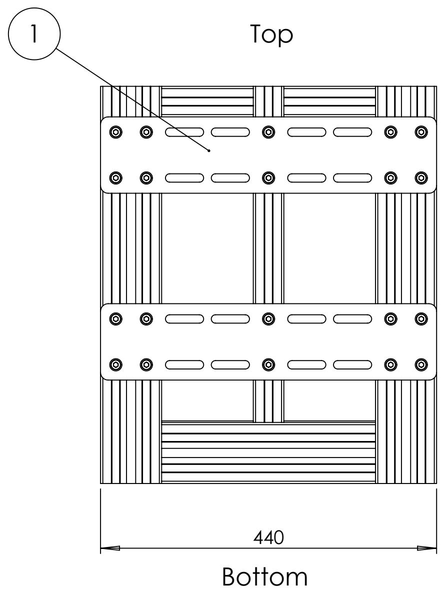

Front

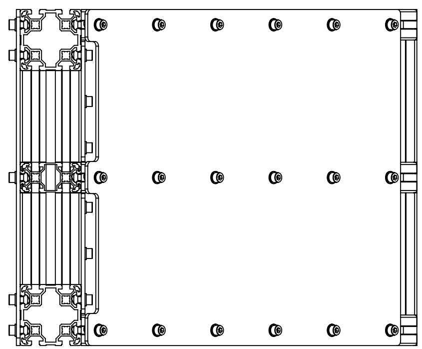

Rear

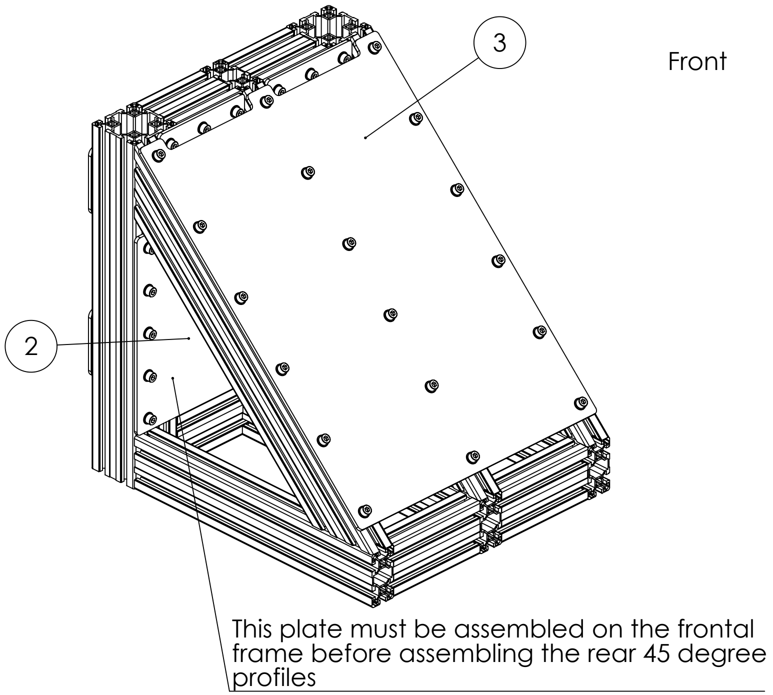

ID	Description	PartNumber	QTY.
1	NVH Support Hole Matrix Plate	EVO-CCBTEST-DW-228-1	2
2	NVH Structure Inner Reinforcement Plate	EVO-CCBTEST-DW-256-1	1
3	NVH Structure Rear Reinforcement Plate	EVO-CCBTEST-DW-255-1	1
4	NVH Support Structure	EVO-CCBTEST-DW-227-1	1
5	Flat washers ISO 7089, 8, 140HV	ISO 7089 / DIN 125-1A - 8 - 140HV	59
6	Screw Hex Socket head cap ISO 4762, M8x16, 8.8	ISO 4762 / DIN 912 - M8x16 - 8.8	59
7	Sliding Block Swivel In N10 M8	3842529300	59

Material: Material <not specified>
Surface Finish: ISO 1302
ISO SYS
Dimensions in mm

EVOLEO TECHNOLOGIES

DOC. TITLE:
CCB NVH Structure

Project Name: CCBTester

Author:	Tiago Silva	Document Reference Number: EVO-CCBTEST-DW-254-1			
Review:	António Sousa	Date: 12/10/2017	last modification: 19/10/2017		Page:
Apprvl:	Rodolfo Martins	Weight:	26888.97 g	Size: A3	1/1
Pa Rev.:	Sara Freitas	Tolerance:	ISO 2768 m K	Scale: 1:7	